An Ecological Study of Hunting Creek

2021

FINAL REPORT

February 2, 2022

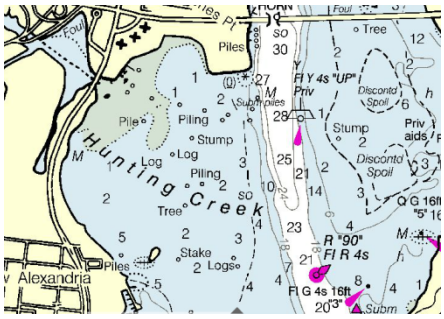

by

R. Christian Jones
Professor, Project Director

T. Reid Nelson
Assistant Professor, Co-Principal Investigator

Benoit Van Aken
Associate Professor, Co-Principal Investigator

Amy Fowler
Assistant Professor, Co-Principal Investigator

Potomac Environmental Research and Education Center
Department of Environmental Science and Policy
Department of Chemistry and Biochemistry
George Mason University

to

Alexandria Renew Enterprises
Alexandria, VA

This page intentionally blank.

Table of Contents

An Ecological Study of Hunting Creek - 2021

Executive Summary

Hunting Creek is an embayment of the tidal Potomac River located just downstream of the City of Alexandria and the I-95/I-495 Woodrow Wilson bridge. This embayment receives treated wastewater from the Alexandria Renew Enterprises wastewater treatment plant and inflow from Cameron Run which drains most of the Cities of Alexandria and Falls Church and much of eastern Fairfax County. The Hunting Creek embayment is bordered on the north by the City of Alexandria and on the west and south by the George Washington Memorial Parkway and associated park land. Due to its tidal nature and shallowness, the embayment does not seasonally stratify vertically, and its water is flushed by rainstorms and may mix readily with the adjacent tidal Potomac River mainstem.

Beginning in 2013 the Potomac Environmental Research and Education (PEREC) in collaboration with Alexandria Renew Enterprises (AlexRenew) initiated a program to monitor water quality and biological communities in the Hunting Creek area including stations in the embayment itself, its tributaries, and the adjacent river mainstem. This document presents study findings from 2020 and compares them with that from the previous seven years. In addition, *Escherichia coli* levels in Hunting Creek and tributaries. And we completed a fourth year of benthic macroinvertebrate and water quality sampling on many tributaries of Cameron Run and Hunting Creek.

The Chesapeake Bay, of which the tidal Potomac River is a major subestuary, is the largest and most productive coastal system in the United States. The use of the Bay as a fisheries and recreational resource has been threatened by overenrichment with nutrients which can cause nuisance algal blooms, hypoxia in stratified areas, loss of submersed aquatic vegetation, and declining fisheries. As a major discharger of treated wastewater into Hunting Creek, AlexRenew has been proactive in decreasing nutrient loading since the late 1970's. Also of concern are *E. coli* and nutrients derived from combined sewer overflows (CSO's) and nonpoint sources within the drainage basin as well as sediments derived from the watershed.

The ecological study reported here provides documentation of the current state of water quality and biological resources in Hunting Creek. Air temperature was above normal in all months. Precipitation closer to normal in 2021 than in the extremely wet year 2018. However, it was again well above normal in 2021, especially in June and August. Water temperature followed a typical seasonal pattern at all tidal stations with highest values approaching 30°C in early June, July, and August. A marked drop in water temperature occurred in late June corresponding with a cool snap and associated precipitation. Specific conductance followed a gradual increase at most tidal stations through early August. Chloride followed a more variable pattern at stations AR1, AR24 and AR25 near the input from the AR treatment plant and some potential CSO flow. Dissolved oxygen peaked in early June at most tidal stations at values above saturation indicating active phytoplankton photosynthesis at this time. Dissolved oxygen was also high near the western shore of Hunting Creek during the July and August water quality mapping cruise. Field pH also peaked in early June at most tidal stations and in particular at the embayment stations AR2 and AR3, further evidence of phytoplankton photosynthesis.

Total alkalinity was in the 60-100 range at all tidal river sites, similar to past years. Total alkalinity was generally 60-100 mg/L as $CaCO_3$ at most embayment and river stations..

Secchi disk transparency showed a distinct seasonal trend at the tidal stations with values higher in the spring at 0.6-0.9 m and lower in the fall at 0.4-0.5 m. Light attenuation exhibited a similar, but less marked trend with one exceptionally low value in late July in Hunting Creek. Turbidity was also very high at AR2 on that date. In the Hunting Creek embayment there was a consistent decline in Secchi disk depth and light attenuation coefficient over the study period. There were also substantial declines in late June and late July corresponding with elevated Cameron Run inflows. Field turbidity readings also reflected these trends. The values of both Secchi and light attenuation indicate water clarity continues to be a problem for SAV recolonization in Hunting Creek.

Ammonia nitrogen was typically below the detection limit (<0.2 mg/L) at all tidal stations so little could be said about its spatial or temporal variation. Nitrate nitrogen showed strong seasonal pattern with lowest values in late July and early August. Nitrite was very low at all tidal stations and did not show consistent seasonal patterns. Organic nitrogen was mostly in the range 0.5-1.0 mg/L at the tidal main stations and showed little seasonal pattern. At the tidal CSO stations there was more variability and spikes of high levels at AR24 and AR25 in early June and late July. Total P at the tidal Main Stations was generally less than 0.1 mg/L. At AR1 and AR24 and AR25 higher values were observed sporadically. All ortho-P values were below the 0.05 detection limit so no patterns could be discerned. N/P ratio consistently pointed to P limitation, with values generally in the 10-30 range being greater than 7.2 threshold in all samples. BOD was consistently below 4 mg/L at most stations. TSS values did not vary much over most stations at dates although there were a few spikes at AR1 and AR25. It is of note that several of the nearshore stations were classified as CSO impact stations and higher levels of certain water quality variables there may reflect CSO impacts.

In the tributaries, seasonal temperature patterns were similar to the tidal stations with the marked drop in late June, but somewhat reduced maximum values near 25°C. In contrast to the tidal stations, specific conductance exhibited a marked seasonal decline especially at the Cameron Run Axis stations probably due to the slow flushing of road salt residuals from surface groundwater. The patterns in chloride, a main component of road salt, backed up these trends in specific conductance.

Dissolved oxygen was at or near saturation at the tributary stations except for AR34 which is at the lower end of the Hoofs Run Axis and influenced by the AR effluent and perhaps by near shore tidal Hunting Creek stations. AR34 showed values at low as 3 mg/L or 30% saturation. Field pH followed a very similar seasonal pattern at all stations with most values centered around 7.5. Lab pH values were even more consistent over time and stations, centered slightly below 7.5. YSI turbidity was very low at all tributary stations on all dates except for AR23, AR13, and AR34. These stations are at the lower end of their axes and near the influence of the AR effluent. Total alkalinity was quite consistent at most stations and throughout the year. Again, the exception was AR23 which often showed elevated values.

Total phosphorus values were frequently below the detection limit of 0.05 mg/L except at AR23, AR13, and AR34, similar to turbidity. Virtually all ortho-P values were below the detection limit of 0.05 mg/L. Organic N at most stations was below 0.5 mg/L. Exceptions again were AR23 and AR34 which had substantially higher and more variable values. Ammonia N was generally near or below detection limits with only one higher value at AR23. Nitrate N was generally low and followed a declining trend at most stations in the Cameron Run Axis. AR23 was often higher. Nitrate on the Hoofs Run Axis was generally somewhat higher, especially at AR33 in the middle of a residential area which was consistently higher reaching 2.5 mg/L. Nitrite N was consistently very low. TSS and VSS were consistently low at most tributary stations. Exceptions again were AR23, AR13, and AR34 which had variable and elevated values.

Correlation analysis was conducted among PEREC-collected water quality parameters from the regular sampling. These reflect relationships over all nine years of the study. Indicators of photosynthesis (DOPPM, DOSAT, Field pH) were highly intercorrelated. Also, measures of particles in the water column and resultant water clarity (turbidity, TSS, Secchi disk depth, and extinction coefficient) were also highly intercorrelated. Indicators of phytoplankton abundance (CHLDI, CHLSF, and VSSSF) were highly intercorrelated. A similar correlation analysis was conducted among AR/Mooney lab parameters. Among the most highly correlated variables in this dataset were TSS and VSS. Total P was positively correlated with organic N, TSS and VSS. Most phosphorus is bound to particles so these correlations make sense. TP was negatively correlated with N to P ratio and this makes sense since it is in the denominator of this ratio. Organic N was highly correlated with TSS, VSS, and BOD. VSS and TSS were highly correlated with BOD.

Since the study began in 2013 it has been noted that certain water quality variables appear to be impacted by major rainfall and runoff events. In this year's report we have tested the correlations between recent runoff coming down Cameron Run and a wide array of water quality variables. This analysis revealed that many variables are strongly correlated with recent stream flow. Specific conductance, chloride, pH, and alkalinity are all significantly reduced by increased streamflow, probably due to the dilution effects of the runoff on the water already in the river. Turbidity, Secchi depth, light attenuation, and TSS are all increased by runoff because solids are either brought in or resuspended by the higher runoff resulting in poorer light penetration.

A fundamental change in the Hunting Creek ecosystem occurred in 2018 with the disappearance of SAV due to high flows that year. SAV has yet to recolonize. Water quality variables that show a clear difference between these two periods using the box plot analysis include Secchi disk depth, light attenuation coefficient, turbidity, TSS, and VSS, all variables related to water clarity.

Phytoplankton biomass as indicated by chlorophyll *a* exhibited two distinct maxima and early June and in early August 2021 at the two Hunting Creek embayment stations (AR2 and AR3). The early June peak occurred during a period of low rainfall and corresponded with high dissolved oxygen and high pH indicating strong photosynthesis by phytoplankton.This peak in late July and early August of 40 µg/L is similar to that attained in 2020 and is among the highest values observed in the nine years of study. At

the river station AR4 chlorophyll values were fairly constant at about 10 µg/L. Phytoplankton cell density at AR2 peaked at the same date as chlorophyll *a* at AR2. Cyanobacteria were the dominant group on that date with a roughly even mixture of *Merismopedia*, *Chroococcus*, and *Oscillatoria*. At AR4 phytoplankton cell density peaked in late July led by green algae and cyanobacteria. Phytoplankton biovolume was generally dominated by diatoms notably *Melosira* and some unidentified pennate diatoms at both AR2 and AR4. Other algae such as *Euglena* and *Peridinium* were also dominant on some occasions.

Phytoplankton biomass as measured by chlorophyll *a* showed a clear increase at both AR2 and AR3 in the post 2018 samples as compared with the pre-2018 samples. The phytoplankton cell count and biovolume data did not show this increase, partially due to the error associated with these counts.

Rotifers were very abundant in early June reaching nearly 8000/L at AR2 and over 4000/L at AR4. As is typical, *Brachionus* was the dominant rotifer. The small cladoceran *Bosmina* had a high short-lived peak in late May of over 500/L. *Diaphanosoma* was the dominant large cladoceran and was very abundant at both AR2 and AR4 and reached maxima in late May and early June, again a period of low precipitation and thus low flushing. *Leptodora* reached a very strong peak of over 6000/m^3 in late May. Among the copepods the immature copepod nauplii reached a strong peak in late May at both AR2 and AR4 and then showed a slow decline thereafter. *Eurytemora* as the most abundant larger copepod with a maxima of over 4000/m^3 in early June at AR4 and almost 2000/m^3 at AR2. *Mesocyclops* was also abundant at AR4.

Some of the zooplankton species did appear to show an effect of the ecosystem change in 2018. The rotifers *Brachionus*, and *Polyarthra* have been more abundant since 2018 than before. Several other taxaa were depressed in 2018, but have recovered including copepod nauplii, the small cladoceran *Bosmina*, and a larger cladoceran *Diaphanosoma*,

2021 marks the ninth year of our fish collections in Hunting Creek. Both trends and inter-annual variability become apparent when comparing the years of data. Total larval density is lower than previous years except for 2018 (a year of high flows) and 2020 (a year with incomplete sampling). Although total abundance was lower, River Herring and other Clupeids remained the most abundant species similar to previous years. Interestingly, White Perch larvae was the second most abundant in 2021, only being surpassed by collections in 2019. Although abundances were somewhat diminished, all four anadromous *Alosa* species were still collected in Hunting Creek, demonstrating that this waterbody remains an important nursery and rearing habitat for these imperiled species of concern.

Trawl sampling was conducted between April and September at stations AR3 and AR4. A total of 731 fishes comprising of at least 16 species were collected with trawls. Collections were dominated by White Perch (71 %). The second most abundant species was Blue Catfish (7.7%), followed by Spottail Shiner and Alewife. An interesting find was the collection of Atlantic Croaker and Hogchoker, two species typically associated with higher salinity waters. The catches at both stations were roughly one third of last year's catches, mainly driven by lower catches of White Perch. Another notable

difference from last year was the absence of three catfishes (Brown Bullhead, Channel Catfish, and Flathead Catfish) in our trawl samples.

A total of 18 seine samples were taken (9 per station), comprising 1739 fishes of at least 19 species (Table 9). Like last year, White Perch (75%) was the dominant species in seine catches followed by Banded Killifish, and Blueback Herring. This continues the trend of greater White Perch dominance seen in 2020 and 2019 as compared with Banded Killifish dominance before 2018 when SAV was very abundant. Similar to previous years, White Perch instead of Banded Killifish was the dominant species collected with fyke nets, representing 76% of the total abundance (Table 12, Figure 63 A & B, 64 A & B) and their catches ramped up in July (Table 13). This resembles the trend seen in seine and trawl collections, where White Perch dominated over Banded Killifish as a likely response to the paucity of SAV.

As in 2018-2020, SAV was virtually absent in 2021 as verified by surveys conducted during datamapping. This is most certainly attributable to the very turbid water in 2018 and continued turbidity at critical periods in 2019, 2020, and 2021 which obstructed light penetration.

Similar to previous years, the macroinvertebrate community at the tidal stations was dominated by Annelids (including Oligochaetes and Leeches) across sites, with Oligochaetes contributing most to this group. Outside of the Annelids, Crustaceans (dominated by gammarid amphipods) were the most abundant group at AR4, while both AR2 and AR3 were dominated by Insect larvae from the Chironomidae family (midges). Each site had their own unique taxa. AR4 had the highest number of unique taxa, with six (three species of gastropods, including the invasive Japanese mystery snails - *Cipangopaludina japonica* and insect larvae from the families Heptageniidae, Aeshnidae, and Leptoceridae). Comparing percent contributions of all non-Annelida taxa across all of the sites, months were dominated by the Crustaceans (July and August), Turbellarians (September) or Insecta (May and June). Ordination analyses of the communities indicated a clear separation between communities by sampling station. This could be due to the type of habitat found at each site; while the habitat at AR2 is mostly leaves and organic debris, the habitat at both AR3 and AR4 is composed of the shells of dead Asian clams.

In 2016 a benthic macroinvertebrate sampling program was implemented for the flowing tributary streams starting with six stations. In 2018 two more stations were added with sampling continuing annually in November. Seventeen taxa were identified across all sites in 2021. In general, the top four most abundant taxa observed across all sites stayed the same as in previous years. In 2021, Turkeycock had the highest abundance of all macroinvertebrates and the four dominant taxa, mostly composed of the Insecta family Philopotamidae. In contrast to previous years in which Hydropsychidae larvae (caddisflies) were the dominant group at the majority of the sites, Philopotamidae were dominant across sites in 2021. Taxa richness across all sites ranged from 5 to 13 taxa, with lowest richness at Backlick Run and highest richness at Timber Branch. Using 10 measures of biological health, we calculated a summary statistic of relative overall health of these streams. Using the criteria for each metric laid out above, two streams were categorized as “good”, three were categorized as “fair”, and three were categorized as “poor. These results are similar to those obtained in recent years. Looking across all sites and years, the taxa that dominates are members of the Insecta family Hydropsychidae.

being the most dominant group 39% of the time across all years and sites. Members within this family are netspinning caddisflies, which live in debris and under stones and spin concave silken nets that face upstream to capture floating or swimming prey. The next most dominant group across all sites and years are members of the Insecta family Chironomidae (28% across all years and sites), known as midges.

Anadromous fish sampling continued in Cameron Run in 2021. During the sampling period, we caught 36 Alewife on a single sampling date, April 8th 2021. However, this abundance of Alewife was similar to our overall Alewife abundance in previous sampling years. Although we did not intercept any adult Blueback Herring this year, we did collect larval Blueback Herring and Alewife indicating that this creek was used for spawning by both species. The finding of river herring adults and larvae in an area above the outflow of the Alexandria Renew Enterprises wastewater reclamation facility signifies that the water of Cameron Run is clean enough to use as spawning habitat for these species of concern.

E. coli studies indicate that virtually the entire area sampled, including the mainstem of the Potomac River (AR-4), is impaired for the bacteriological water quality criterion (*E. coli*) content under Section 9VAC25-260-170 of the Virginia Water Quality Standards that apply to primary contact recreational use surface waters. Even though over the period 2014 – 2017, both the percent exceedances and average counts suggested worsening of the water conditions, these trends are not observed for the period 2018 - 2021. One shore station showed exceedance of 235 CFUs per 100 mL on all sampling dates: AR-13 on Hooffs Run near a CSO outfall. All other stations on shore showed exceedance of 235 CFUs per 100 mL on at least 5 sampling dates out of 10. Six shore stations showed exceedance in at least 8 sampling dates: AR-13, AR-24, AR-25, AR-30, AR-33, AR-34, and AR-35. As usual, off-shore stations showed less exceedances: 4 or less over all sampling dates. Sampling additional sites in Hooffs Run/Cameron Run as was done in 2020 and 2021 indicate that Hooffs Run is a significant contributor of the Hunting Creek contamination by *E. coli*. Similarly, sampling additional sites on the Potomac River by the Royal St. CSO indicate a contribution of this CSO to *E. coli* contamination of the receiving water. Unlike what was observed in several prior years, in 2021 we did not detect significant correlation between the *E. coli* numbers and the Cameron Run flow

We recommend that:

1. The basic ecosystem monitoring should continue. A range of climatic conditions is needed to effectively establish baseline conditions in Hunting Creek. Interannual, seasonal and spatial patterns are starting to appear, but need validation with future years's data. With record rainfall and runoff, 2018 provided a glimpse of the vulnerability of the system to flushing and sediment related effects which eliminated SAV from Hunting Creek. Continued monitoring will allow us to assess the resiliency of the ecosystem; i.e., how quickly will it recovery from a very wet year. With the continued absence of SAV from Hunting Creek, the system has remained in a degraded state.
2. Water quality mapping should be continued. This provides much needed spatial resolution of water quality patterns as well as allowing mapping of SAV distributions.

3. Fyke nets have proven to be a useful new gear to enhance fish collections and should be continued.
4. Anadromous fish sampling is an important part of this monitoring program and has gained interest now that the stock of river herring has collapsed generally, and a moratorium on these taxa has been established in 2012. The discovery and continue presence of river herring spawning in Cameron Run increases the importance of continuing studies of anadromous fish in the study area.
5. We recommend continuing the more intensive *E. coli* sampling plan which seems to be giving better insight into the dynamics of *E. coli* in the study area.
6. We recommend that continuing macroinvertebrate studies the tributaries of Hunting Creek to further ascertain overall aquatic biota health and that tidal benthos sampling should continue and the data should be more thoroughly examined.

List of Abbreviations

BOD	Biochemical oxygen demand
cfs	cubic feet per second
DO	Dissolved oxygen
ha	hectare
l	liter
LOWESS	locally weighted sum of squares trend line
m	meter
mg	milligram
MGD	Million gallons per day
NS	not statistically significant
NTU	Nephelometric turbidity units
SAV	Submersed aquatic vegetation
SRP	Soluble reactive phosphorus
TP	Total phosphorus
TSS	Total suspended solids
um	micrometer
VSS	Volatile suspended solids
#	number

The Aquatic Monitoring Program for the Hunting Creek Area of the Tidal Freshwater Potomac River 2021

FINAL REPORT
February 2, 2022

by

R. Christian Jones
Professor, Department of Environmental Science and Policy
Director, Potomac Environmental Research and Education Center
George Mason University
Project Director

T. Reid Nelson
Assistant Professor, Department of Environmental Science and Policy
George Mason University
Co-Principal Investigator

Amy Fowler
Assistant Professor, Department of Environmental Science and Policy
George Mason University
Co-Principal Investigator

to

Alexandria Renew Enterprises
Alexandria, VA

ACKNOWLEDGEMENTS

The authors wish to thank the numerous individuals and organizations whose cooperation, hard work, and encouragement have made this project successful. We wish to thank the Alexandria Renew Enterprises especially CEO Karen Pallansch for her vision in initiating the study and to Blake Hamilton, Aster Tekle, and Ashley Tatge of Alex Renew for their advice and assistance during the study.

Without a dedicated group of field and laboratory workers this project would not have been possible. Thanks go to Laura Birsa for managing water quality/plankton/benthos field trips and to field/lab workers Chelsea Gray, Tabitha King, Alex Mott, David Tolentino, Sam Mohney, Ben Stablow, Alexis Berger, and Liam Palmer.. Benthic samples were analyzed with the help of Dasha Maslyukova; Liam Palmer; Katheryn Hout; Cathryn Mcvicker; Shel Johnson; Helene Pinto; Kelly Grantz . *E. coli* samples were collected and processed with the assistance of Aaron Newborn, Fanella Zamcho, Ayesah Karamat, and Alison Gomeiz. Dr. Saiful Islam conducted all phytoplankton counts. Claire Buchanan served as a voluntary consultant on plankton identification.

This work would not have been possible without Dr. Kim de Mutsert ensuring that a field crew and resources were in place to continue working during the Co-PI transition. We thank her for her dedication to this project from its inception and during this transitory period. We also thank Rachel Kelmartin for taking a large role in the field collection and laboratory processing of these fishes, the work would not have been completed without her. Finally, we thank Daya Hall-Stratton Breanna Hart, Sammie Alexander, and Beverly Bachman for their assistance throughout the project.

INTRODUCTION

This section reports the results of the ninth year of an aquatic monitoring program conducted for Alexandria Renew Enterprises by the Potomac Environmental Research and Education Center (PEREC) in the College of Science at George Mason University. This year we resumed the full year of data collection after a partial shutdown in 2020 due to COVID restrictions.

This work was in response to a request from Karen Pallansch, Chief Executive Officer of Alexandria Renew Enterprises (Alex Renew), operator of the wastewater reclamation and reuse facility (WRRF) which serves about 350,000 people in the City of Alexandria and the County of Fairfax in northern Virginia. The study is patterned on the long-running Gunston Cove Study which PEREC has been conducting in partnership with the Fairfax County Department of Public Works and Environmental Services since 1984. The goal of these projects is to provide baseline data and on-going trend analysis of the ecosystems receiving reclaimed water from wastewater treatment facilities with the objective of adaptive management of these valuable freshwater resources. This will facilitate the formulation of well-grounded management strategies for maintenance and improvement of water quality and biotic resources in the tidal Potomac. A secondary but important educational goal is to provide training for Mason graduate and undergraduate students in water quality and biological monitoring and assessment.

Setting of Hunting Creek

Hunting Creek is an embayment of the tidal Potomac River located just downstream of the City of Alexandria and the Woodrow Wilson Bridge. Waters are shallow with the entire embayment having a depth of 2 m or less at mean tide. According to the "Environmental Atlas of the Potomac Estuary" (Lippson et al. 1981), the mean depth of Hunting Creek is 1.0 m, the surface area is 2.26 km^2, and the volume of 2.1 x 10^6 m^3.

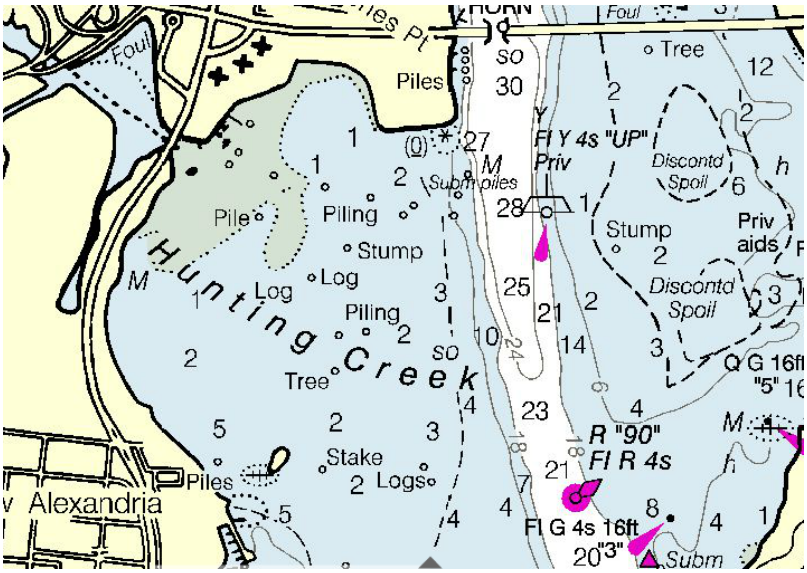

On the left is the Hunting Creek embayment. The Woodrow Wilson Bridge spans the tidal Potomac River at the top of the map. The Potomac River main channel is the whitish area running from north to south through the middle of the map. Soundings (numbers on the map) are in feet at mean low water. For the purposes of this report "Hunting Creek" will extend to the head of tide, roughly to Telegraph Rd. as the is VA DEQ's definition.

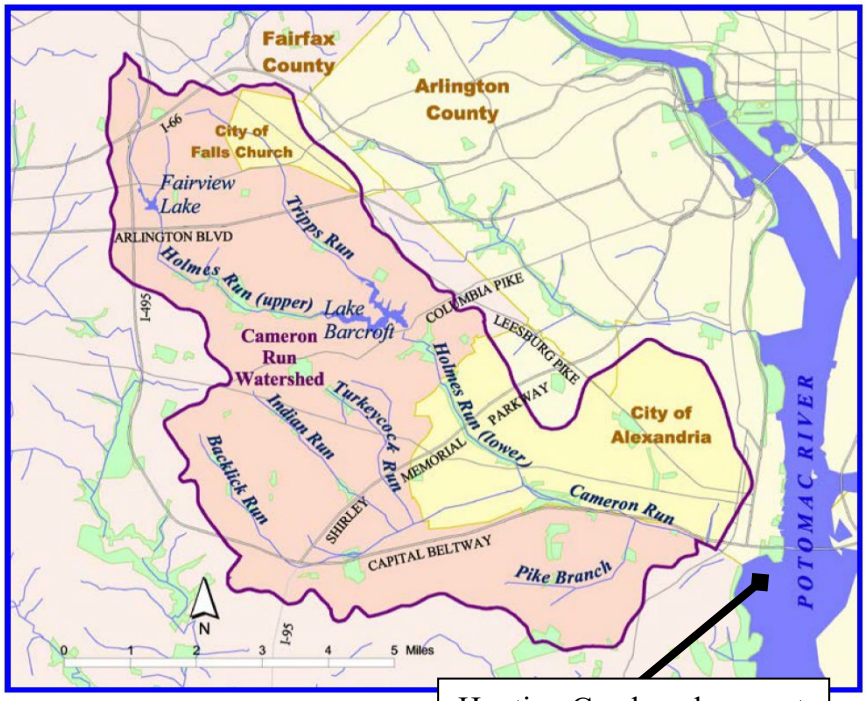

On the left is a map of the Hunting Creek watershed. Cameron Run is the freshwater stream which drains the vast majority of the watershed of Hunting Creek. The watershed is predominantly suburban in nature with areas of higher density commercial and residential development. The watershed has an area of 44 square miles and drains most of the Cities of Alexandria and Falls Church and much of east central Fairfax County. A major aquatic feature of the watershed is Lake Barcroft. The suburban land uses in the watershed are a source of nonpoint pollution to Hunting Creek.

Hunting Creek embayment

The Alex Renew WRRF serves an area similar in extent to the Cameron Run watershed with the addition of some areas along the Potomac shoreline from Four Mile Run to Dyke Marsh. The effluent of the Alexandria Renew Enterprises plant enters the upper tidal reach of Hunting Creek under the Rt 1/I-95 interchange.

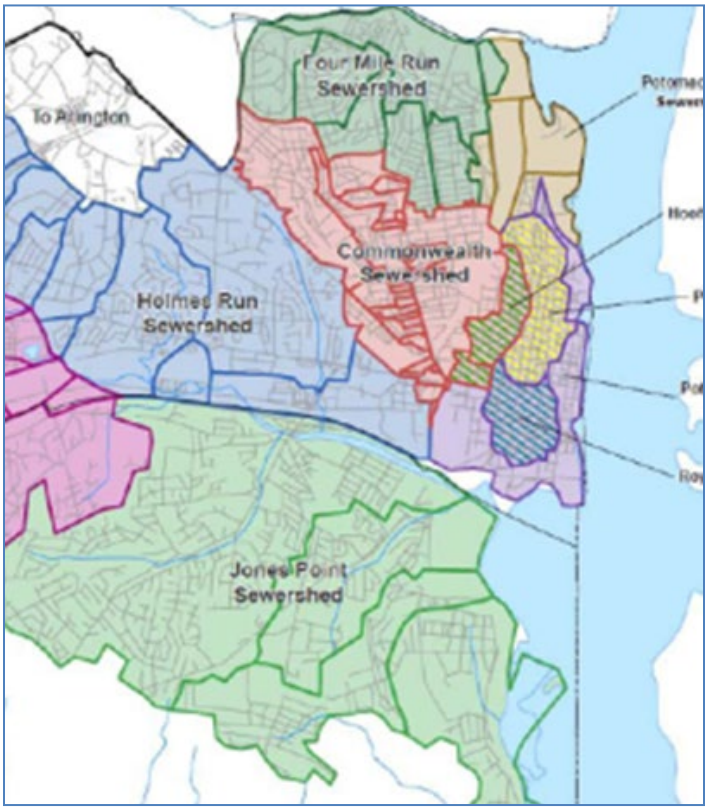

The map at the left shows the sewersheds which contribute to the AlexRenew WRRF. Of particular note are the shaded areas within the City of Alexandria. These sewersheds (Hooffs Run, Pendleton, and Royal St.) all contain combined sewers meaning that domestic wastewater is co-mingled with street runoff. Under most conditions, all of this water is directed to the AlexRenew WRRF for treatment. But in extreme runoff conditions (like torrential rains), some may be diverted directly into the tidal Potomac via a Combined Sewer outfalls (CSOs).

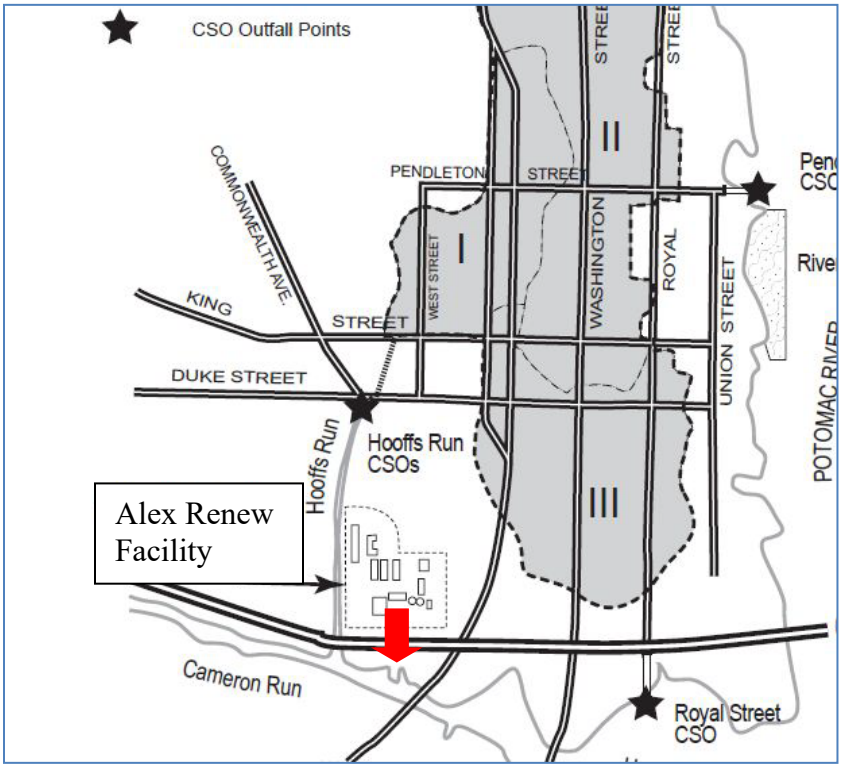

The map at the left is an enlargement of the area where the Alex Renew WRRF is found and where the discharge sites of the CSO's are located. Note the close proximity of two of the CSO's to the Alex Renew WRRF discharge (shown as red arrow).

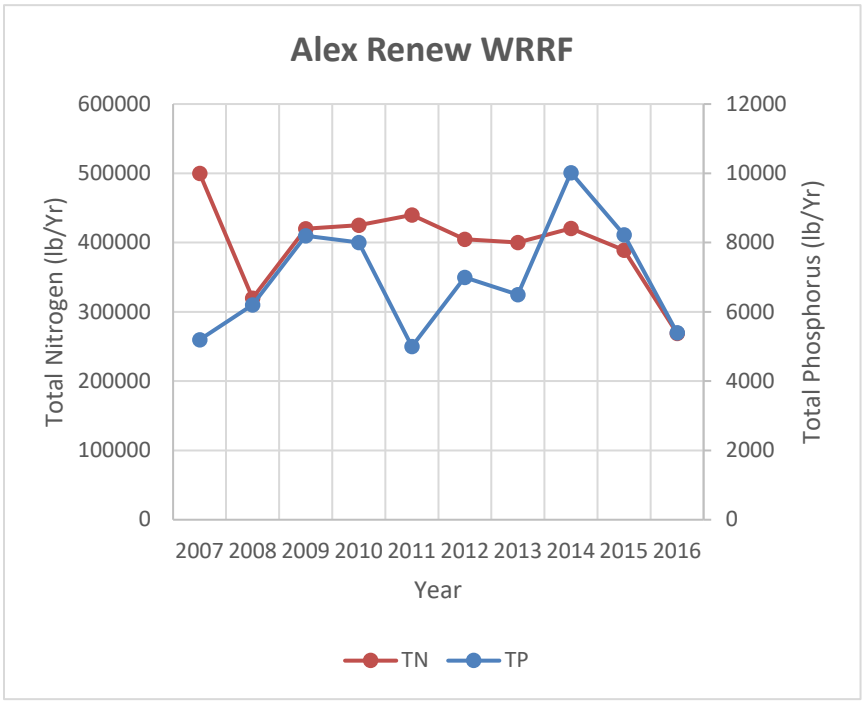

The graph at the left shows the loading of nitrogen and phosphorus from the Alexandria Renew WRRF for seven recent years. Loadings of both nutrient elements were among the lowest in the last decade in 2016: 269,000 lb/yr for nitrogen and 5,400 lb/yr for phosphorus.

Ecology of the Freshwater Tidal Potomac

The tidal Potomac River is an integral part of the Chesapeake Bay tidal system and at its mouth the Potomac is contiguous to the bay proper. The tidal Potomac is often called a subestuary of the Chesapeake Bay and as such it is the largest subestuary of the bay in terms of size and amount of freshwater input. The mixing of freshwater with saltwater is the hallmark of an estuary. While the water elevation in an estuary is "sea level", the water contained in an estuary is not pure sea water such as found in the open ocean. Pure ocean sea water has a salt concentration of about 35 parts per thousand by weight (ppt). Water in Chesapeake Bay ranges from about 30 ppt near its mouth to 0 ppt in the upper reaches where there is substantial freshwater inflow such as in the upper tidal Potomac River. Salinity at a given location is determined by the balance between freshwater input and salt water mixing in from the ocean. It generally varies with season being lower in spring when freshwater inflows are greater and higher in summer when there is less freshwater inflow. In the Hunting Creek study area, the salinity is essentially 0 yearround.

Figure 2. The tidal Potomac River and Estuary.

(map courtesy USGS)

The tidal Potomac is generally divided into three salinity zones as indicated by the map to the left:
-Estuarine or Mesohaline zone (6-14 ppt)
-Transition or Oligohaline zone (0.5-6 ppt)
-Tidal River or Tidal Fresh zone (<0.5 ppt)
Hunting Creek is in the upper part of the Tidal River/Tidal Fresh zone and as such it never experiences detectable salinity

Within the tidal freshwater zone, the flora and fauna are generally characterized by the same species that would occur in a freshwater lake in this area and the food web is similar. Primary producers are freshwater species of submersed aquatic vegetation (SAV) such as native taxa *Vallisneria americana* (water celery), *Potomogeton* spp, (pondweeds), and *Ceratophyllum* (coontail) as well as introduced species such as *Hydrilla verticallata* (hydrilla) and *Myriophyllum spicatum* (water milfoil). Historical accounts indicate that most of the shallow areas of the tidal freshwater Potomac were colonized by SAV when observations were made around 1900 (Carter et al. 1985).

The other group of important primary producers are phytoplankton, a mixed assemblage

of algae and cyanobacteria which may turn over rapidly on a seasonal basis. The dominant groups of phytoplankton in the tidal freshwater Potomac are diatoms (considered a good food source for aquatic consumers) and cyanobacteria (considered a less desirable food source for aquatic consumers). For the latter part of the 20th century, the high nutrient loadings into the river favored cyanobacteria over both diatoms and SAV resulting in large production of undesirable food for consumers. In the last decade or so, as nutrient reductions have become manifest, cyanobacteria have decreased and diatoms and SAV have increased. Recently, since 2018, SAV has declined to very low levels in the Hunting Creek embayment, due apparently to high river and tributary flows in 2018 which resulted in flushing of the SAV from the embayment.

The biomass contained in the cells of phytoplankton nourishes the growth of zooplankton and benthic macroinvertebrates which provide an essential food supply for the juvenile and smaller fish. These in turn provide food for the larger fish like striped bass and largemouth bass. The species of zooplankton and benthos found in the tidal fresh zone are similar to those found in lakes in the area, but the fish fauna is augmented by species that migrate in and out from the open interface with the estuary.

Resident fish species include typical lake species such as sunfish (*Lepomis* spp.), bass (*Micropterus* spp.), and crappie (*Pomoxis* spp.) as well as estuarine species such as white perch (*Morone americana*) and killifish (*Fundulus* spp.). Species which spend part of their year in the area include striped bass (*Morone saxitilis*) and river herrings and shad (*Alosa* spp.). Non-native fish species have also become established in the tidal freshwater Potomac such as northern snakehead (*Channa argus*) and blue catfish (*Ictalurus furcatus*).

Larval fishes are transitional stages in the development of juvenile fishes. They range in development from newly hatched, embryonic fish to juvenile fish with morphological features similar to those of an adult. Many fishes such as clupeids (herring family), white perch, striped bass, and yellow perch disperse their eggs and sperm into the open water. The larvae of these species are carried with the current and termed “ichthyoplankton”. Other fish species such as sunfish and bass lay their eggs in “nests” on the bottom and their larvae are rare in the plankton.

After hatching from the egg, the larva draws nutrition from a yolk sack for a few days. When the yolk sack diminishes to nothing, the fish begins a life of feeding on other organisms. This post yolk sack larva feeds on small planktonic organisms (mostly small zooplankton) for a period of several days. It continues to be a fragile, almost transparent larva and suffers high mortality to predatory zooplankton and juvenile and adult fishes of many species, including its own. When it has fed enough, it changes into an opaque juvenile, with greatly enhanced swimming ability. It can no longer be caught with a slow-moving plankton net, but is soon susceptible to capture with the seine or trawl net.

METHODS

A. Profiles and Plankton: Sampling Day

Tidal Stations

Sampling was conducted on a semimonthly basis at stations representing both the Hunting Creek embayment and the Potomac mainstem (Figure 1a). Two stations (AR 2 & 3) were located in the Hunting Creek embayment proper. A fourth station (AR 4) was located in the river channel about 100 m upstream from Buoy 90. Dates for sampling as well as weather conditions on sampling dates and immediately preceding days are shown in Table 1. Note that certain dates had significant rainfall in days preceding sampling which may have impacted conditions in Hunting Creek due to it shallow nature and relatively large watershed contributing runoff.

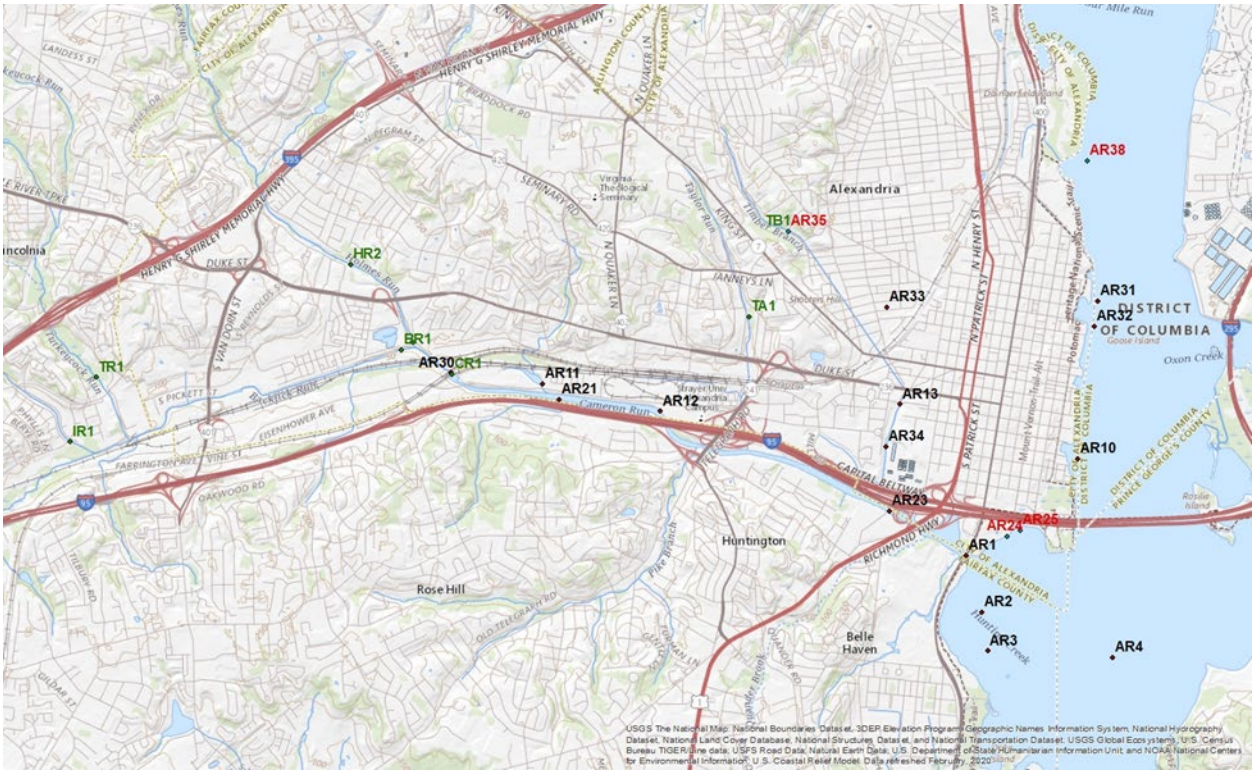

Table 1. Water quality monitoring stations.

Station ID	Access Type	Sample Type	Other Sampling	Location Description	Latitude	Longitude
AR1	Shore	Surface Grab	None	Hunting Cr at the GW Parkway Bridge	38.78992	-77.05126
AR2	Boat	Surface Bottom	Plankton Benthos	Northern portion of Hunting Cr.	38.78509	-77.04951
AR3	Boat	Surface Bottom	Benthos	Southern portion of Hunting Cr.	38.78181	-77.04890
AR4	Boat	Surface Bottom	Plankton Benthos	Potomac River Mainstem off Hunting Cr.	38.78124	-77.03529
AR10	Boat	Surface Grab	None	Potomac River North of Wilson Bridge	38.79816	-77.03907
AR12	Shore	Surface Grab	None	Last Riffle of Cameron Run near Beltway crossing	38.80218	-77.08467
AR13	Shore	Surface Grab	None	Hoff's Run upstream of CSO 003 and 004 outfalls	38.80278	-77.05848
AR21	Shore	Surface Grab	None	South side of Cameron Run downstream from Lake Cook drain	38.80318	-77.09565
AR23	Shore	Surface Grab	None	South side of upper Hunting Creek across from AlexRenew outfall	38.79372	-77.05966
AR24	Shore	Surface Grab	None	Hunting Creek north shore W. of Royal Street CSO outfall	38.79156	-77.04680
AR25	Shore	Surface Grab	None	Hunting Creek north shore E. of Royal Street CSO outfall	38.79205	-77.04538
AR30	Shore	Surface Grab	None	Cameron Run upstream near metro rail bridge	38.80545	-77.10745
AR32	Boat	Surface Grab	None	Potomac River Mainstem just S of Orinoco Bay CSO outfall	38.80940	-77.03727
AR33	Shore	Surface Grab	None	Hooffs Run at Linden St.	38.81103	-77.05993
AR34	Shore	Surface Grab	None	Hooffs Run at Alex Renew	38.79918	-77.05997
AR35	Shore	Surface Grab	None	Timber Branch at Ivy Hill Cemetery	38.8175	-77.07065
AR38	Boat	Surface Grab	None	Potomac River Mainstem near Daingerfield Island	38.82348	-77.03802

For the purpose of graphical analysis the stations were parsed into groups as follow:
Tidal Main Stations: AR1, AR2, AR3, AR4
Tidal CSO Impact Stations: AR10 (control), AR25 (Royal St CSO), AF24 (Royal St CSO), AR32 (Orinoco Bay CSO), AR38 (control)
Cameron Run Axis Tributaries: AR30, AR21, AR12, AR23
Hooffs Run Axis Tributaries: AR35, AR33, AR13, AR34

Table 2
Hunting Creek Study: Sampling Dates and Weather Data for 2021

	Type of Sampling						Avg Daily Temp (°C)		Precipitation (cm)	
Date	WP	B	D	T	S	F*	1-Day	3-Day	1-Day	3-Day
April 14	X						13.9	14.3	0.76	0.98
April 16				X	X		11.7	13.1	0	0.77
May 7				X	X		13.9	16.3	0.13	0.28
May 12	X	X					15.6	16.1	0	T
May 20				X			25.6	22.4	0	0
May 26	X						27.2	23.0	2.29	3.15
June 3				X	X	X	23.9	22.2	0.25	0.25
June 9	X	X					28.3	28.1	T	0.04
June 17				X	X	X	21.1	22.4	0	T
June 23	X						20.0	23.0	0	0.99
July 1				X	X		27.2	28.9	3.23	3.30
July 8	X						26.1	28.0	0.61	0.61
July 13			X							
July 15				X	X	X	27.8	28.7	0	T
July 27	X	X					29.4	29.1	0	0.94
August 5				X	X	X	25.0	24.4	0	0
August 9			X				28.3	25.9	0	0.61
August 10	X	X					28.9	28.0	1.65	1.65
August 19				X	X		28.9	28.0	0.05	2,46
August 24	X						29.4	28.3	0	0.06
Sept 9	X	X		X	X	X	23.3	24.4	0.64	0.65

Type of Sampling: WP: Water quality (samples to AlexRenew Lab), profiles and plankton, B: benthos, D: dataflow (water quality mapping), T: fish collected by trawling, S: fish collected by seining. F: fish collected by fyke net. T under Precipitation equals “trace”. X indicates full station suite on that date. *fyke nets were not set in 2020 due to reduced crew and lack of SAV.

Sampling was initiated about 9:00 am. Four types of measurements or samples were obtained depending on the station. At stations AR2, AR3, and AR4 (Tidal Main Stations), (1) depth profiles of temperature, conductivity, dissolved oxygen, pH, and irradiance

(photosynthetically active radiation, PAR) measured directly in the field; (2) water samples for GMU lab determination of chlorophyll *a* and phytoplankton species composition and abundance (phytoplankton at AR2 and AR4 only); (3) water samples for determination of N and P forms, BOD, COD, alkalinity, hardness, suspended solids, chloride, and pH by the Alexandria Renew Enterprises lab; (4) net sampling of zooplankton and ichthyoplankton (AR2 and AR4 only).

Profiles of temperature, conductivity, and dissolved oxygen were conducted at each Tidal Main station using a YSI 6600 datasonde with temperature, conductivity, dissolved oxygen and pH probes. Measurements were taken at 0.3 m increments from surface to bottom at the embayment stations. In the river measurements were made with the sonde at depths of 0.3 m and 2.0 m increments to the bottom. At the other three groups of stations, one sonde measurement was collected at the time of water collection. Meters were checked for calibration before and after sampling. At Tidal Main Stations (except AR1) profiles of irradiance (photosynthetically active radiation, PAR) were collected with a LI-COR underwater flat scalar PAR probe. PAR measurements were taken at 10 cm intervals to a depth of 1.0 m. Simultaneous measurements were made with a terrestrial probe in air during each profile to correct for changes in ambient light if needed. Secchi depth was also determined. The readings of at least two crew members were averaged due to variability in eye sensitivity among individuals. If the Secchi disk was still visible at the bottom or if its path was block by SAV while still visible, a proper reading could not be obtained.

At Tidal Main Stations (except AR2), a 1-L sample was constructed from equal volumes of water collected at each of three depths (0.3 m below the surface, middepth, and 0.3 m off of the bottom) using a submersible bilge pump. At AR2 only two depths were used. A 100-mL aliquot of the 1-L sample was preserved immediately with acid Lugol's iodine for later identification and enumeration of phytoplankton at stations AR2 and AR4. The remainder of the samples were placed in an insulated cooler with ice. A separate 1-liter surface sample was collected from 0.3 m using the submersible bilge pump and placed in the insulated cooler with ice for lab analysis of surface chlorophyll *a*.

At selected embayment and river mainstream sampling stations (AR2, AR3, and AR4), 2-liter samples were collected at each station from just below the surface (0.3 m) and near the bottom (0.3 m off bottom) at each station using the submersible pump. At other tidal and tributary stations, 2-liter samples were collected by hand from just below the surface. The 2-L samples were promptly delivered to either the Alexandria Renew Laboratory or the Prince William Mooney Laboratory for determination of nitrogen, phosphorus, BOD, TSS, VSS, pH, total alkalinity, and chloride. Surface water grab samples were collected in sterile 1-L containers at all stations for *E. coli* determination (see *E. coli* chapter). These were promptly delivered to Dr. Van Aken's lab at Potomac Science Center for analysis.

At stations AR2 and AR4, microzooplankton was collected by pumping 32 liters from each of three depths (0.3 m, middepth, and 0.3 m off the bottom) through a 44 μm mesh sieve. The sieve consisted of a 12-inch long cylinder of 6-inch diameter PVC pipe with a piece of 44 μm nitex net glued to one end. The 44 μm cloth was backed by a larger mesh cloth to protect it. The pumped water was passed through this sieve from each depth and then the collected microzooplankton was backflushed into the sample bottle. The resulting sample was treated with

about 50 mL of club soda and then preserved with formalin containing a small amount of rose bengal to a concentration of 5-10%.

At stations AR2 and AR4, macrozooplankton was collected by towing a 202 µm net (0.3 m opening, 2 m long) for 1 minute at each of three depths (near surface, middepth, and near bottom). Ichthyoplankton (larval fish) was sampled by towing a 333 µm net (0.5 m opening, 2 m long) for 2 minutes at each of the same depths at Stations AR2 and AR4. In the embayment, the boat traveled from AR2 toward AR3 during the tow while in the river the net was towed in a linear fashion along the channel. Macrozooplankton tows were about 300 m and ichthyoplankton tows about 600 m. Actual distance depended on specific wind conditions and tidal current intensity and direction, but an attempt was made to maintain a constant slow forward speed (approximately 3 miles per hour) through the water during the tow. The net was not towed directly in the wake of the engine. A General Oceanics flowmeter, fitted into the mouth of each net, was used to establish the exact towing distance. During towing the three depths were attained by playing out rope equivalent to about 1.5-2 times the desired depth. Samples which had obviously scraped bottom were discarded and the tow was repeated. Flowmeter readings taken before and after towing allowed precise determination of the distance towed and when multiplied by the area of the opening produced the total volume of water filtered.

Macrozooplankton were preserved immediately with rose bengal formalin with club soda pretreatment. Ichthyoplankton was preserved in 70% ethanol. Macrozooplankton was collected on each sampling trip; ichthyoplankton collections ended after July because larval fish were normally not found after this time.

Benthic macroinvertebrate samples were collected monthly at stations AR2, AR3, and AR4. Three samples were collected at each station using a petite ponar grab. The bottom material was first passed through a 5 mm screen to catch leaves, shells, and other large particles which might contribute to habitat for benthic fauna. The material passing through this coarse screen was was then sieved through a 0.5 mm stainless steel sieve and resulting organisms were preserved in rose bengal formalin for lab analysis.

Samples for water quality determination were maintained on ice and delivered to the Alexandria Renew Enterprises (AlexRenew) Laboratory or Prince William Mooney Lab by 2 pm on sampling day and returned to GMU by 3 pm. At GMU 10-15 mL aliquots of both depth-integrated and surface samples were filtered through 0.45 µm membrane filters (Gelman GN-6 and Millipore MF HAWP) at a vacuum of less than 10 lbs/in^2 for chlorophyll a and pheopigment determination. During the final phases of filtration, 0.1 mL of $MgCO_3$ suspension (1 g/100 mL water) was added to the filter to prevent premature acidification. Filters were stored in 20 mL plastic scintillation vials in the lab freezer for later analysis. Seston dry weight (TSS) and seston organic weight (VSS) were measured by filtering 200-400 mL of depth-integrated sample through a pretared glass fiber filter (Whatman 984AH).

Tributary Stations

At tributary stations, 2-liter samples were collected by hand from just below the surface.

This water was promptly delivered to the nearby Alexandria Renew Laboratory or Prince William Mooney Lab for determination of nitrogen, phosphorus, BOD, TSS, VSS, pH, total alkalinity, and chloride. While at the site, water temperature, specific conductance, dissolved oxygen, pH, and turbidity were taken at 0.1 m depth with a YSI ProDDS minisonde. Surface water grab samples were collected at all of these stations for *E. coli* determination (see *E. coli* chapter).

Sampling day activities were normally completed by 5:30 pm.

B. Profiles and Plankton: Follow-up Analyses

Chlorophyll *a* samples were processed using an overnight soaking procedure which has been shown to give comparable results to the traditional homogenization process. (Huntley et al. 1987). The filters had been stored in the freezer in 20 mL plastic scintillation vials. 15 mL of 90% acetone was added to each vial and the vials were shaken. They were placed in the refrigerator overnight. The next day they were mixed and assayed fluorometrically.

Chlorophyll *a* concentration in the extracts was determined fluorometrically using a Turner Designs Trilogy fluorometer configured for chlorophyll analysis as specified by the manufacturer. The instrument was calibrated using standards obtained from Turner Designs. Chlorophyll was determined and then after acidification with 2 drops of 10% HCl pheophytin was determined. Chlorophyll filters were stored in the freezer pending analysis in October.

Phytoplankton species composition and abundance was determined using the inverted microscope-settling chamber technique (Lund et al. 1958). Ten milliters of well-mixed algal sample were added to a settling chamber and allowed to stand for several hours. The chamber was then placed on an inverted microscope and random fields were enumerated. At least two hundred cells were identified to species and enumerated on each slide. Counts were converted to number per mL by dividing number counted by the volume counted. Biovolume of individual cells of each species was determined by measuring dimensions microscopically and applying volume formulae for appropriate solid shapes.

Microzooplankton and macrozooplankton samples were rinsed by sieving a well-mixed subsample of known volume and resuspending it in tap water. This allowed subsample volume to be adjusted to obtain an appropriate number of organisms for counting and for formalin preservative to be purged to avoid fume inhalation during counting. One mL subsamples were placed in a Sedgewick-Rafter counting cell and whole slides were analyzed until at least 200 animals had been identified and enumerated. A minimum of two slides was examined for each sample. References for identification were: Ward and Whipple (1959), Pennak (1978), and Rutner-Kolisko (1974). Zooplankton counts were converted to number per liter (microzooplankton) or per cubic meter (macrozooplankton) with the following formula:

Zooplankton (#/L or #/m^3) = $NV_s/(V_cV_f)$
where N = number of individuals counted
V_s = volume of reconstituted sample, (mL)
V_c = volume of reconstituted sample counted, (mL)

V_f = volume of water sieved, (L or m^3)

Larval fish were picked from the ethanol-preserved ichthyoplankton samples with the aid of a stereo dissecting microscope. Identification of ichthyoplankton was made to family and further to genus and species where possible. If the number of animals in the sample exceeded several hundred, then the sample was split with a plankton splitter and the resulting counts were multiplied by the subsampling factor. The works Hogue et al. (1976), Jones et al. (1978), Lippson and Moran (1974), and Mansueti and Hardy (1967) were used for identification. The number of ichthyoplankton in each sample was expressed as number per 10 m^3 using the following formula:

Ichthyoplankton (#/10m^3) = 10N/V
where N = number ichthyoplankton in the sample
V = volume of water filtered, (m^3)

C. Adult and Juvenile Fish

Fishes were sampled by trawling at stations AR3 and AR4, and seining at stations AR5 and AR6 (Figure 1b). For trawling, a try-net bottom trawl with a 15-foot horizontal opening, a ¾ inch square body mesh and a ¼ inch square cod end mesh was used. The otter boards were 12 inches by 24 inches. Towing speed was 2-3 miles per hour and tow length was 5 minutes. The trawls were towed upriver parallel to the channel at AR4, and following the curve away from the channel at AR3. The direction of tow should not be crucial. Dates of sampling and weather conditions are found in Table 1.

Seining was performed with a bag seine that was 50 feet long, 3 feet high, and made of knotted nylon with a ¼ inch square mesh. The bag is located in the middle of the net and measures 3 ft^3. The seining procedure was standardized as much as possible. The net was stretched out perpendicular to the shore with the shore end right at the water line. The net was then pulled parallel to the shore for a distance of 100 feet by a worker at each end moving at a slow walk. Actual distance was recorded if in any circumstance it was lower than 100 feet. At the end of the prescribed distance, the offshore end of the net was swung in an arc to the shore and the net pulled up on the beach to trap the fish. Dates for seine sampling were the same as those for trawl sampling (Table 1).

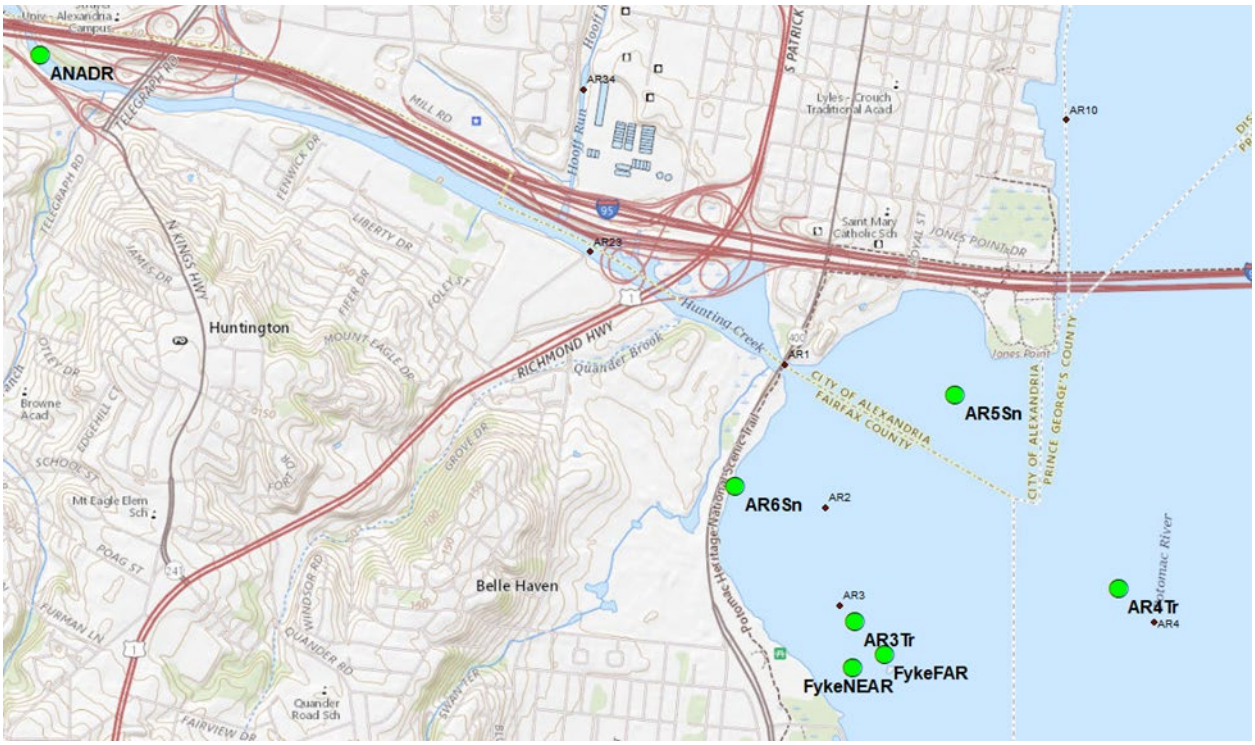

Figure 1b. Hunting Creek area of the Tidal Potomac River showing fish monitoring stations – Large Green circles. Stations with Tr in name are trawl stations; those with Sn in name are seine stations and those with Fyke in name are fyke stations. ANADR is the anadromous station. Water quality stations shown as small symbols and lettering for comparison.

Due to extensive submerged aquatic vegetation (SAV) cover in Hunting Creek, we adjusted our sampling regime in years of high SAV growth to include fyke netting. Two fyke nets were set in the area close to AR3 (Figure 1). The fyke net sampling stations are called 'fyke near' and 'fyke far' in reference to their distance from shore. These fyke nets were set within areas of former SAV to sample the fish community that uses that area as habitat. Fyke nets were set for 4 hours to passively collect fish. The fyke nets have 5 hoops, a 1/4 inch mesh size, 16 feet wings and a 32 feet lead. Fish enter the net by actively swimming and/or due to tidal motion of the water. The lead increases catch by capturing the fish swimming parallel to the wings. Fyke nets were not set in 2020 due to crew limitations under COVID. Trawling in this location (AR3) continued throughout the year in 2021 (Table 1).

After the catch from each of these three gear types was hauled in, the fishes were measured for standard length and total length to the nearest mm. Standard length is the distance from the front tip of the snout to the end of the vertebral column and base of the caudal fin. This is evident in a crease perpendicular to the axis of the body when the caudal fin is pulled to the side. Total length is the distance from the tip of the snout to the tip of the longer lobe of the caudal fin, measured by straightening the longer lobe toward the midline.

If the identification of the fish was not certain in the field, a specimen was preserved in 70% ethanol and identified later in the lab. All fishes retained for laboratory analysis or

identification were first euthanized by submerging them in an ice sludge conforming to the IACUC protocol. Identification was based on characteristics in dichotomous keys found in several books and articles, including Jenkins and Burkhead (1983), Hildebrand and Schroeder (1928), Loos et al (1972), Dahlberg (1975), Scott and Crossman (1973), Bigelow and Schroeder (1953), Eddy and Underhill (1978), Page and Burr (1998), and Douglass (1999).

The number of fykes, seines, and trawls completed each sampling day is shown below:

Date	Fyke	Seine	Trawl
2021-04-16	0	2	2
2021-05-07	0	2	2
2021-05-20	0	0	4
2021-06-03	2	2	2
2021-06-17	2	2	2
2021-07-01	0	2	2
2021-07-15	2	2	2
2021-08-05	2	2	2
2021-08-19	0	2	2
2021-09-09	2	2	2

D. Submersed Aquatic Vegetation

Data on coverage and composition of submersed aquatic vegetation (SAV) are generally obtained from the SAV webpage of the Virginia Institute of Marine Science (http://www.vims.edu/bio/sav). Information on this web site is obtained from aerial photographs near the time of peak SAV abundance as well as ground surveys which are used to determine species composition. We also recorded SAV relative abundance on a 0-3 scale at 4 minute intervals using visual observations and rake tow during data mapping cruises.

E. Benthic Macroinvertebrates

Benthic macroinvertebrates were sampled monthly using a petite ponar sampler at embayment stations AR2, AR3, and AR4. Triplicate samples were collected at each station monthly. Field processing of benthic samples was described earlier. In the laboratory benthic samples were rinsed with tap water through a 0.5 mm sieve to remove formalin preservative and resuspended in tap water. All organisms were picked, sorted, identified and enumerated. Debris contained in the ponar samples which was collected in the 5 mm sieve was dried and weighed in the lab.

In 2021 benthic invertebrates were also sampled at selected flowing tributary stations which possessed natural riffle-run areas. At each site one-minute kick samples were collected at one riffle and one run and composited in a single bottle. The sample was preserved with formalin

to a concentration of 5%. In the lab the sample was sieved through a 0.5 mm mesh (same as the kick net) and thoroughly washed with tap water before picking and sorting. Following sorting animals were enumerated by taxon and held in ethanol-glycerin. Sampling sites for tributary macroinvertebrate sampling are shown in Figure 1c.

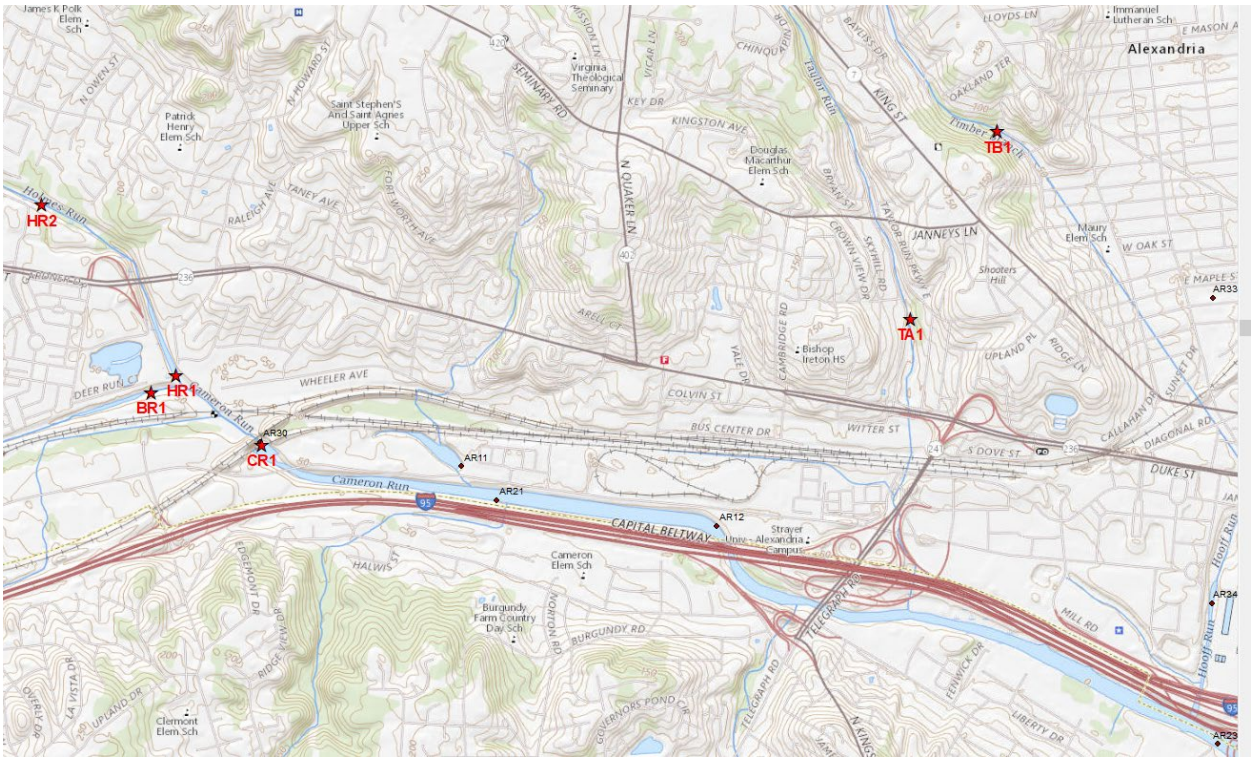

Figure 1c. Benthic sampling stations on flowing tributaries of Cameron Run. CR1: Cameron Run: HR1, HR2: Holmes Run; BR: Backlick Run; IR: Indian Run; TR: Turkeycock Run.

F. Water Quality Mapping (Dataflow)

On two additional dates in 2021 *in situ* water quality mapping was conducted by slowly transiting through much of the Hunting Creek study area as water was pumped through a chamber containing a YSI EXO sonde equipped with temperature, specific conductance, dissolved oxygen, pH, turbidity, and chlorophyll probes. Readings were recorded at 15 second intervals along with simultaneous GPS position readings. Every 4 minutes SAV relative abundance by species was recorded and every 4 minutes water samples were collected for extracted chlorophyll and TSS determination. These surveys allowed a much better understanding of spatial patterns in water quality within the Hunting Creek area which facilitated interpretation of data from the fixed stations. This approach is in wide use in the Chesapeake Bay region by both Virginia and Maryland under the name “dataflow”.

G. Data Analysis

Data for each parameter were entered into spreadsheets (Excel or SigmaPlot) for graphing of temporal and spatial patterns. SYSTAT was used for statistical calculations and to

create illustrations of the water quality mapping cruises. JMP v8.0.1was used for fish graphs. Other data analysis approaches are explained in the text.

RESULTS

A. Climatic and Hydrologic Factors - 2021

In 2021 temperature was above normal in all months (Table 3). There were 38 days with maximum temperature above 32.2ºC (90ºF) in 2021 as in 2020 which is well above the median number over the past decade. Precipitation was closer to normal in 2021 than in the extremely wet year 2018. However, it was again well above normal in 2021, especially in June and August.

Table 3. Meteorological Data for 2021. National Airport. Monthly Summary.

	Air Temp (ºC)		Precipitation (cm)	
MONTH				
March	10.8	(8.1)	9.7	(9.1)
April	14.7	(13.4)	5.6	(7.0)
May	19.1	(18.7)	9.6	(9.7)
June	24.9	(23.6)	14.0	(8.0)
July	27.3	(26.2)	10.8	(9.3)
August	27.3	(25.2)	23.1	(8.7)
September	23.1	(21.4)	10.3	(9.6)

Note: 2021 monthly averages or totals are shown accompanied by long-term monthly averages (1971-2000). Source: Local Climatological Data. National Climatic Data Center, National Oceanic and Atmospheric Administration.

River and tributary stream flow in 2021 were close to average for all months except September in the Potomac mainstem, but in Cameron Run were well above average in June, August, and September (Table 4).

Table 4. Monthly mean discharge at USGS Stations representing freshwater flow into the study area. (+) 2021 month > 2x Long Term Avg. (-) 2021 month < ½ Long Term Avg.

	Potomac River at Little Falls (cfs)		**Cameron Run at Wheeler Ave (cfs)**	
	2021	**Long Term Average**	**2021**	**Long Term Average**
March	21614	23600	64.2	55
April	15746	20400	45.6	42
May	7978	15000	43.6	41
June	6884	9030	73.4 (+)	38
July	3022	4820	53.6	31
August	2748	4550	142.1 (+)	28
September	14873 (+)	5040	86.5 (+)	38

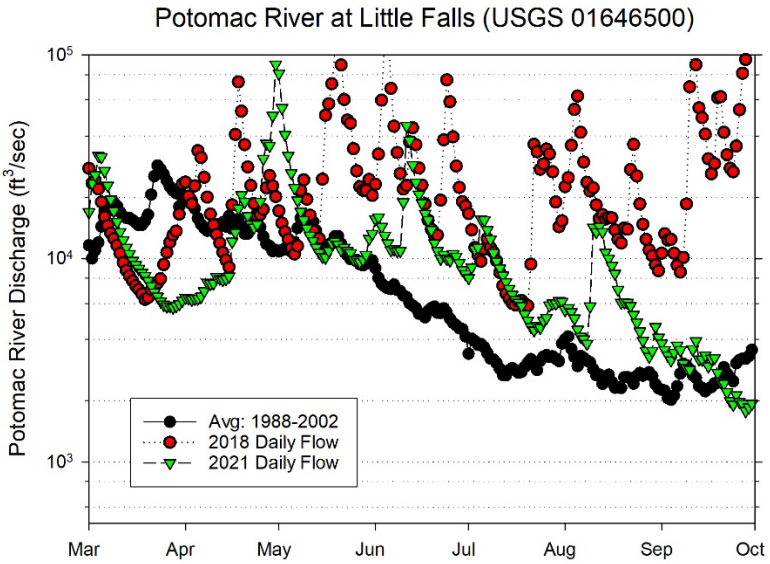

In a tidal freshwater system like the Potomac River, river flow entering from upstream is important in maintaining freshwater conditions and also serves to bring in dissolved and particulate substances from the watershed. High freshwater flows may also flush planktonic organisms downstream and bring in suspended sediments that decrease water clarity. The volume of river flow per unit time is referred to as "river discharge" by hydrologists. Note the general long term seasonal pattern of higher discharges in winter and spring and lower discharges in summer and fall.

Figure 2. Mean Daily Discharge: Potomac River at Little Falls (USGS Data). Month tick is at the beginning of the month.

These same patterns were seen in the graphs of daily river flow when compared to long-term averages (Figure 2). The long-term average shows a steadily decreasing trend from April through September. In 2021 this general seasonal pattern was observed except for the notable surges in June, July, and September which have the potential to strongly impact the ongoing growth of SAV and plankton in the river. Discharge in Cameron Run showed many short-lived pulses during June, August, and September. (Figure 3).

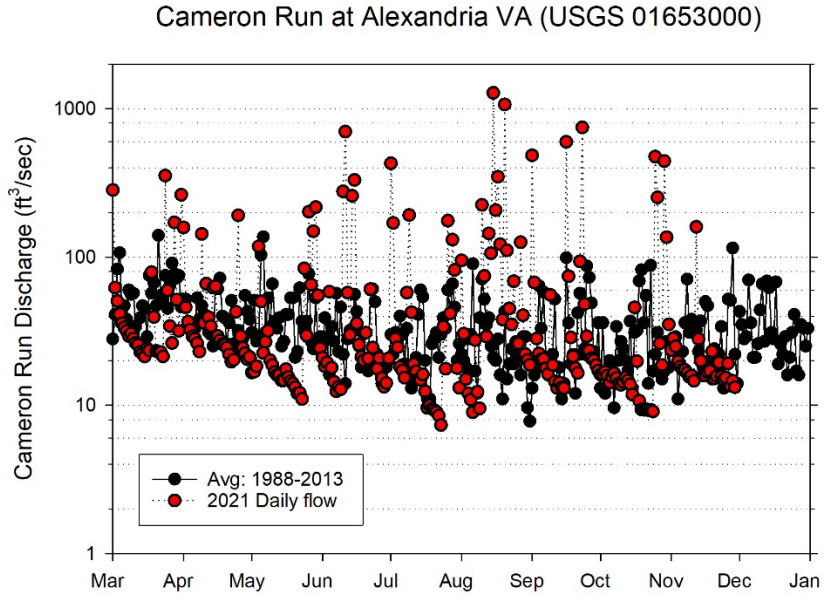

In the Hunting Creek region of the tidal Potomac, freshwater discharge is occurring from both the major Potomac River watershed upstream (measured at Little Falls) and from immediate tributaries, principally Cameron Run which empties directly into Hunting Creek. The gauge on Cameron Run at Wheeler Avenue is located just above the head of tide and covers most area which contributes runoff directly to the Hunting Creek embayment from the watershed. The contributing area to the Wheeler Ave gauge is 33.9 sq mi. (USGS)

.

Figure 3. Mean Daily Discharge: Cameron Run at Alexandria (Wheeler Ave) (USGS Data).

B. Physico-chemical Parameters: Embayment and River Stations – 2021

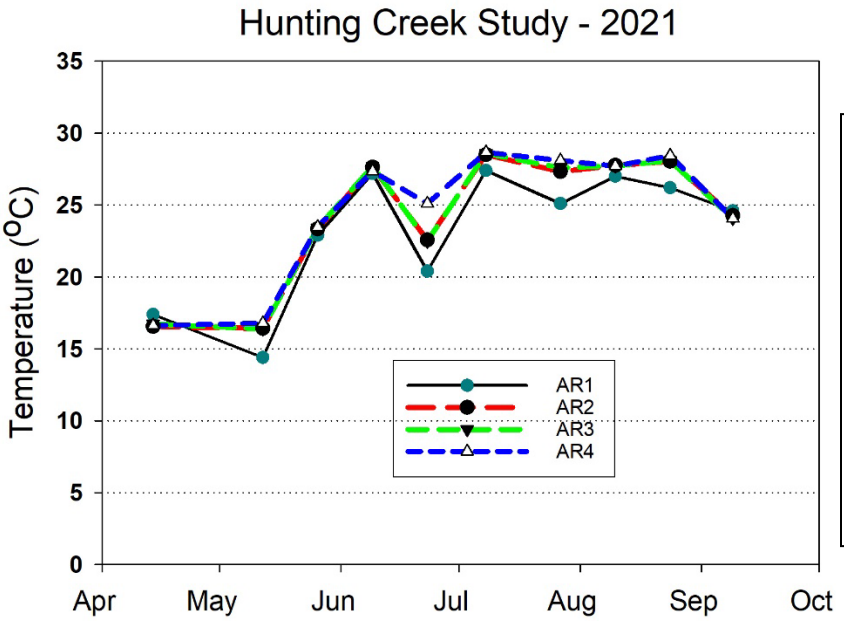

Water temperature is an important factor affecting both water quality and aquatic life. In a well-mixed system like the tidal Potomac, water temperatures are generally fairly uniform with depth. In a shallow mixed system such as the tidal Potomac, water temperature often closely tracks daily changes in air temperature.

Figure 4. Water Temperature (°C). Tidal Main Stations. Month tick is at first day of month.

Water temperature followed the typical seasonal pattern at Tidal Main Stations (Figure 4). Temperatures in mid-July approached 30°C and remained high for August and September. A marked drop was observed in late June. Similar patterns were observed at the Tidal CSO Impact Stations with the exception that AR24 and AR25 were consistently 2-5 degrees cooler (Figure 5).

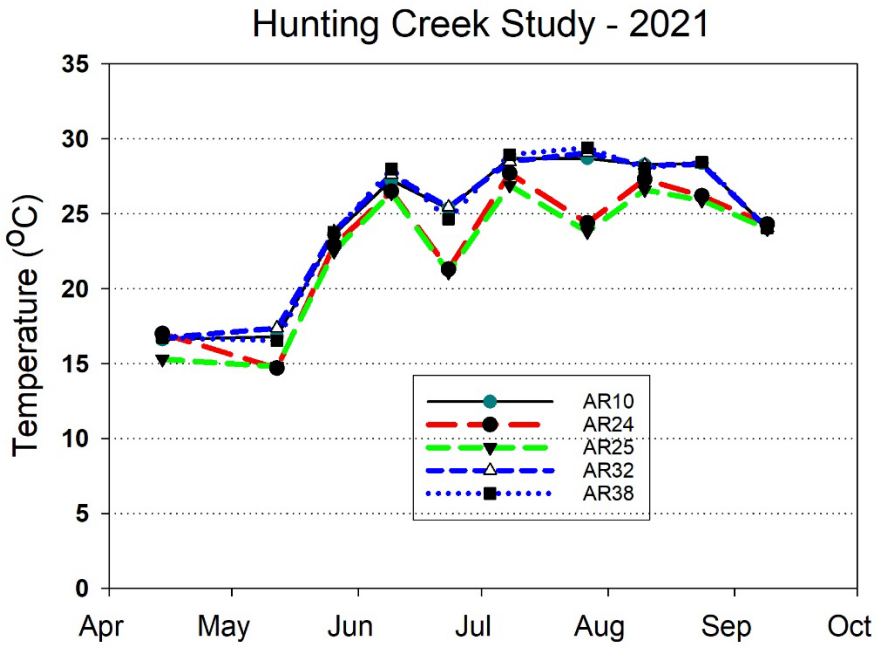

In this section of the report, we have placed the stations into two groups: Tidal Main Stations which were sited to get general conditions in the tidal open water in Hunting Creek and the Potomac mainstem. The second group was Tidal CSO Impact Stations that were situated above and below CSO outfalls to examine their effects on tidal water quality.

Figure 5. Water Temperature (°C). Tidal CSO Impact Stations.

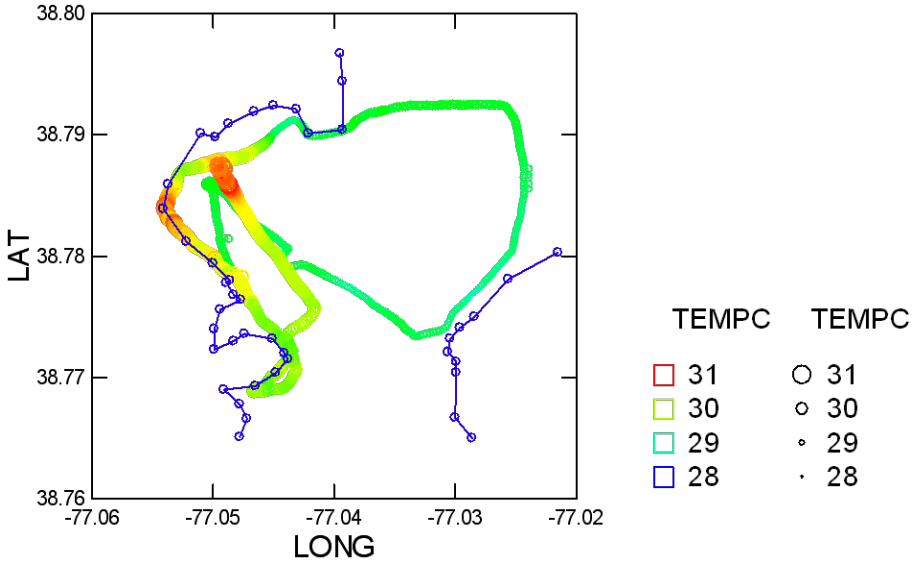

Figure 6a. Water Quality Mapping July 13, 2021. Temperature (°C).

Mapping of water temperature was conducted on July 13 and August 9, 2021 (Figure 6a,b). Water temperature ranged from 28 to 31°C in July and 26.5 to 28.5°C. There was a clear pattern of higher temperatures in the Hunting Creek embayment although some of that might be due to the warming of water as the day progressed.

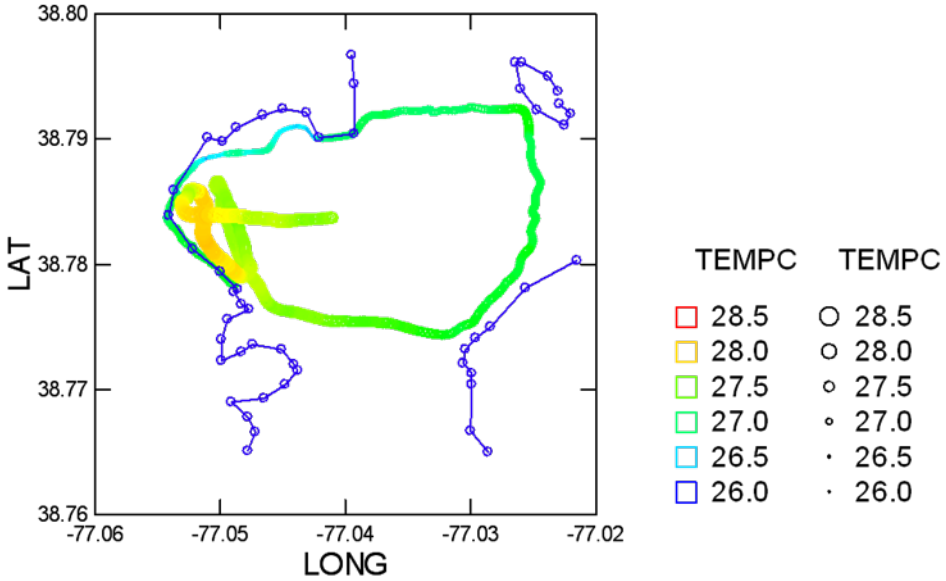

Figure 6b. Water Quality Mapping. August 9, 2021. Temperature (°C).

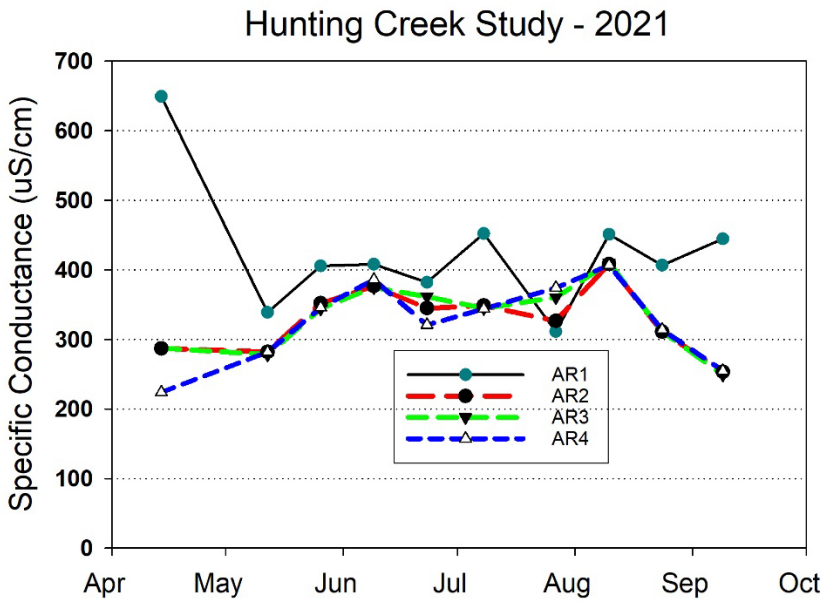

Specific conductance measures the capacity of the water to conduct electricity standardized to 25°C. This is a measure of the concentration of dissolved ions in the water. In freshwater, conductivity is relatively low. Ion concentration generally increases slowly during periods of low freshwater inflow and decreases during periods of high freshwater inflow. Sewage treatment facilities can be a source of elevated conductivity. In winter road salts can be a major source of conductivity in urban streams.

Figure 7. Specific Conductance (µS/cm). Tidal Main Stations. Month tick is at first day of month.

Specific conductance followed a gradual increase at most Tidal Main stations through early August. It was quite high at AR1 in April, but similar to the other sites for the rest of the year (Figure 7). Values at other stations were quite similar. AR10, AR32, and AR38 exhibited similar and slowly increasing values that were similar to most of the Tidal Main Stations. AR24 and AR25 on the north shore of Hunting Creek were more variable with peaks in early June, early July, and early August.

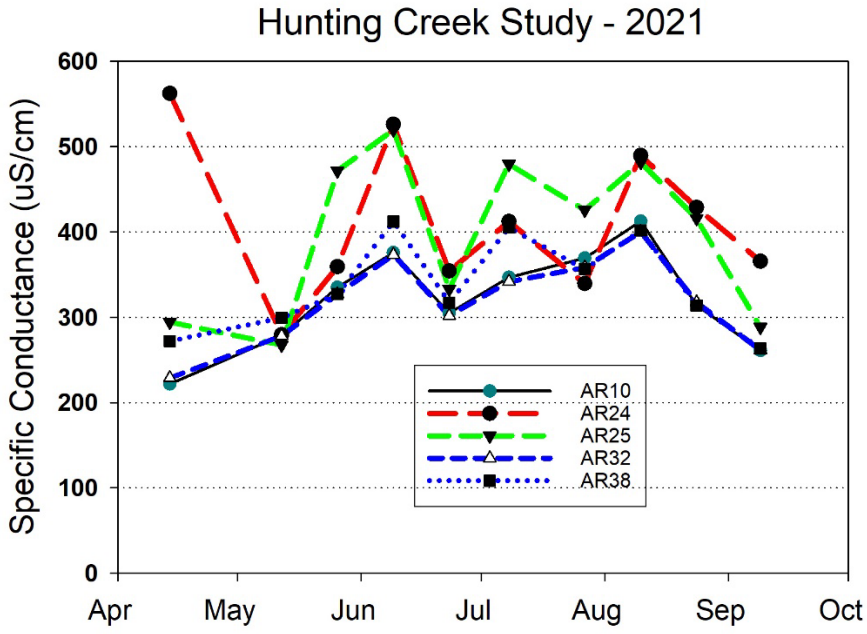

Figure 8. Specific Conductance (µS/cm). Tidal CSO Impact Stations.

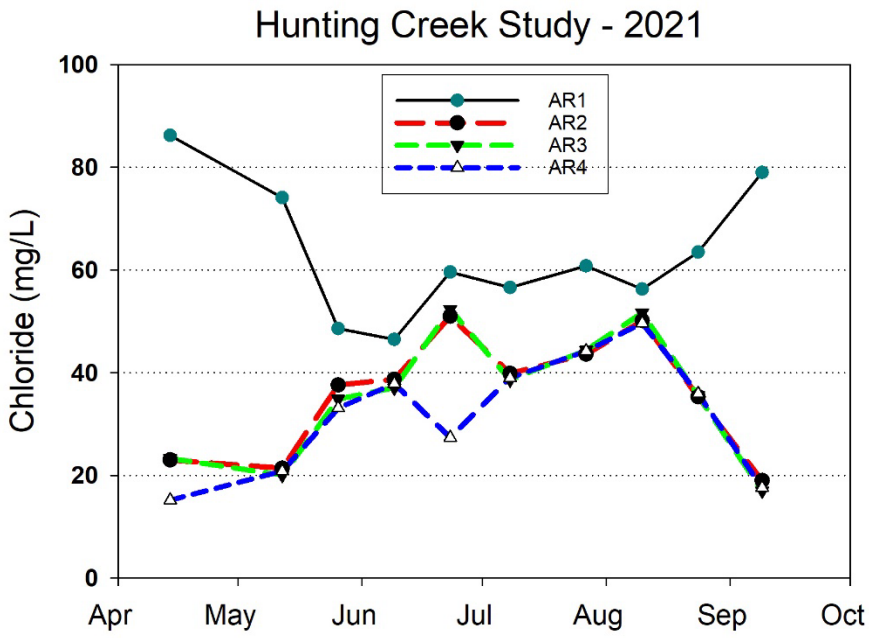

Chloride ion (Cl-) is a principal contributor to conductance. Major sources of chloride in the study area are sewage treatment plant discharges, road salt, and brackish water from the downriver portion of the tidal Potomac. Chloride concentrations observed in the Hunting Creek area are very low relative to those observed in brackish, estuarine, and coastal areas of the Mid-Atlantic region. Chloride may increased slightly in late summer or fall when brackish water from down estuary may reach the area as freshwater discharge declines.

Figure 9. Chloride (mg/L). Tidal Main Stations. Month tick is at first day of month.

Chloride exhibited a similar pattern to specific conductance at most of the tidal main stations increasing from April through August. AR1 again showed high values in April before coming closer to the other stations in late may through August (Figure 9). AR10, AR32, and AR38, located on the mainstem of the Potomac, followed a seasonal pattern similar to most of the Tidal Main Stations whereas AR24 and AR25 were more variable with peaks in early June and early July (Figure 10).

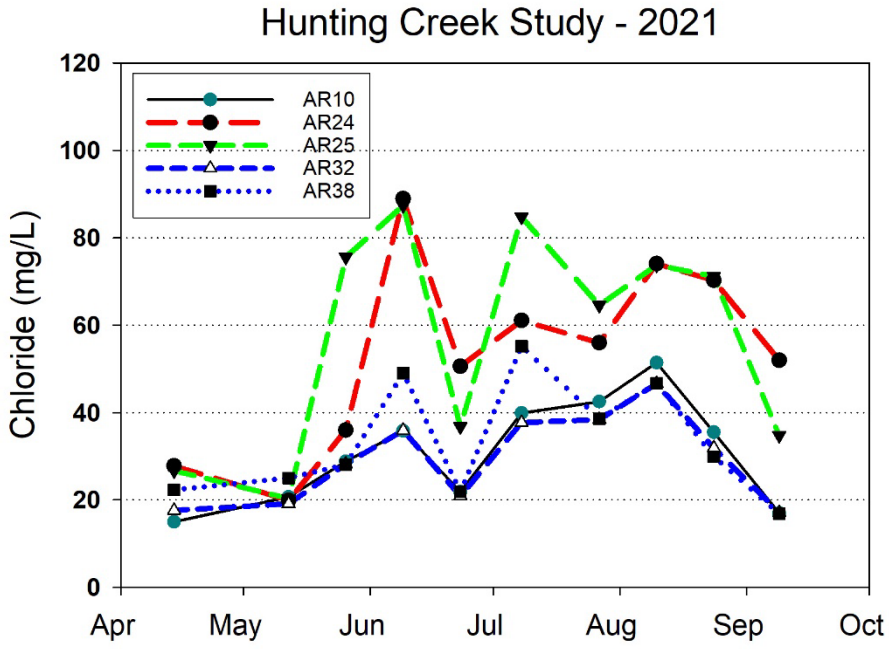

Figure 10. Chloride (mg/L). Tidal CSO Impact Stations

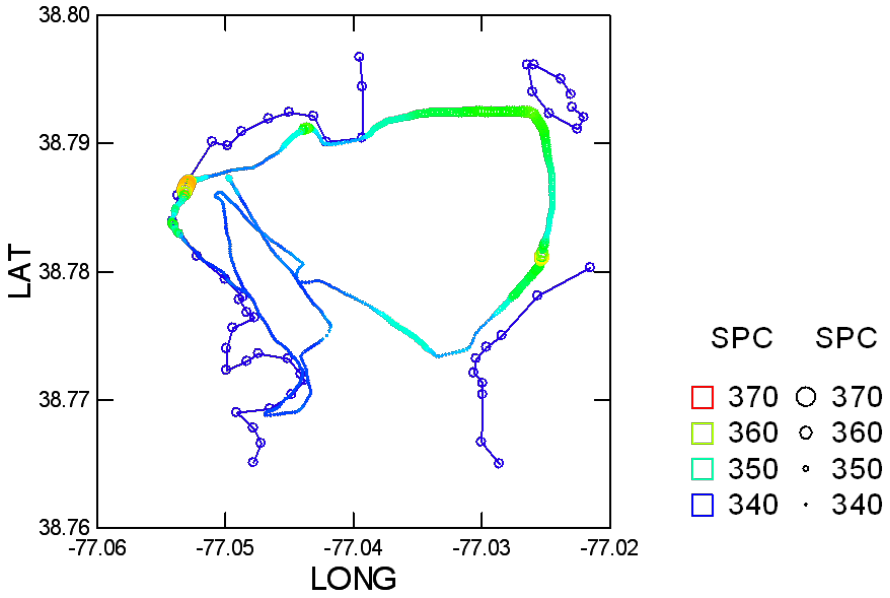

Figure 16a. Water Quality Mapping. July 13, 2021. Specific Conductance (uS/cm).

On July 13 specific conductance was about 340 uS/cm in most of the Hunting Creek embayment. Slightly higher values were observed in the river mainstem and near the shoreline of Huntiing Creek.On August 9 showed that lower values (400-430 uS/cm) were found over most of the study area with higher values (440-460 uS/cm) found along the northwest corner of Hunting Creek near the entrance of water to the embayment under the GW Parkway bridge. This reflects water slightly higher in ions, probably attributable to the Alex Renew effluent.

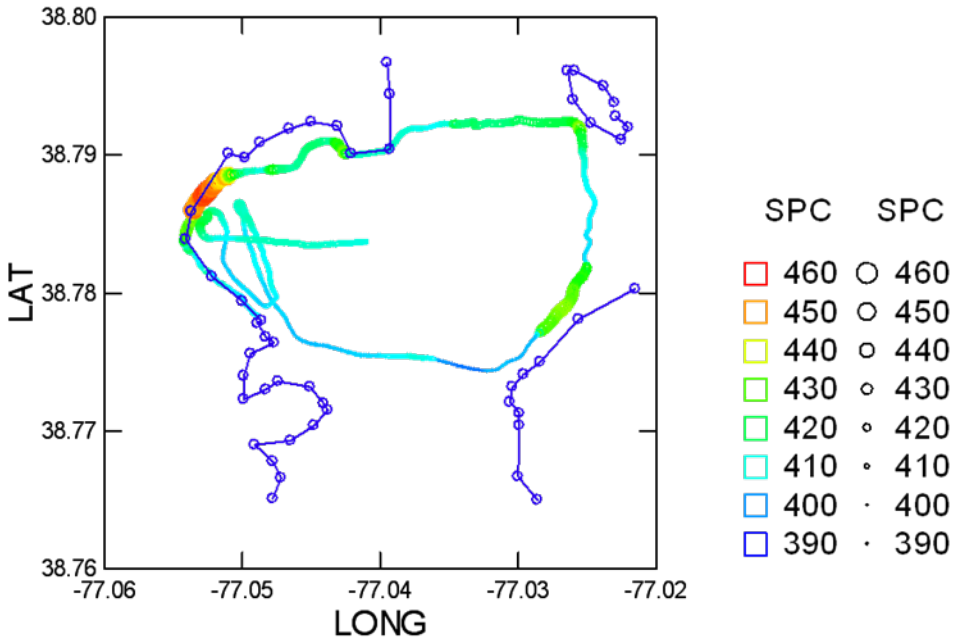

Figure 16b. Water Quality Mapping. August 9, 2021. Specific Conductance (uS/cm).

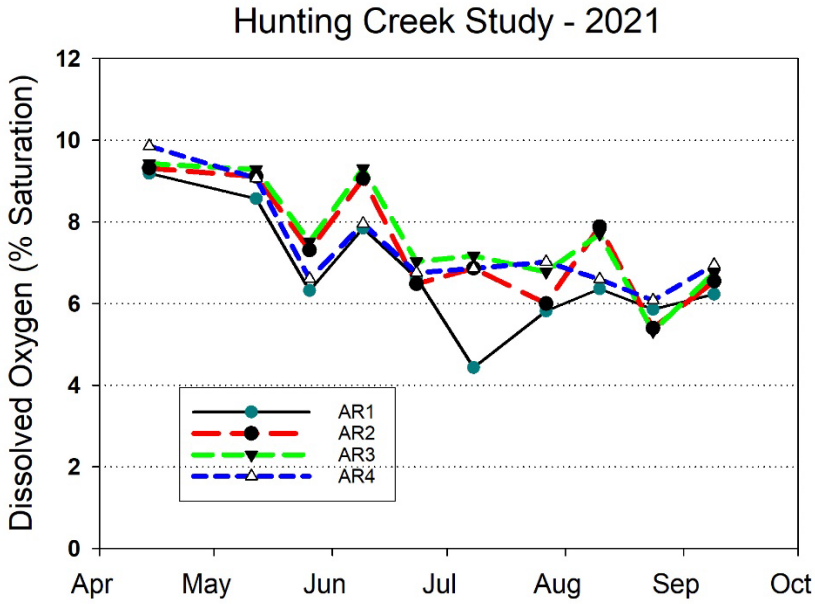

Oxygen dissolved in the water is required by freshwater animals for survival. The standard for dissolved oxygen (DO) in most surface waters is 5 mg/L. Oxygen concentrations in freshwater are in balance with oxygen in the atmosphere, but oxygen is only weakly soluble in water so water contains much less oxygen than air. This solubility is determined by temperature with oxygen more soluble at low temperatures.

Figure 12. Dissolved Oxygen (mg/L). Tidal Main Stations. Month tick is at first day of month.

The general pattern for dissolved oxygen (mg/L) at Tidal Main Stations was a gradual decline from April through September (Figure 12). Looking at DO as percent saturation (Figure 13), values were more consistent seasonally. A peak was observed at all stations in early June. A significant decline was seen at AR1 in early July.

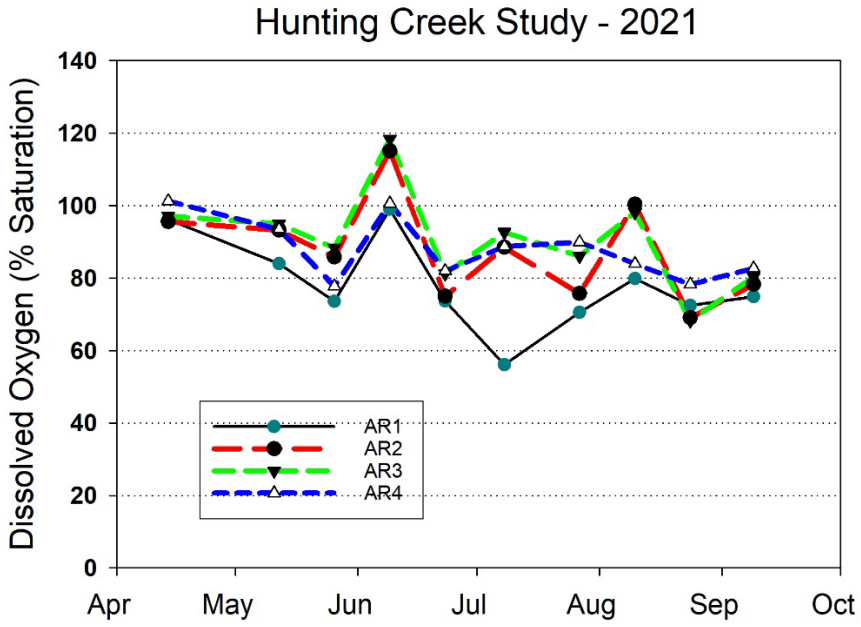

The temperature effect on oxygen concentration can be removed by calculating DO as percent saturation. This allows examination of the balance between photosynthesis and respiration both of which also impact DO. Photosynthesis adds oxygen to the water while respiration removes it. Values above 120% saturation are indicative of intense photosynthesis while values below 80% reflect a preponderance of respiration or decomposition.

Figure 13. Dissolved Oxygen (% saturation). Tidal Main Stations. Month tick is at first day.

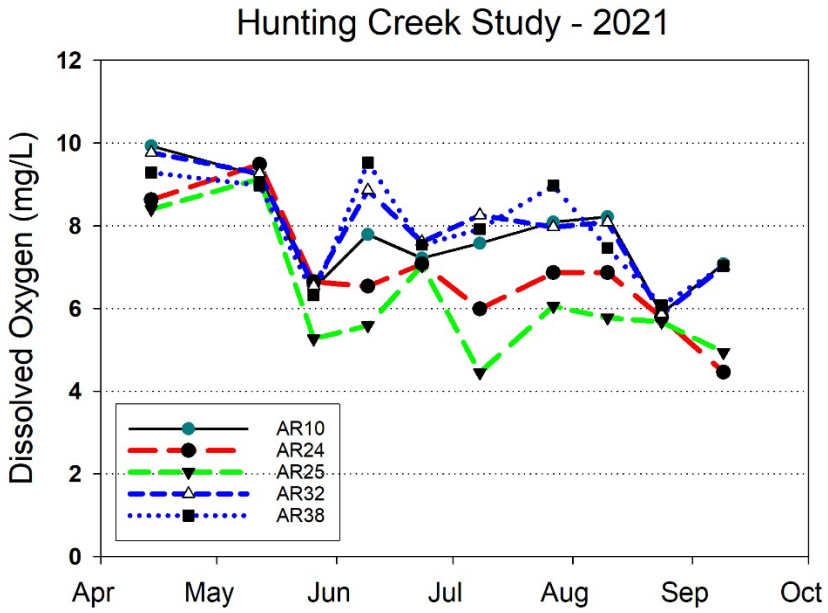

Figure 14. Disssolved oxygen (mg/L). Tidal CSO Impact Stations.

At the Tidal CSO Impact Stations there was general decline at AR10, AR32, and AR38 except in late May when there was an abrupt drop (Figure 14). The two stations in northern Hunting Creek bracketing the CSO outfall (AR24 and AR25) exhibited generally lower values than the other stations. DO as percent saturation (Figure 15) showed similar trends. The levels at AR24 and AR25 were substanially lowere for most of the year than the other stations..

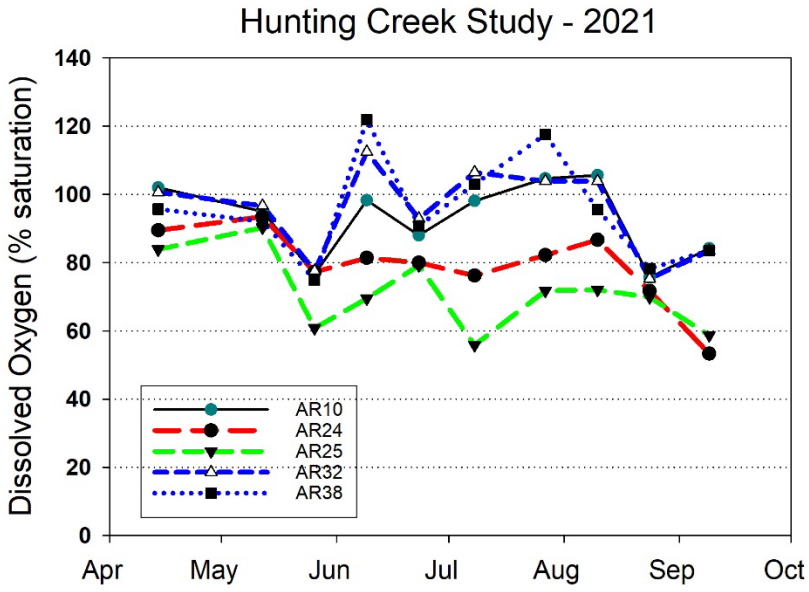

Figure 15. Dissolved oxygen (% saturation). Tidal CSO Impact Stations.

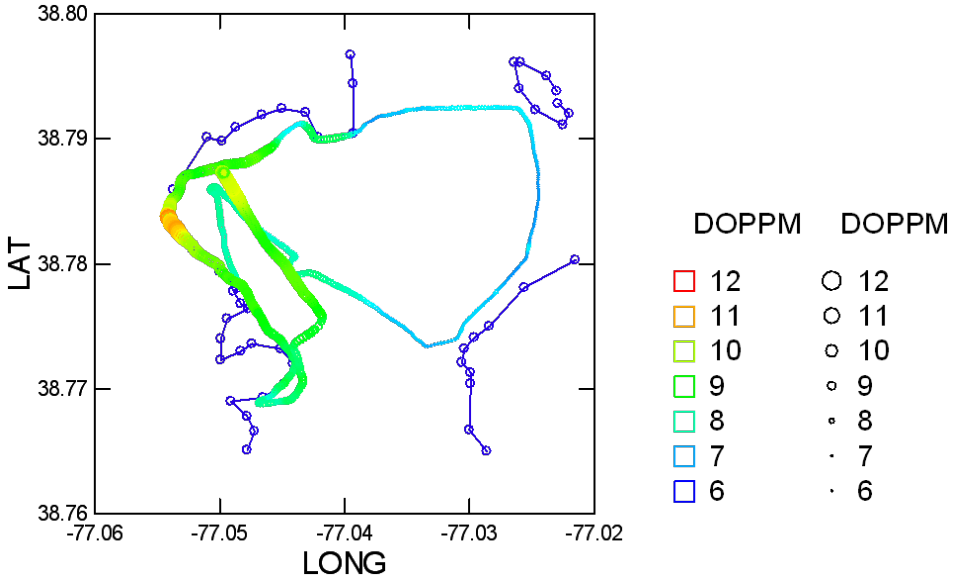

Figure 16a. Water Quality Mapping. July 13, 2021. Dissolved oxygen (mg/L).

On July 13 DO values were higher in the Hunting Creek embayment attained 150% saturation wheras in the river mainstem values were well below saturation with values typically about 7 mg/L (16a,b). this suggests active photosynthesis in the cove and more respiration in the river.

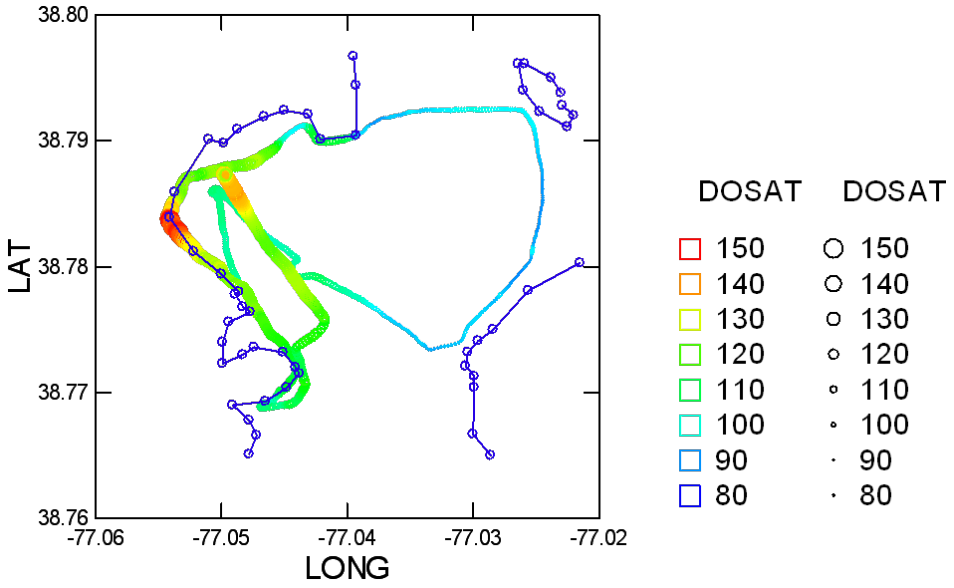

Figure 16b. Water Quality Mapping. July 13, 2021. Dissolved oxygen (percent saturation)

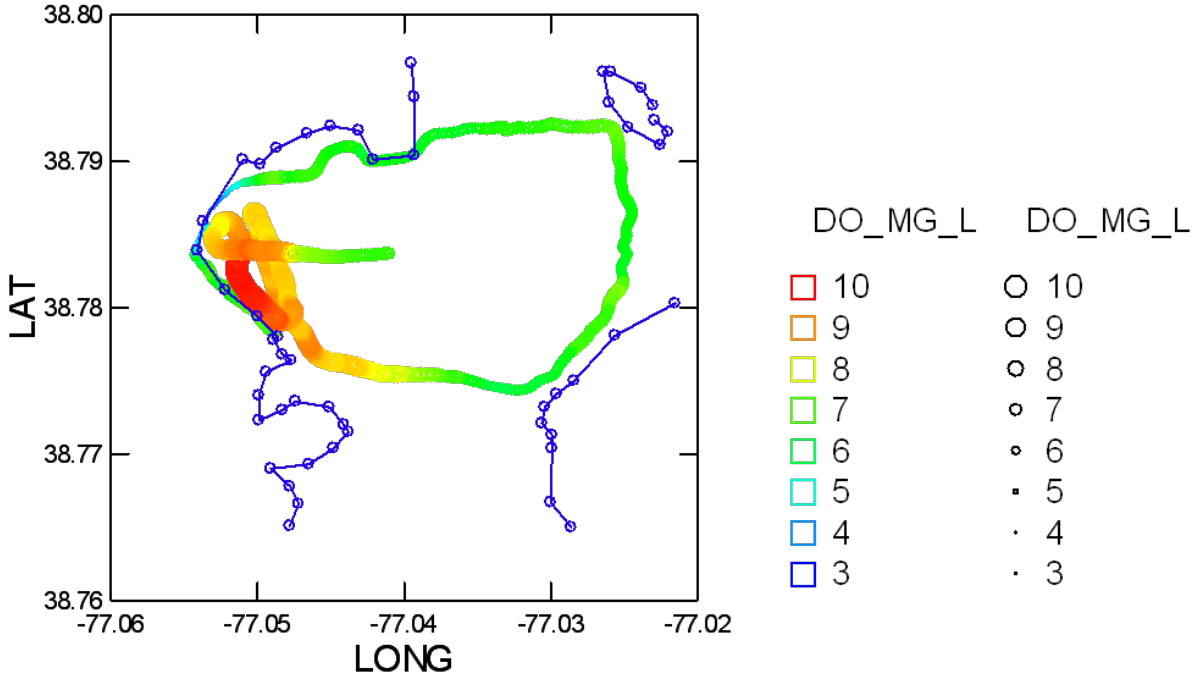

Figure 16a. Water Quality Mapping. August 9, 2021. Dissolved oxygen (mg/L).

Water quality mapping of dissolved oxygen on August 9, 2021 revealed higher values of up to 10 mg/L and 130% saturation in the Hunting Crkk embayment while values of 6-7 mg/L and slightly below saturation in the Potomac mainstem (Figure 16a,b). This spatial pattern suggests strong photosynthetic activity by phytoplankton in Hunting Creek.

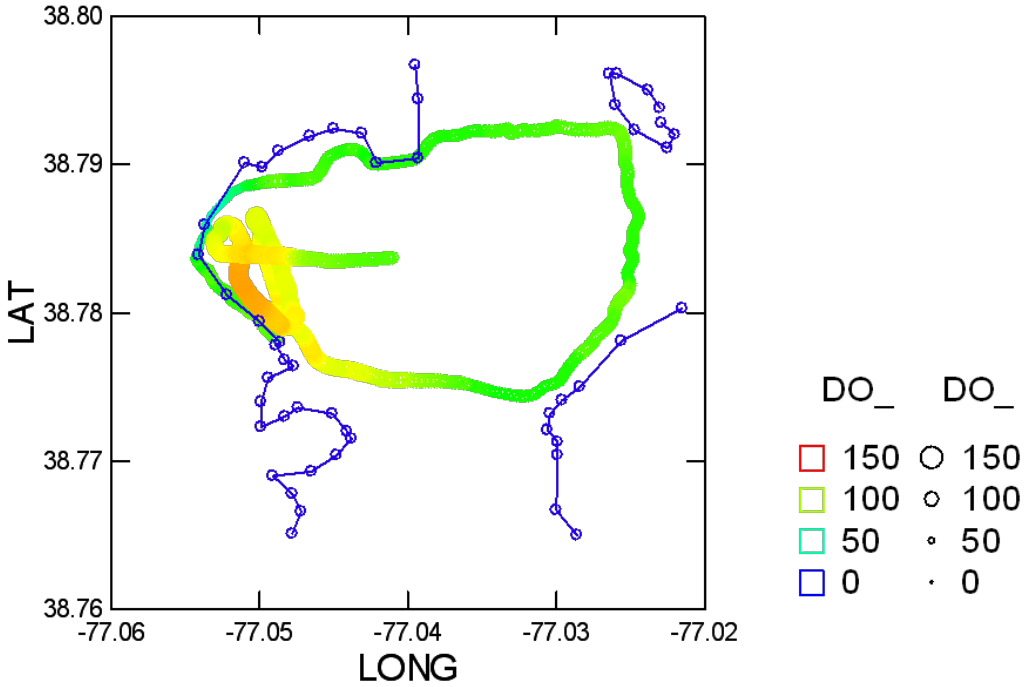

Figure 16b. Water Quality Mapping. August 9, 2021. Dissolved oxygen (percent saturation)

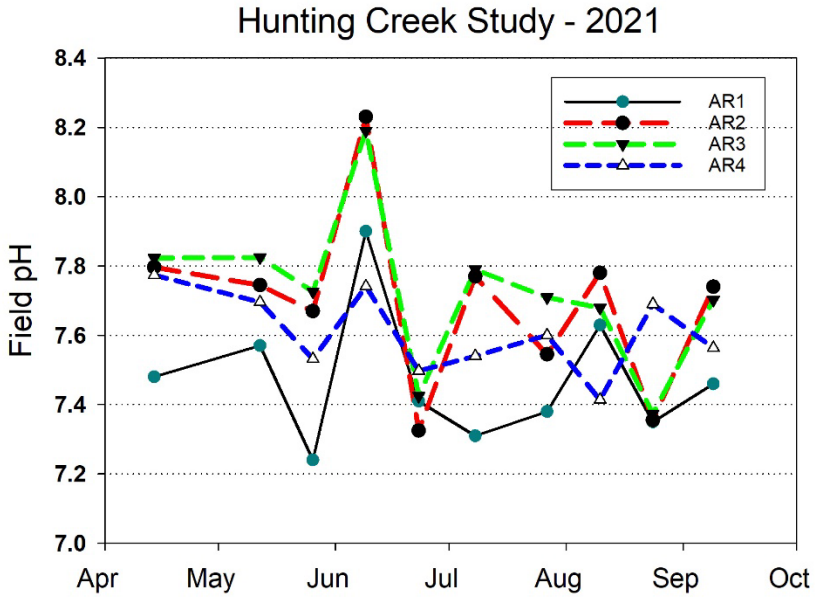

pH is a measure of the concentration of hydrogen ions (H+) in the water. Neutral pH in water is 7. Values between 6 and 8 are often called circumneutral, values below 6 are acidic and values above 8 are termed alkaline. Like DO, pH is affected by photosynthesis and respiration. In the tidal Potomac, pH above 8 indicates active photosynthesis and values above 9 indicate intense photosynthesis. A decrease in pH following a rainfall event may be due to acids in the rain or in the watershed.

Figure 17. Field pH. Tidal Main Stations. Month tick is at first day of month.

While variable from week to week, field pH values remained in a fairly narrow range (7.2-7.8) with little seasonal pattern at the Tidal Main Stations (Figures 17). The one exception was in early June at AR2 and AR 3 when a pH of 8.2 was attained. In the tidal CSO impact stations pH was generally lower at AR24 and AR25 (Field 18).

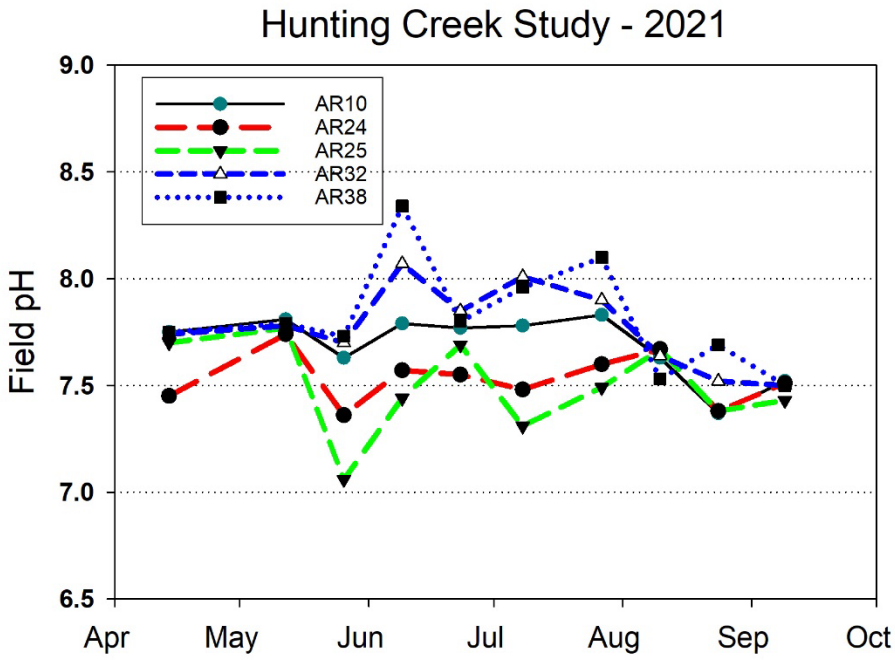

pH may be measured in the field or in the lab. Field pH is more reflective of in situ conditions while lab pH is done under more stable and controlled laboratory conditions and is less subject to error. Newer technologies such as the Hydrolab and YSI sondes used in GMU field data collection are more reliable than previous field pH meters and should give results that are most representative of values actually observed in the river.

Figure 18. Field pH. Tidal CSO Impact Stations. Month tick is at first day of month.

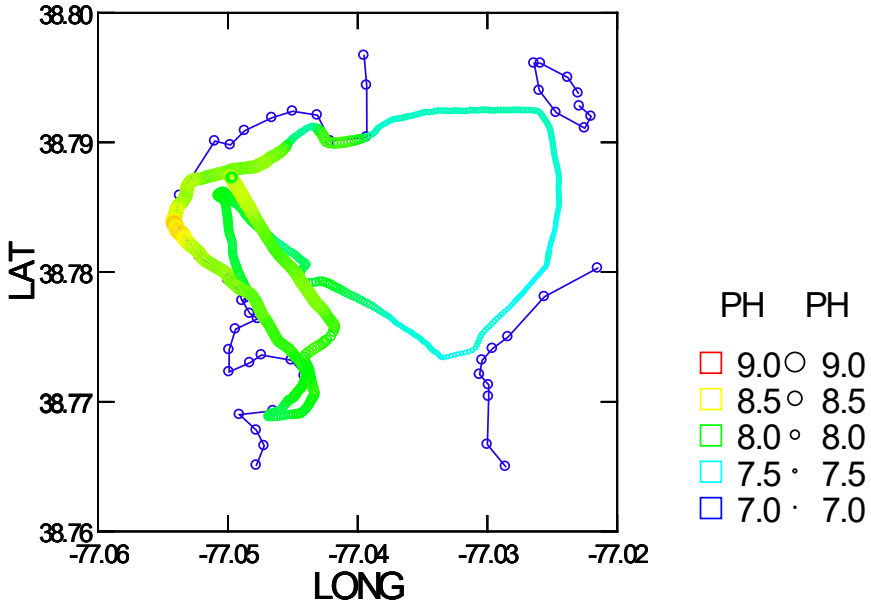

Figure 19a. Water Quality Mapping. July 13, 2021. pH.

Water quality mapping of pH showed a spatial pattern similar to dissolved oxygen (Figure 19a,b). Values above 8.0 were found in the Hunting Creek embayment which, like dissolved oxygen, suggests significant photosynthesis by phytoplankton.

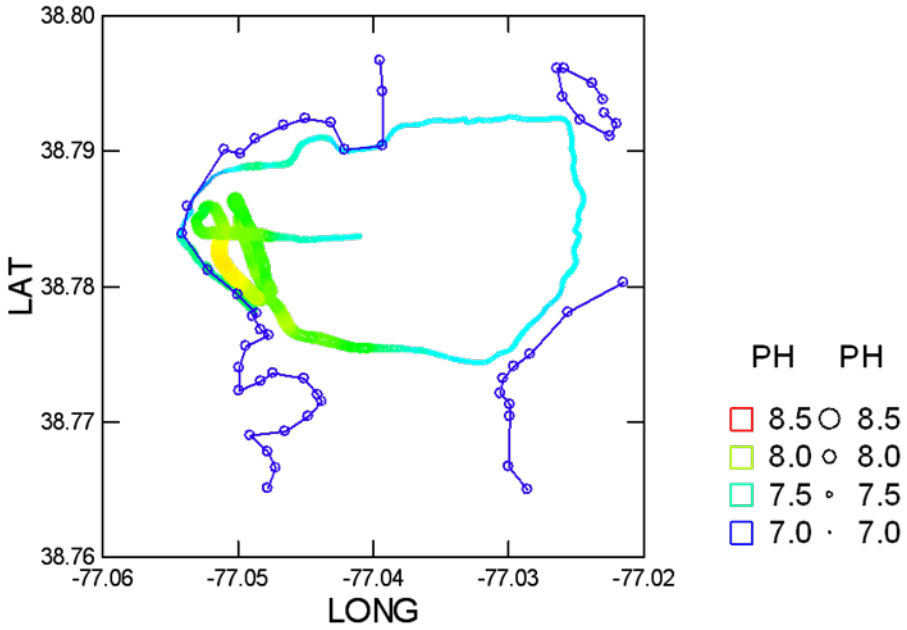

Figure 19b. Water Quality Mapping. August 21, 2021. pH.

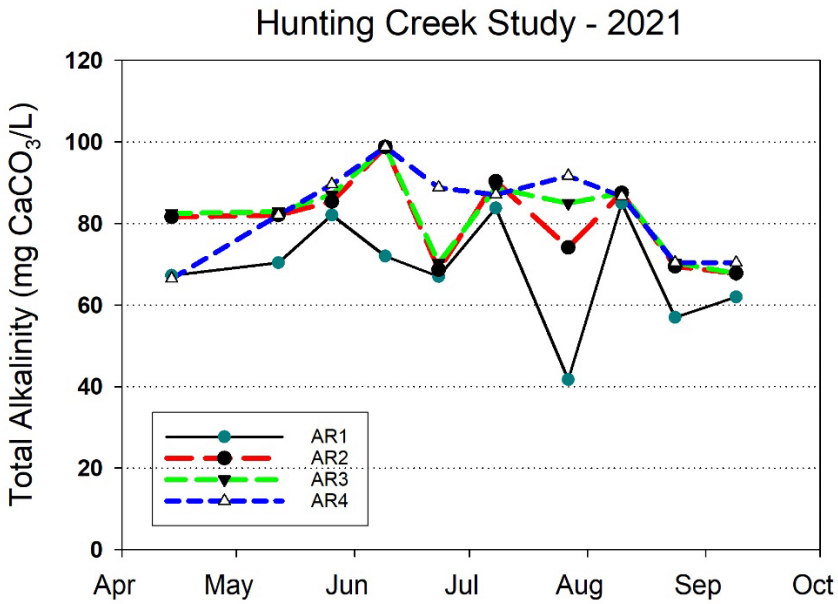

Total alkalinity measures the amount of bicarbonate and carbonate dissolved in the water. In freshwater this corresponds to the ability of the water to absorb hydrogen ions (acid) and still maintain a near neutral pH. Alkalinity in the tidal freshwater Potomac generally falls into the moderate range allowing adequate buffering without carbonate precipitation.

Figure 20. Total Alkalinity (mg/L as $CaCO_3$). Tidal Main Stations. Month tick is at first day.

Total alkalinity was fairly constant at the tidal main stations except for a marked dip in late July at AR1 (Figure 20). AR10, AR32, and AR38 were fairly constant at 80-100 mg/L except that AR32 was much lower at the beginning and the end of the year (Figure 21). AR24 and AR25 were consistently somewhat lower than the other stations.

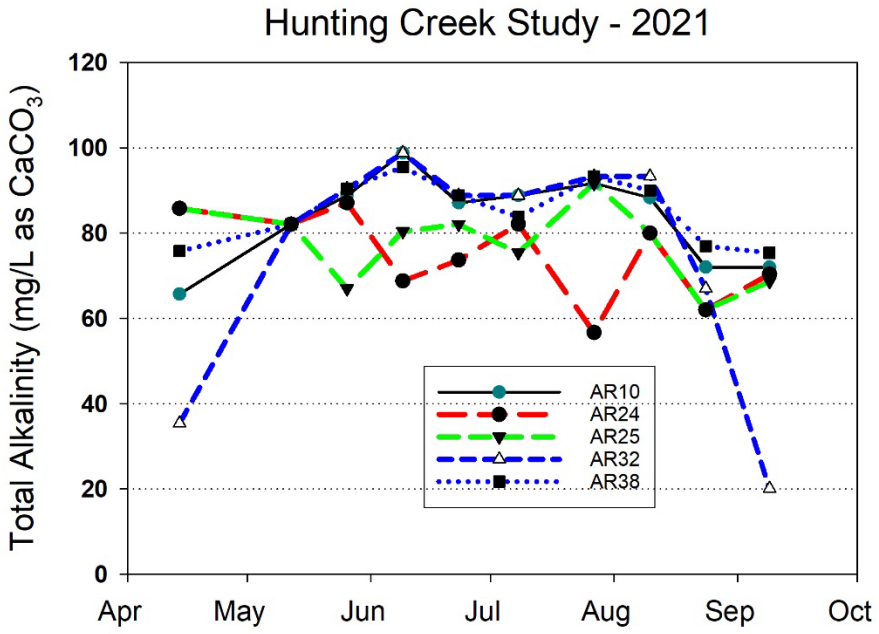

Figure 21. Total Alkalinity (mg/L as CaCO3). Tidal CSO Impact Stations.

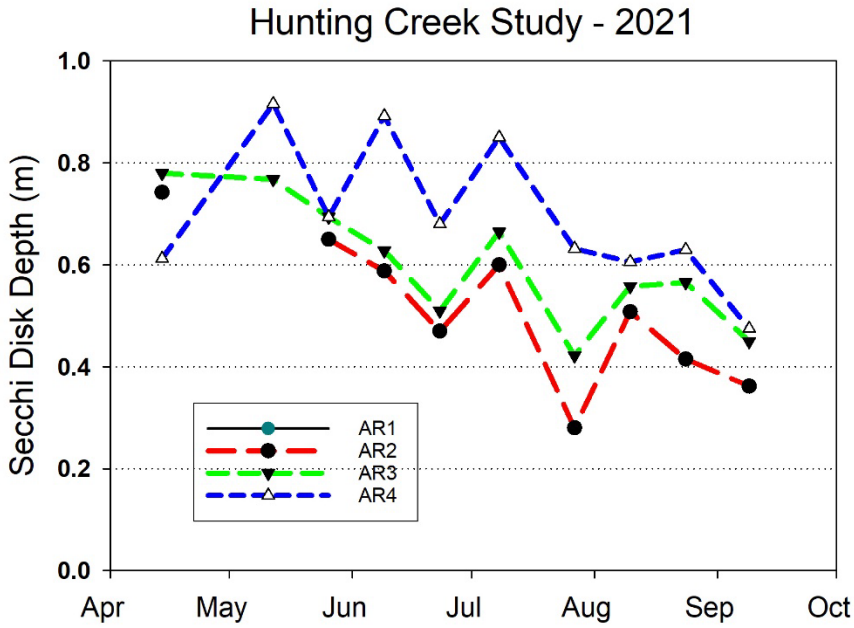

Secchi Depth is a measure of the transparency of the water. The Secchi disk is a flat circle of thick sheet metal or plywood about 6 inches in diameter which is painted into alternate black and white quadrants. It is lowered on a calibrated rope or rod to a depth at which the disk disappears. This depth is termed the Secchi Depth. This is a quick method for determining how far light is penetrating into the water column. Light is necessary for photosynthesis and thereby for growth of aquatic plants and algae.

Figure 22. Secchi Disk Depth (m). Tidal Main Stations. Month tick is at first day of month.

Water clarity as reflected by Secchi disk did showed a fairly consistent seasonal decline at AR2 and AR3 with peak in early July followed by a marked decline in late July (Figure 22). At AR4 values hovered at about 0.8 m for most of the year before dropping somewhat in the fall. Light attenuation coefficient (Figure 23) was generally lower in the river (AR4) and higher in the embayments. A strong decline was observed in late July similar to that in Secchi Depth.

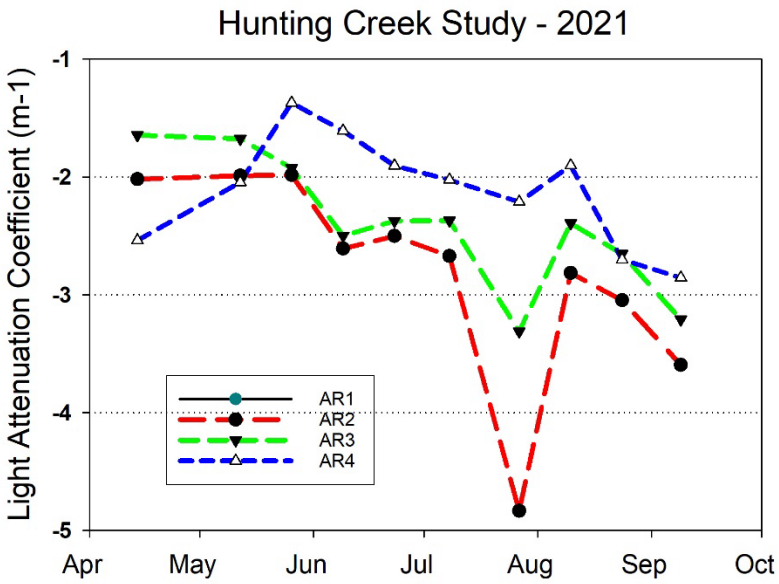

Light Attenuation is another approach to measuring light penetration. This is determined by measuring light levels at a series of depths starting near the surface. The resulting relationship between depth and light is fit to a semi-logarithmic curve and the resulting slope is called the light attenuation coefficient. This relationship is called Beer's Law. It is analogous to absorbance on a spectrophotometer. The greater the light attenuation, the faster light is absorbed with depth. More negative values indicate greater attenuation. Greater attenuation is due to particulate and dissolved material which absorbs and deflects light.

Figure 23. Light Attenuation Coefficient (m^{-1}). Tidal Main Stations. Month tick is at first day of month.

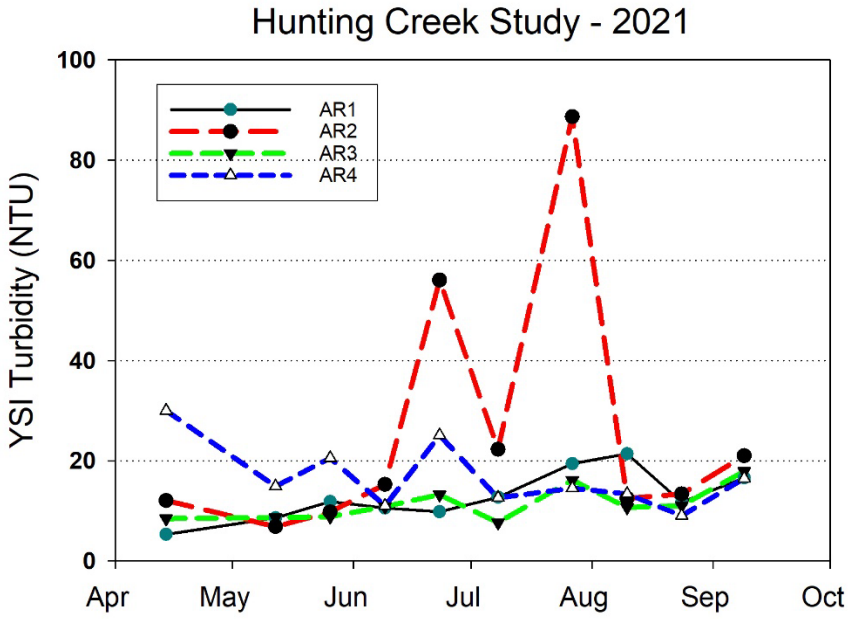

Turbidity is yet a third way of measuring light penetration. Turbidity is a measure of the amount of light scattering by the water column. Light scattering is a function of the concentration and size of particles in the water. Small particles scatter more light than large ones (per unit mass) and more particles result in more light scattering than fewer particles.

Figure 24. Turbidity (NTU). Tidal Main Stations. Month tick is at first day of month.

Turbidity values were generally low to moderate (<20 NTU) at the Tidal Main Stations (Figure 24). The exceptions were two very high values at AR2 in late June and late July which correspond with the low Secchi disk readings and high light attenuation observed earlier. At the Tidal CSO impact stations values were generally below 20 NTU (Figure 25). Much higher values were observed on two dates at AR24 and AR25. These may have been due to disturbance of the bottom during sample collection as these two stations are accessed from shore.

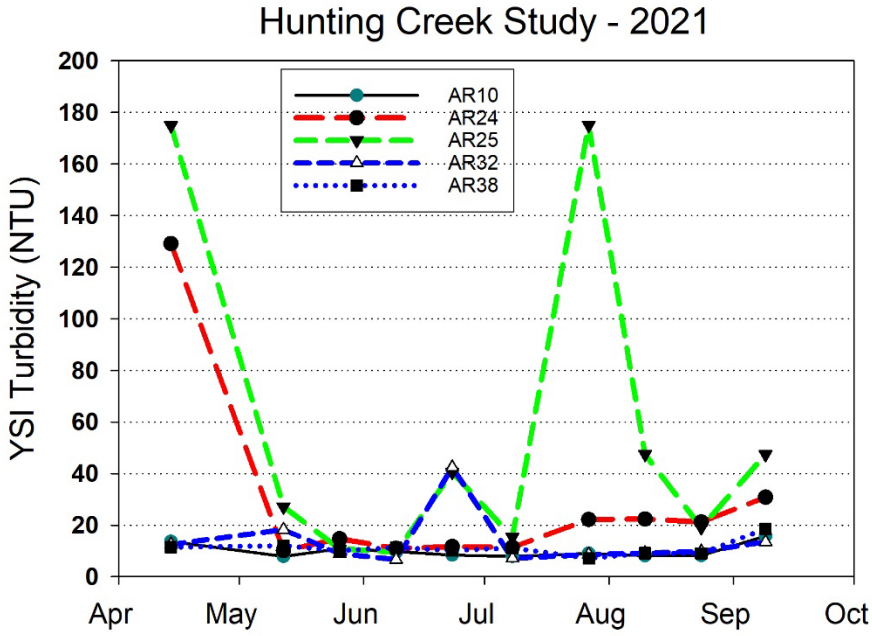

Figure 25. Turbidity (NTU). Tidal CSO Impact Stations.

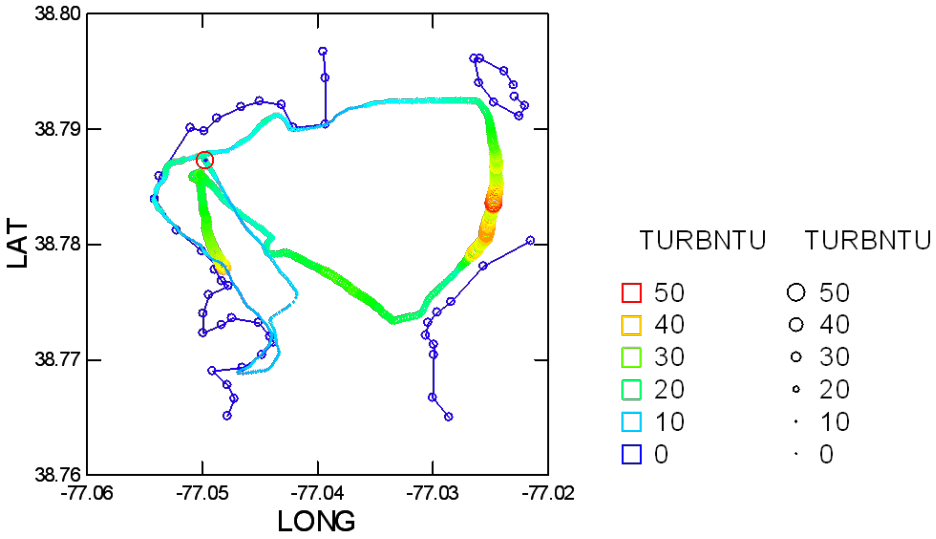

Figure 26a. Water Quality Mapping. June 13, 2021. Turbidity YSI.

Turbidity was generally quite low through much of the study area on both dates with values typically about 10 NTU. Some higher values were found on the Maryland side of the river (Figure 26a).Substantially higher values were observed near the boat launch area and near the GW Parkway bridge (Figure 26b).

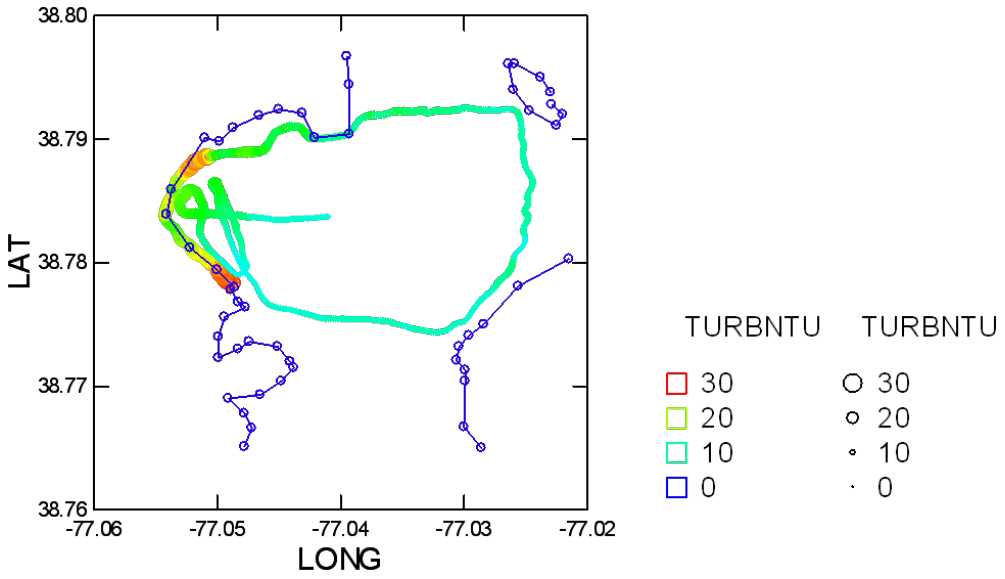

Figure 26b. Water Quality Mapping. August 9, 2021. Turbidity YSI.

.

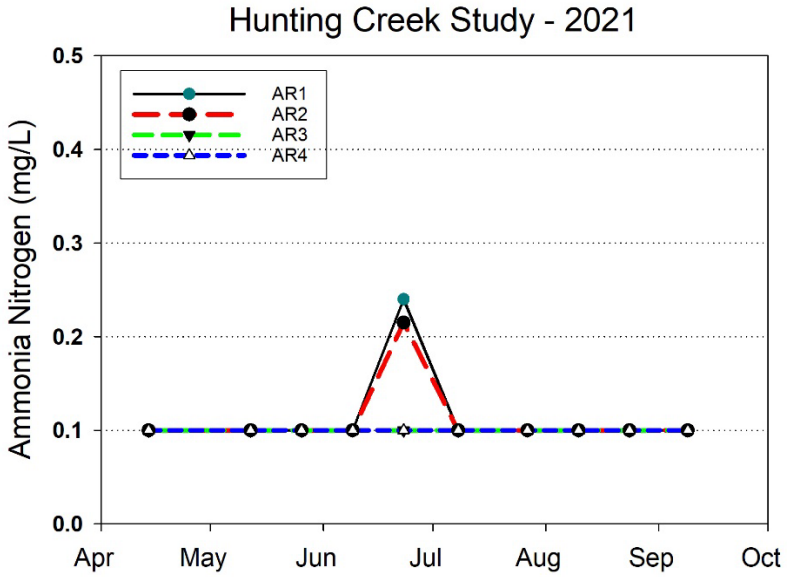

Ammonia nitrogen measures the amount of ammonium ion (NH_4^+) and ammonia gas (NH_3) dissolved in the water. Ammonia nitrogen is readily available to algae and aquatic plants and acts to stimulate their growth. While phosphorus is normally the most limiting nutrient in freshwater, nitrogen is a close second. Ammonia nitrogen is rapidly oxidized to nitrate nitrogen when oxygen is present in the water so high ammonia levels suggest proximity to a source.

Figure 27. Ammonia Nitrogen (mg/L). Tidal Main Stations. Month tick is at first day of month.

Ammonia nitrogen was consistently low (<0.2 mg/L, the detection limit) for almost the entire study period at both Tidal Main and Tidal CSO impact stations (Figure 27&28). Slightly higher values were seen on some dates especially at AR24 and AR25. Most of the values for ammonia nitrogen were reported as below detection limit at which time values equal to ½ of the detection limit were used in graphing.

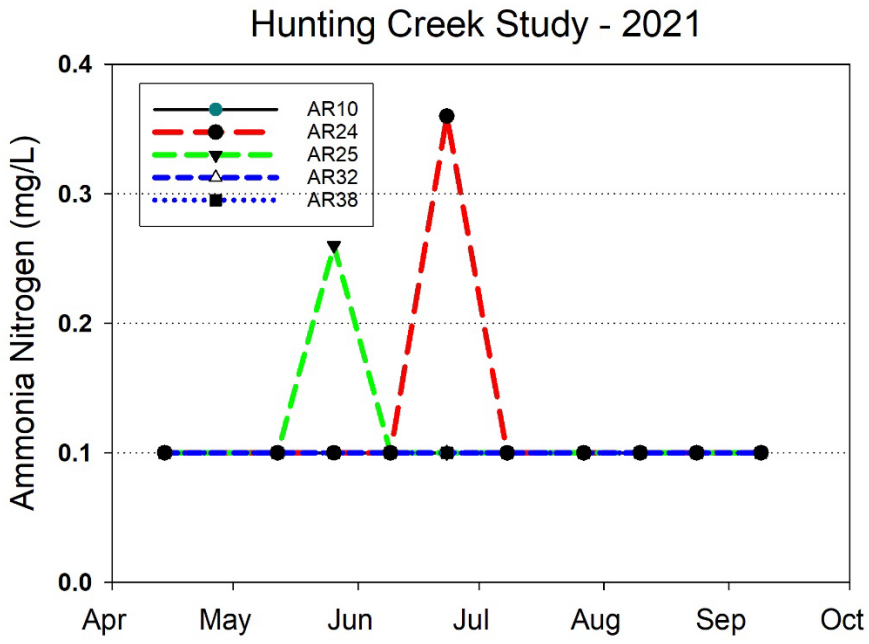

Figure 28. Ammonia Nitrogen (mg/L). Tidal CSO Impact Stations.

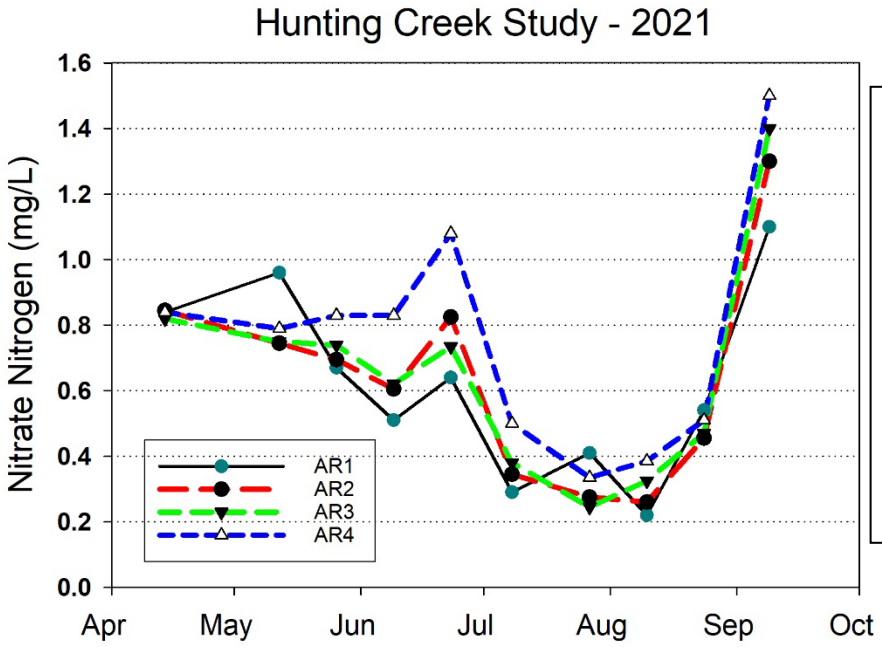

Nitrate Nitrogen refers to the amount of N that is in the form of nitrate ion (NO_3^-). Nitrate ion is the most common form of nitrogen in most well oxidized freshwater systems. Nitrate concentrations are increased by input of wastewater, nonpoint sources, and oxidation of ammonia in the water. Nitrate concentrations decrease when algae and plants are actively growing and removing nitrogen as part of their growth.

Figure 29. Nitrate Nitrogen (mg/L). Tidal Main Stations. Month tick is at first day of month.

At the Tidal Main stations, nitrate nitrogen levels showed a general pattern of decrease from April through early August with a strong uptick in September (Figure 29). There was also a peak in late June especially at AR4, the river station. A similar pattern was observed at the Tidal CSO Impact stations with a more obvious uptick at all stations in late June (Figure 30).

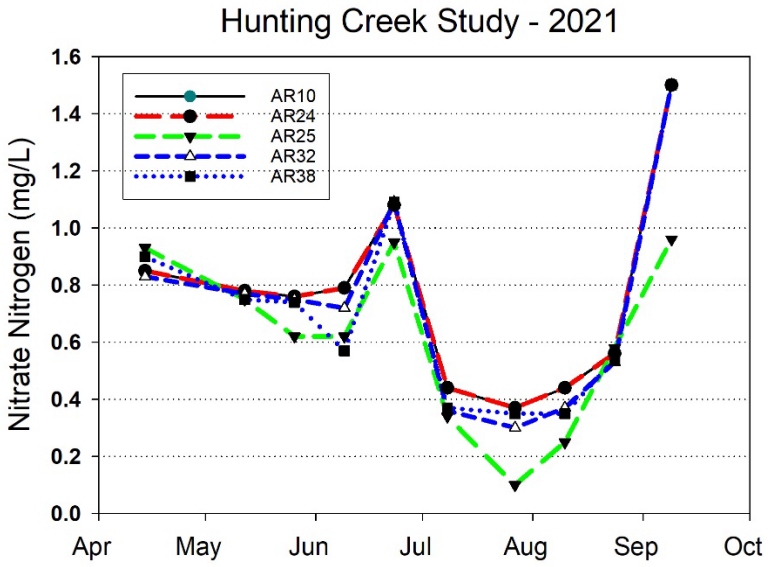

Figure 30. Nitrate Nitrogen (mg/L). Tidal CSO Impact Stations.

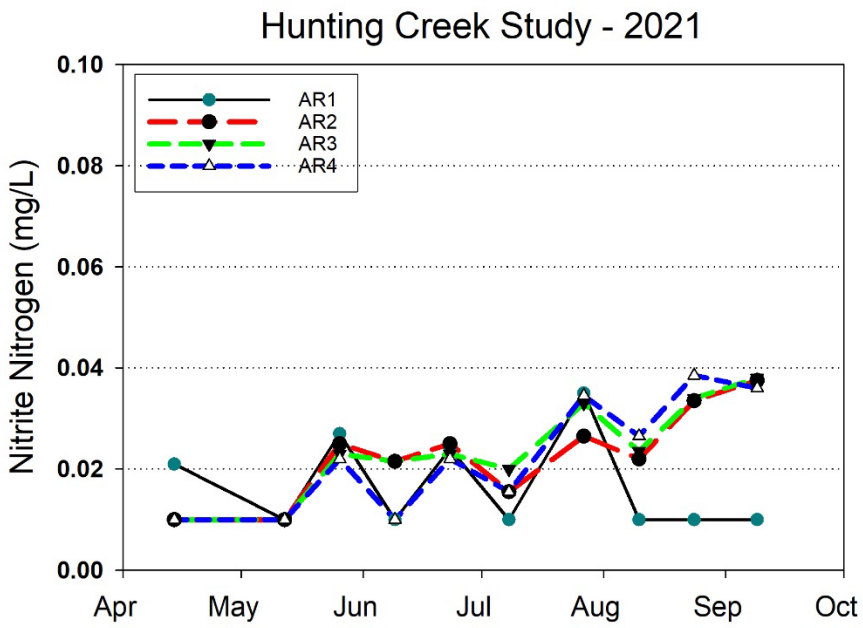

Nitrite nitrogen consists of nitrogen in the form of nitrite ion (NO_2^-). Nitrite is an intermediate in the oxidation of ammonia to nitrate, a process called nitrification. Nitrite is usually in very low concentrations unless there is active nitrification.

Figure 31. Nitrite Nitrogen (mg/L). Tidal Main Stations. Month tick is at first day of month.

Nitrite nitrogen was generally low (<0.04 mg/L) at all stations throughout the year (Figures 31&32). There was little consistent seasonal pattern.

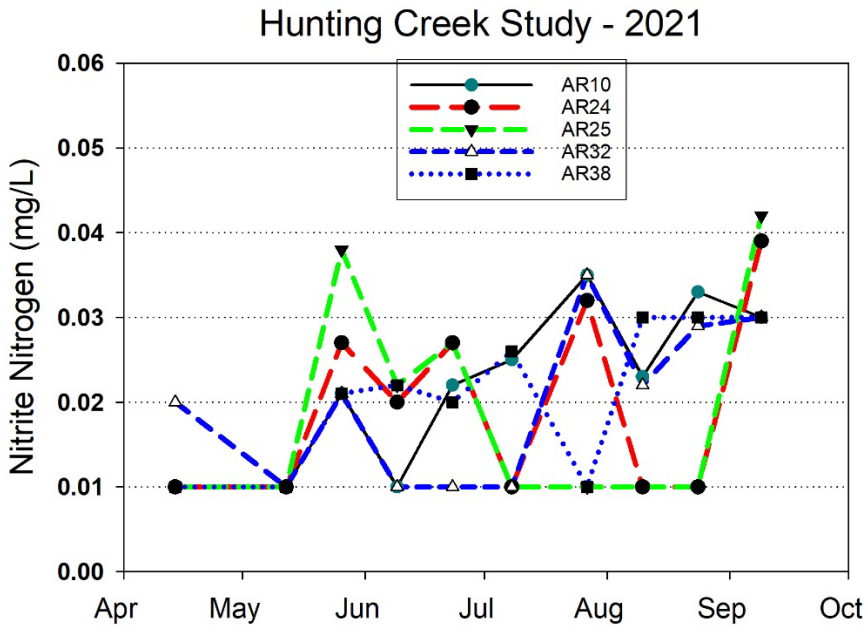

Figure 32. Nitrite Nitrogen (mg/L). Tidal CSO Impact Stations.

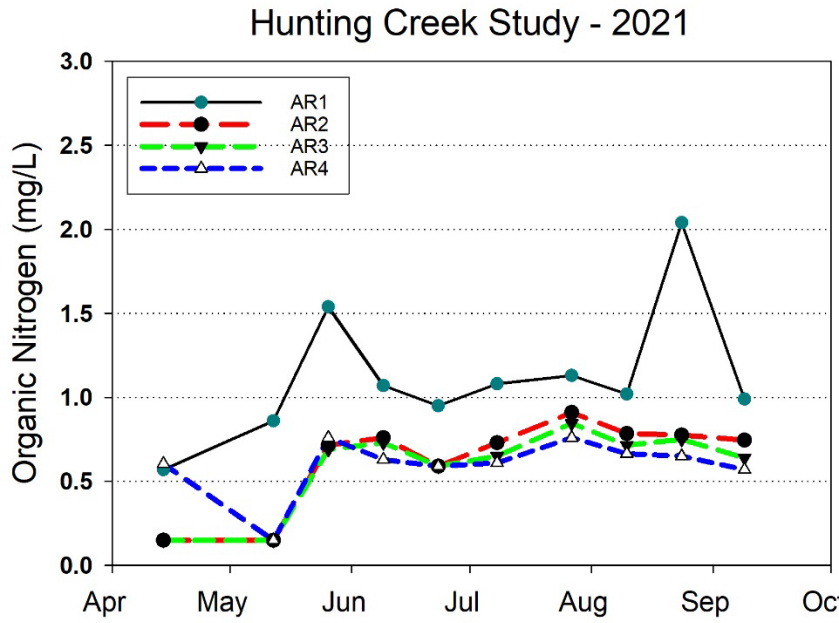

Organic nitrogen measures the nitrogen in dissolved and particulate organic compounds in the water. Organic nitrogen comprises algal and bacterial cells, detritus (particles of decaying plant, microbial, and animal matter), amino acids, urea, and small proteins. When broken down in the environment, organic nitrogen results in ammonia nitrogen. Organic nitrogen is determined as the difference between total Kjeldahl nitrogen and ammonia nitrogen.

Figure 33. Organic Nitrogen (mg/L). Tidal Main Stations. Month tick is at first day of month.

Organic nitrogen values were generally in the range of 0.2-1.0 mg/L at most stations throughout the year at both Tidal Main and CSO Impact stations (Figures 33&34). AR1, AR24, and AR25 were consistently higher.

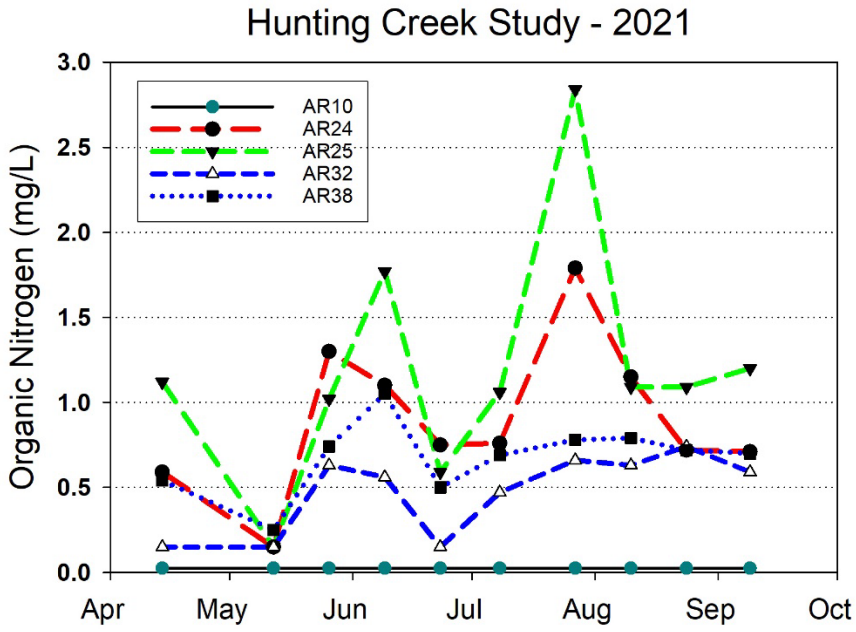

Figure 34. Organic Nitrogen (mg/L). Tidal CSO Impact Stations.

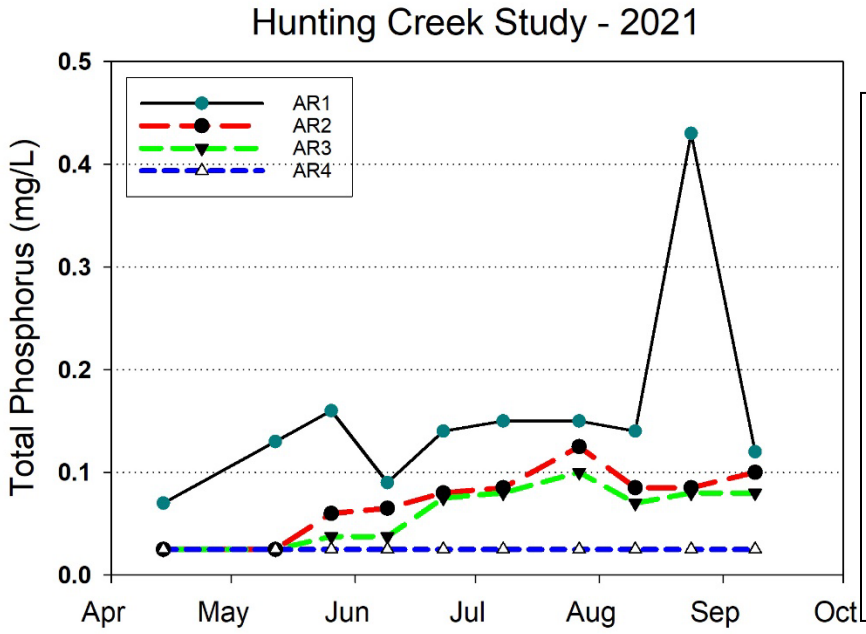

Phosphorus (P) is often the limiting nutrient in freshwater ecosystems. As such the concentration of P can set the upper limit for algal growth. Total phosphorus is the best measure of P availability in freshwater since much of the P is tied up in biological tissue such as algal cells. Total P includes phosphate ion (PO_4^{-3}) as well as phosphate inside cells and phosphate bound to inorganic particles such as clays.

Figure 35. Total Phosphorus (mg/L). Tidal Main Stations. Month tick is at first day of month.

Total phosphorus did not vary much through the year at most stations remaining in the 0.05 to 0.10 range (Figures 35&36). Higher values were observed at AR1, AR24, and AR25 along the northern shore of Hunting Creek similar to organic nitrogen.

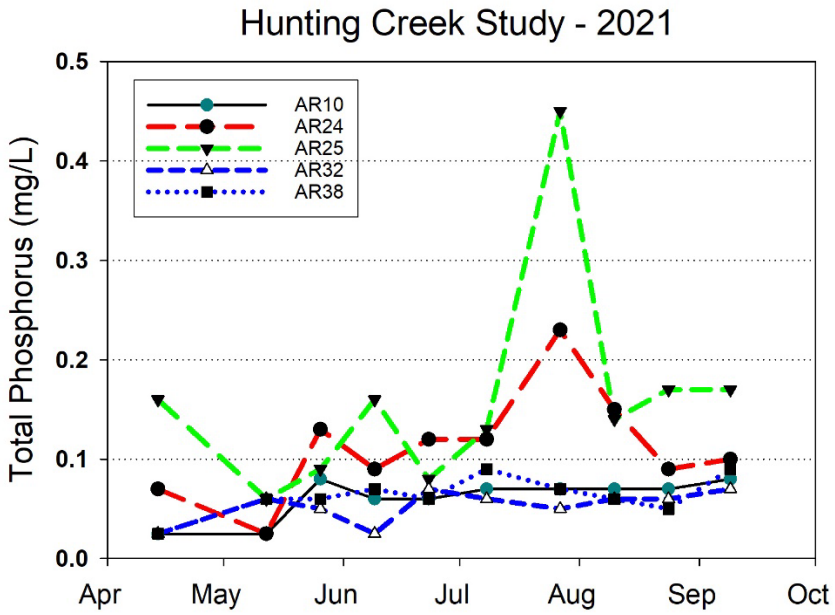

Figure 36. Total Phosphorus (mg/L). Tidal CSO Impact Stations.

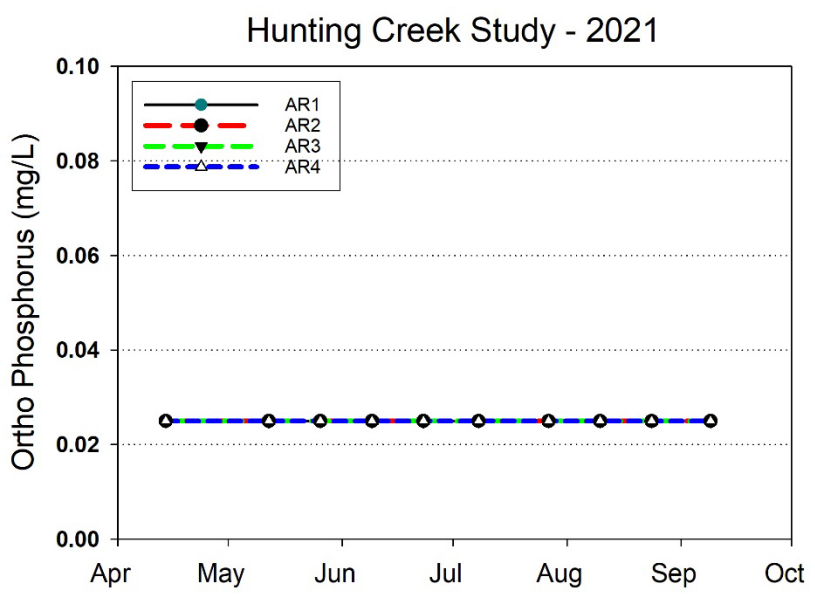

Soluble reactive phosphorus (SRP) is a measure of phosphate ion (PO_4^{-3}). Phosphate ion is the form in which P is most available to primary producers such as algae and aquatic plants in freshwater. However, SRP is often inversely related to the activity of primary producers because they tend to take it up so rapidly. So, higher levels of SRP indicate either a local source of SRP to the waterbody or limitation by a factor other than P.

Figure 37. Soluble Reactive Phosphorus (mg/L). Tidal Main Stations. Month tick is at first day of month.

Ortho-phosphorus values were all below the detection limit of 0.05 mg/L and thus were represented as half the detection limit (Figures 37&38). Little can be said other than that.

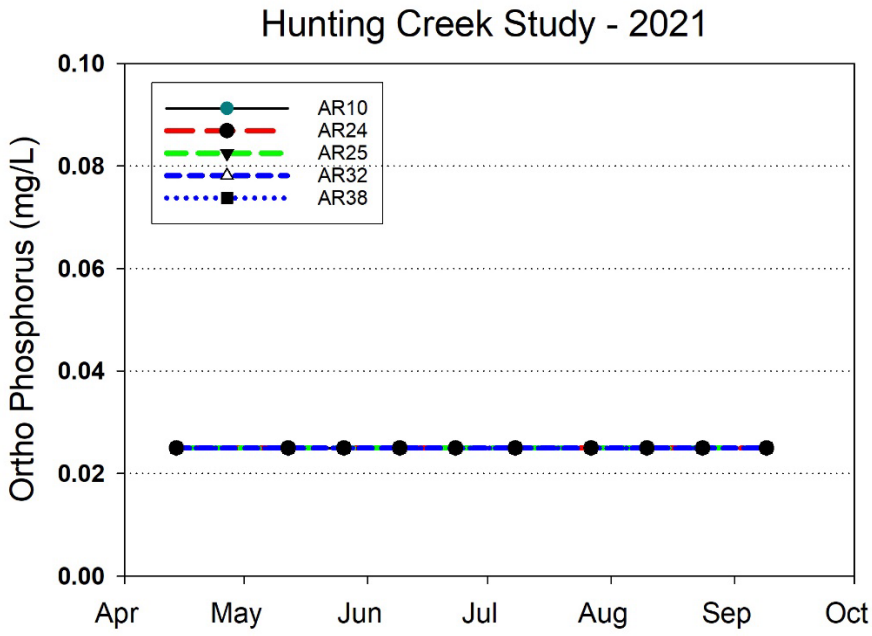

Figure 38. Soluble Reactive Phosphorus (mg/L). Tidal CSO Impact Stations.

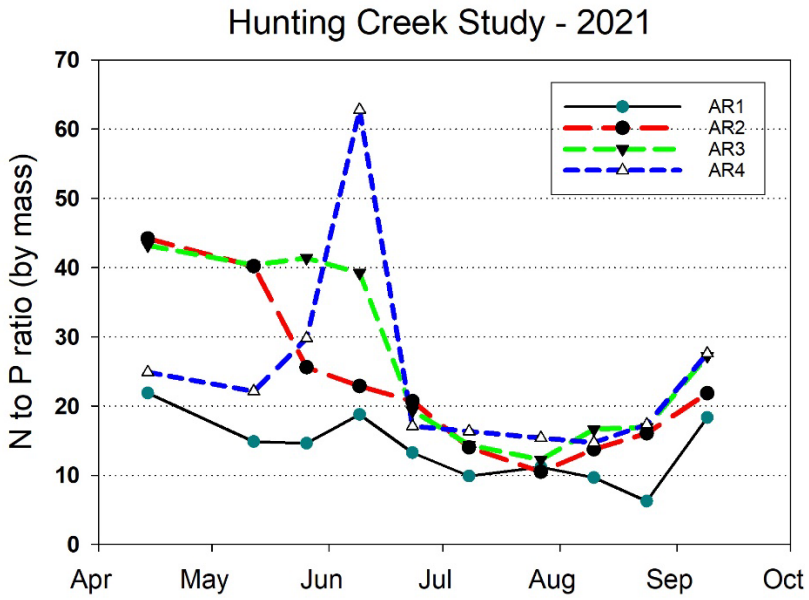

N:P ratio is determined by summing all of the components of N (ammonia, nitrate, nitrite, and organic nitrogen) and dividing by total P. This ratio gives an indication of whether N or P is more likely to be limiting primary production in a given freshwater system. Generally, values above 7.2 are considered indicative of P limitation while values below 7.2 suggest N limitation. N limitation could lead to dominance by cyanobacteria who can fix their own N from the atmosphere.

Figure 39. N/P Ratio (by mass). Tidal Main Stations. Month tick is at first day of month.

N/P ratio consistently pointed to P limitation, with values generally in the 10-30 range being greater than 7.2 threshold in all samples (Figure 39). One sample at AR1 in late August approached the threshold for N limitation of 7.2. In the Tidal CSO Impact Stations values were again above 10 in almost all samples with a general trend for higher values in the April to June period and lower and more uniform values thereafter (Figure 40).

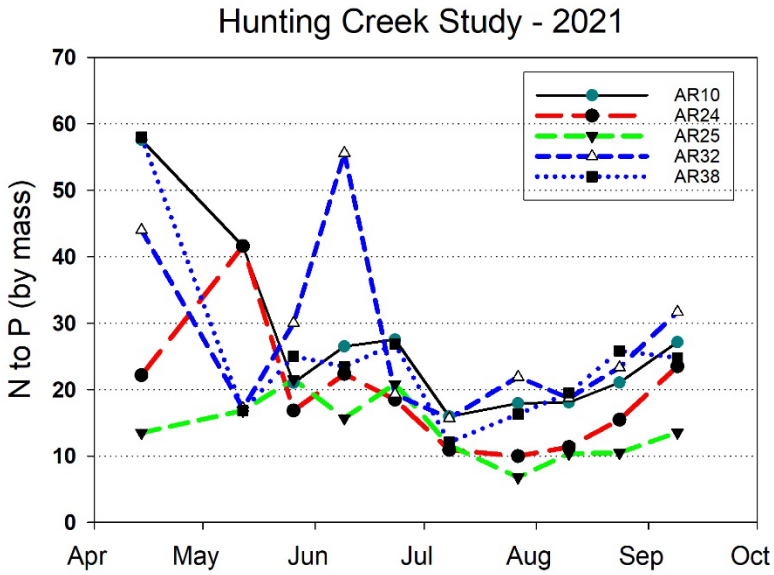

Figure 40. N/P Ratio (by mass). Tidal CSO Impact Stations.

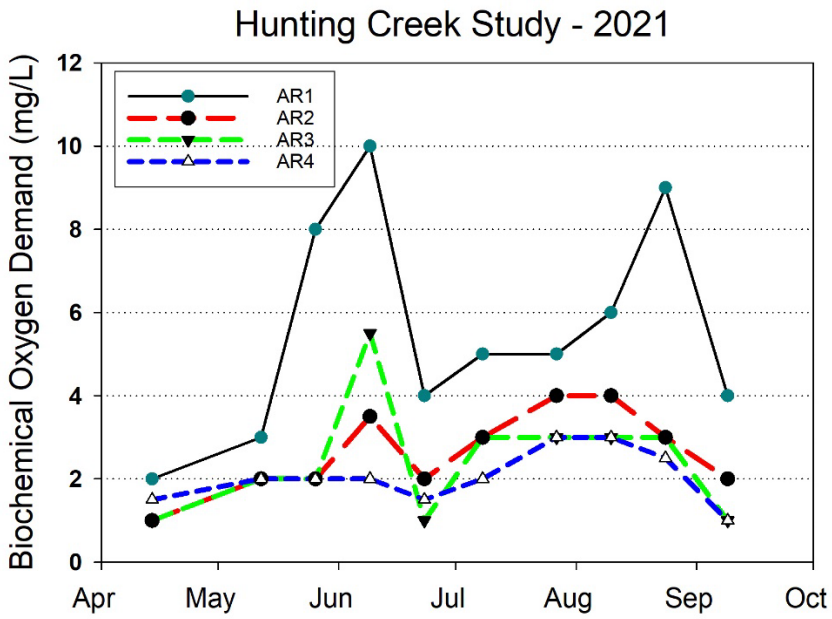

Biochemical oxygen demand (BOD) measures the amount of decomposable organic matter in the water as a function of how much oxygen it consumes as it breaks down over a given number of days. Most commonly the number of days used is 5. BOD is a good indicator of the potential for oxygen depletion in water. BOD is composed both dissolved organic compounds in the water as well as microbes such as bacteria and algae which will respire and consume oxygen during the period of measurement.

Figure 41. Biochemical Oxygen Demand (mg/L). Tidal Main Stations. Month tick is at first day of month.

BOD was consistently less than 4 mg/L at AR2, AR3, and AR4 (Figure 41). At AR1 values were greater than 4 on several dates and as high as 10. At the AR24 and AR25 values were often above 4, but at other Tidal CSO Impact stations values of 1-4 were observed (Figure 42).

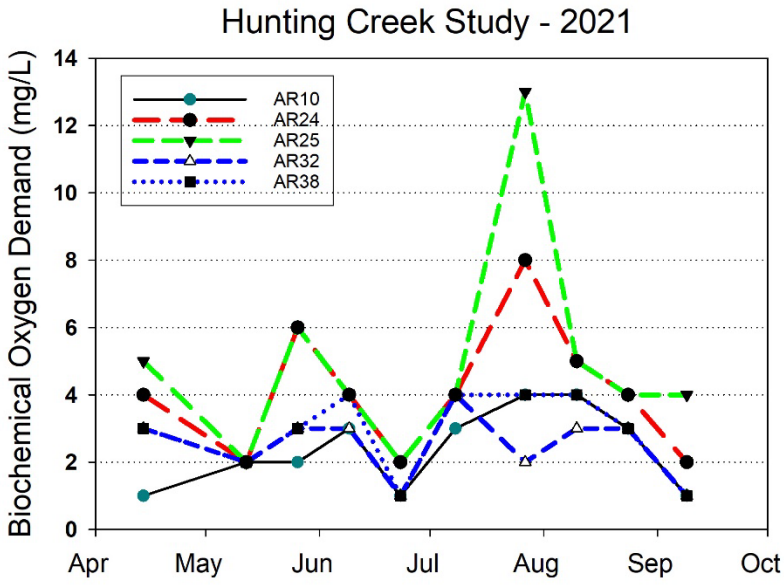

Figure 42. Biochemical Oxygen Demand (mg/L). Tidal CSO Impact Stations.

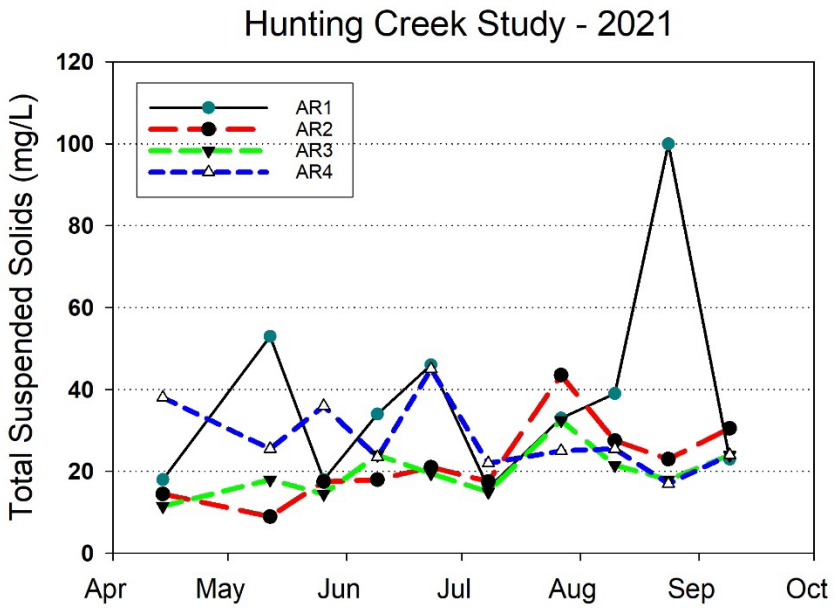

Total suspended solids (TSS) is measured by filtering a known amount of water through a fine filter which retains all or virtually all particles in the water. This filter is then dried and the weight of particles on the filter determined by difference. TSS consists of both organic and inorganic particles. During periods of low river and tributary inflow, organic particles such as algae may dominate. During storm flow periods or heavy winds causing resuspension, inorganic particles may dominate.

Figure 43. Total Suspended Solids (mg/L). Tidal Main Stations. Month tick is at first day of month.

Total suspended solids was generally in the range 15-40 mg/L at the Tidal Main Stations and at AR10, AR32, and AR38 (Figures 43&44). Again, higher values were observed at AR1, AR24, and AR25 similar to organic nitrogen and total phosphorus.

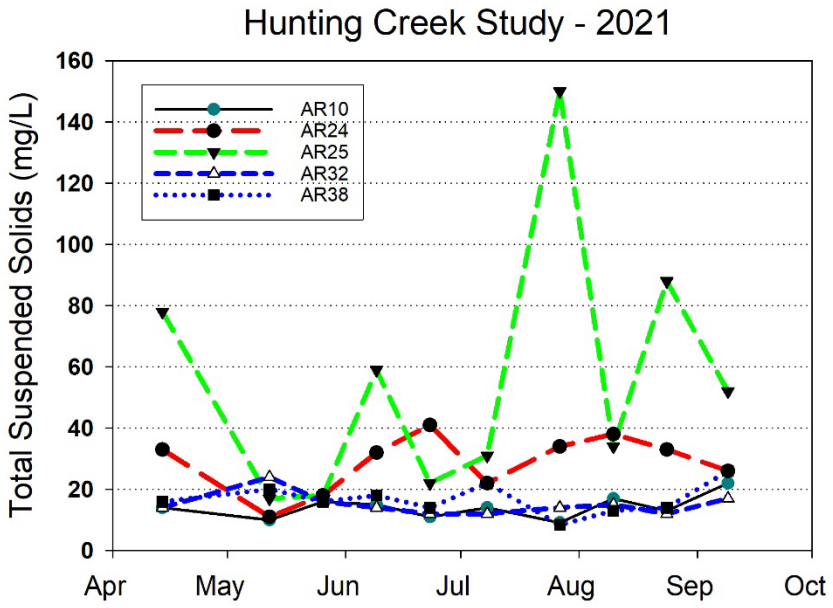

Figure 44. Total Suspended Solids. Tidal CSO Impact Stations.

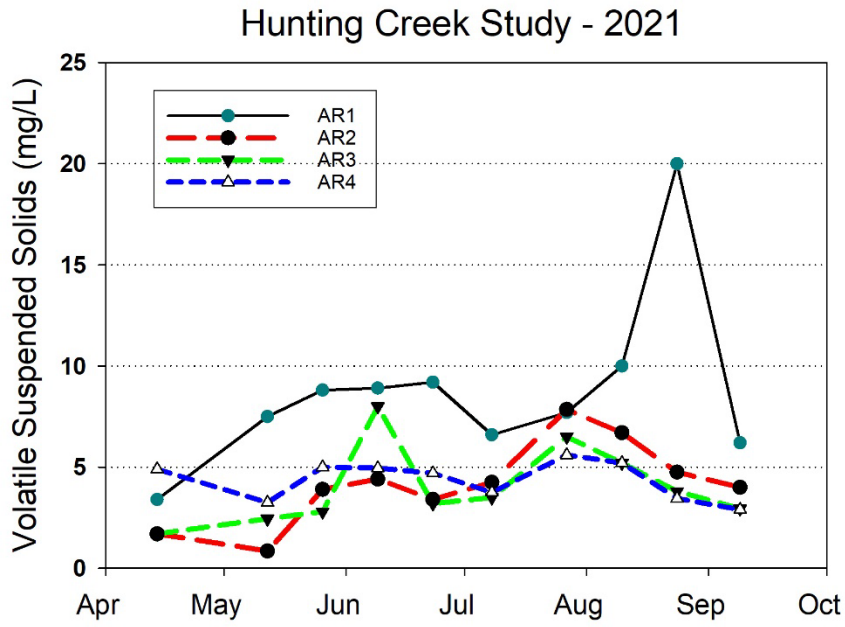

Volatile suspended solids (VSS) is determined by taking the filters used for TSS and then ashing them to combust (volatilize) the organic matter. The organic component is then determined by difference. VSS is a measure of organic solids in a water sample. These organic solids could be bacteria, algae, or detritus. Origins include sewage effluent, algae growth in the water column, or detritus produced within the waterbody or from tributaries. In summer in Gunston Cove a chief source is algal (phytoplankton) growth.

Figure 45. Volatile Suspended Solids (mg/L). Tidal Main Stations. Month tick is at first day of month.

VSS values followed similar patterns. At the Tidal Main Stations and AR32 and AR38 values remained in the 2-6 mg/L range (Figures 45&46). Higher values were observed at AR1, AR24, and AR25 and once at AR32.

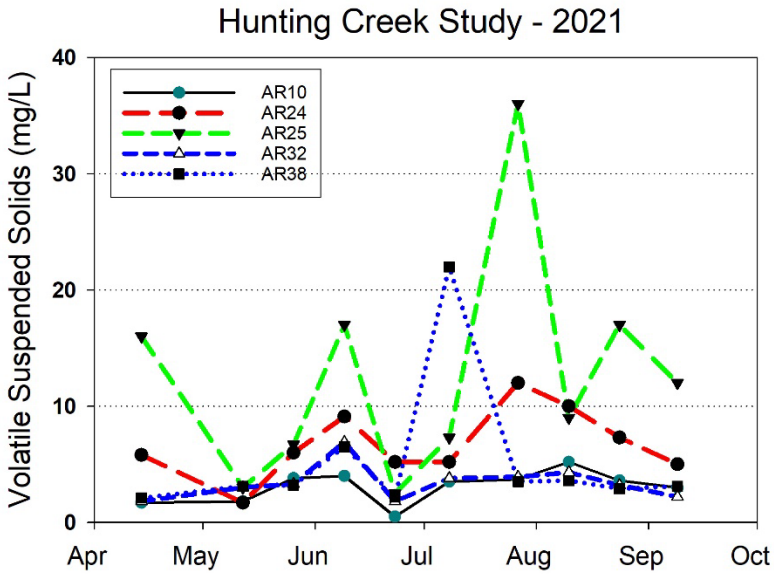

Figure 46. Volatile Suspended Solids (mg/L). Tidal CSO Impact Stations.

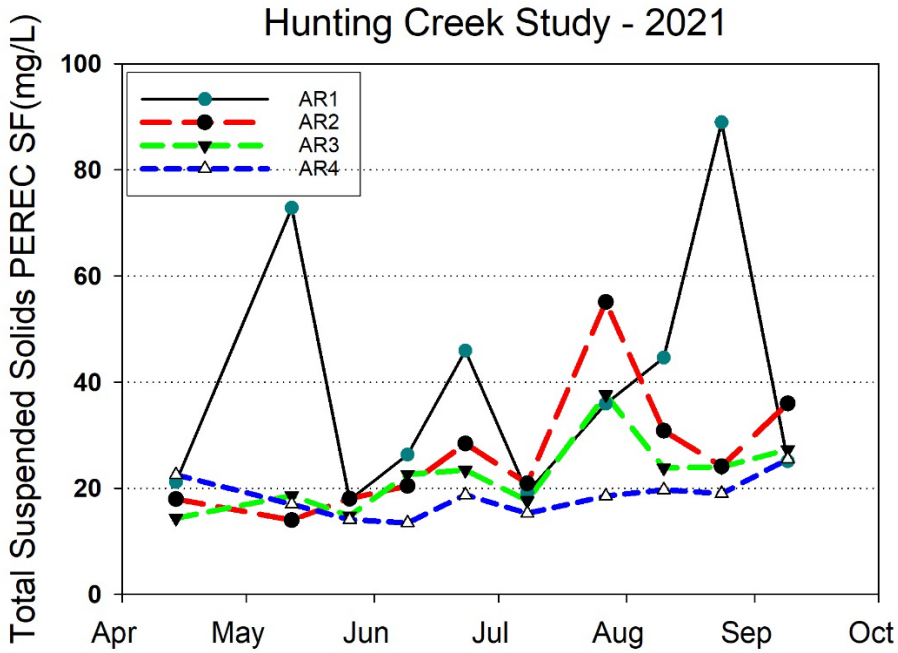

Figure 47. Total Suspended Solids. PEREC. Tidal Main Stations.

PEREC staff conducted TSS and VSS at the Tidal Main Stations. Again, AR2, AR3, and AR4 were generally in the 15-40 mg/L range for TSS while AR1 was higher on several occasions (Figure 47). AR2, AR3, and AR4 were less than 10 mg/L for VSS and showed a seasonal decline while AR1 showed higher values (Figure 48).

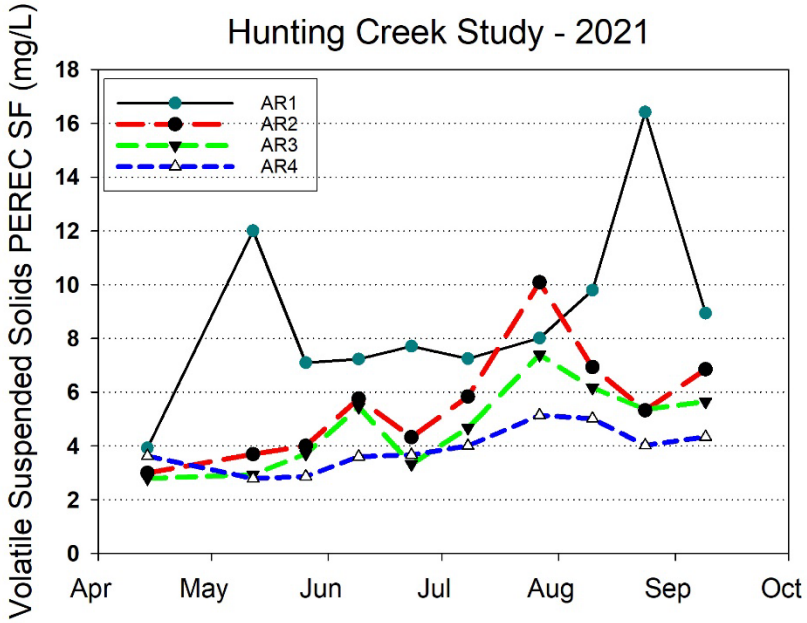

Figure 48. Volatile Suspended Solids. PEREC. Tidal CSO Impact Stations.

C. Physico-chemical Parameters: Tributary Stations – 2021

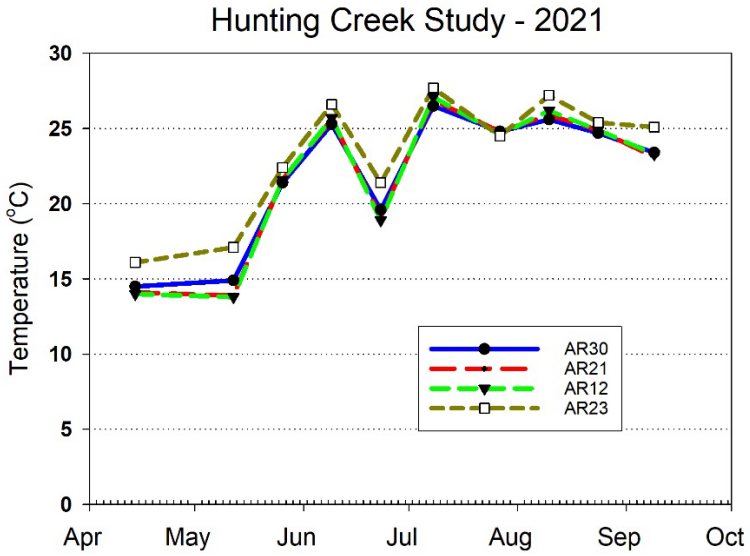

Figure 49. Water Temperature (ºC). GMU Field Data. Cameron Run Axis Tributaries. Month tick is at first day of month.

Water quality data for the tributary stations was graphed in two sets for each parameter: Cameron Run Axis stations running the length of Cameron Run and Hooffs Run Axis stations along the Hooffs Run Axis. Stations are arranged in the legends from upstream to downstream. Temperatures at almost all stations closely followed air temperatures (Figure 49&50). During summer, the Cameron Run Axis stations ran above 25°C while the Hooffs Run Axis stations were below 25°C.

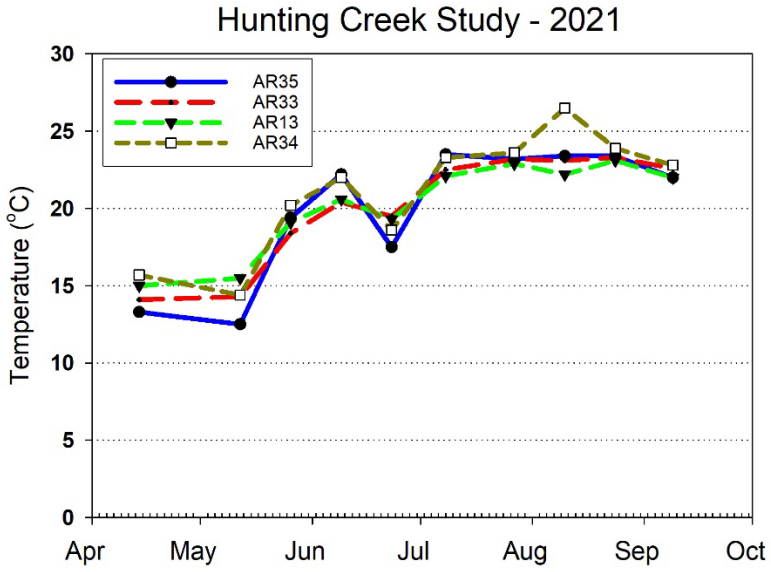

Figure 50. Water Temperature (ºC). GMU Field Data. Hooffs Run Axis Tributaries. Month tick is at first day of month.

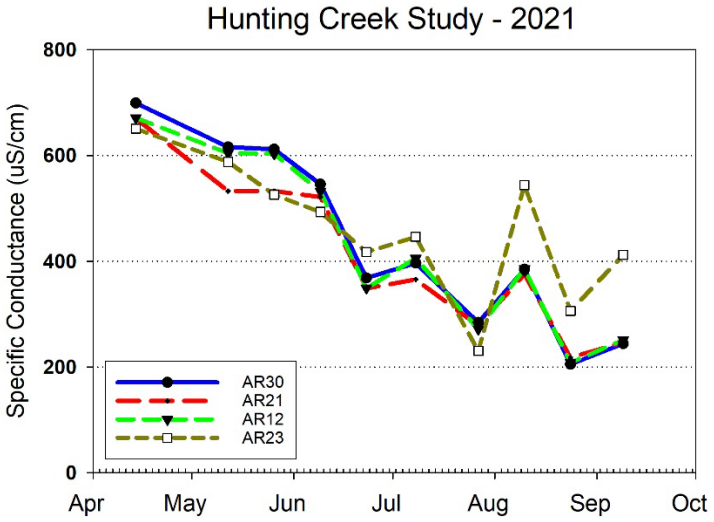

Figure 51. Specific Conductance (uS/cm). GMU Field Data. Cameron Run Axis Tributaries. Month tick is at first day of month.

Specific conductance was generally in the 200-700 uS/cm range and showed a clear decrease seasonally at the Cameron Run Axis stations (Figure 51). At the Hooffs Run Axis stations specific conductance started out the year somewhat lower and showed only a weak decline seasonally until September (Figure 52). The high values in spring in Cameron Run could be due to residual road salt in near surface groundwater that gradually leaked out through the year.

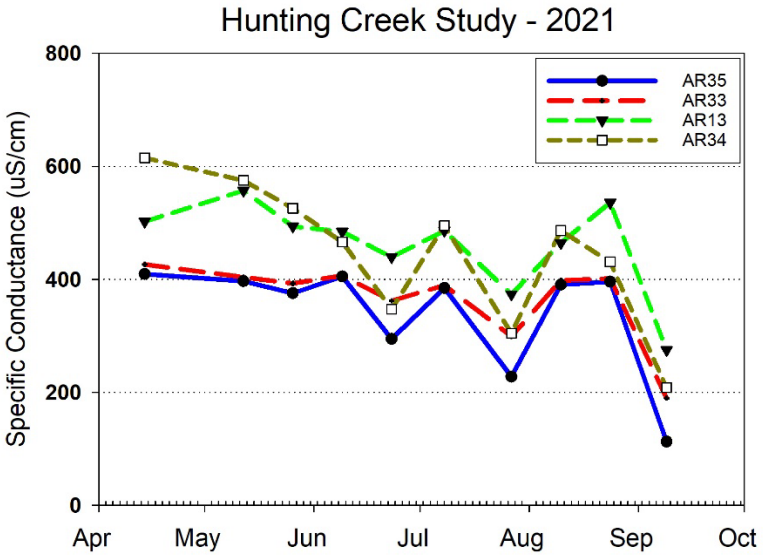

Figure 52. Specific Conductance (uS/cm). GMU Field Data. Hooffs Run Axis Tributaries. Month tick is at first day of month.

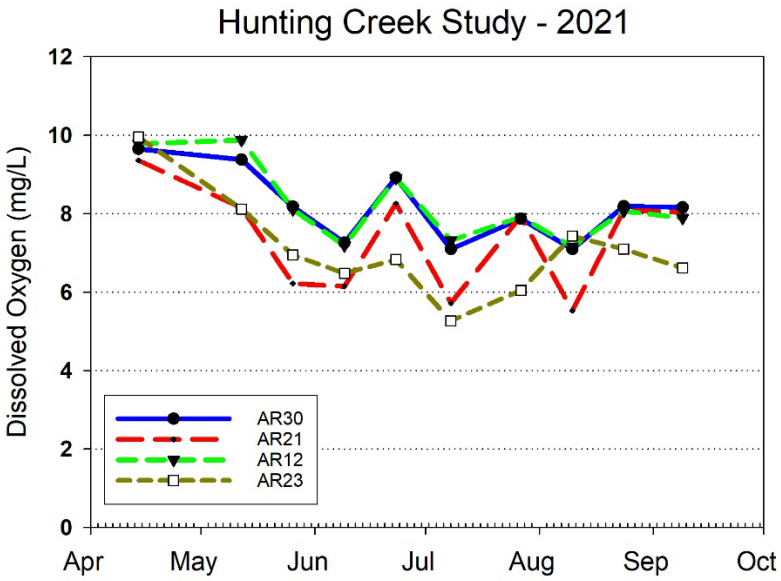

Figure 53. Dissolved Oxygen (mg/L) GMU Field Data. Cameron Run Axis stations. Month tick is at first day of month.

Dissolved oxygen (mg/L) at most of the Cameron Run Axis stations showed a seasonal pattern of declining values through the year reaching lows of 6-8 mg/L in July through September (Figure 53). Most of this trend was due to temperature effects since percent saturation values were in the 70-100% range with little seasonal pattern (Figure 54). And again, AR34 showed lower and variable values.

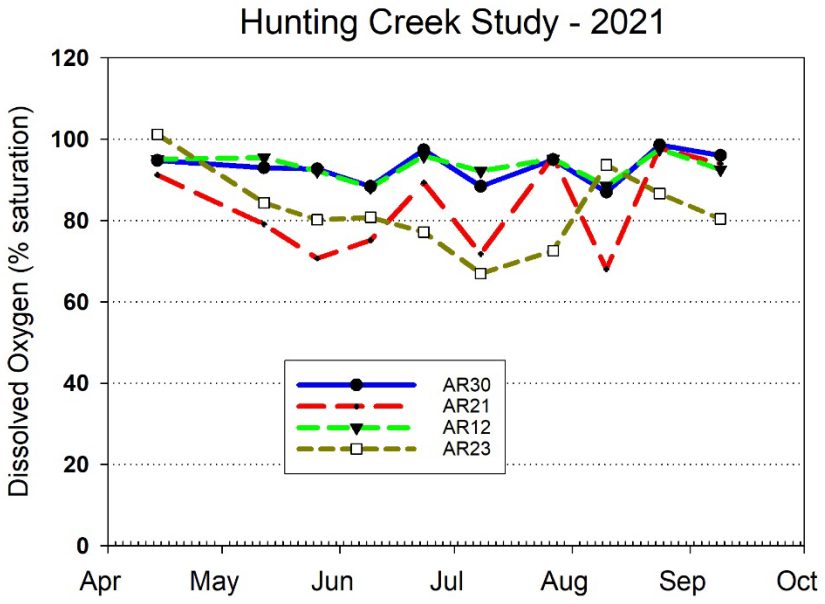

Figure 54. Dissolved Oxygen (% saturation) GMU Field Data. Cameron Run Axis stations. Month tick is at first day of month.

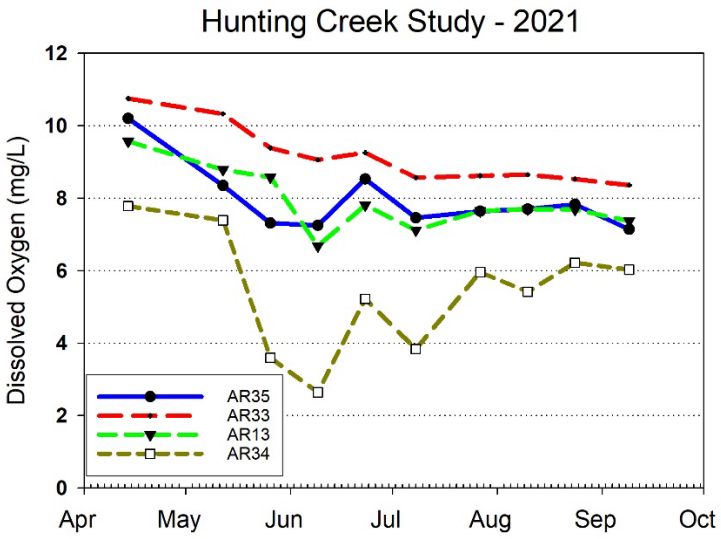

Figure 55. Dissolved Oxygen (mg/L) GMU Field Data. Hooffs Run Axis stations. Month tick is at first day of month.

A similar pattern was observed in the Hooffs Run Axis stations with the exception of AR34 which had lower values particularly in the summer dropping below 3 mg/L in early June (Figures 55&56).

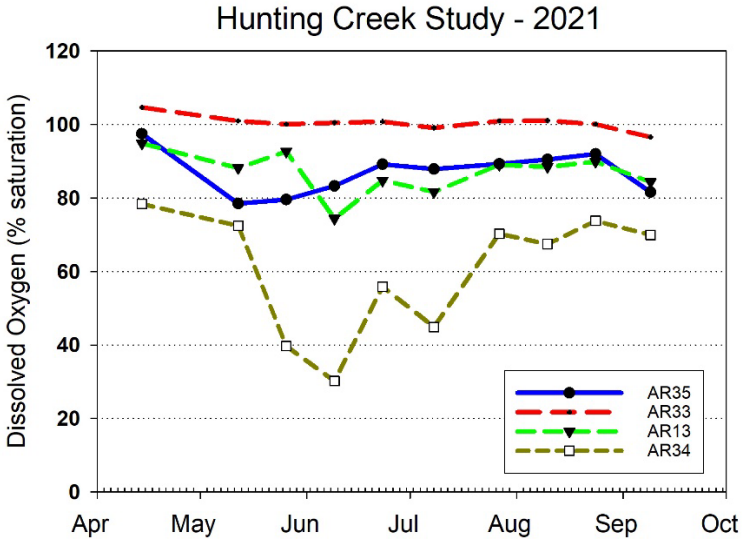

Figure 56. Dissolved Oxygen (% saturation) GMU Field Data. Hooffs Run Axis stations. Month tick is at first day of month.

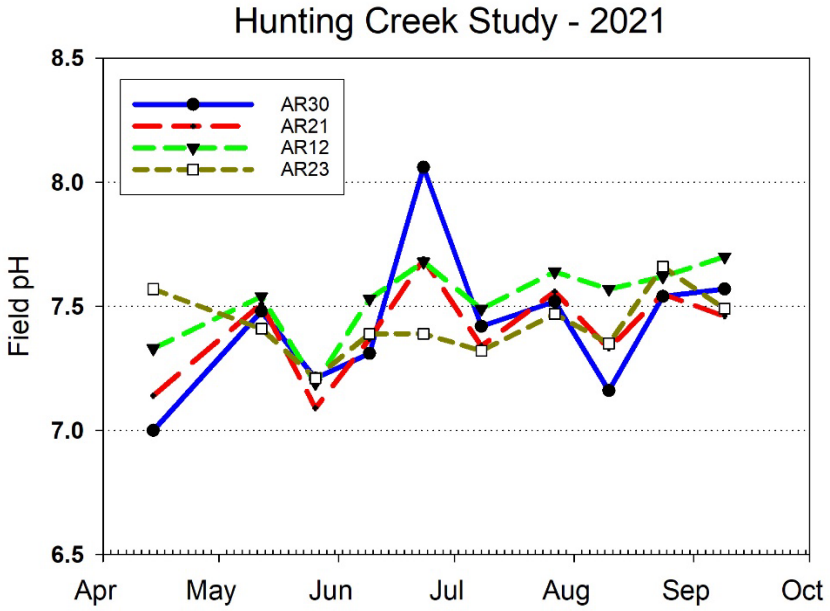

Figure 57. Field pH. GMU Field Data. Cameron Run Axis stations. Month tick is at first day of month.

Field pH followed a very similar seasonal pattern at all stations with most values centered around 7.5 (Figure 57). The highest value observed was 8.1 at AR30 in late June. AR35, AR33, and AR12 typically had relatively high values (Figure 58).

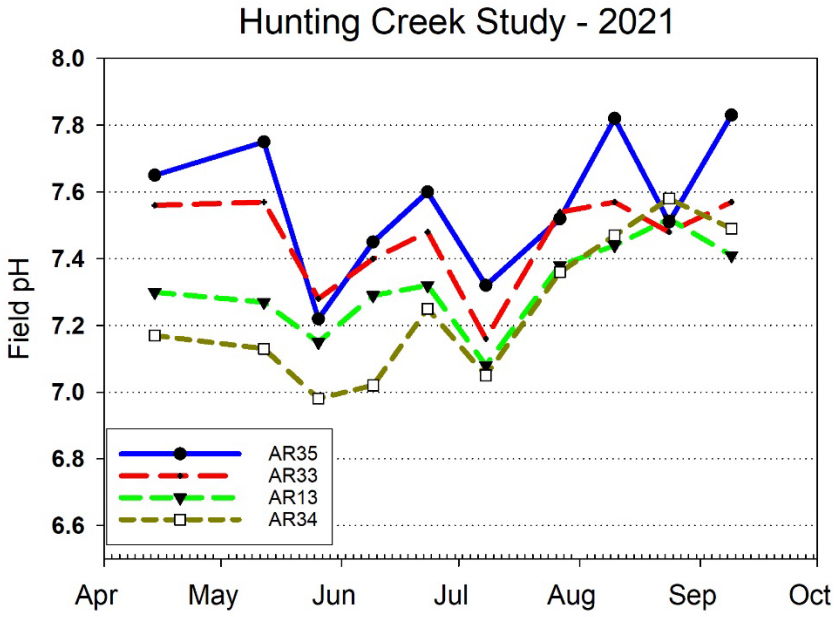

Figure 58. Field pH. GMU Field Data. Hooffs Run Axis stations. Month tick is at first day of month.

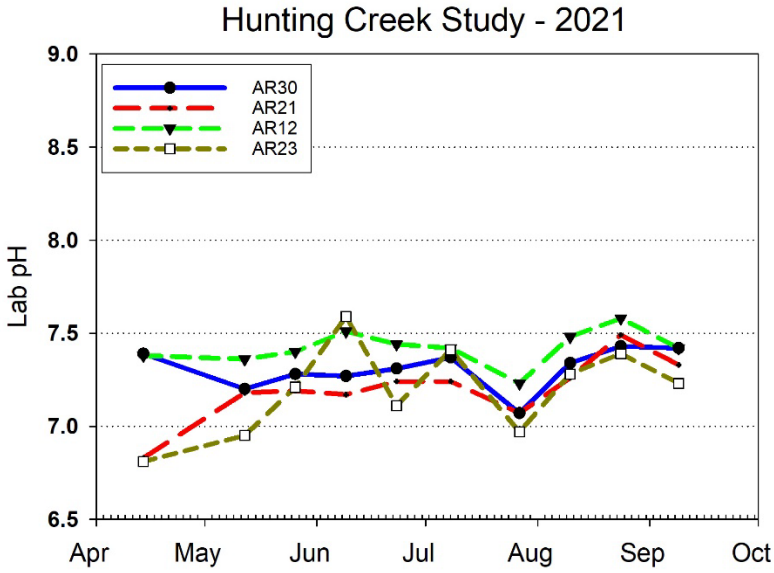

Figure 59. Lab pH. Alex Renew Lab Data. Cameron Run Axis stations. Month tick is at first day of month.

Lab pH values were more tightly grouped but again were generally in the range 7 to 7.5 (Figure 59&60).

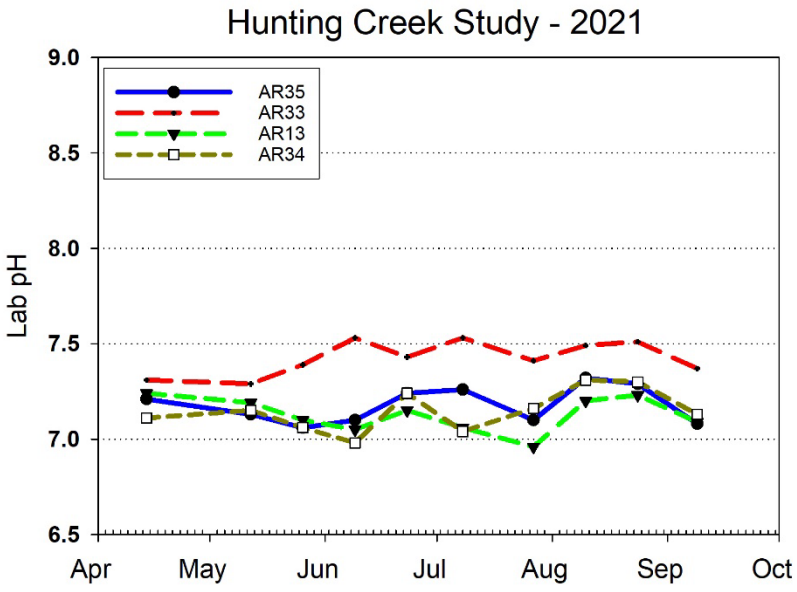

Figure 60. Lab pH. Alex Renew Lab Data. Hooffs Run Axis stations. Month tick is at first day of month.

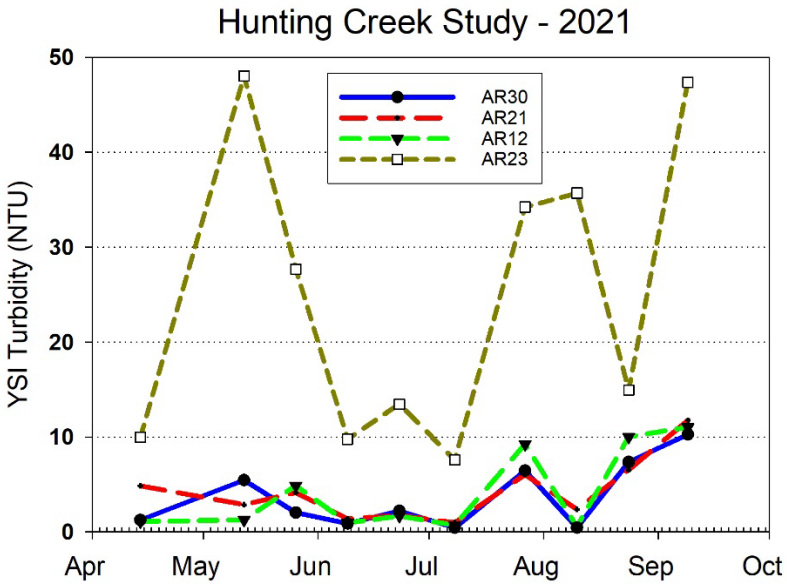

Figure 61. YSI Turbidity. GMU Field Data. Cameron Run Axis stations. Month tick is at first day of month.

YSI Turbidity was generally below 10 NTU at most stations (Figures 61&62). Conspicuously different were AR23, AR34, and AR13. AR13 and AR34 are along lower Hooffs Run and AR34 is in upper Hunting Creek just below Hooffs Run and across from the Alex Renew effluent.

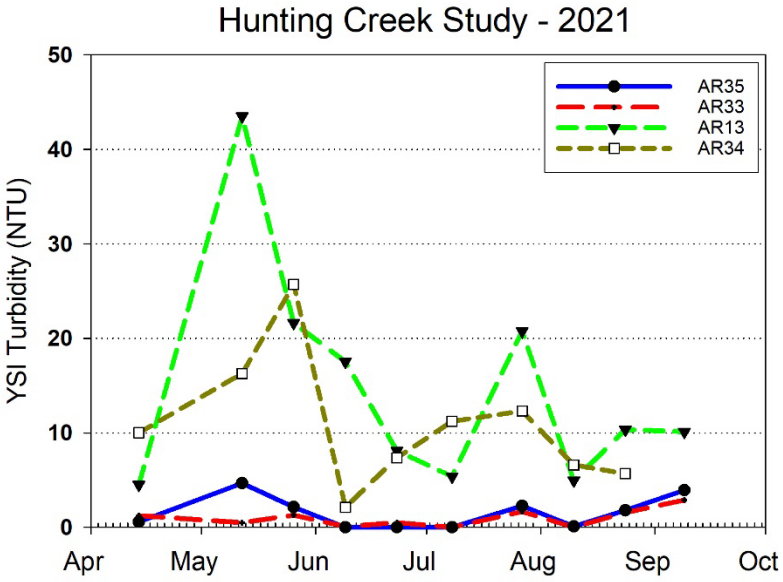

Figure 62. YSI Turbidity. GMU Field Data. Hooffs Run Axis stations. Month tick is at first day of month.

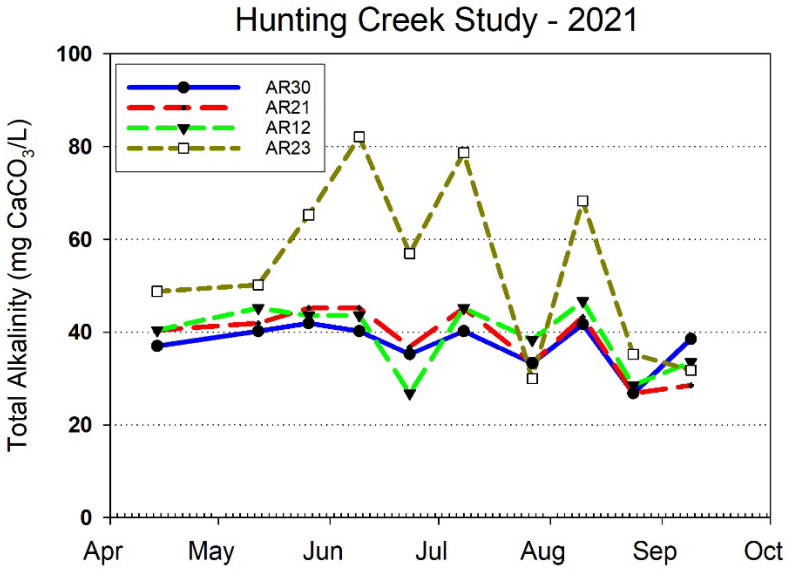

Figure 63. Total Alkalinity (mg/L as $CaCO_3$) AlexRenew Lab Data. Cameron Run Axis stations. Month tick is at first day of month.

Total alkalinity was generally in the 30-50 mg/L range with little seasonal change observed. (Figure 63&64). Clearly different was AR23 which often had much higher values. This may have been attributable to the fact that AR23 is directly across from the Alex Renew effluent discharge.

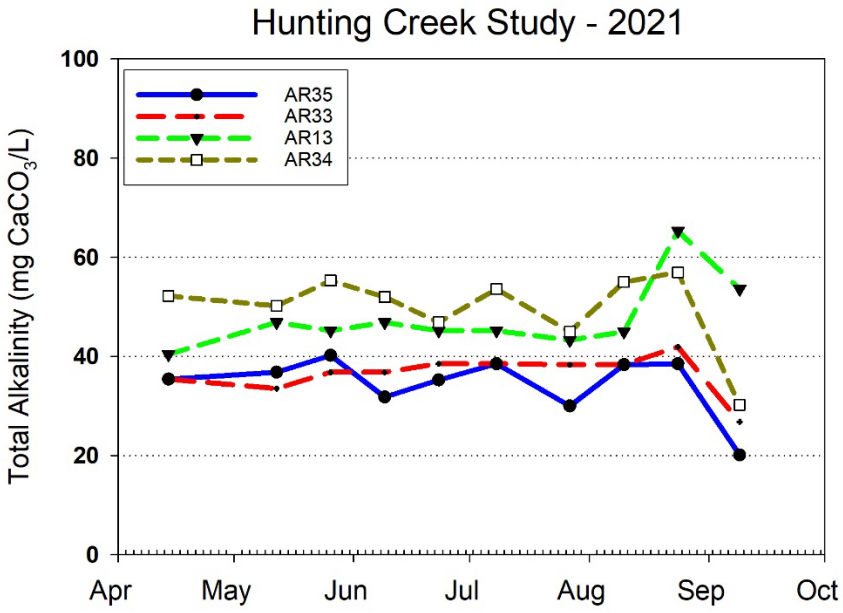

Figure 64. Total Alkalinity (mg/L as $CaCO_3$) AlexRenew Lab Data. Hooffs Run Axis stations. Month tick is at first day of month.

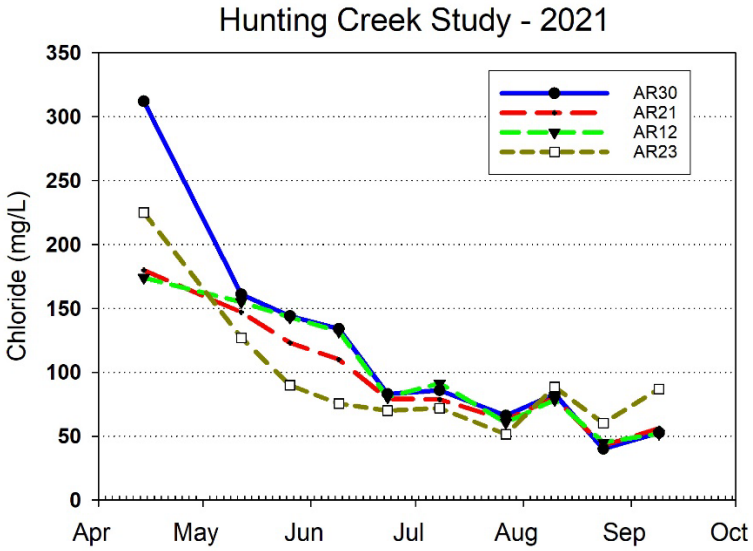

Figure 65. Chloride (mg/L) AlexRenew Lab Data. Cameron Run Axis stations. Month tick is at first day of month.

Similar to conductivity, chloride levels showed a strong pattern of decrease from April through to mid-September (Figure 65&66). Also similar to conductivity the trend in chloride levels was stronger in the Cameron Run Axis stations than in the Hooffs Run Axis stations. With highest values at AR30, farthest up in the watershed, this trend points towards road salts from the entire watershed causing the elevated values in April and gradually declining through dilution during the year.

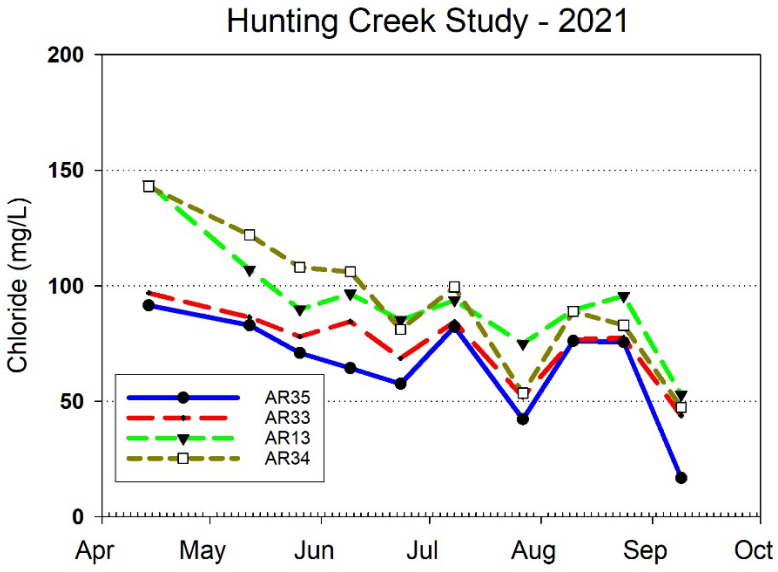

Figure 66. Chloride (mg/L) AlexRenew Lab Data. Hooffs Run Axis stations. Month tick is at first day of month.

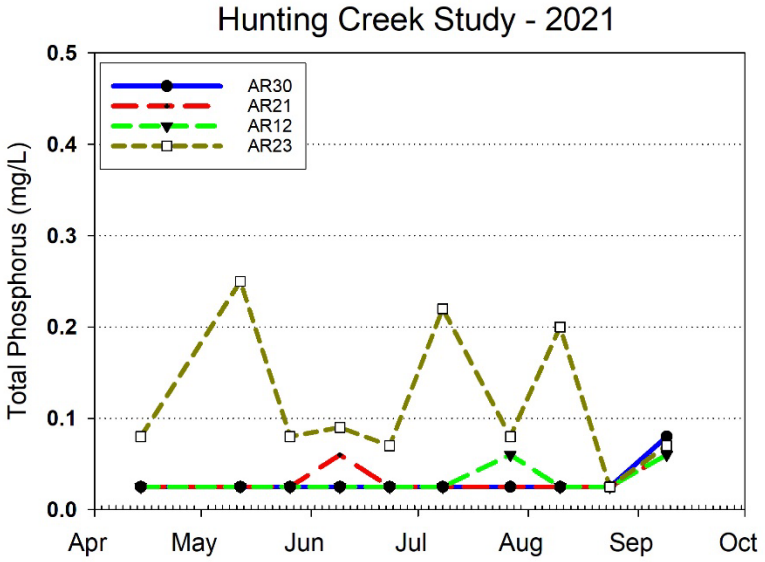

Figure 67. Total Phosphorus (mg/L) AlexRenew Lab Data. Cameron Run Axis stations. Month tick is at first day of month.

The detection limit for total phosphorus was 0.05 mg/L and samples less than the detection limit are graphed as 0.025 mg/L. Total phosphorus levels were generally relatively low at most tributary stations (<0.05 mg/L) and did not vary much seasonally (Figure 67). Highest values along the Cameron Run axis were observed at AR23 at the end of the axis. Values along the Hooffs Run axis were also generally below detection limit at AR33 and AR35 (furthest upstream) (Figure 68). At the lower end of this axis AR13 and AR34 numerous higher values were observed with an increasing seasonal trend at AR34.

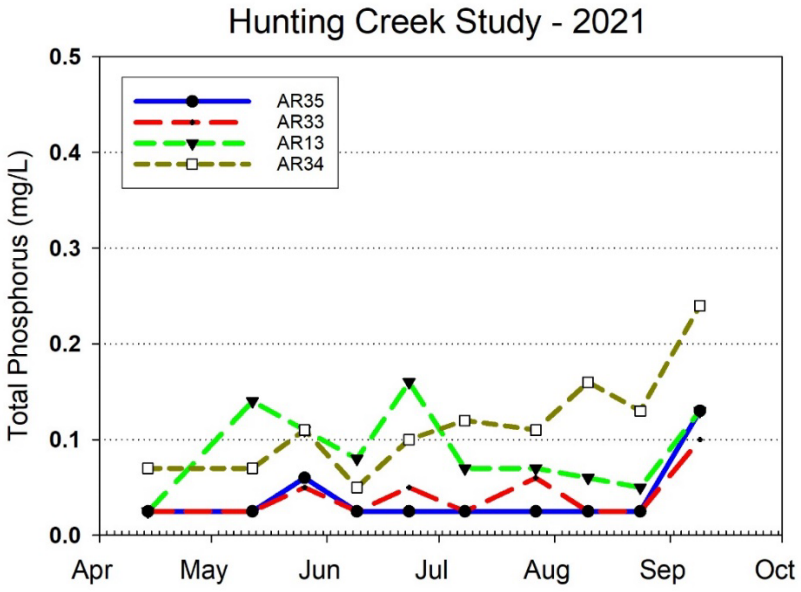

Figure 68. Total Phosphorus (mg/L) AlexRenew Lab Data. Hooffs Run Axis stations. Month tick is at first day of month.

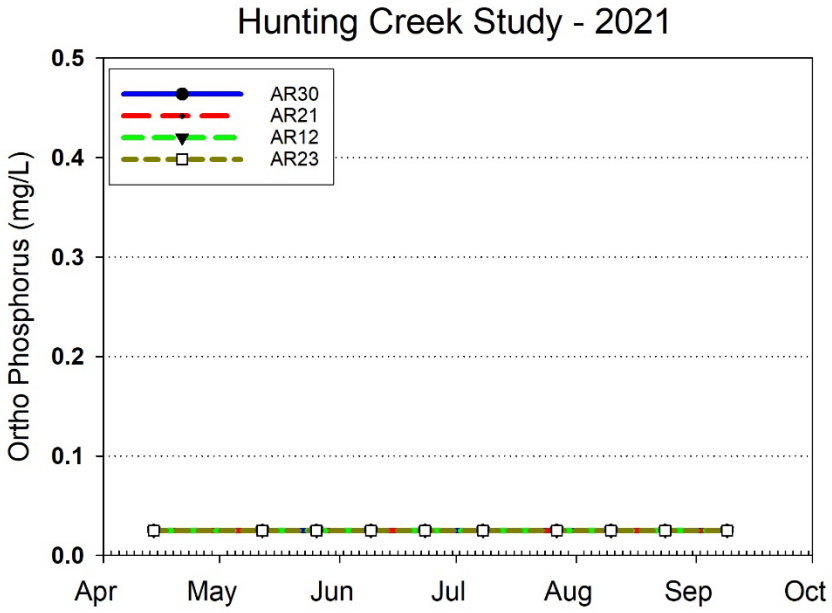

Figure 69. Ortho-Phosphorus (mg/L) AlexRenew Lab Data. Cameron Run Axis stations. Month tick is at first day of month.

Ortho phosphorus levels were almost always below the detection limit of 0.05 mg/L (Figures 69&70). Some slightly higher readings were observed at AR35 and AR33 on the last sampling date.

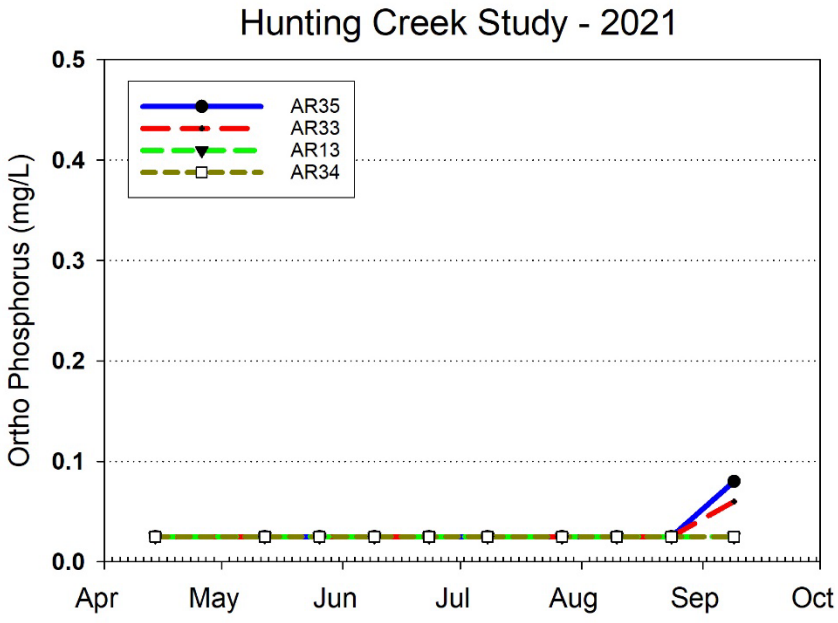

Figure 70. Ortho-Phosphorus (mg/L) AlexRenew Lab Data. Hooffs Run Axis stations. Month tick is at first day of month.

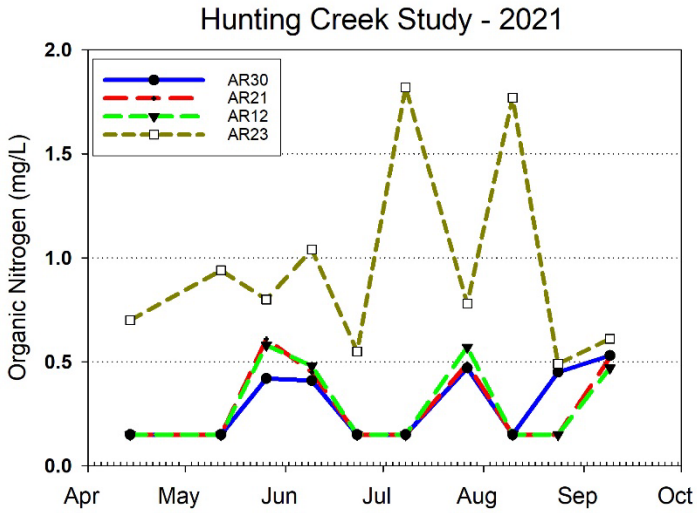

Figure 71. Organic Nitrogen (mg/L) AlexRenew Lab Data. Cameron Run Axis stations. Month tick is at first day of month.

Tributary levels of organic nitrogen are depicted in Figures 71&72. Values were generally below 0.5 mg/L at most stations with little obvious pattern. However, at AR23 values were significantly higher and at AR34 higher values and an increasing trend were observed.

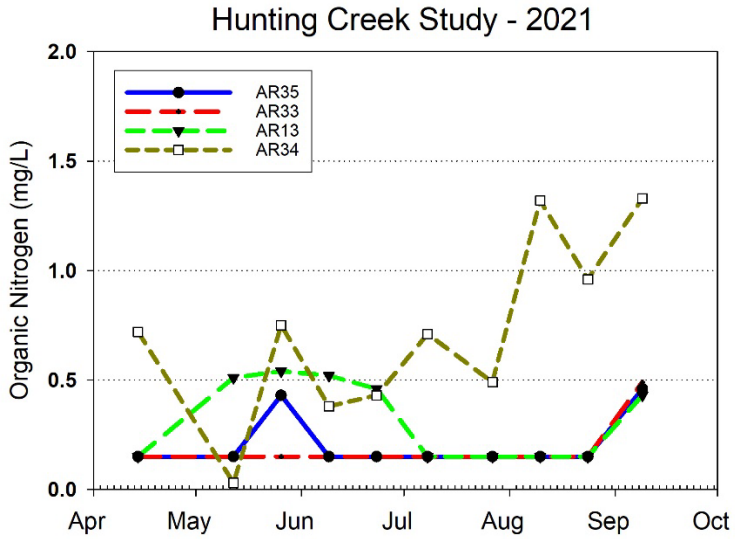

Figure 72. Organic Nitrogen (mg/L) AlexRenew Lab Data. Hooffs Run Axis stations. Month tick is at first day of month.

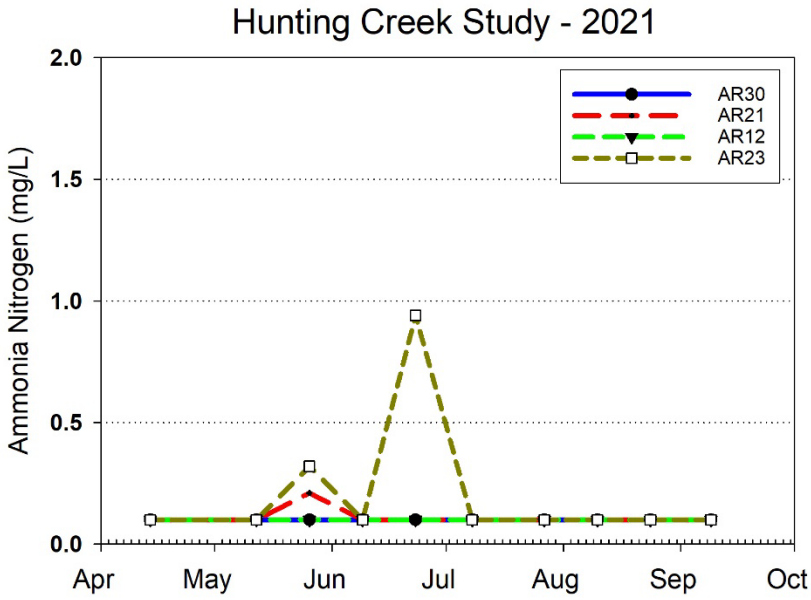

Figure 73. Ammonia Nitrogen (mg/L) AlexRenew Lab Data. Cameron Run Axis stations. Month tick is at first day of month.

Ammonia nitrogen values were below the 0.2 mg/L limit of detection in most samples from both axes (Figure 73&74). However, some slightly higher values were observed at AR23 and AR34.

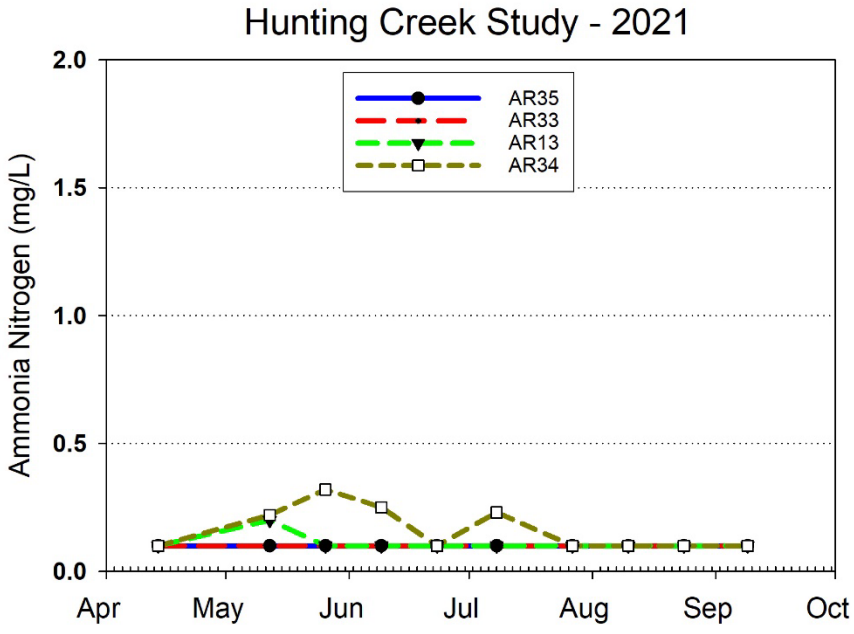

Figure 74. Ammonia Nitrogen (mg/L) AlexRenew Lab Data. Hooffs Run Axis stations. Month tick is at first day of month.

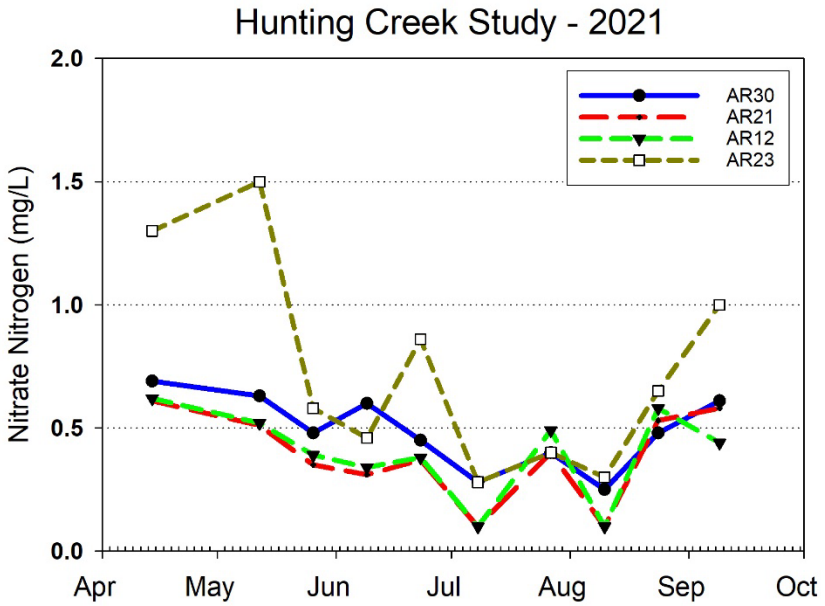

Figure 75. Nitrate Nitrogen (mg/L) AlexRenew Lab Data. Cameron Run Axis stations. Month tick is at first day of month.

Nitrate nitrogen values was generally below 0.7 mg/L along the Cameron Run Axis except at AR23 (Figure 75). Along the Hooffs Run Axis values were consistently higher, particularly at AR 33 which averaged about 2.0 mg/L (Figure 76). The higher values for nitrate in the Hooffs Run Axis reflects the highly density residential and commercial land uses in that watershed which often hive elevated nitrate levels.

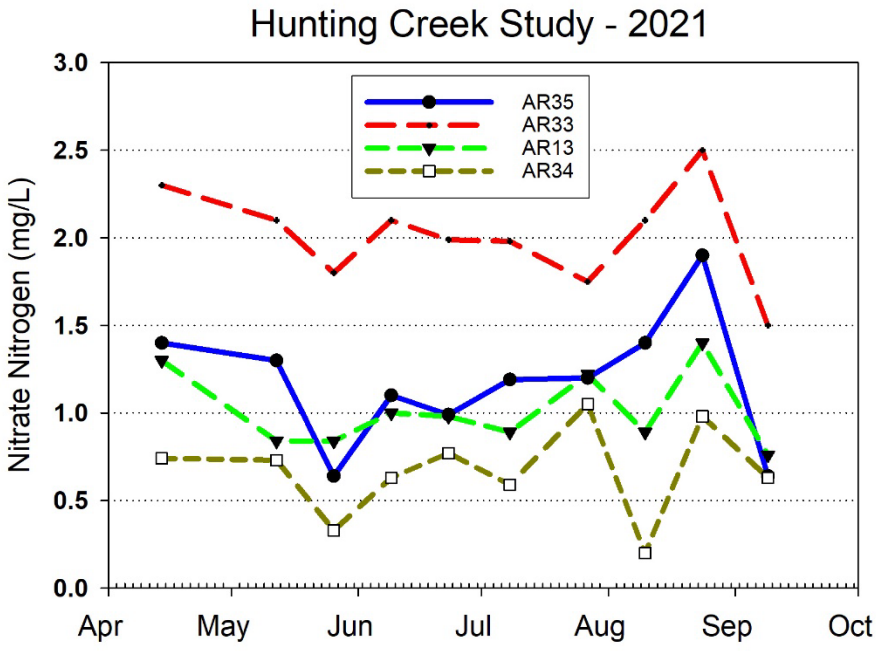

Figure 76. Nitrate Nitrogen (mg/L) AlexRenew Lab Data. Hooffs Run Axis stations. Month tick is at first day of month.

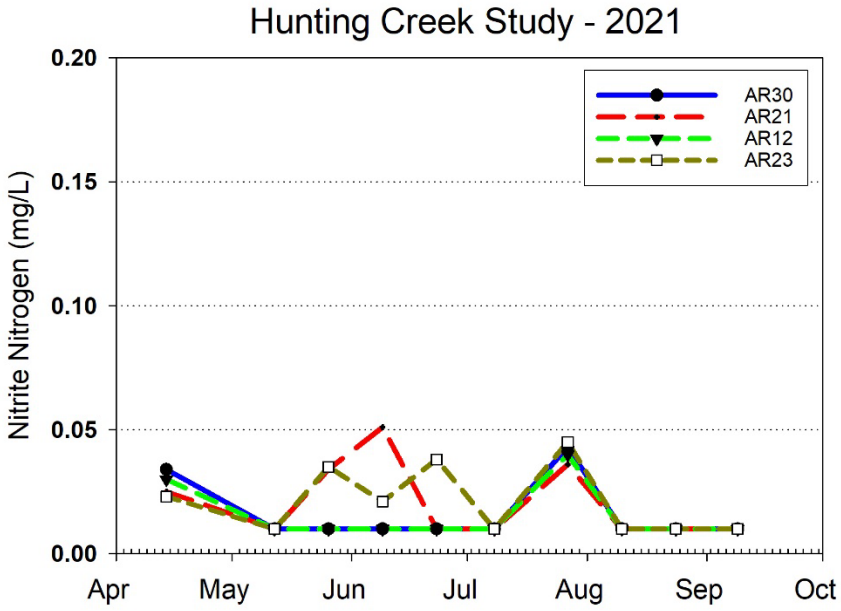

Figure 77. Nitrite Nitrogen (mg/L) AlexRenew Lab Data. Cameron Run Axis stations. Month tick is at first day of month.

Nitrite nitrogen was generally quite low (<0.04) at all stations most of the time (Figures 77&78). The highest value observed was 0.8 mg/L at AR13 in late July.

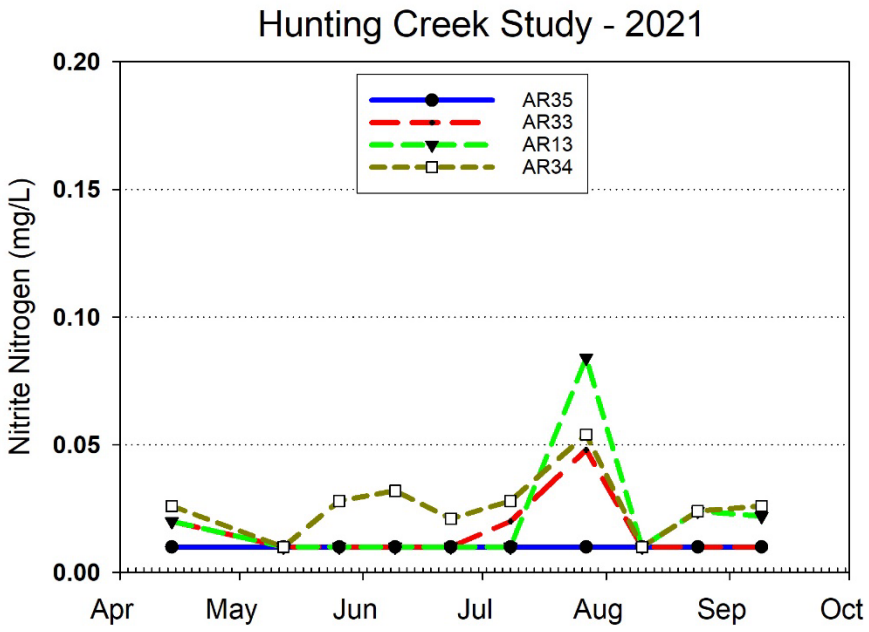

Figure 78. Nitrite Nitrogen (mg/L) AlexRenew Lab Data. Hooffs Run Axis stations. Month tick is at first day of month.

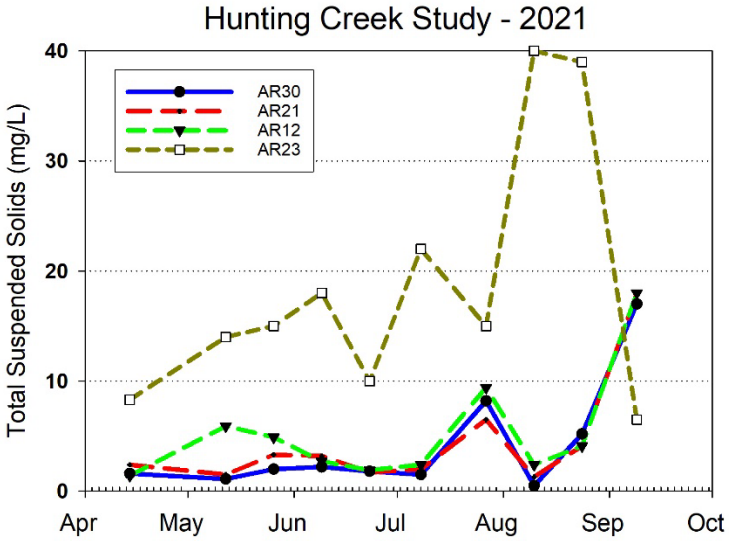

Figure 79. Total Suspended Solids (mg/L) AlexRenew Lab Data. Cameron Run Axis stations. Month tick is at first day of month.

Total suspended solids concentrations at Cameron Run Axis stations was generally below 10 mg/L (Figure 79). The exception was AR23 in upper Hunting Creek near the Alex Renew outfall which consistently had much higher values. TSS was also quite low (<10 mg/L) at most stations in the Hooffs Run Axis for most of the year (Figure 80). The exceptions were AR13 and AR34 in lower Hooffs Run which often had higher readings.

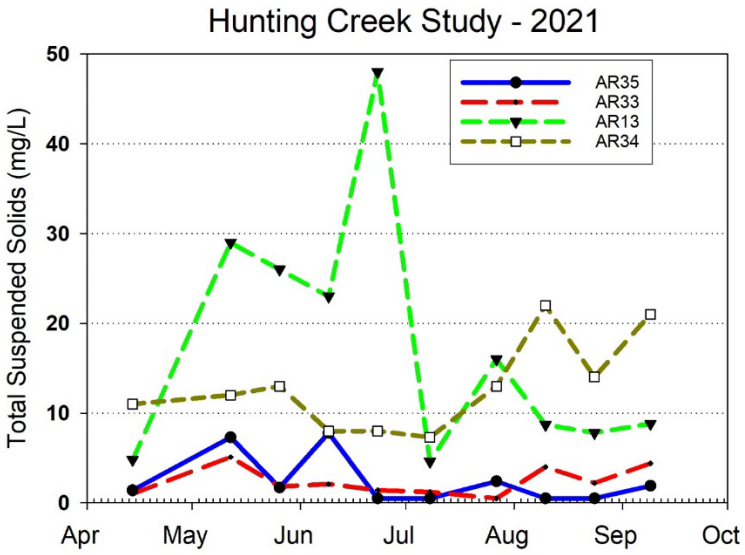

Figure 80. Total Suspended Solids (mg/L) AlexRenew Lab Data. Hooffs Run Axis stations. Month tick is at first day of month.

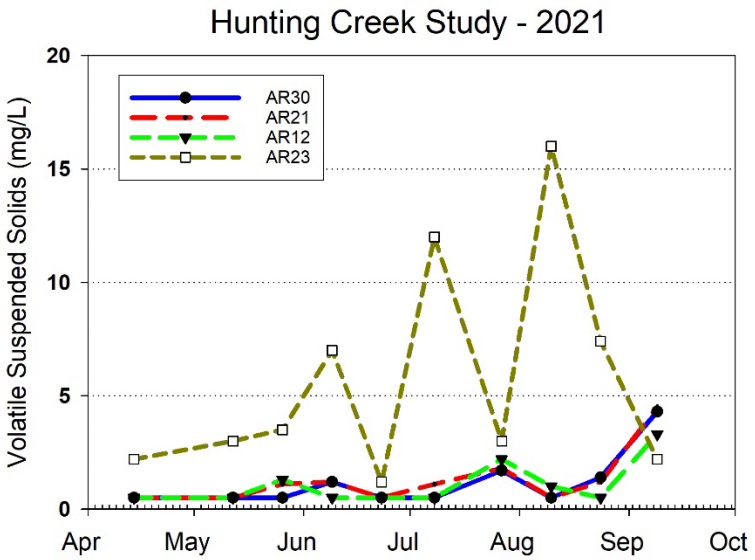

Figure 81. Volatile Suspended Solids (mg/L) AlexRenew Lab Data. Cameron Run Axis stations. Month tick is at first day of month.

VSS along the Cameron Run Axis was generally half of TSS with highest values at AR23 again (Figure 81). VSS values were below 5 mg/L on the last sampling date. For the Hooffs Run Axis stations, most values were again below 5 mg/L (Figure 82). However, higher readings were observed sometimes at AR13 and AR34 at the lower end of the Hooffs Run Axis.

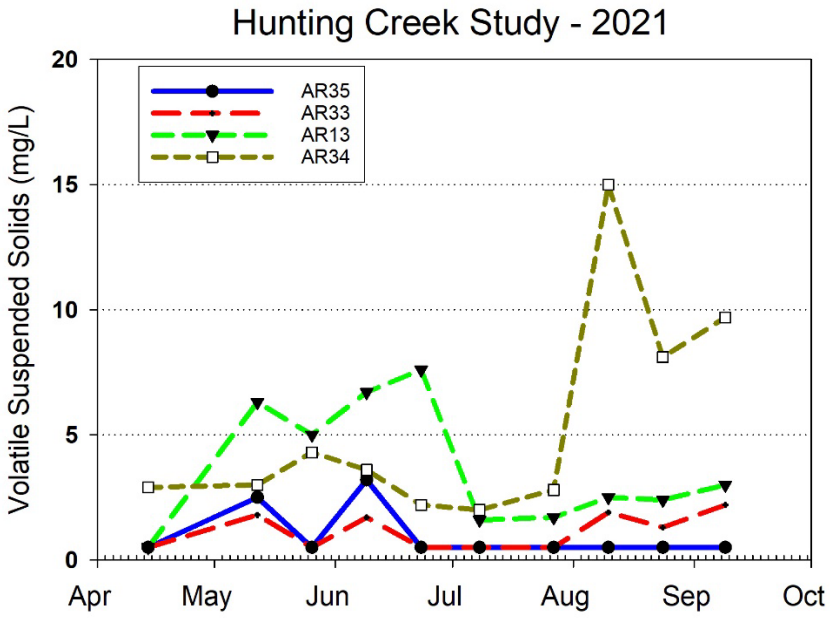

Figure 82. Volatile Suspended Solids (mg/L) AlexRenew Lab Data. Hooffs Run Axis stations. Month tick is at first day of month.

D. Phytoplankton - 2021

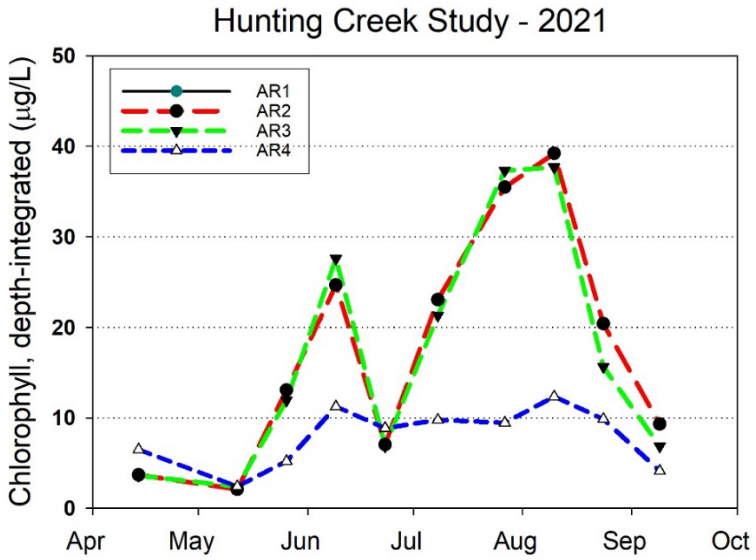

Chlorophyll *a* is a measure of the amount of algae growing in the water column. These suspended algae are called phytoplankton, meaning "plant wanderers". In addition to the true algae (greens, diatoms, cryptophytes, etc.) the term phytoplankton includes cyanobacteria (sometimes known as "blue-green" algae). Both depth-integrated and surface chlorophyll values are measured due to the capacity of phytoplankton to aggregate near the surface under certain conditions.

Figure 83. Chlorophyll *a* (µg/L). Depth-integrated. GMU Lab Data. Month tick is at the first day of month.

Depth-integrated chlorophyll *a* values at AR2 and AR3 (the embayment stations) were very similar throughout the year with peak values of about 25 µg/L in early June and 40 µg/L in early August (Figure 83). In the river values showed less seasonal pattern and remained at about 10 µg/L from June through August. Similar values were observed in surface chlorophyll a at AR2, AR3, and AR4 (Figure 84). Values at AR1 were similar to those at the other stations until August and September when higher levels were observed. It was during this period that the datamappinig was conducted which showed high chlorophyll levels in the embayment near AR1.

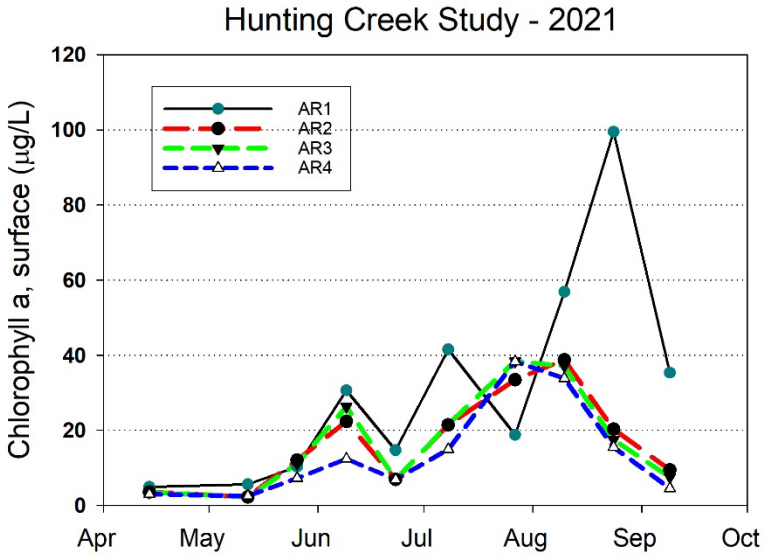

In the tidal freshwater Potomac generally, there is very little difference in surface and depth-integrated chlorophyll levels because tidal action keeps the water well-mixed which overcomes any potential surface aggregation by the phytoplankton. Summer chlorophyll concentrations above 30 ug/L are generally considered characteristic or eutrophic conditions.

Figure 84. Chlorophyll *a* (µg/L). Surface. GMU Lab Data. Month tick is at first day of month.

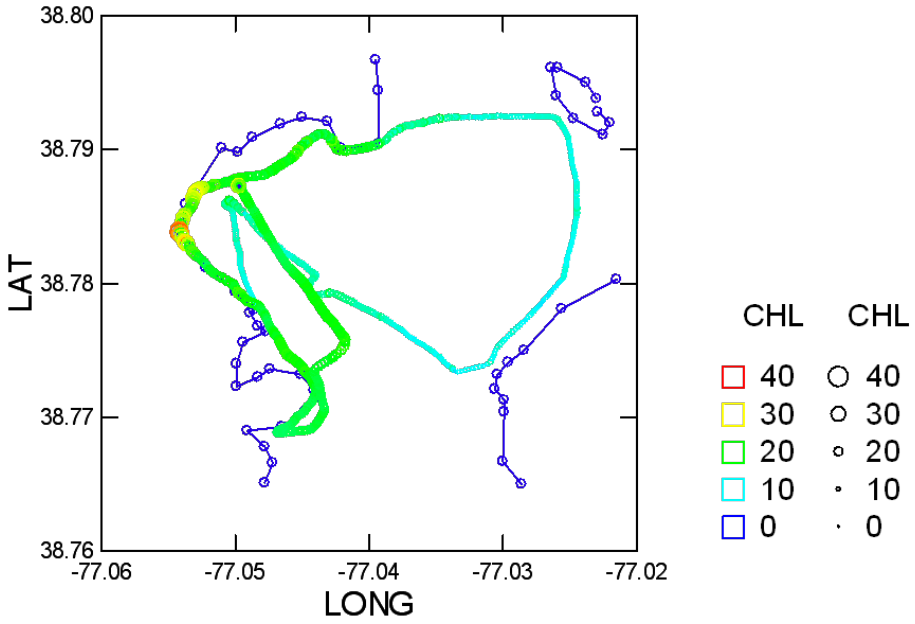

Figure 85a. Water Quality Mapping. June 13, 2021. Chlorophyll YSI (µg/L).

On both dates water quality mapping showed that chlorophyll a was generally quite low throughout most of the study area (Figure 85a,b). The exception was inner Hunting Creek near the shoreline where values as high as 30 ug/L were observed. This pattern correlated well with the patterns in dissolved oxygen and pH, consistent with the hypothesis of substantial phytoplankton activity in the inner Hunting Creek area.

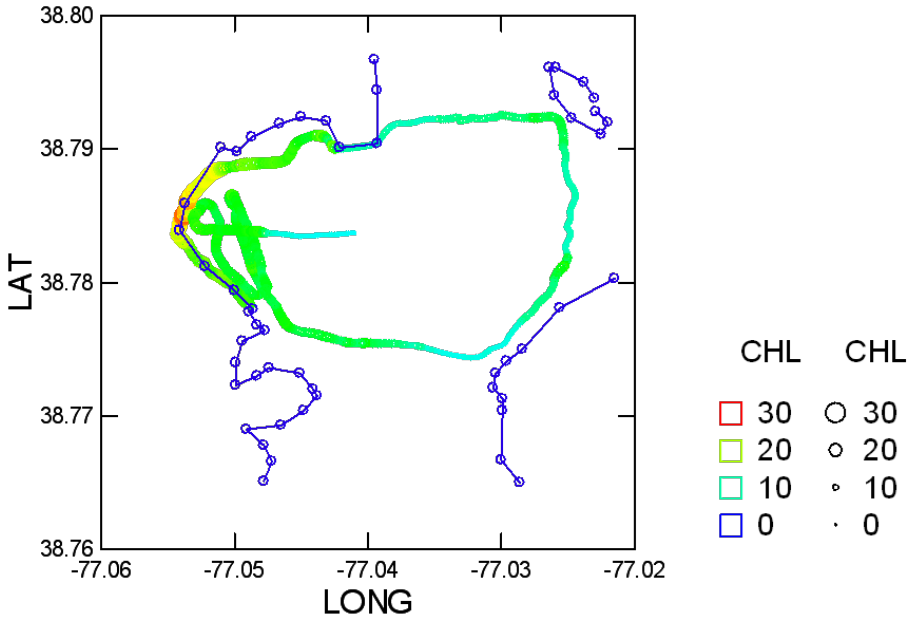

Figure 85b. Water Quality Mapping. August 9, 2021. Chlorophyll YSI (µg/L).

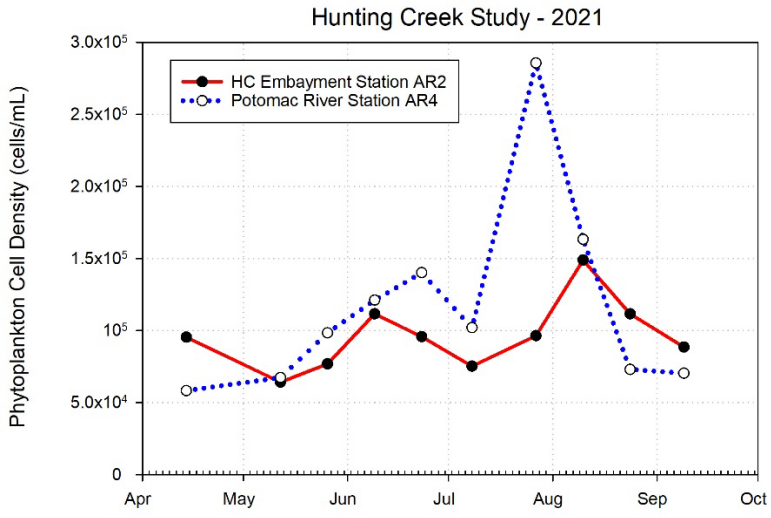

Figure 89. Phytoplankton Cell Density (cells/mL).

Phytoplankton cell density provides a measure of the number of algal cells per unit volume. This is a rough measure of the abundance of phytoplankton, but does not discriminate between large and small cells. Therefore, a large number of small cells may actually represent less biomass (weight of living tissue) than a smaller number of large cells. However, small cells are typically more active than larger ones so cell density is probably a better indicator of activity than of biomass. The smaller cells are mostly cyanobacteria.

In 2021 phytoplankton cell density exhibited a strong peak in the river in late July and a lesser peak in Hunting Creek embayment in early August (Figure 89). Total biovolume exhibited a strong peak in the river in early June and a lesser peak in the embayment in late July (Figure 90).

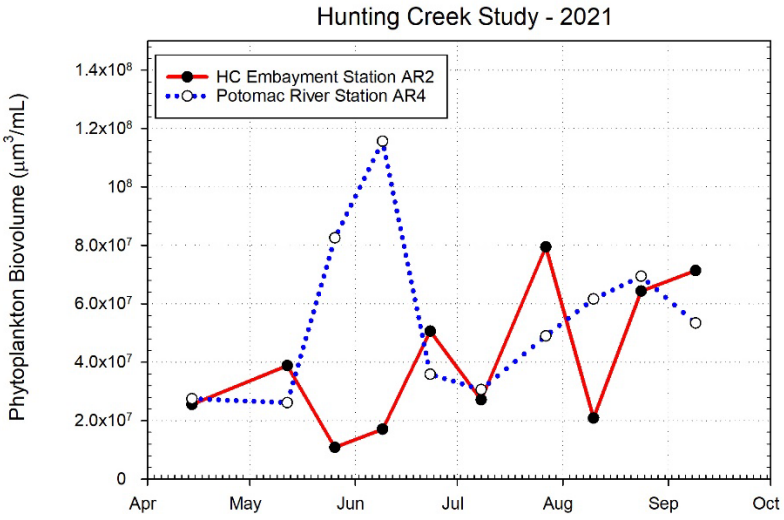

Figure 90. Phytoplankton Biovolume (um^3/mL).

The volume of individual cells of each species is determined by approximating the cells of each species to an appropriate geometric shape (e.g. sphere, cylinder, cone, cube, etc.) and then making the measurements of the appropriate dimensions under the microscope. Total phytoplankton biovolume (shown here) is determined by multiplying the cell density of each species by the biovolume of each cell of that species. Biovolume accounts for the differing size of various phytoplankton cells and is probably a better measure of biomass. However, it does not account for the varying amount of water and other nonliving constituents in cells.

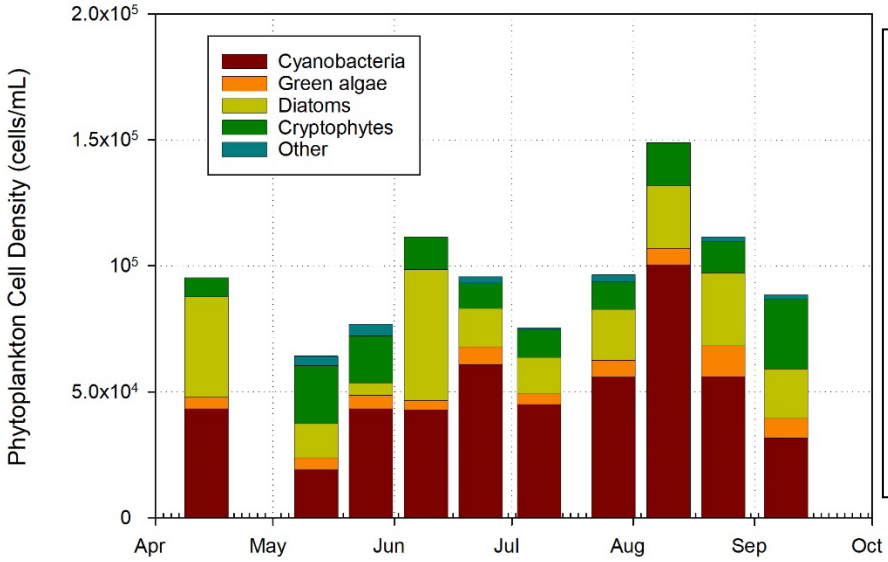

Total phytoplankton cell density can be broken down by major group. **Cyanobacteria** are sometimes called "blue-green algae". **Other** includes euglenoids and dinoflagellates. Due to their small size cyanobacteria typically dominate cell density numbers. Their numbers are typically highest in the late summer reflecting an accumulation of cells during favorable summer growing conditions.

Figure 91. Phytoplankton Density by Major Group (cells/mL). Hunting Creek.

Phytoplankton cell density at AR2 was generally dominated by cyanobacteria.(Figure 91). Diatoms were generally subdominant. In the river mainstem (AR4), cyanobacteria were less dominant with green algae and diatoms sometimes dominant (Figure 92).

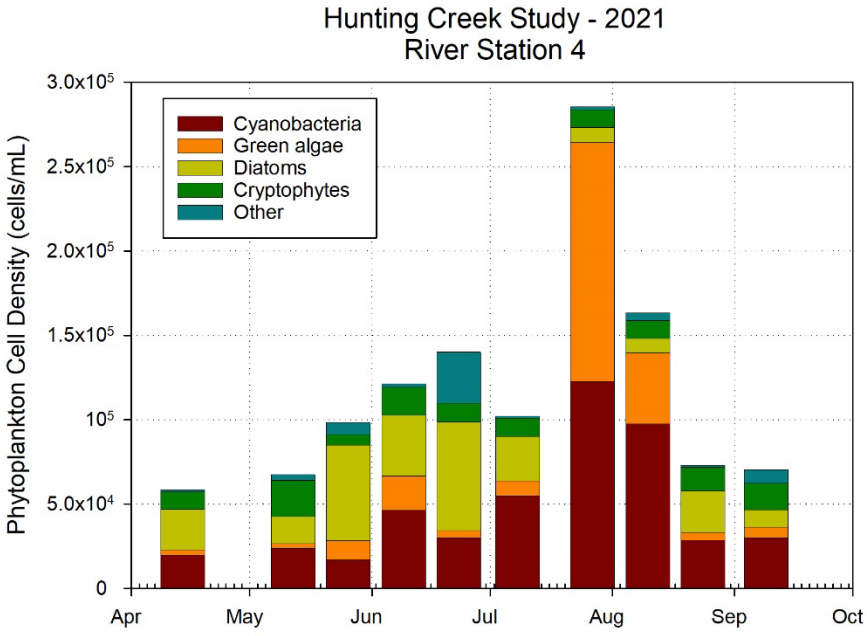

In the river cyanobacteria normally follow similar patterns as in the embayments, but may attain lower abundances. This is probably due to the deeper water column which leads to lower effective light levels and greater mixing. Other groups such as diatoms and green algae tend to be more important on a relative basis than in the embayments.

Figure 92. Phytoplankton Density by Major Group (cells/mL). River.

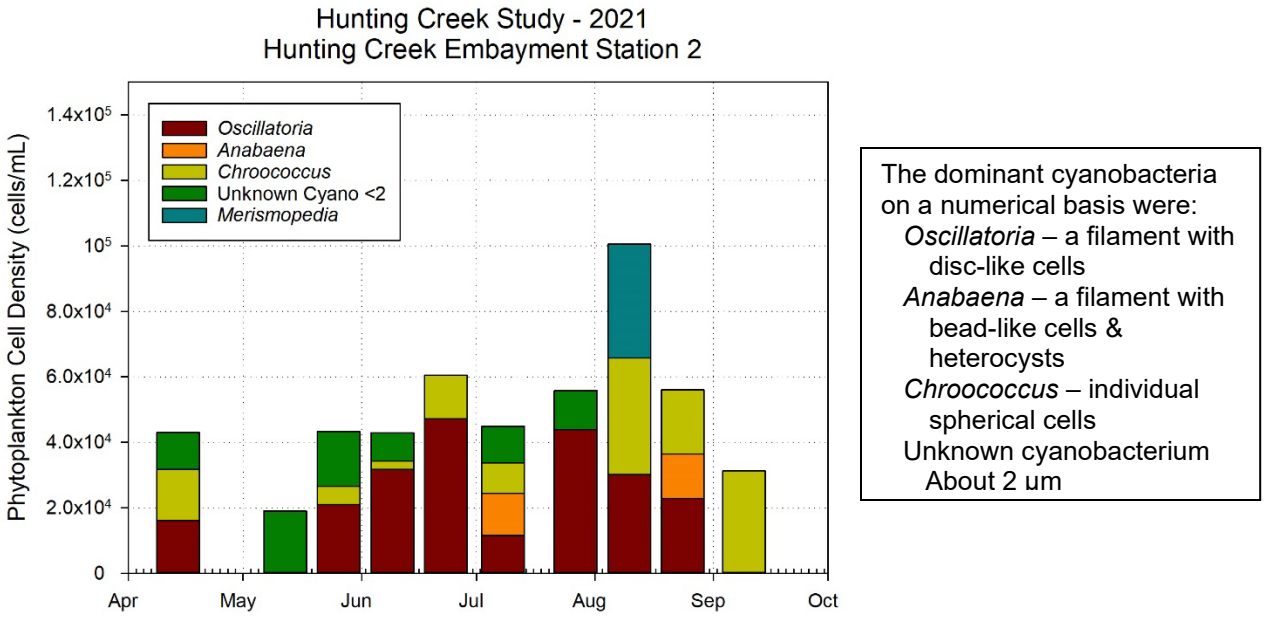

Figure 93. Phytoplankton Density by Dominant Cyanobacteria (cells/mL). Hunting Creek.

Oscillatoria and *Chroococcus*,were the most important cyanobacteria in cell density at the embayment station (AR2) (Figure 93). In the river mainstem this was also true (Figure 94). *Chroococcus* and *Anabaena* were subdominant.

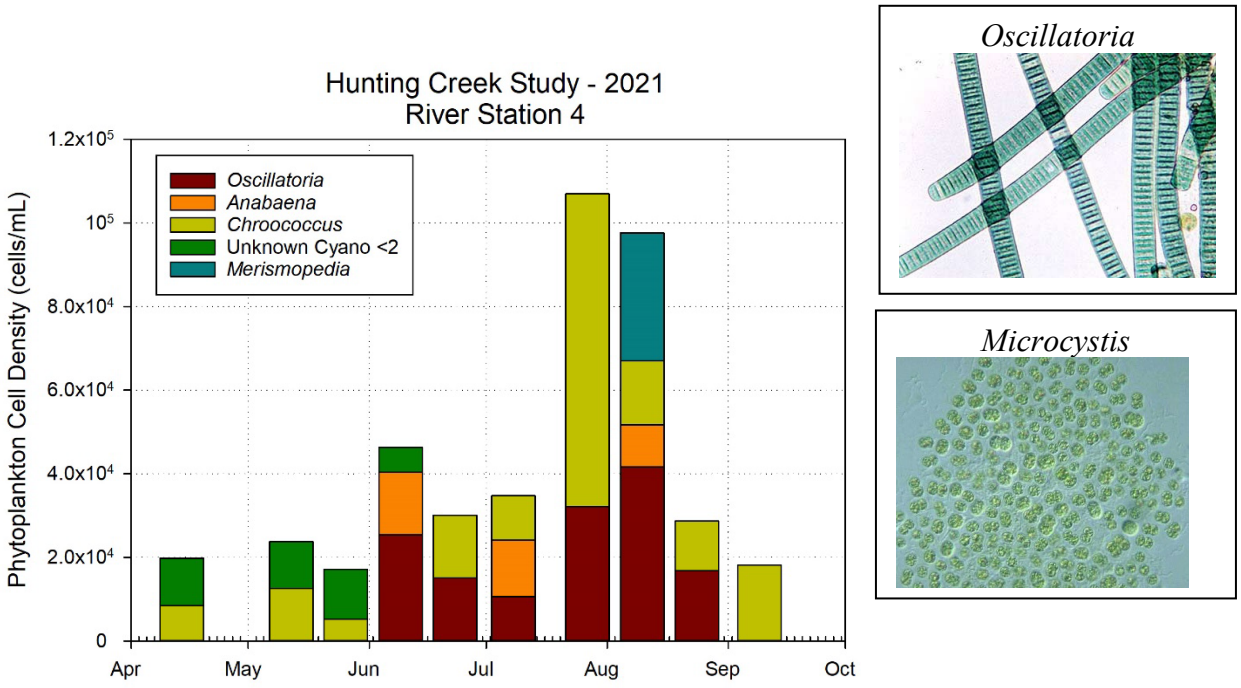

Figure 94. Phytoplankton Density by Dominant Cyanobacteria (cells/mL). River.

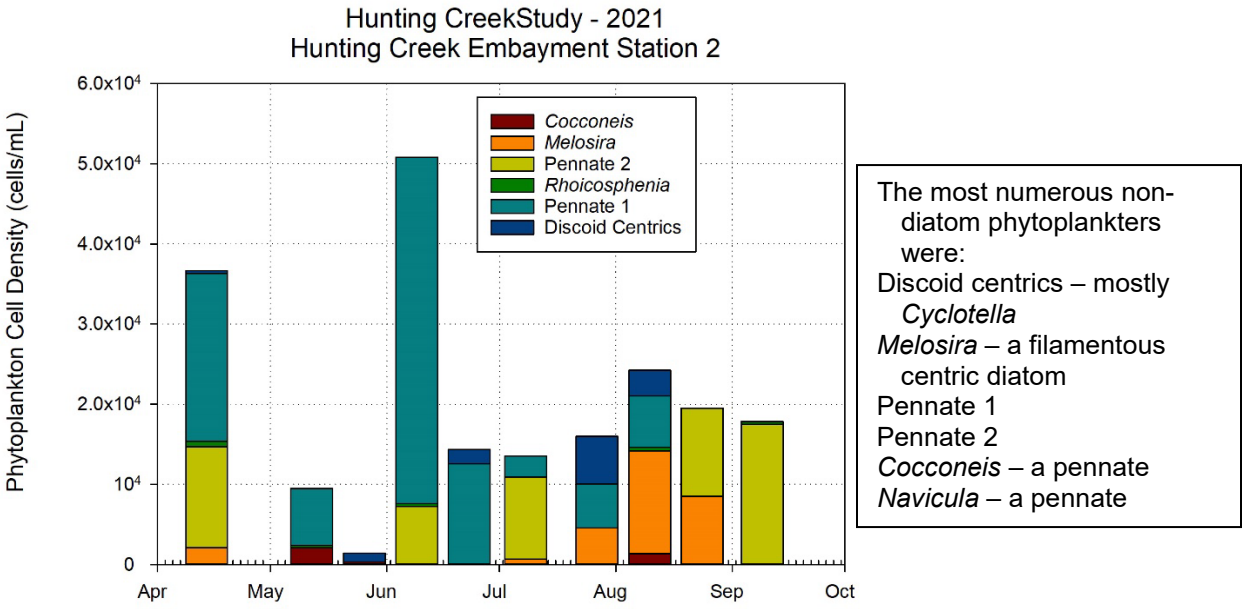

Figure 95. Phytoplankton Density (#/mL) by Dominant Diatom Taxa. Hunting Creek.

Diatom cell density dominance was variable in the embayment. In Spring Pennate 1 was dominant and later in summer *Melosira* and Pennate2 were dominant (Figure 95). At AR4 Pennate 1 and Pennate 2 were dominant for most of the year with *Melosira* important in spring (Figure 96).

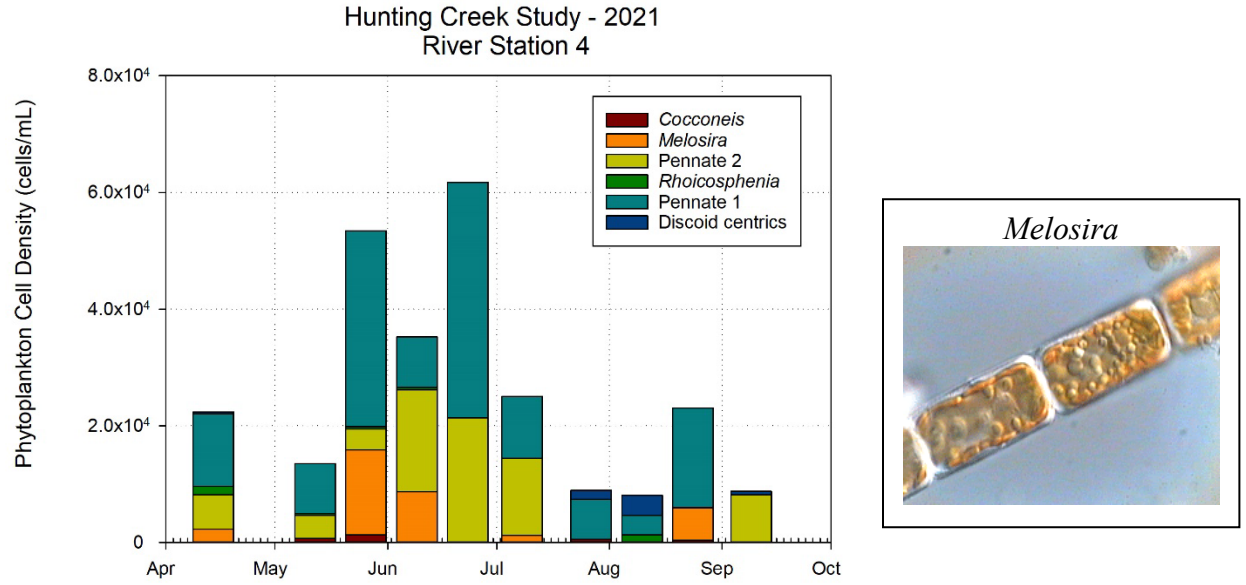

Figure 96. Phytoplankton Density (#/mL) by Dominant Diatom Taxa. River.

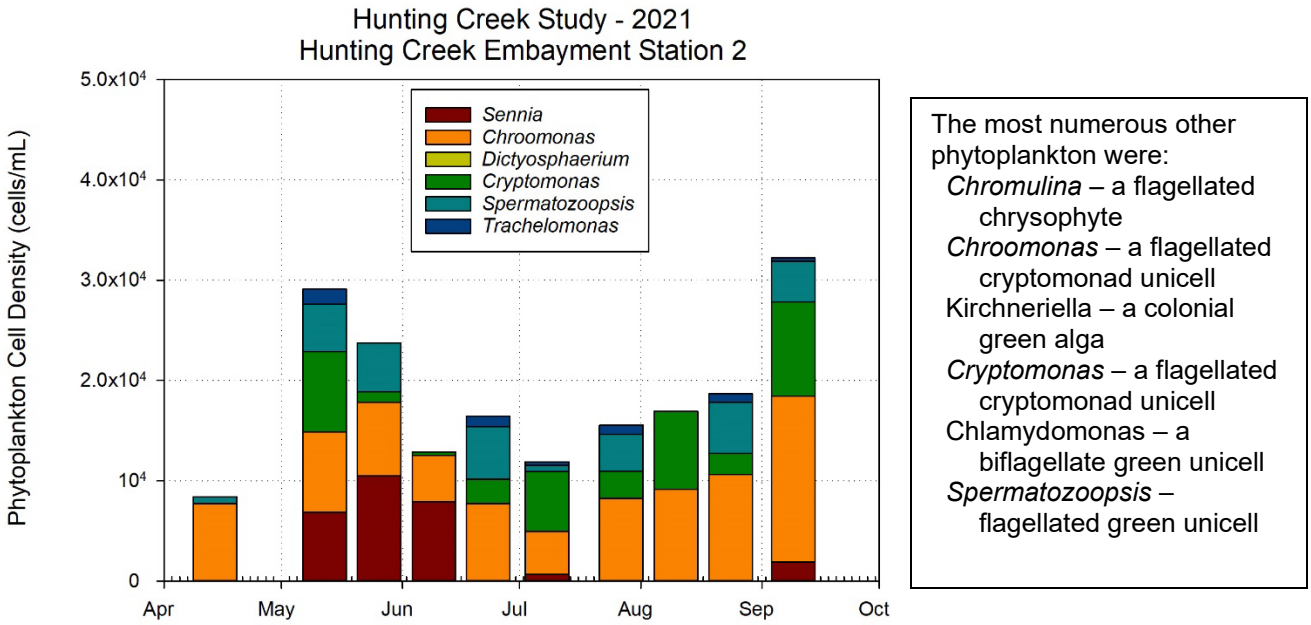

Figure 97. Phytoplankton Density (#/mL) by Dominant Other Taxa. Hunting Creek.

Phytoplankton species that were neither cyanobacteria nor diatoms were grouped together as "other" for these graphs; these included most numerous taxa of green algae, cryptophytes, euglenoids, and dinoflagellates. The cryptophyte *Chroomonas* was abundant in every month at AR2 (Figure 97). At AR4 the green alga *Dictyospherium* was very abundant in late July; in other samples *Chroomonas* was most abundant (Figure 98).

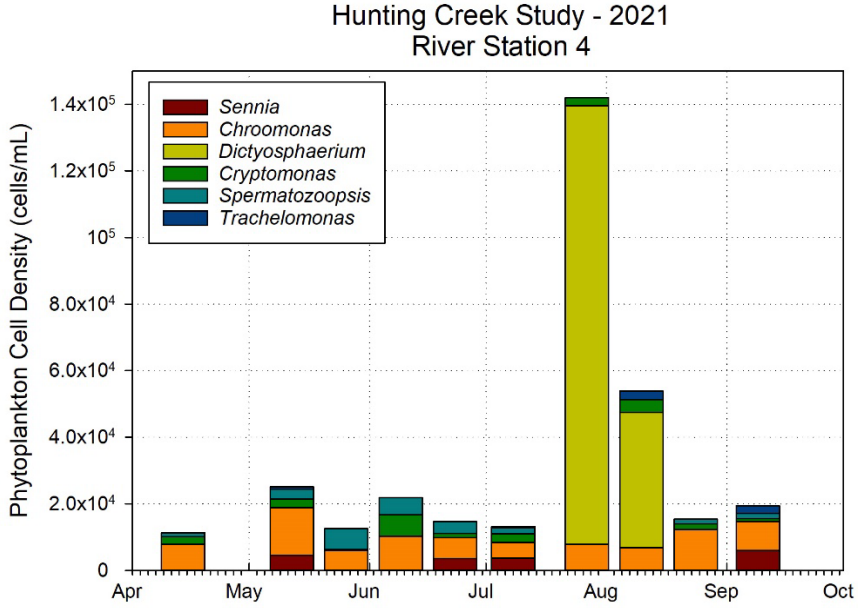

Figure 98. Phytoplankton Density (#/mL) by Dominant Other Taxa. River.

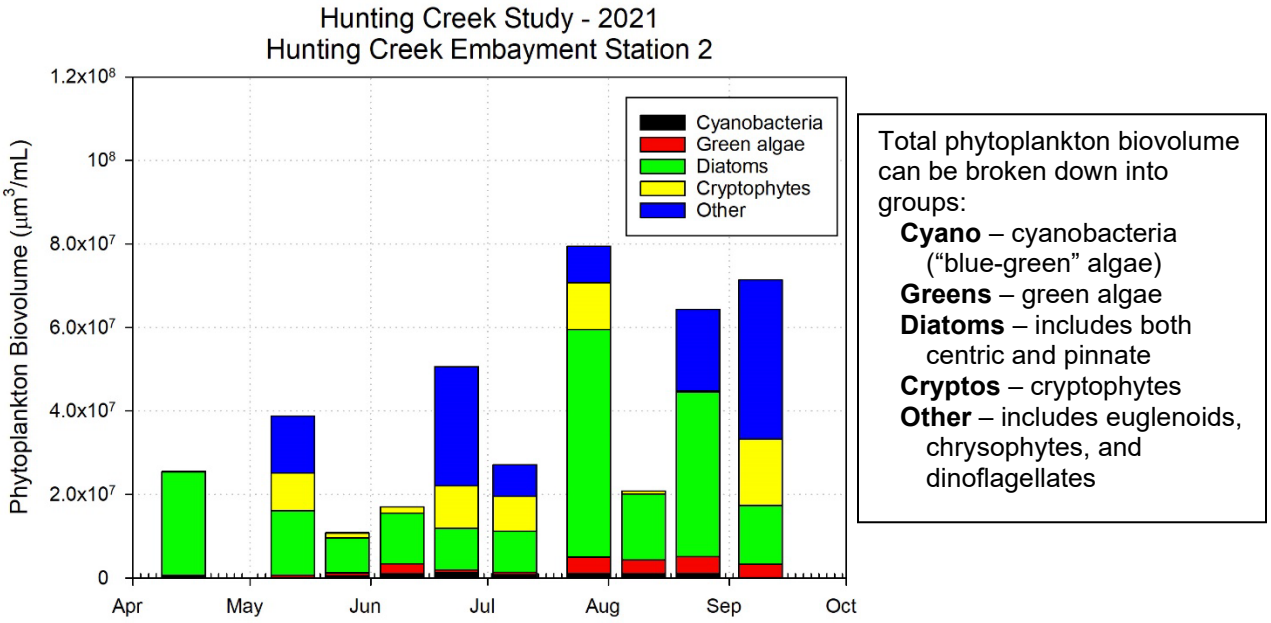

Figure 99. Phytoplankton Biovolume (um³/mL) by Major Groups. Hunting Creek.

In 2021 at AR2 in Hunting Creek diatoms were dominant in biovolume in every month (Figure 99). At AR4 in the river, diatoms were dominant on some dates while Other algae were dominant on other dates (Figure 100).

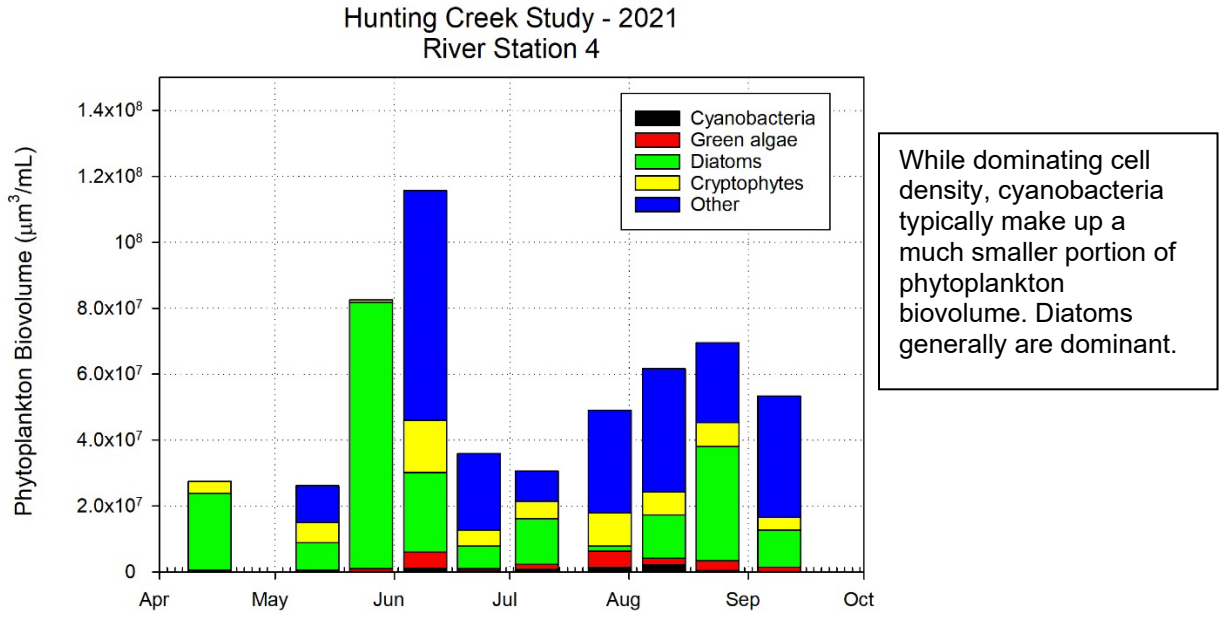

Figure 100. Phytoplankton Biovolume (um³/mL) by Major Groups. River.

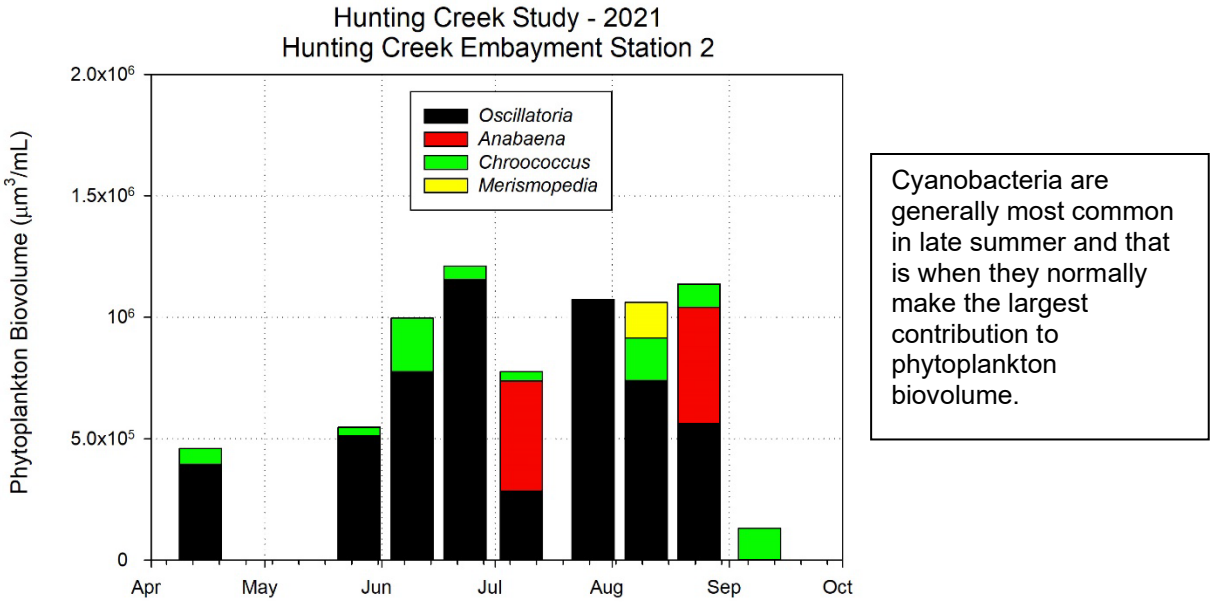

Figure 101. Phytoplankton Biovolume (um³/mL) by Cyanobacteria Taxa. Hunting Creek.

Among the cyanobacteria *Oscillatoria* was dominant on most dates at both stations (Figures 101&102). However, in certain samples at AR4 *Anabaena* or *Merismopedia* were co-dominant.

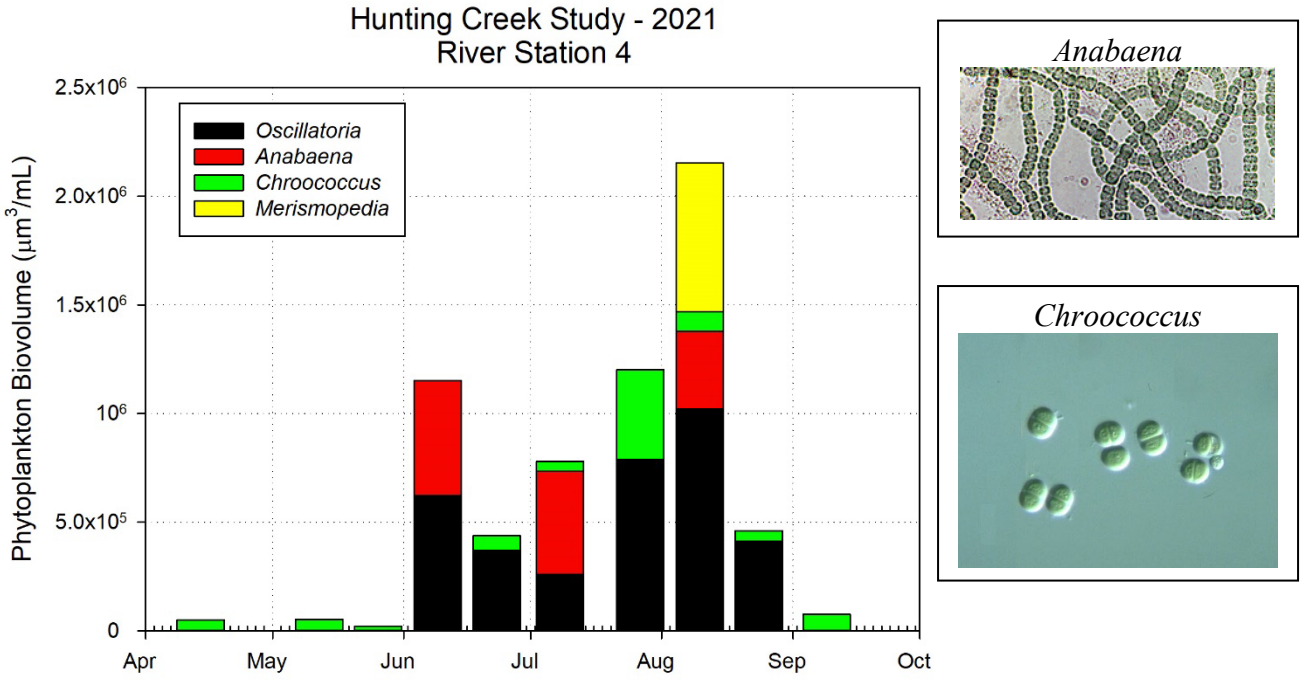

Figure 102. Phytoplankton Biovolume (um³/mL) by Cyanobacterial Taxa. River.

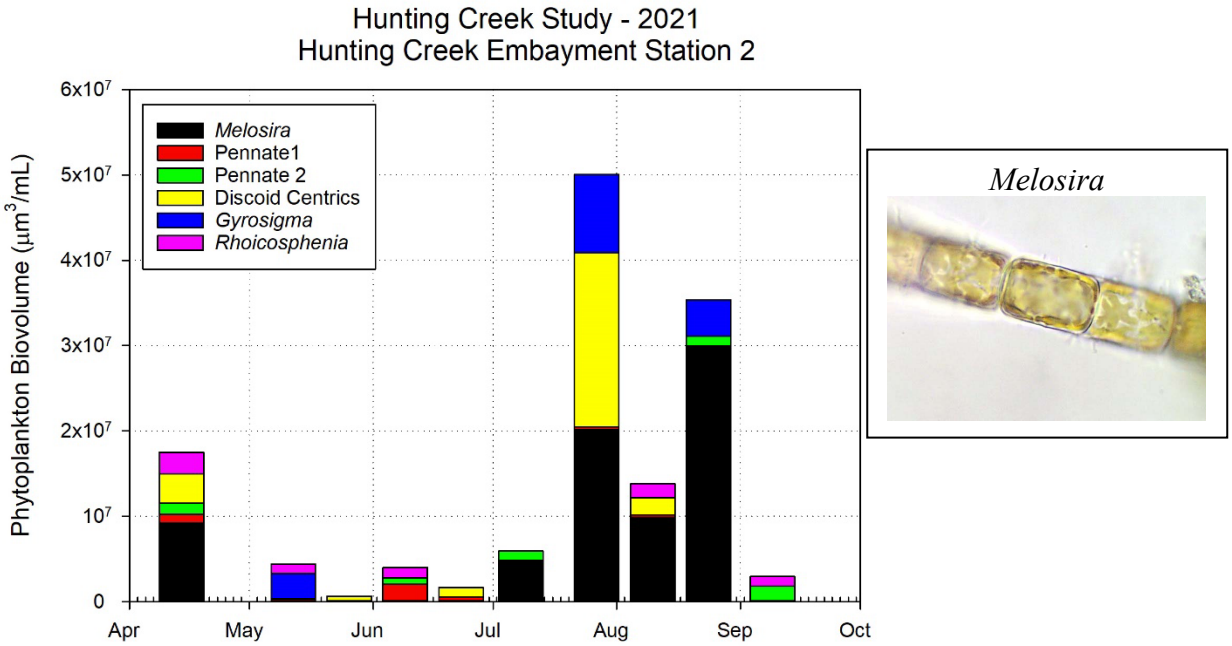

Figure 103. Phytoplankton Biovolume (um³/mL) by Dominant Diatom Taxa. Hunting Creek.

At both stations, *Melosira* was the dominant on most dates (Figures 103&104). Discoid centrics were also important in some samples.

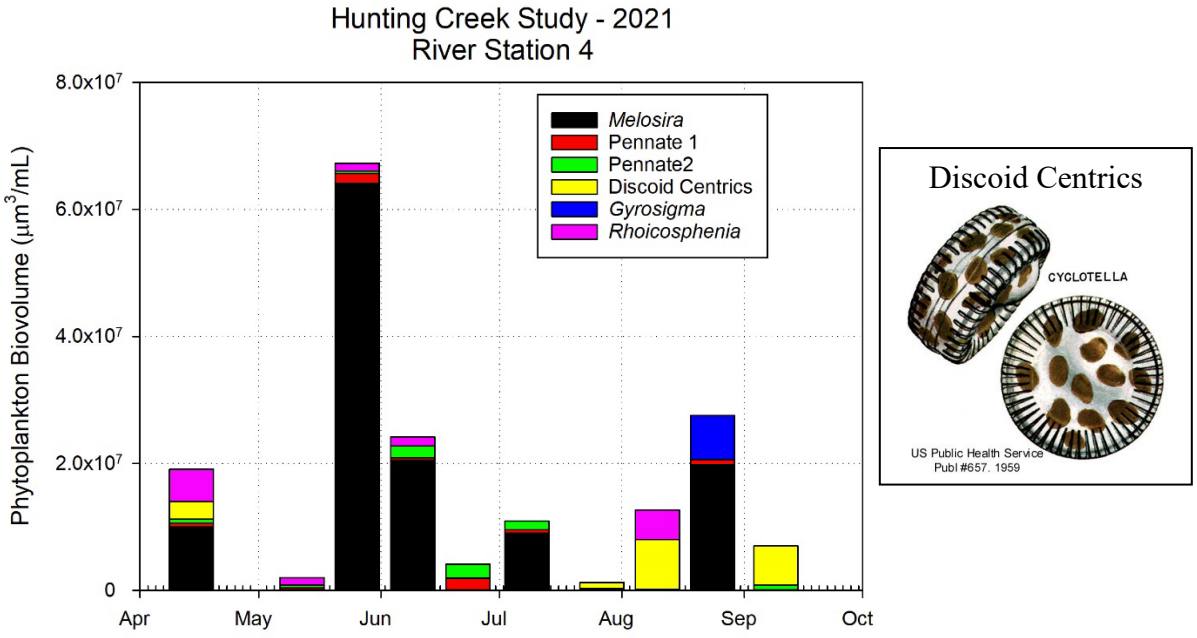

Figure 104. Phytoplankton Biovolume (um³/mL) by Dominant Diatom Taxon. River.

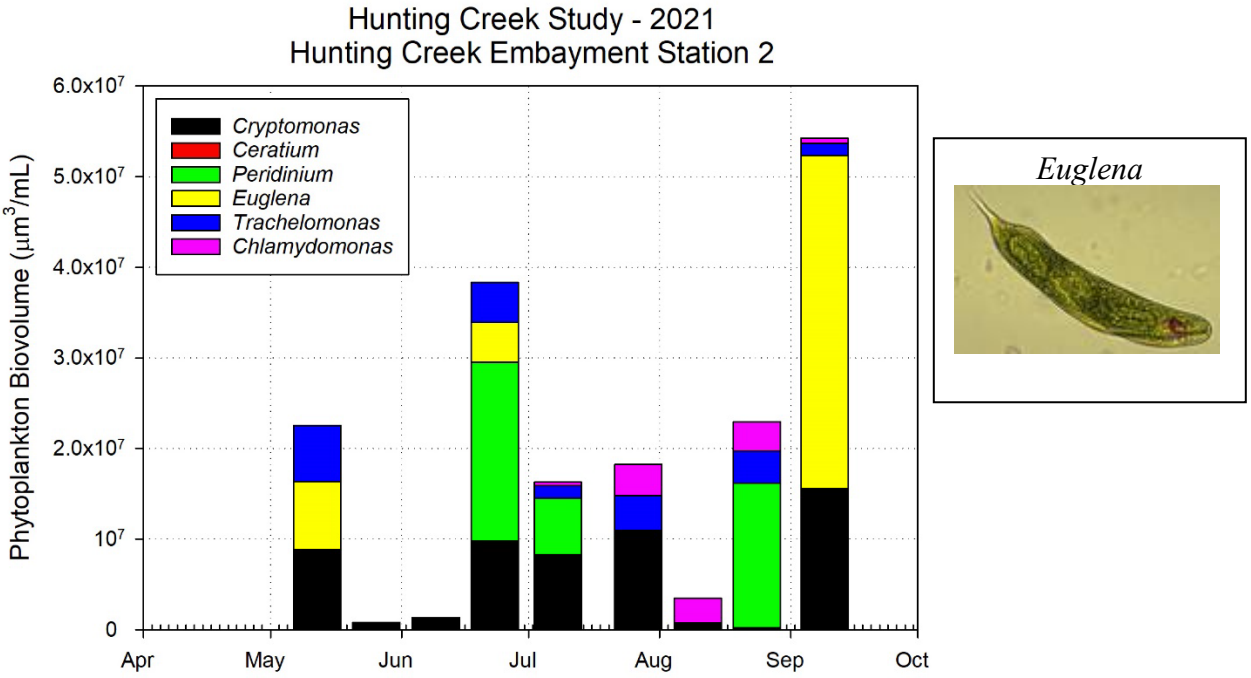

Figure 105. Phytoplankton Biovolume (um³/mL) by Dominant Other Taxa. Hunting Creek.

In the embayment the dinoflagellate *Peridinium* and the cryptophyte *Cryptomonas* dominated biovolume in most samples at AR2 (Figure 105). The dinoflagellate *Peridinium* and the euglenoid Euglena were consistently important (Figure 106). The dinoflagellate *Ceratium* made a strong showing at one sample at AR4.

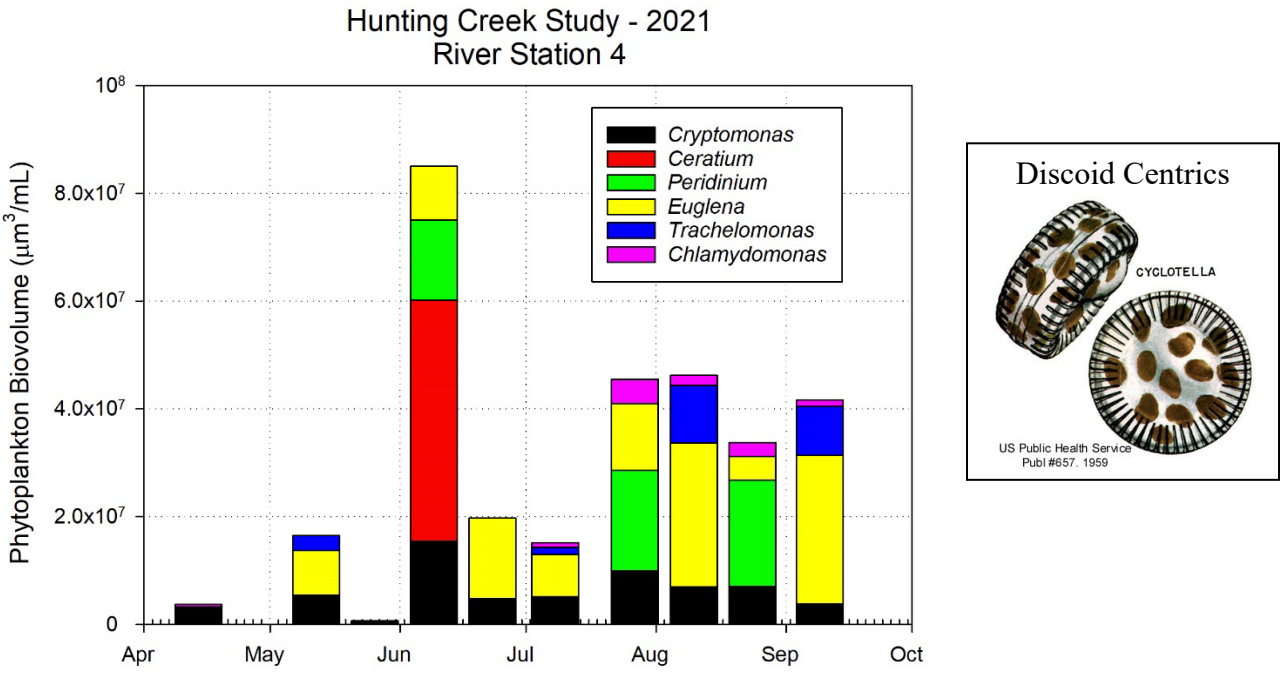

Figure 106. Phytoplankton Biovolume (um³/mL) by Dominant Other Taxon. River.

E. Zooplankton – 2021

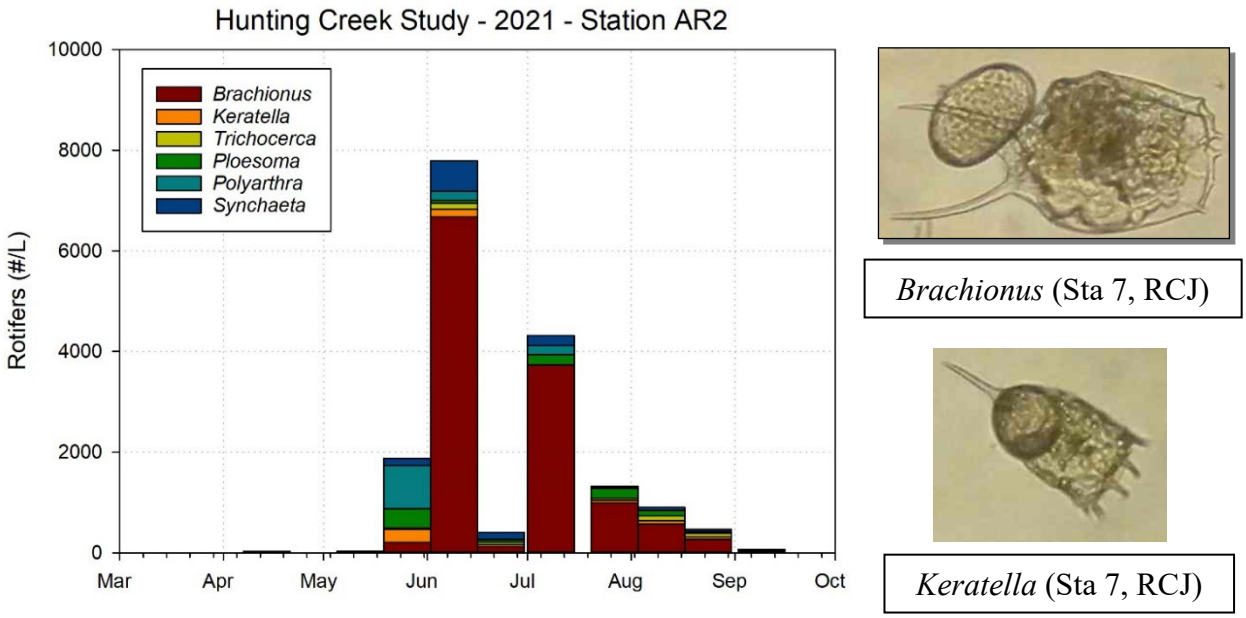

Figure 107. Rotifer Density by Dominant Taxa (#/L). Hunting Creek.

At the embayment station AR2, rotifer populations quite high in early June and early July with *Brachionus* being the dominant genus in 2021 (Figure 107). In late May *Polyarthra* was dominant, but in all other samples *Brachionus* was dominant. In the river at AR4, rotifer populations followed a similar pattern at levels about half of that at AR2 (Figure 108). As at AR2, the maximum number of rotifers was observed in early June. *Brachionus* was again dominant in most samples, but other taxa played a somewhat more important role.

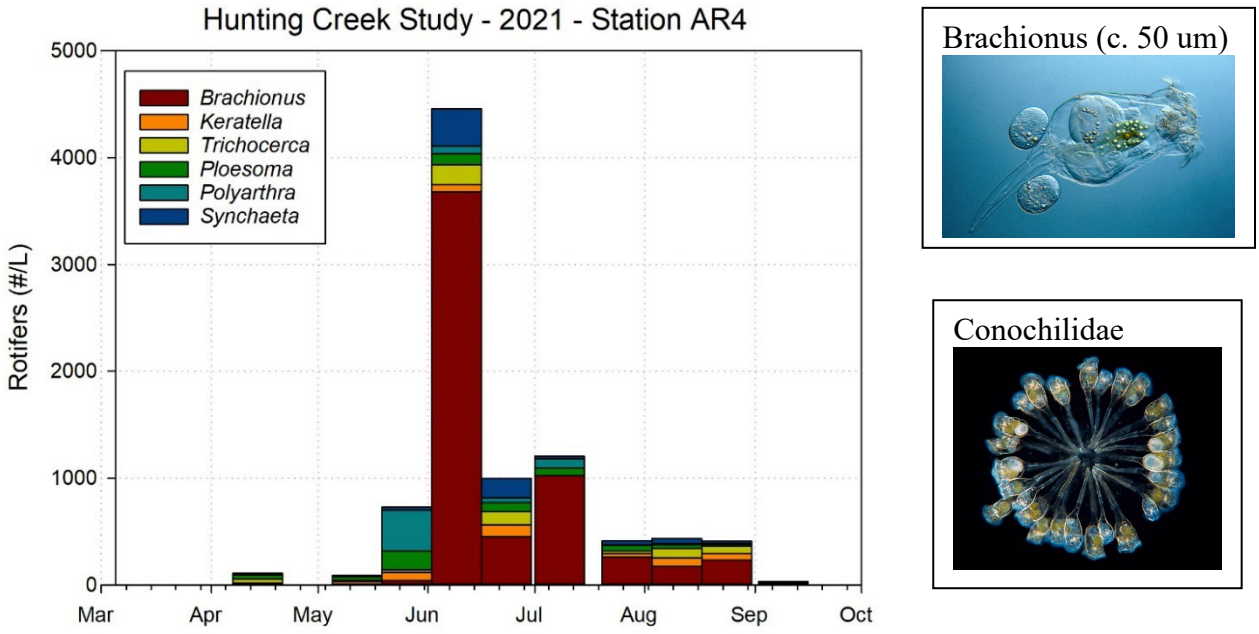

Figure 108. Rotifer Density by Dominant Taxa (#/L). River.

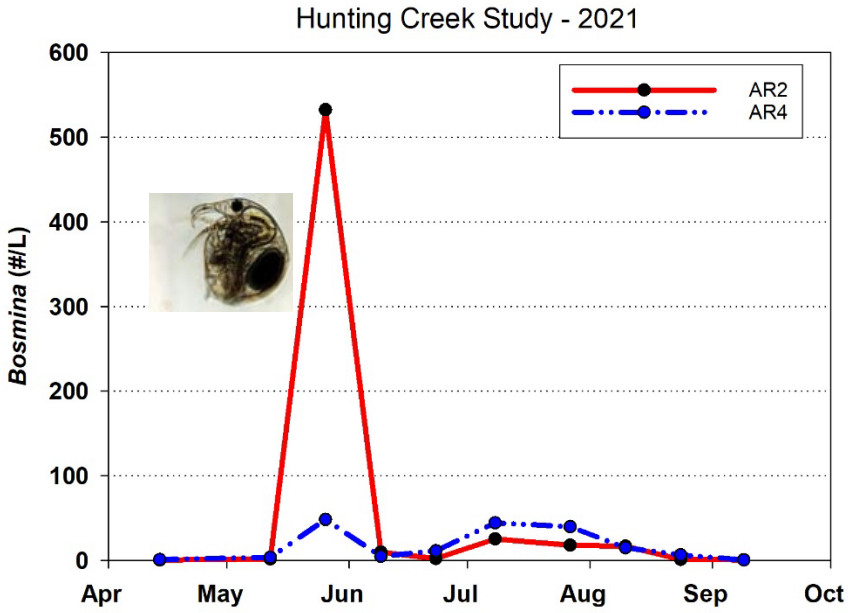

Bosmina is a small-bodied cladoceran, or "waterflea", which is common in lakes and freshwater tidal areas. It is typically the most abundant cladoceran with maximum numbers generally about 100-1000 animals per liter. Due to its small size and relatively high abundances, it is enumerated in the micro-zooplankton samples. *Bosmina* can graze on smaller phytoplankton cells, but can also utilize some cells from colonies by knocking them loose.

Figure 109. *Bosmina* Density by Station (#/L).

At the embayment station AR2 the small cladoceran *Bosmina* was generally quite low for most of the year, but underwent a significant bloom in late May of over 500/L (Figure 109). In the river *Bosmina* exhibited similar levels except that the late May peak was much reduced. *Diaphanosoma,* typically the most abundant larger cladoceran in the tidal Potomac, exhibited large peaks in late May and early June at both AR2 and AR4, exceeding 1000/m^3 at both stations (Figure 110). A secondary peak was observed at AR4 in early July.

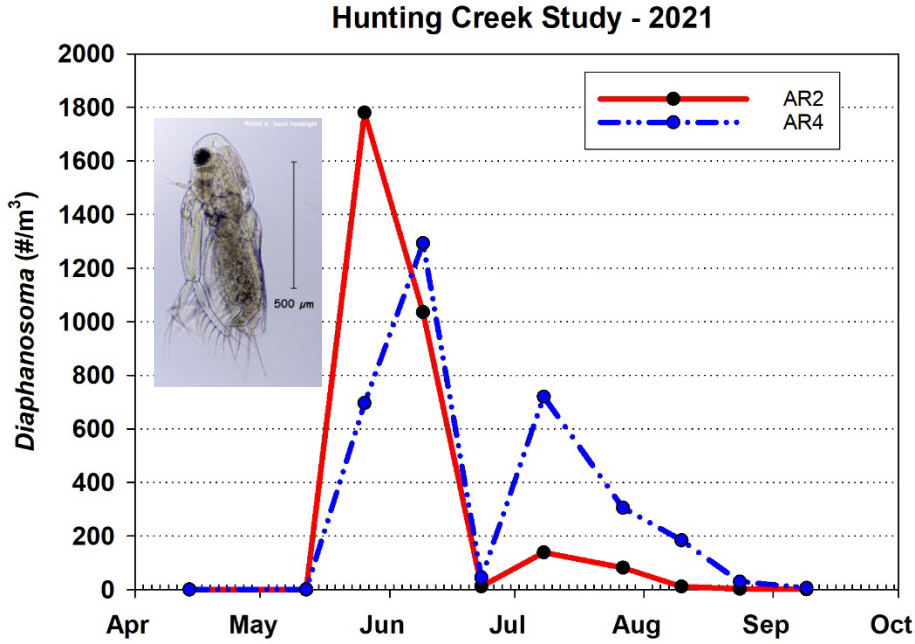

Diaphanosoma is the most abundant larger cladoceran found in the tidal Potomac River. It generally reaches numbers of 1,000-10,000 per m^3 (which would be 1-10 per liter). Due to their larger size and lower abundances, *Diaphanosoma* and the other cladocera are enumerated in the macrozooplankton samples. *Diaphanosoma* prefers warmer temperatures than some cladocera and is often common in the summer.

Figure 110. *Diaphanosoma* Density by Station (#/m^3).

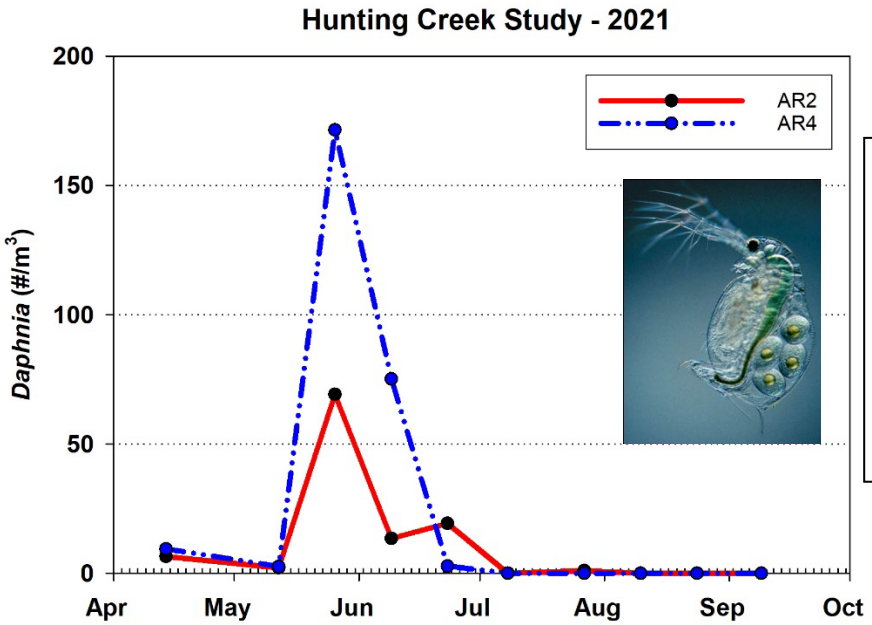

Daphnia, the common waterflea, is one of the most efficient grazers of phytoplankton in freshwater ecosystems. In the tidal Potomac River it is present, but has not generally been as abundant as *Diaphanosoma*. It is typically most common in spring.

Figure 111. *Daphnia* Density by Station (#/m^3).

Daphnia was only moderately abundant in 2021 with peak values at AR2 and AR4 in late May (Figure 111). *Ceriodaphnia* showed a similar peak in late May at AR2 (Figure 112).

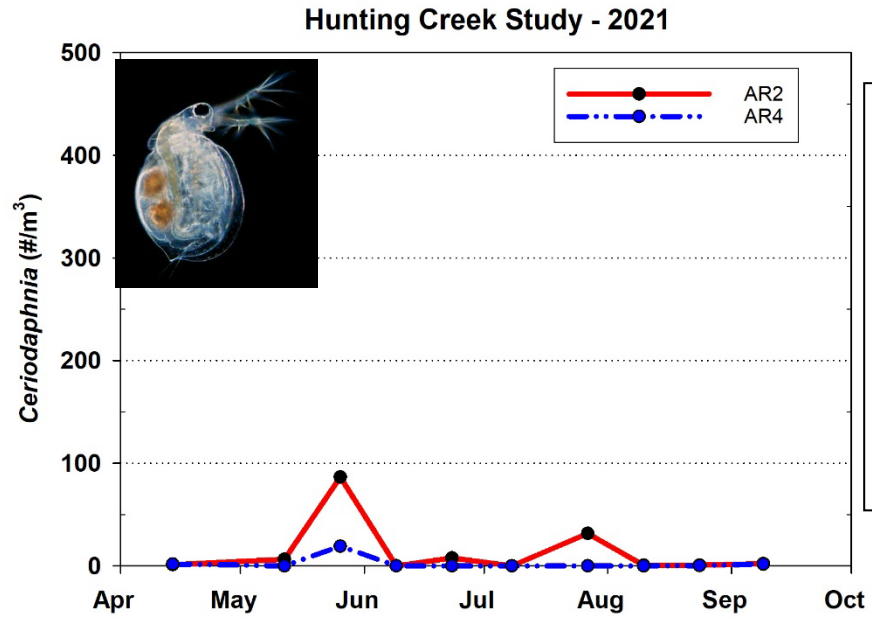

Ceriodaphnia, another common large-bodied cladoceran, is usually present in numbers similar to *Daphnia*. Like all waterfleas, the juveniles look like miniature adults and grow through a series of molts to a larger size and finally reach reproductive maturity. Most reproduction is asexual except during stressful environmental conditions.

Figure 112. *Ceriodaphnia* Density by Station (#/m^3).

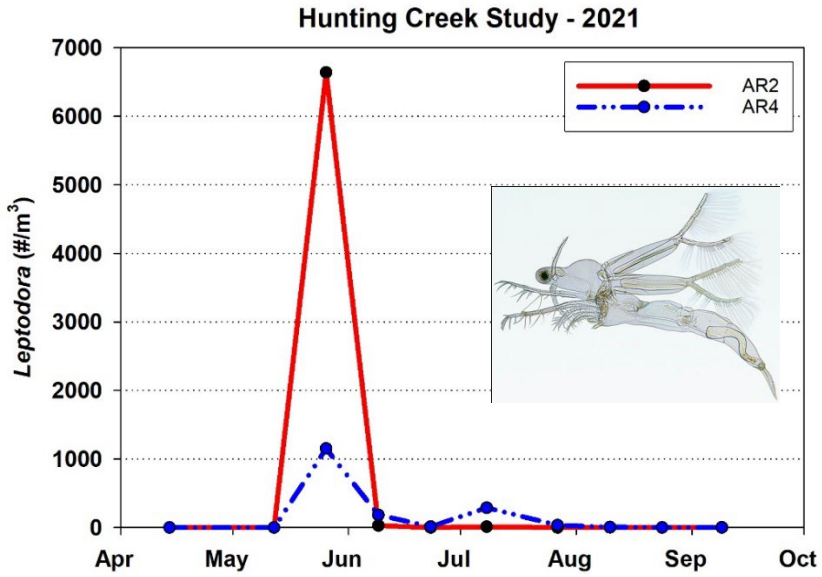

Leptodora is substantially larger than the other cladocera mentioned. Also different is its mode of feeding – it is a predator on other zooplankton. It normally occurs for brief periods in the late spring or early summer.

Figure 113. *Leptodora* Density by Station (#/m^3).

Leptodora, the large cladoceran predator, was found at extremely high values in late May at AR2 and at moderately high levels at AR4 on that date (Figure 113). Otherwise, it was rare. Chydorid cladercera were found in the river at moderate levels but were almost entirely missing at AR2 (Figure 114).

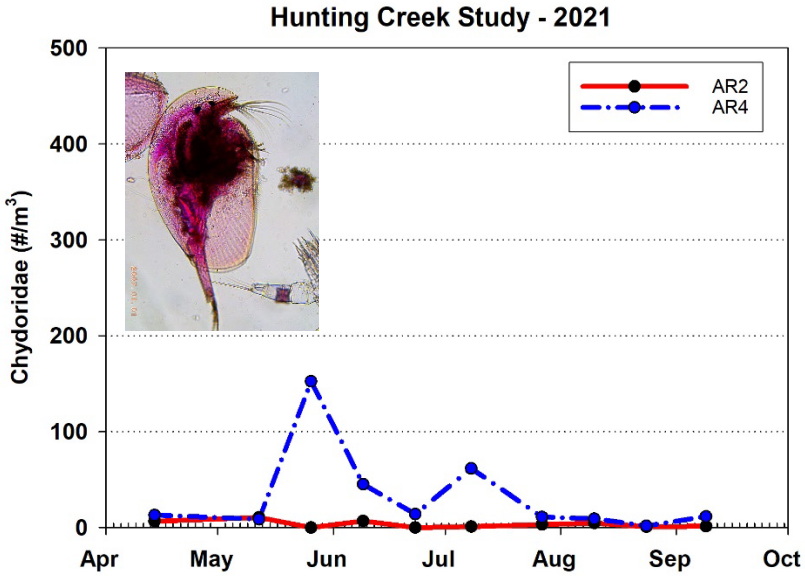

Figure 114. Chydoridae Density by Station (#/m^3). (photo: L. Birsa from HC samples)

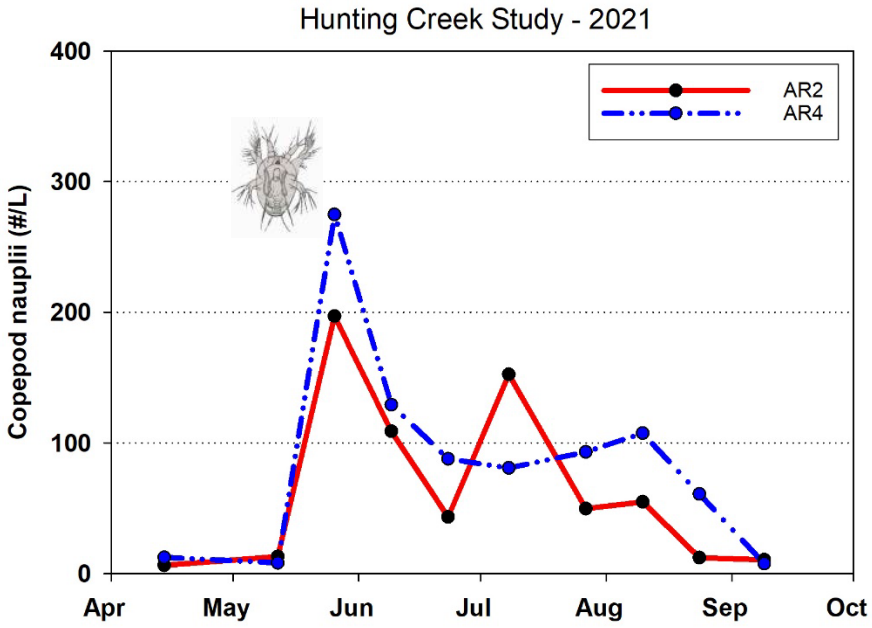

Copepod eggs hatch to form an immature stage called a nauplius. The nauplius is a larval stage that does not closely resemble the adult and the nauplii of different species of copepods are not easily distinguished so they are lumped in this study. Copepods go through 5 naupliar molts before reaching the copepodid stage which is morphologically very similar to the adult. Because of their small size and high abundance, copepod nauplii are enumerated in the micro-zooplankton samples.

Figure 115. Copepod Nauplii Density by Station (#/L).

Copepod nauplii, the larval stage of copepods, were the most numerous group of crustacean zooplankton. At AR2 they peaked at 200/L in late May and at 150/L in early July. At AR4 they peaked at nearly 300/L in late May and 100/L in early August (Figure 115). In the river *Eurytemora*, a large calanoid copepod, was present at high values of over 4000/m^3 at AR4 in early June and declined slowly through the summer with two secondary peaks. At AR2 a maximum of nearly 2000/m^3, but declined rapidly thereafter (Figure 116).

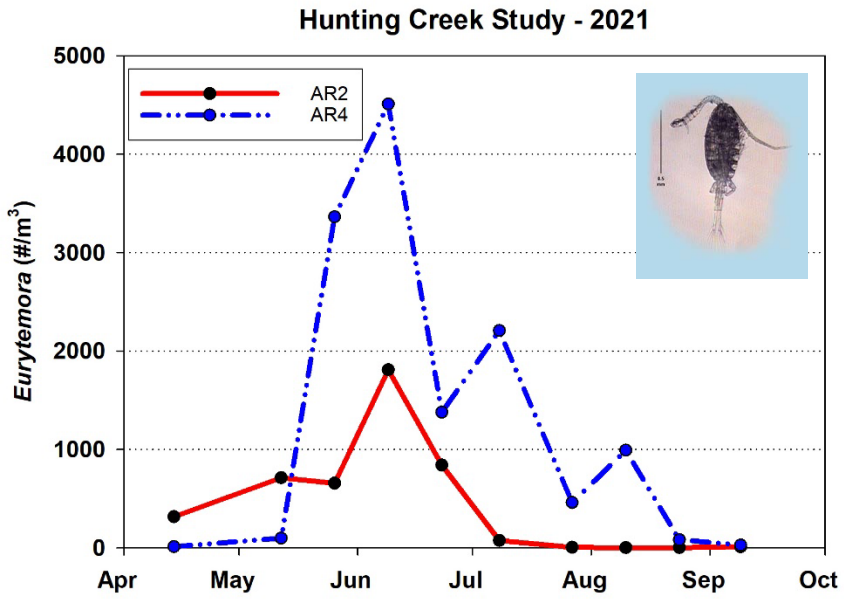

Eurytemora affinis is a large calanoid copepod characteristic of the freshwater and brackish areas of the Chesapeake Bay. *Eurytemora* is a cool water copepod which often reaches maximum abundance in the late winter or early spring. Included in this graph are adults and those copepodids that are recognizable as *Eurytemora*.

Figure 116. *Eurytemora* Density by Station (#/m^3).

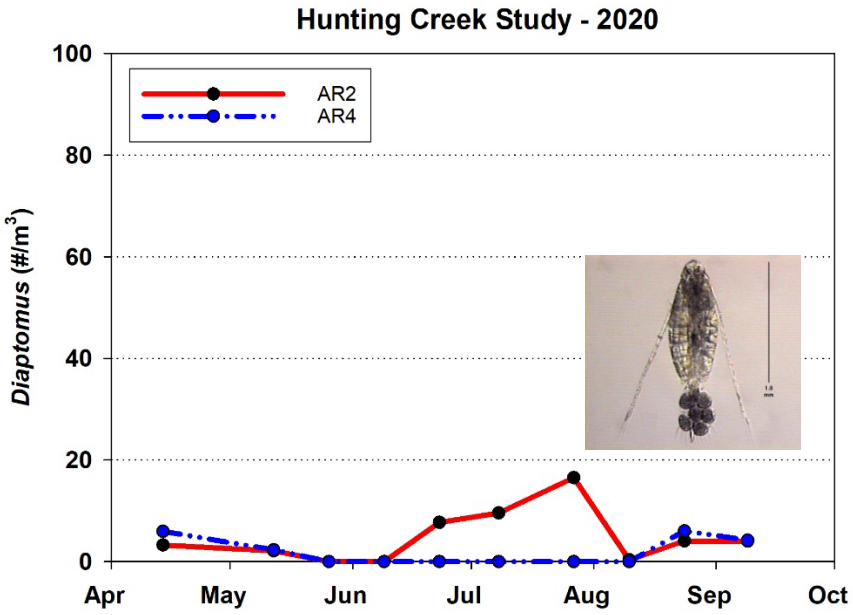

Diaptomus pallidus is a calanoid copepod often found in moderate densities in the Gunston Cove area. *Diaptomus* is an efficient grazer of algae, bacteria, and detrital particles in freshwater ecosystems Included in this graph are adults and those copepodids that are recognizable as *Diaptomus*.

Figure 117. *Diaptomus* Density by Station (#/m^3).

Diaptomus was present at only very low levels in 2021 (Figure 117). *Mesocyclops* exhibited two distinct peaks at AR4 in early June and a larger one in early July at nearly 1400/m^3 (Figure 118). *Mesocyclops* was less abundant at AR2 with one minor peak in early June.

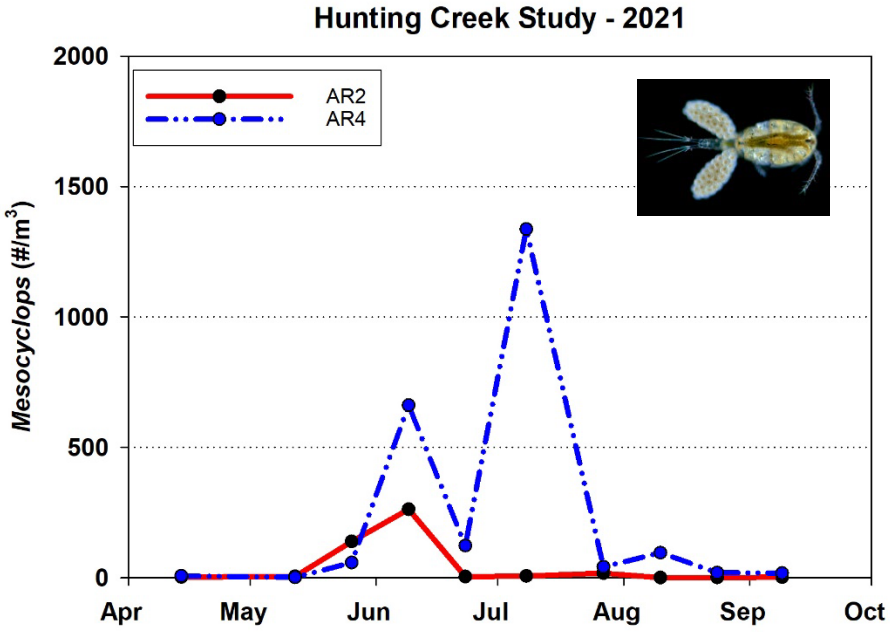

Cyclopoids are the other major group of planktonic copepods. Cyclopoids feed on individual particles suspended in the water including small zooplankton as well as phytoplankton. In this study we have lumped all copepodid and adult cyclopoids together.

Figure 118. *Mesocyclops* by Station (#/m^3).

F. Ichthyoplankton – 2021

We collected 14 samples (7 at AR2 and 7 at AR4) during the months April through July and found an average total larval density of 299 larvae of at least 11 species per 10 m^3 (Table 5). The dominant family was Clupeidae, of which Gizzard Shad (*Dorosoma cepedianum*) had the highest density with an average larval density of 87 larvae per 10 m^3. Unknown Clupeids had the second highest density with an average of 77 larvae per 10 m^3, closely followed by Blueback Herring (*Alosa aestivalis*) and Alewife (*Alosa pseudoharengus*) with 57 and 52 larvae per 10 m^3 respectivley. Another clupeid present that could positively be identified to the species level was Hickory Shad (*Alosa mediocris*) at an average of 3 larvae per 10 m^3. White Perch a semi-anadromous species also was abundant in our ichthyoplankton samples with 17 larvae per 10 m^3 on average. The density of clupeid larvae has a clear seasonal pattern as a result of the spring spawning season of most clupeids that occurs higher upstream. Clupeid larvae in Figure 119 include Blueback Herring, Hickory Shad, Alewife, American Shad and Gizzard Shad. These have similar spawning patterns, so they are lumped into one group for this analysis. Clupeids peaked in late-may and then rapidly decreased by late-June (Figure 119). Of these clupeids, Alewife and Blueback Herring are the two species that make up river herring, of which we describe the spawning population at the end of this report. White Perch larvae attained their highest density on average at 8 larvae per 10 m^3 during May as well (Figure 120), and disappeared from the samples by mid-June. Highest densities of other larvae (not Clupeids or Moronids) were also found at the end of May (Figure 121).

Table 5. Total larval density (#/10m^3) in Hunting Creek (AR2) and the Potomac River (AR4) and the mean among these stations in 2021.

Scientific Name	Common Name	AR2	AR4	Average
Alosa aestivalis	Blueback Herring	21.49	90.65	56.07
Alosa mediocris	Hickory Shad	1.59	4.34	2.96
Alosa pseudoharengus	Alewife	14.73	88.47	51.60
Alosa sapidissima	American Shad	0.15	0.19	0.17
Alosa sp.	unk. Alosa species	0.17	0.00	0.09
Carpiodes cyprinus	Quillback	0.00	0.19	0.10
Clupeidae	unk. clupeid species	7.71	145.04	76.38
Dorosoma cepedianum	Gizzard Shad	35.88	136.63	86.26
Eggs	eggs	0.00	0.00	0.00
Lepomis sp.	unk. sunfish	0.19	0.00	0.09
Menidia beryllina	Inland Silverside	2.64	2.24	2.44
Morone americana	White Perch	12.59	21.08	16.83
Perca flavescens	Yellow Perch	0.00	0.58	0.29
Unidentified	unidentified	3.33	7.44	5.39
Total		**100.47**	**496.87**	**298.67**

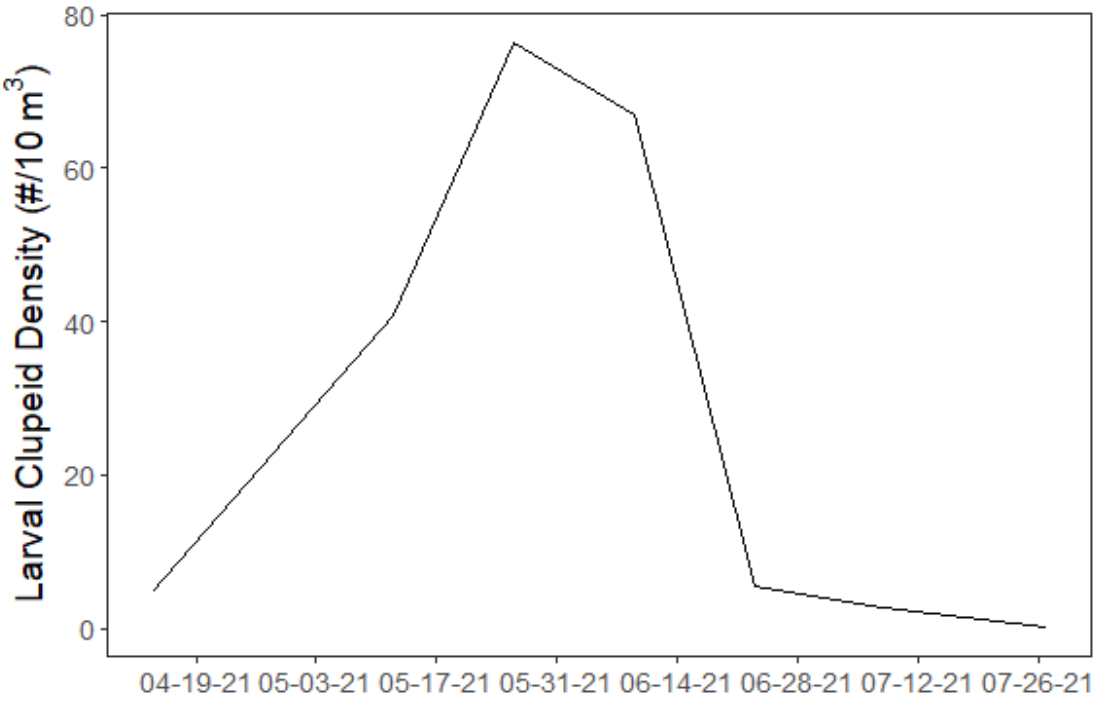

Figure 119. Density of clupeid larvae per $10m^3$.

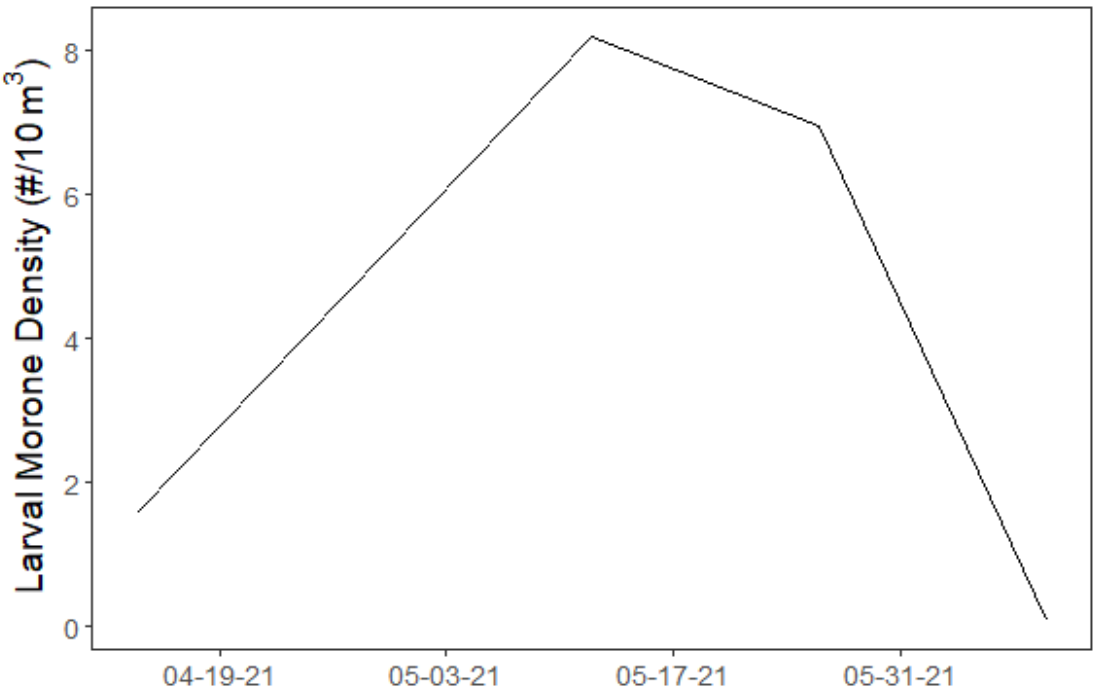

Figure 120. Density of *Morone sp.* (white perch and striped bass) per $10m^3$.

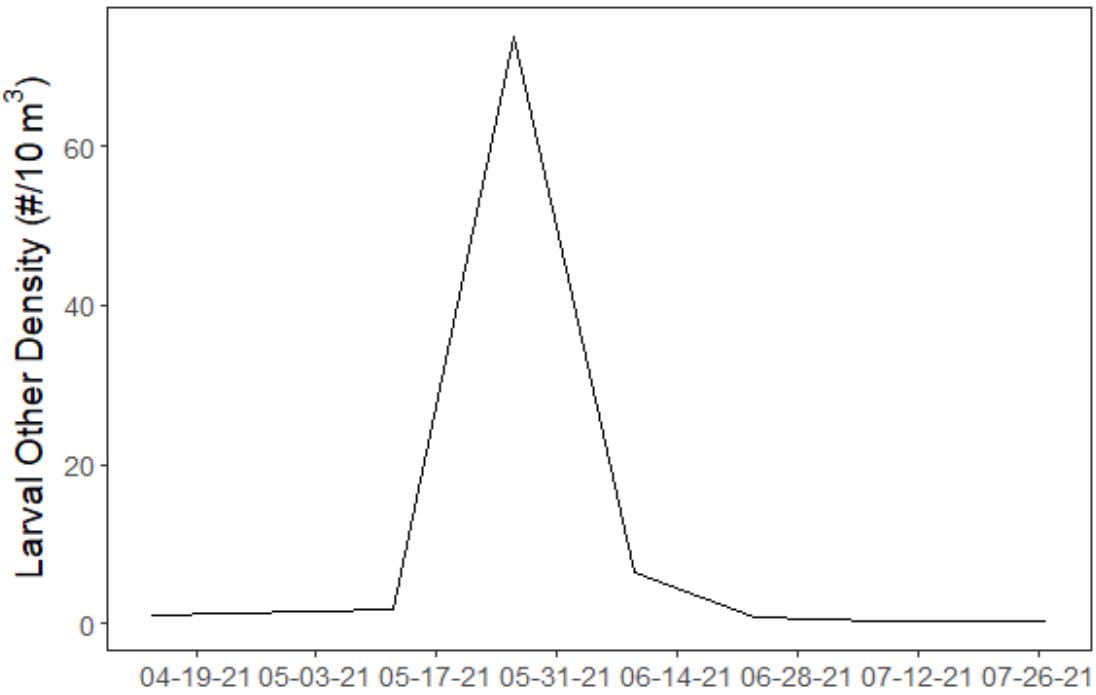

Figure 121. Density of other larvae per $10m^3$.

G. Adult and juvenile fishes – 2021

Trawls

Trawl sampling was conducted between April 16 and September 9 at stations 3 and 4. A total of 731 fishes comprising of at least 16 species were collected with trawls (Table 6). Collections were dominated by White Perch (70.99 %). The second most abundant species was Blue Catfish (7.66%), followed by Spottail Shiners and Alewife (Tables 6 and 7). An interesting find was the collection of Atlantic Croaker and Hogchoker, two species typically associated with higher salinity waters.

Our highest catch occurred on September 9, due to the high abundance of White Perch in that trawl sample (Table 7). Catches were similar among AR3 and AR4; however, more River Herring were collected at station 3 (Table 8). At both stations, catches of White Perch were mostly responsible for the total catch. The catches at both stations were roughly one third of last year's catches, mainly driven by lower catches of White Perch. White Perch was the dominant species as in previous years. Another notable difference from last year was the absence of other catfishes (Brown Bullhead, Channel Catfish, and Flathead Catfish) in our trawl samples. We only collected 2 White Bullhead, but did collect Bluegill, Carp, Goldfish, and Striped Bass, which were absent in last year's trawls.

White Perch (*Morone americana*) was the dominant species in all months sampled, except for April, which was dominated by Spottail Shiner (*Notropis hudsonius*) (Figure 60 A&B). With the

exception of April, Blue Catfish were present in all remaining months and *Alosa* species were present starting in June.

Table 6. Adult and juvenile fish collected by trawling. Hunting Creek - 2021.

Scientific Name	Common Name	Abundance	Percent
Morone americana	White Perch	519	70.99
Ictalurus furcatus	Blue Catfish	56	7.66
Notropis hudsonius	Spottail Shiner	48	6.57
Alosa pseudoharengus	Alewife	18	2.46
Alosa sp.	unk. Alosa species	17	2.33
Anchoa mitchilli	Bay anchovy	17	2.33
Morone sp.	unk. perch/bass species	13	1.78
Etheostoma olmstedi	Tessellated Darter	8	1.09
Dorosoma cepedianum	Gizzard Shad	7	0.96
Alosa aestivalis	Blueback Herring	6	0.82
Cyprinus carpio	Carp	5	0.68
Lepomis macrochirus	Bluegill	5	0.68
Lepomis gibbosus	Pumpkinseed	4	0.55
Ameiurus catus	White Bullhead	2	0.27
Carassius auratus	Goldfish	2	0.27
Morone saxatilis	Striped Bass	2	0.27
Micropogonias undulatus	Atlantic Croaker	1	0.14
Trinectes maculatus	Hogchoker	1	0.14
Total		**731**	**100.00**

Table 7. Adult and juvenile fish collected by trawling on each sampling date.

Scientific Name	Common Name	4-16	5-7	5-20	6-3	6-17	7-1	7-15	8-5	8-19	9-9	Total
Alosa aestivalis	Blueback Herring	0	0	0	0	0	0	0	0	4	2	6
Alosa pseudoharengus	Alewife	0	0	0	0	0	0	0	0	2	16	18
Alosa sp.	unk. Alosa sp.	0	0	0	0	2	3	1	5	1	5	17
Ameiurus catus	White Bullhead	0	0	0	0	0	0	0	0	0	2	2
Anchoa mitchilli	Bay anchovy	0	0	0	0	0	0	0	0	9	8	17
Carassius auratus	Goldfish	0	0	1	0	1	0	0	0	0	0	2
Cyprinus carpio	Carp	1	0	1	3	0	0	0	0	0	0	5
Dorosoma cepedianum	Gizzard Shad	0	0	0	0	0	2	3	0	2	0	7
Etheostoma olmstedi	Tessellated Darter	1	0	1	0	0	0	1	3	0	2	8
Ictalurus furcatus	Blue Catfish	0	0	3	0	2	0	4	0	21	26	56
Lepomis gibbosus	Pumpkinseed	1	0	1	0	0	0	1	0	0	1	4
Lepomis macrochirus	Bluegill	1	0	2	0	0	0	0	0	0	2	5
Micropogonias undulates	Atlantic Croaker	0	0	1	0	0	0	0	0	0	0	1
Morone americana	White Perch	4	24	9	9	29	7	24	50	66	297	519
Morone saxatilis	Striped Bass	0	1	0	0	0	0	0	0	0	1	2
Morone sp.	unk. Morone sp.	0	0	0	13	0	0	0	0	0	0	13
Notropis hudsonius	Spottail Shiner	7	2	9	1	2	8	6	1	6	6	48
Trinectes maculatus	Hogchoker	0	0	0	0	0	0	0	0	1	0	1
Total		**15**	**27**	**28**	**26**	**36**	**20**	**40**	**59**	**112**	**368**	**731**

Table 8. Adult and juvenile fish collected by trawling at each station.

		Station	
Scientific Name	**Common Name**	**AR3**	**AR4**
Alosa aestivalis	Blueback Herring	2	4
Alosa pseudoharengus	Alewife	16	2
Alosa sp.	unk. Alosa species	12	5
Ameiurus catus	White Bullhead	0	2
Anchoa mitchilli	Bay anchovy	8	9
Carassius auratus	Goldfish	2	0
Cyprinus carpio	Carp	2	3
Dorosoma cepedianum	Gizzard Shad	6	1
Etheostoma olmstedi	Tessellated Darter	7	1
Ictalurus furcatus	Blue Catfish	22	34
Lepomis gibbosus	Pumpkinseed	4	0
Lepomis macrochirus	Bluegill	5	0
Micropogonias undulatus	Atlantic Croaker	1	0
Morone americana	White Perch	204	315
Morone saxatilis	Striped Bass	2	0
Morone sp.	unk. perch/bass species	13	0
Notropis hudsonius	Spottail Shiner	30	18
Trinectes maculatus	Hogchoker	0	1
Total		**336**	**395**

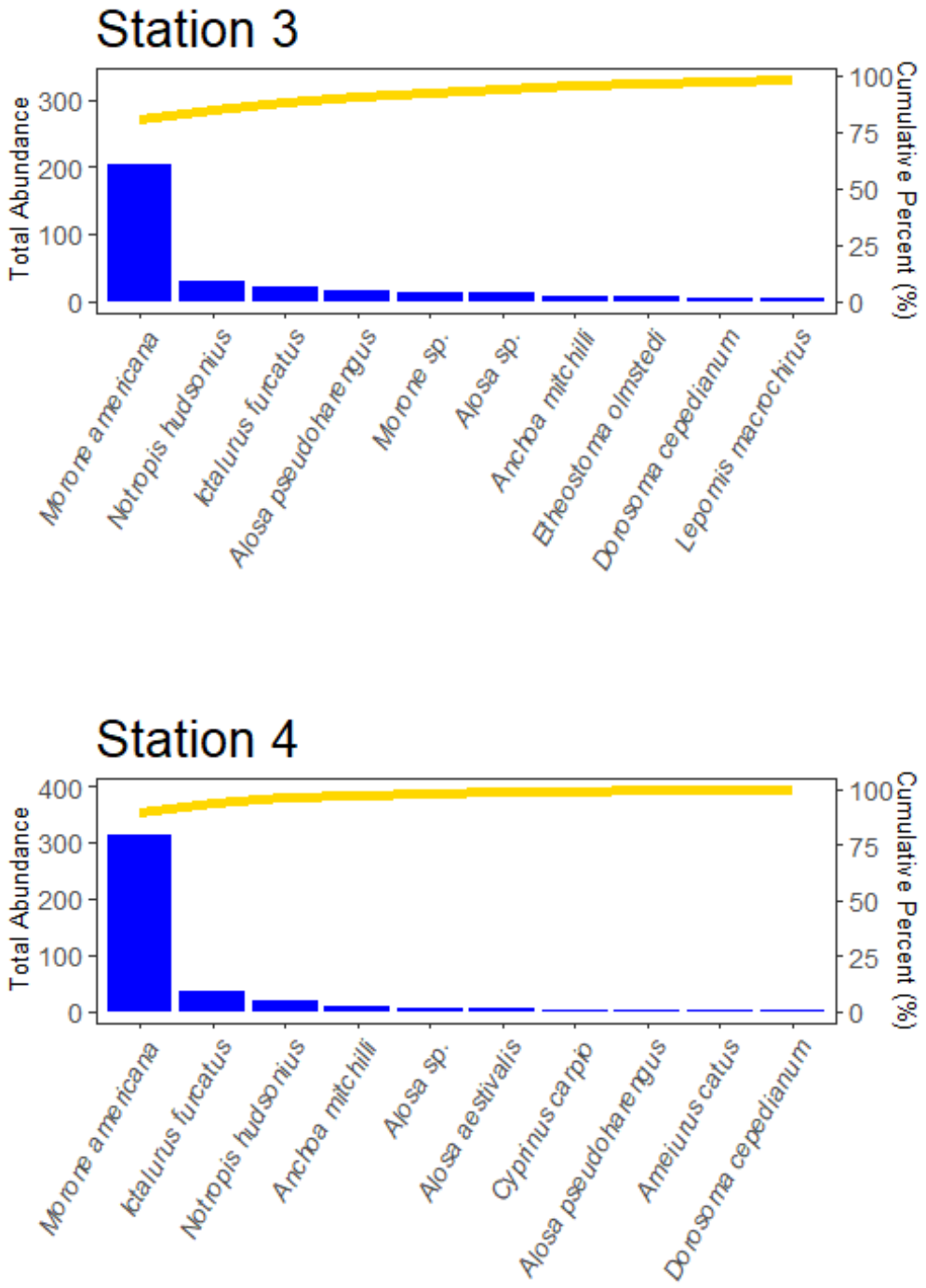

Figure 122A and B. Pareto chart of adult and juvenile fishes collected by trawling. Dominant species by station in total abundance and cumulative percentage of total for Station AR3 (top) and Station AR4 (bottom).

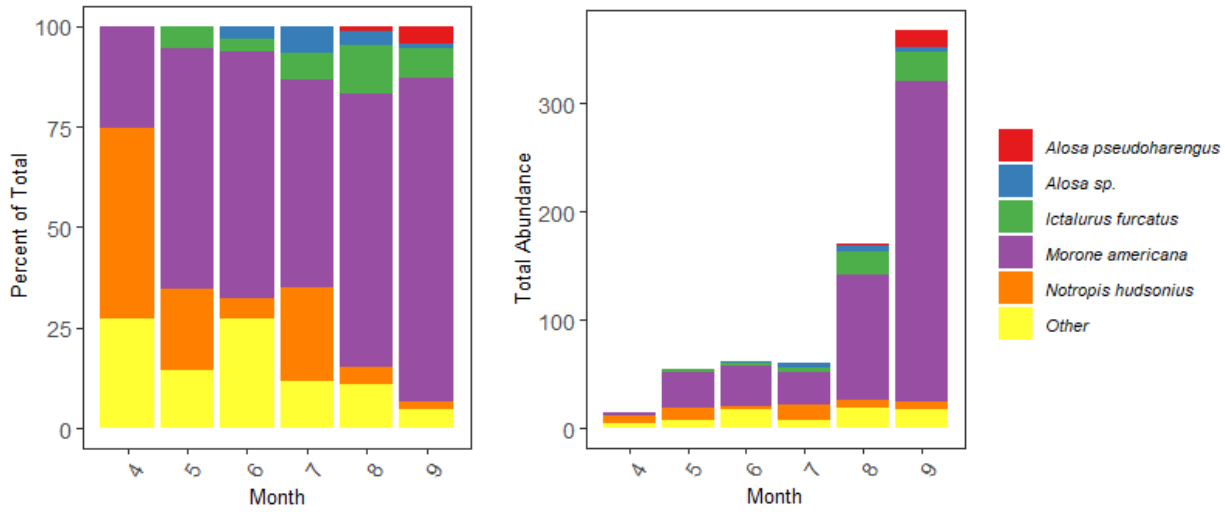

Figure 123 A&B. Adult and juvenile fishes collected by trawling. Dominant species by month in percentage of total (A) and total abundance (B).

Seines

Seine sampling was conducted between April 16 and September 9 at station 5 and 6; however, there was not enough water present to get to our seine sites on May 20th. These two stations were selected as sites with shallow sloping shorelines that would enable us to tow a beach seine. The net was towed up onto the beach unless high water completely submerged the beach. In those cases, the net was towed into the boat. A total of 18 seine samples were taken (9 per station), comprising 1739 fishes of at least 19 species (Table 9). Like last year, White Perch (74.98%) was the dominant species in seine catches followed by Banded Killifish, and Blueback Herring. This continues the trend of greater White Perch dominance seen in 2020 and 2019.

Banded Killifish were collected from April to September and White Perch were collected from June through September. White Perch abundance was > 100 individuals during June, July, and August and Banded Killifish were relatively abundant (> 38 individuals) all months except September (Table 10). The total number of specimens at station 6 was higher than station 5, given that most all White perch were collected at station 6 (Table 10). More Banded Killifish were collected at station 6 as well, but Blueback Herring abundance were greater at station 5. Evenness distribution of abundance over multiple species (Blueback Herring, Banded Killifish, White Perch) was higher at station 5 than station 6, due to the dominance of White Perch at station 6 (Figure 105A&B). Blueback Herring was the most dominant species in station 5, driven by high abundances during September collections, with total abundance of fishes lower than station 6 (Table 11, Figure 106A&B)

Table 9. Total adult and juvenile fish collected by seining.

Scientific Name	Common Name	Abundance	Percent
Alosa aestivalis	Blueback Herring	284	16.33
Alosa pseudoharengus	Alewife	8	0.46
Alosa sapidissima	American Shad	2	0.12
Alosa sp.	unk. Alosa species	71	4.08
Anchoa mitchilli	Bay anchovy	5	0.29
Brevoortia tyrannus	Atlantic Menhaden	12	0.69
Carpiodes cyprinus	Quillback	6	0.35
Dorosoma cepedianum	Gizzard Shad	13	0.75
Dorosoma petenense	Threadfin Shad	29	1.67
Etheostoma olmstedi	Tessellated Darter	21	1.21
Fundulus diaphanus	Banded Killifish	342	19.67
Fundulus heteroclitus	Mummichog	50	2.88
Gambusia holbrooki	Mosquitofish	1	0.06
Lepisosteus osseus	Longnose Gar	1	0.06
Menidia beryllina	Inland Silverside	42	2.42
Micropterus dolomieu	Smallmouth Bass	1	0.06
Micropterus salmoides	Largemouth Bass	5	0.29
Morone americana	White Perch	827	47.56
Notropis hudsonius	Spottail Shiner	18	1.04
Strongylura marina	Atlantic Needlefish	1	0.06
Total		**1739**	**100.00**

Table 10. Adult and juvenile fish collected by seining on each sampling date.

Scientific Name	Common Name	4-16	5-7	6-3	6-17	7-1	7-15	8-5	8-19	9-9	Total
Alosa aestivalis	Blueback Herring	0	0	0	1	0	0	0	9	274	284
Alosa pseudoharengus	Alewife	1	0	1	0	0	0	3	1	2	8
Alosa sapidissima	American Shad	0	0	1	1	0	0	0	0	0	2
Alosa sp.	unk. Alosa	0	0	0	0	0	5	2	3	61	71
Anchoa mitchilli	Bay anchovy	0	0	0	0	0	0	0	0	5	5
Brevoortia tyrannus	Atlantic Menhaden	0	0	0	0	0	0	0	12	0	12
Carpiodes cyprinus	Quillback	0	0	0	5	0	1	0	0	0	6
Dorosoma cepedianum	Gizzard Shad	0	0	0	0	0	4	1	1	7	13
Dorosoma petenense	Threadfin Shad	0	0	0	0	0	0	2	26	1	29
Etheostoma olmstedi	Tessellated Darter	0	0	1	1	5	0	7	7	0	21
Fundulus diaphanus	Banded Killifish	38	4	50	31	73	43	84	9	10	342
Fundulus heteroclitus	Mummichog	0	0	8	2	0	40	0	0	0	50
Gambusia holbrooki	Mosquitofish	0	0	0	0	0	0	0	0	1	1
Lepisosteus osseus	Longnose Gar	0	0	0	0	0	1	0	0	0	1
Menidia beryllina	Inland Silverside	31	0	0	1	0	0	1	6	3	42
Micropterus dolomieu	Smallmouth Bass	0	0	0	0	0	0	1	0	0	1
Micropterus salmoides	Largemouth Bass	0	0	0	0	0	5	0	0	0	5
Morone americana	White Perch	0	0	29	257	290	128	111	4	8	827
Notropis hudsonius	Spottail Shiner	0	0	0	0	0	0	1	0	17	18
Strongylura marina	Atlantic Needlefish	0	0	0	0	0	1	0	0	0	1
Total		**70**	**4**	**90**	**299**	**368**	**228**	**213**	**78**	**389**	**1739**

Table 11. Adult and juvenile fish collected by seining at each station.

		Station	
Scientific Name	**Common Name**	**5**	**6**
Alosa aestivalis	Blueback Herring	179	105
Alosa pseudoharengus	Alewife	5	3
Alosa sapidissima	American Shad	1	1
Alosa sp.	unk. Alosa species	16	55
Anchoa mitchilli	Bay anchovy	5	0
Brevoortia tyrannus	Atlantic Menhaden	0	12
Carpiodes cyprinus	Quillback	0	6
Dorosoma cepedianum	Gizzard Shad	3	10
Dorosoma petenense	Threadfin Shad	0	29
Etheostoma olmstedi	Tessellated Darter	20	1
Fundulus diaphanus	Banded Killifish	113	229
Fundulus heteroclitus	Mummichog	2	48
Gambusia holbrooki	Mosquitofish	0	1
Lepisosteus osseus	Longnose Gar	1	0
Menidia beryllina	Inland Silverside	5	37
Micropterus dolomieu	Smallmouth Bass	0	1
Micropterus salmoides	Largemouth Bass	0	5
Morone americana	White Perch	80	747
Notropis hudsonius	Spottail Shiner	2	16
Strongylura marina	Atlantic Needlefish	1	0
Total		**433**	**1306**

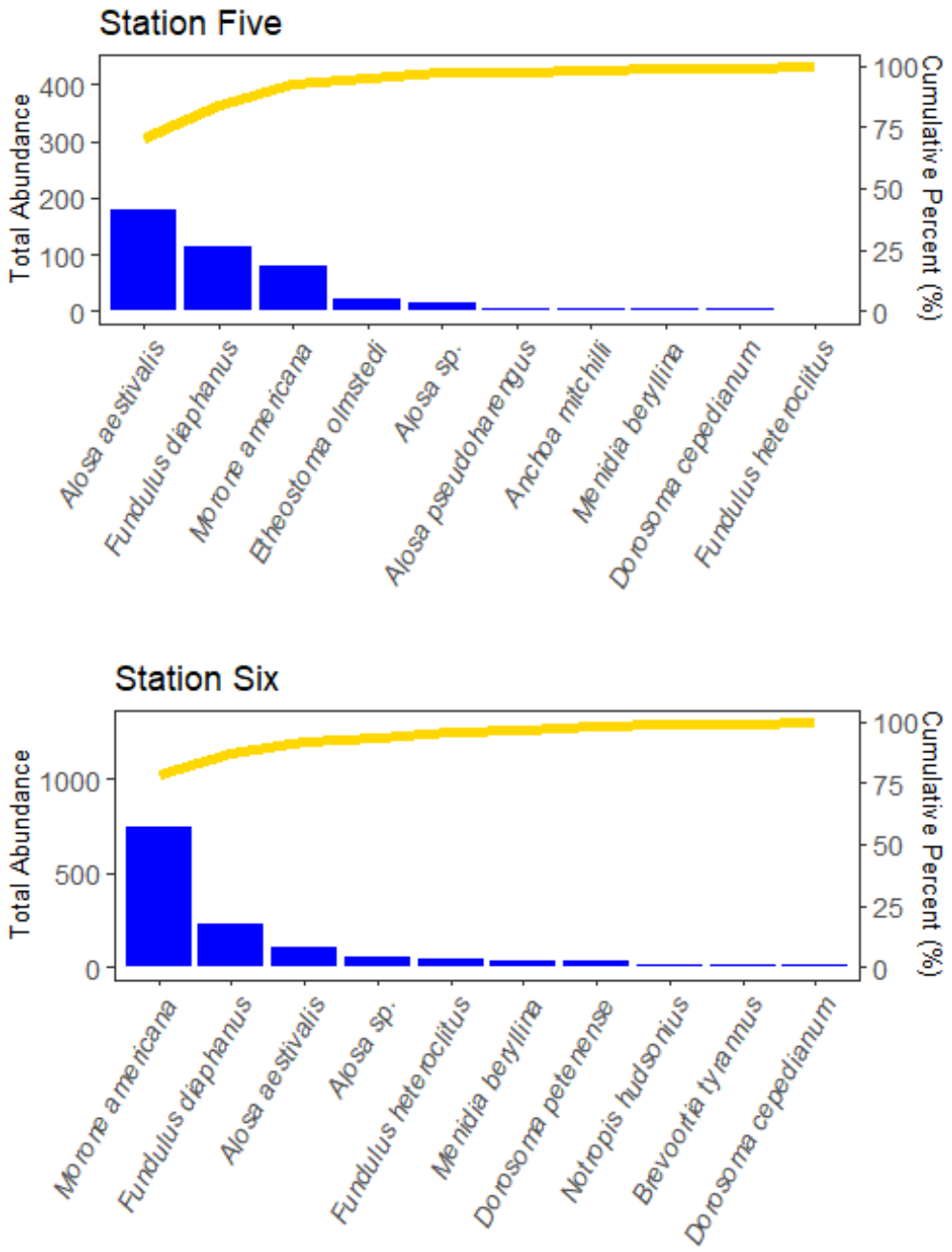

Figure 124A and B. Pareto chart of adult and juvenile fishes collected by seining. Dominant species by station in total abundance and cumulative percentage of total for Station 5 (top) and Station 6 (bottom).

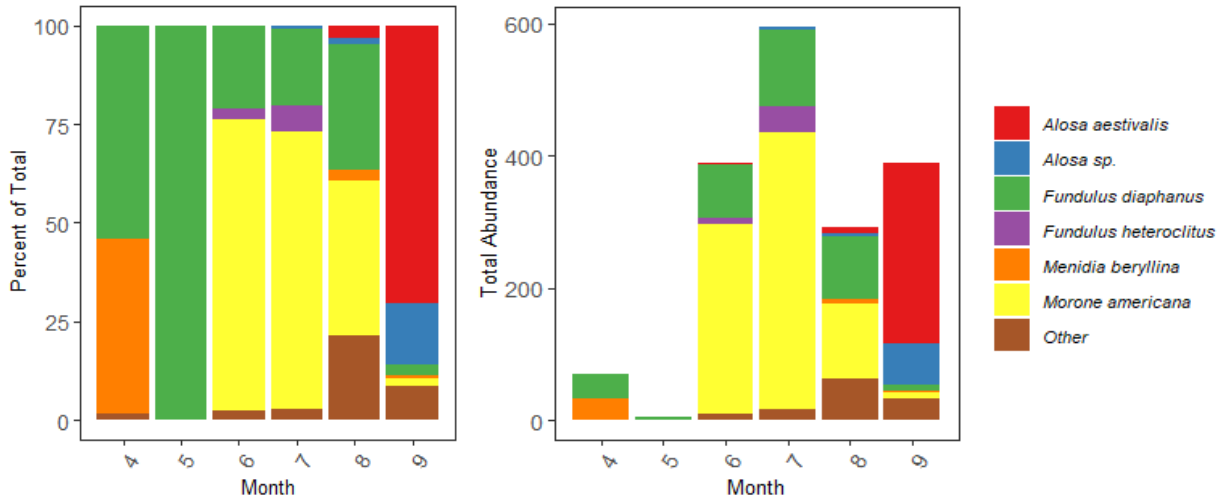

Figure 125A and B. Adult and juvenile fish collected by seining. Dominant species by month in percentage of total (A) and total abundance (B).

Fyke Nets

Fyke nets were set from June to September, but could not be set prior to June given low crew sizes, and inclement weather precluded a sampling event in July and August. Both fyke nets were set near trawl station 3 (Figure 1). Similar to 2018 and 2019, fyke net catches were less than with the trawl or seine, given that only 42 fishes representing 8 species were collected (Table 12). Once again, SAV cover was low in 2021, which makes the trawl more effective resulting in a higher catch, and the fyke nest less effective because they are not hidden as well with less dense aquatic plant beds. This highlights the importance of using different gear types to accurately monitor species abundance trends. Previously, fyke nets were effective in 2017 when the SAV cover was much higher, with high fish abundance reflective of a diversity of species utilizing the SAV habitat.

Table 12. Adult and juvenile fish collected by fyke nets.

Scientific Name	Common Name	Abundance	Percent
Alosa aestivalis	Blueback Herring	1	2.27
Alosa sp.	unk. Alosa species	1	2.03
Dorosoma cepedianum	Gizzard Shad	2	4.59
Fundulus diaphanus	Banded Killifish	1	2.28
Lepomis macrochirus	Bluegill	1	2.03
Menidia beryllina	Inland Silverside	2	4.36
Morone americana	White Perch	32	75.95
Notropis hudsonius	Spottail Shiner	3	6.49
Total		42	100.00

Similar to previous years, White Perch instead of Banded Killifish was the dominant species collected with fyke nets, representing 76% of the total abundance (Table 12, Figure 63 A & B, 64 A & B) and their catches ramped up in July (Table 13). This resembles the trend seen in seine and trawl collections, where White Perch dominated over Banded Killifish as a likely response to the paucity of SAV. The catch was dominated by White Perch at the Fyke Near Station and most fishes were collected at that station (Table 14).

Table 13. Adult and juvenile fish collected by fyke nets on each sampling date.

Scientific Name	Common Name	6-3	6-17	7-15	8-5	9-9	Total
Alosa aestivalis	Blueback Herring	0	0	0	0	1	1
Alosa sp.	unk. Alosa species	0	1	0	0	0	1
Dorosoma cepedianum	Gizzard Shad	0	0	1	1	0	2
Fundulus diaphanus	Banded Killifish	0	0	1	0	0	1
Lepomis macrochirus	Bluegill	0	1	0	0	0	1
Menidia beryllina	Inland Silverside	2	0	0	0	0	2
Morone americana	White Perch	0	0	19	9	4	32
Notropis hudsonius	Spottail Shiner	0	1	2	0	0	3
Total		**2**	**3**	**23**	**10**	**5**	**42**

Table 14. Adult and juvenile fish collected by fyke nets at each station

		Station	
Scientific Name	**Common Name**	**Fyke Far**	**Fyke Near**
Alosa aestivalis	Blueback Herring	0	1
Alosa sp.	unk. Alosa species	0	1
Dorosoma cepedianum	Gizzard Shad	2	0
Fundulus diaphanus	Banded Killifish	0	1
Lepomis macrochirus	Bluegill	1	0
Menidia beryllina	Inland Silverside	0	2
Morone americana	White Perch	9	23
Notropis hudsonius	Spottail Shiner	2	1
Total		**13**	**28**

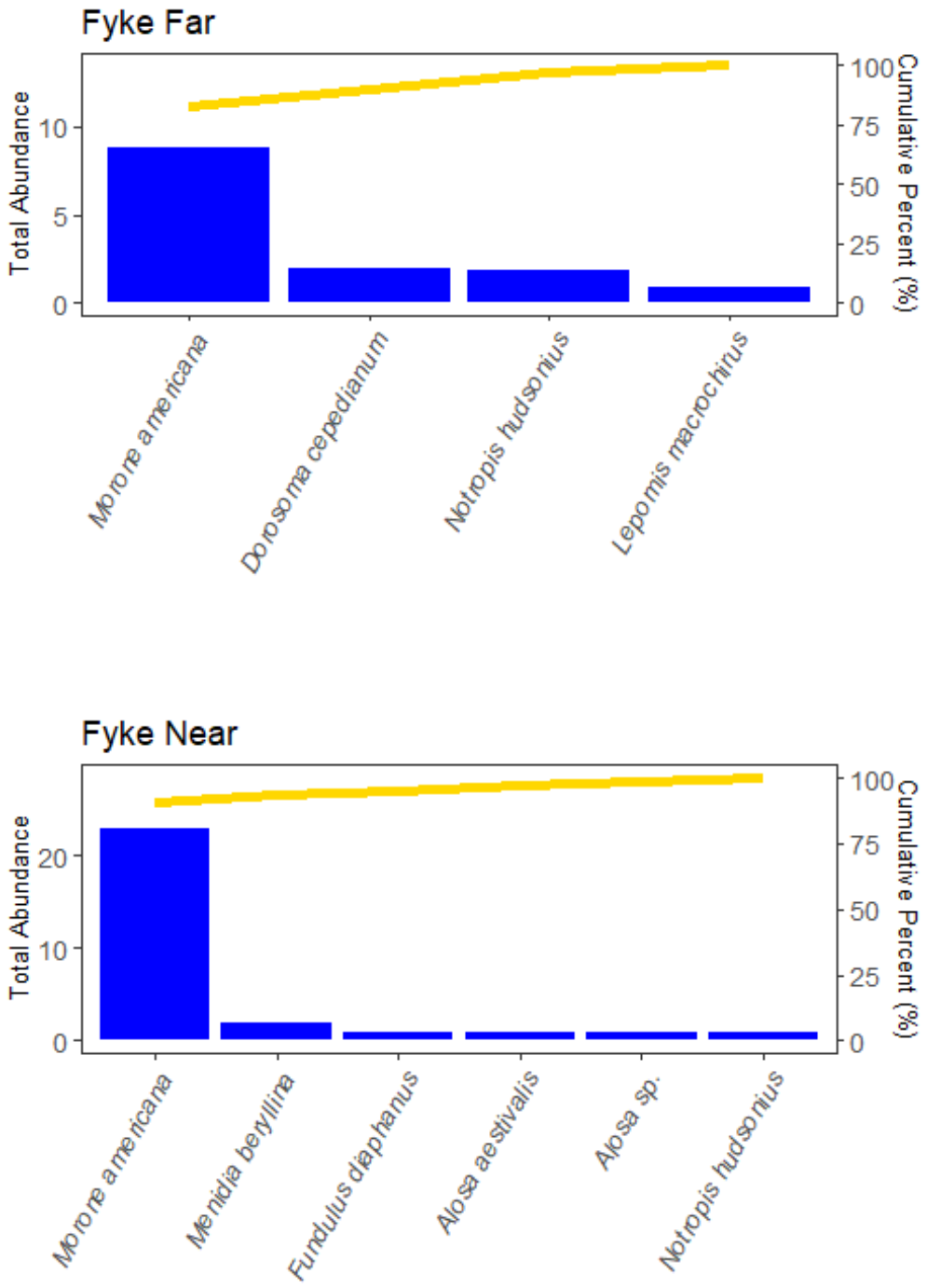

Figure 126A and B. Pareto chart of adult and juvenile fishes collected by fyke nets. Dominant species by station in total abundance and cumulative percentage of total for the Near Fyke (top) and Far Fyke (bottom). Text

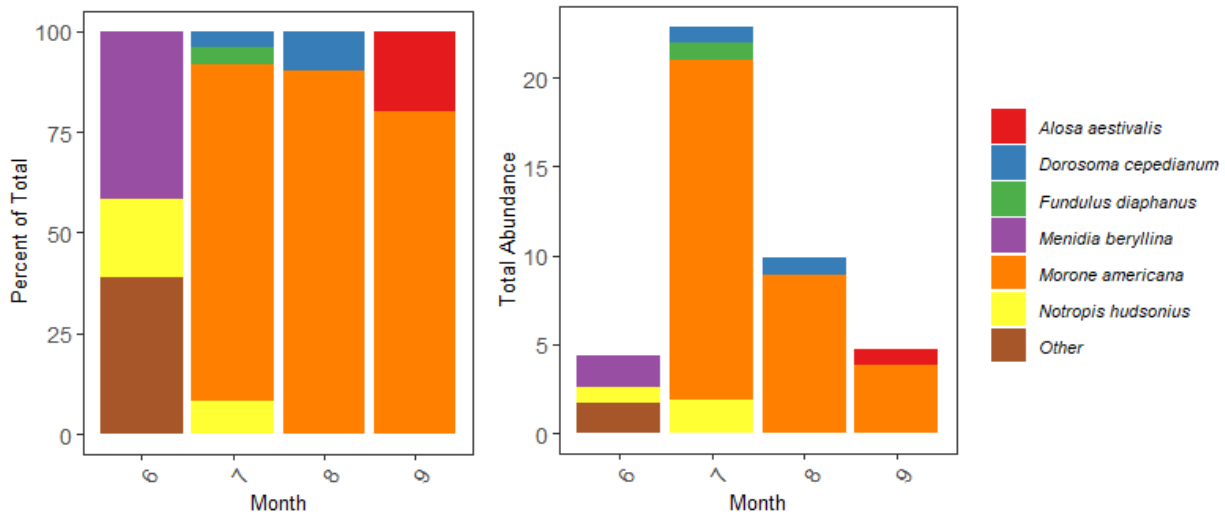

Figure 127A and B. Adult and juvenile fish collected by fyke nets. Dominant species by month in percentage of total (A) and total abundance (B).

H. Submersed Aquatic Vegetation – 2021

SAV data overflights by VIMS were conducted in 2019 and the aerial imagery is available (Figure 107). This imagery shows very little SAV coverage in 2019 compared with recent typical pre-2018 years. While the VIMS reports are not available yet for 2021, the cruises that we conducted and the transects that were done on August 9 (Table 12) indicate that the 2021 imagery will look very similar.

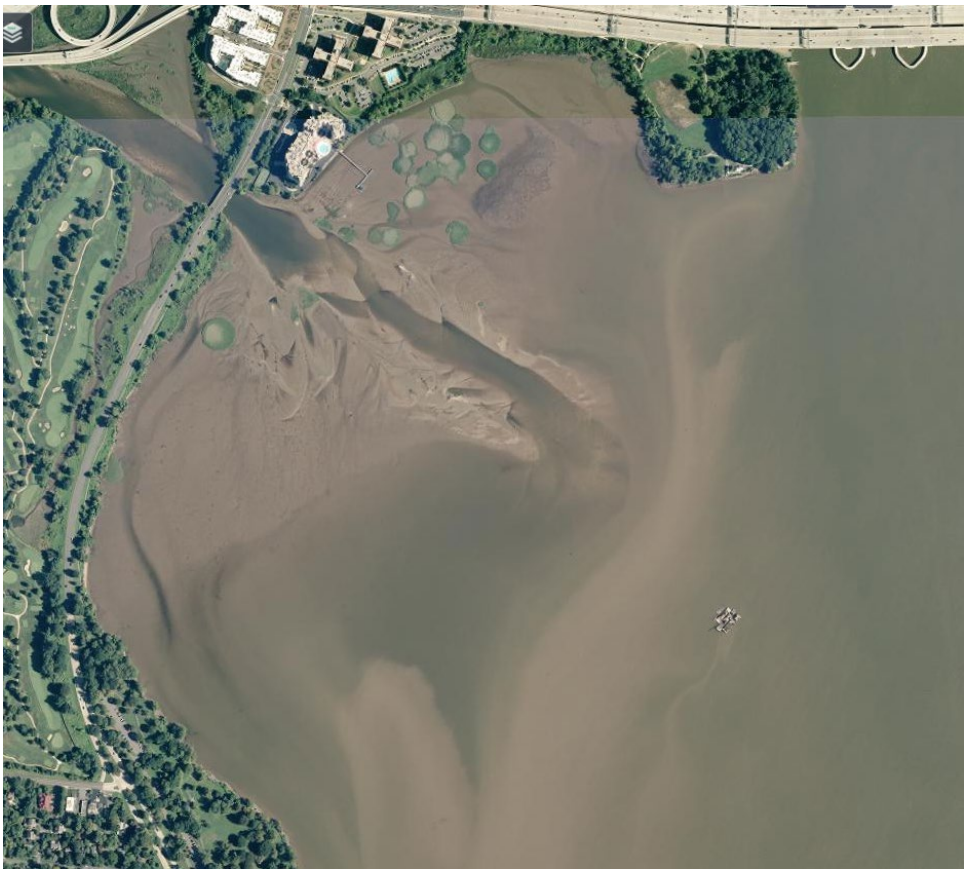

Figure 128. Aerial imagery of Hunting Creek taken in late summer 2019. http://web.vims.edu/bio/sav/savwabmap/ downloaded March 3, 2020.

All SAV taxa were greatly reduced in 2018 and virtually absent in 2019 (Table 12). Coontail, a native species, which was dominant in 2017 was greatly reduced in 2018 and absent in 2019. This decline most certainly started with the very turbid water in 2018 which obstructed light penetration. In 2019, conditions were somewhat better, but at key times in the year light penetration dropped following runoff events and this inhibited SAV recovery. Transects measured in 2020 and 2021 failed to find any SAV.

Table 12. Average Density of Submersed Aquatic Vegetation Species in Transects. Average included all sites with water depth less than or equal to 2 m. 2017-2021. Density scale: 0 (absent) – 4 (very abundant).

		Average Density per sample by SAV Species - 2020	
Taxon Scientific Name	Taxon Common Name	Aug 21, 2020	Aug 9, 2021
Ceratophyllum demersum	Coontail	0	0
Heteranthera dubia	Water Stargrass	0	0
Hydrilla verticillata	Hydrilla	0	0
Najas guadalupensis	Southern Naiad	0	0
Najas minor	Spiny Naiad	0	0
Various	Filamentous algae	0	0

		Average Density per sample by SAV Species - 2019	
Taxon Scientific Name	Taxon Common Name	July 16	August 19
Ceratophyllum demersum	Coontail	0	0
Heteranthera dubia	Water Stargrass	0	0
Hydrilla verticillata	Hydrilla	0.04	0
Najas guadalupensis	Southern Naiad	0	0
Najas minor	Spiny Naiad	0	0
Various	Filamentous algae	0	0

		Average Density per sample by SAV Species - 2018	
Taxon Scientific Name	Taxon Common Name	July 16	August 28
Ceratophyllum demersum	Coontail	0.20	0.10
Heteranthera dubia	Water Stargrass	0.07	0
Hydrilla verticillata	Hydrilla	0.43	0.27
Najas guadalupensis	Southern Naiad	0.02	0.07
Najas minor	Spiny Naiad	0.07	0
Various	Filamentous algae	0.09	0

		Average Density per sample by SAV Species - 2017	
Taxon Scientific Name	Taxon Common Name	July 12	August 10
Ceratophyllum demersum	Coontail	1.76	1.74
Heteranthera dubia	Water Stargrass	0.19	1.19
Hydrilla verticillata	Hydrilla	0.78	0.32
Najas guadalupensis	Southern Naiad	0.20	0
Najas minor	Spiny Naiad	0.45	0.21
Various	Filamentous algae	0.03	0.43

I. Benthic Macroinvertebrates - 2021

River and Embayment Samples

Triplicate petite ponar samples were collected from AR2, AR3, and AR4 monthly from May through September.

Taxonomic Groups: Annelid worms (mainly Oligochaetes with a few Leeches) were found in high numbers at each site over all dates (Table 13; Figure 129). Overall, they accounted for 74% of all benthic organisms found. Oligochaetes were by far the dominant taxonomic annelid, being found in all samples in substantial number. Leeches were less common but found across all sites throughout the sampling period. Insects were the second highest group in abundance across sites and dates, accounting for 14.2% of all individuals accounted for and, more importantly, for the greatest number of distinct taxa (five taxa) (Table 13). Chironomids were by far the most numerous and omnipresent insect taxon. The other insect taxa were present in only a few samples. Crustaceans (including amphipods and isopods) were the third highest group in abundance across sites and dates, accounting for 6.4% of all individuals. Gammarid amphipods (scuds) dominated this group with the isopod *Cyathura polita* being the second most common crustacean (Table 13; Figure 129). The remainder of the taxonomic groups accounted for minor components of the overall abundance and were generally most common at AR4 (Table 13). These included Bivalvia (1.1% of total abundance), Turbellaria (i.e., flatworms) (4.0%), and Gastropoda (0.5%). The bivalve group was composed of both the invasive Asian clam, *Corbicula fluminea*, and a native fingernail clam from the Sphaeriidae family. The gastropod (i.e., snails) group was composed of invasive Japanese mystery snails (*Cipangopaludina japonica*) from the family Viviparidae and native Pleurocerid snails (*Elmina virginica*) and limpets (*Ferrissia rivularis*), all of which were only found at AR4 (Table 13).

Spatial trends: The average abundance of organisms per ponar sample was highest at AR2, but this was entirely attributable to the large number of oligochaetes at that station. AR3 had the lowest average number of organisms per ponar sample. All three sites were dominated by Annelida, driven by high abundances of Oligochaeta (Figure 129A). Site AR4 had a higher diversity of taxa (13 taxa) than either of the other sites (both of which had 7 taxa). Due to the high abundance of Annelida across all sites, additional analyses were conducted with non-Annelida taxa. All gastropods, both native and non-native, were found only at AR4. Bivalves were the most abundant at AR4, but a single native fingernail clam was present only at AR3. When examining all non-Annelida taxa, Insects (driven by Chironomidae) were the dominant group in percent contribution at AR2 (94%) and AR3 (71%), while Crustaceans dominated at AR4 (44%) (Figure 129C). Other taxa varied in their percent contribution by site. For example, Bivalvia were more dominant at AR3, while Gastropoda contributed little to the average abundances and were found only at AR4.

Temporal trends: Members of Annelida, composed of oligochaetes and leeches, were the dominant taxa recorded during all months (Figure 129B). There was a seasonal increase in crustaceans driven by Gammarid amphipods, which peaked during July and August most likely due to recruitment. Bivalve average abundances, dominated by the invasive Asian clam *Corbicula fluminea*, remained low, but relatively stable, over the sampling period and were highest during July. Average abundances of Turbellaria fluctuated, with lowest abundance

during the beginning of the summer and increasing to the highest values during August. The average abundance of Insecta remained relatively stable over the sampling period; with lowest average abundances during September and highest abundances in August, mostly driven by the numbers of midge larvae (Chironomidae) found in the samples. Three gastropod species were found during the sampling period; the average abundances of these species were relatively low with the highest abundances recorded in September. Comparing percent contributions of all non-Annelida taxa across all of the sites, months were dominated by either the Insecta (May – 37%, June – 89%), Crustacean (July – 51%, August – 36%) or the Turbellarians (September – 33%) (Figure 129D). Overall, larger increases in abundances and relative percent contributions over the sampling period for many of the taxa described above are in direct relation to seasonal changes and recruitment.

Table 13. Taxa Identified in Hunting Creek Tidal Benthic Samples. Taxa identified with an asterisk were found on three or more station-dates and were included in the multivariate analysis (see below).

Taxon	Common Name	Average # / ponar		
		AR2	AR3	AR4
Platyhelminthes*	Flatworms	1	1	22.3
Nematoda	Roundworms	1.7	0	0
Annelida-Oligochaeta*	Oligochaete worms	215.7	78.1	66.2
Annelida-Hirudinea*	Leeches	1	2.5	1
Bivalva-Corbicula*	Asiatic clams	0	1	6.2
Bivalvia- Sphaeriidae	Fingernail clams	0	1	0
Gastropoda-Viviparidae	Mystery snails	0	0	1.25
Gastropoda-Pleuroceridae-*Elmina virginica**	Pleurocerid snail	0	0	4.2
Gastropoda-Ancylidae-*Ferrissia rivularis*	Limpet	0	0	2.3
Crustacea-Isopoda-Cyathura*	Isopods	0	1	1.2
Crustacea-Amphipoda-Gammarus*	Amphipods	2.5	0	34.9
Diptera-Chironomidae*	Midges	48.0	7.5	13.3
Ephemeroptera-Heptageniidae	Flatheaded mayflies	0	0	1
Ephemeroptera-Leptophlebiidae	Prong-gilled mayflies	1	0	0
Odonata-Aeshnidae	Darner dragonflies	0	0	1
Trichoptera-Leptoceridae	Long-horned caddisflies	0	0	1
	TOTAL	270.9	92.1	155.85

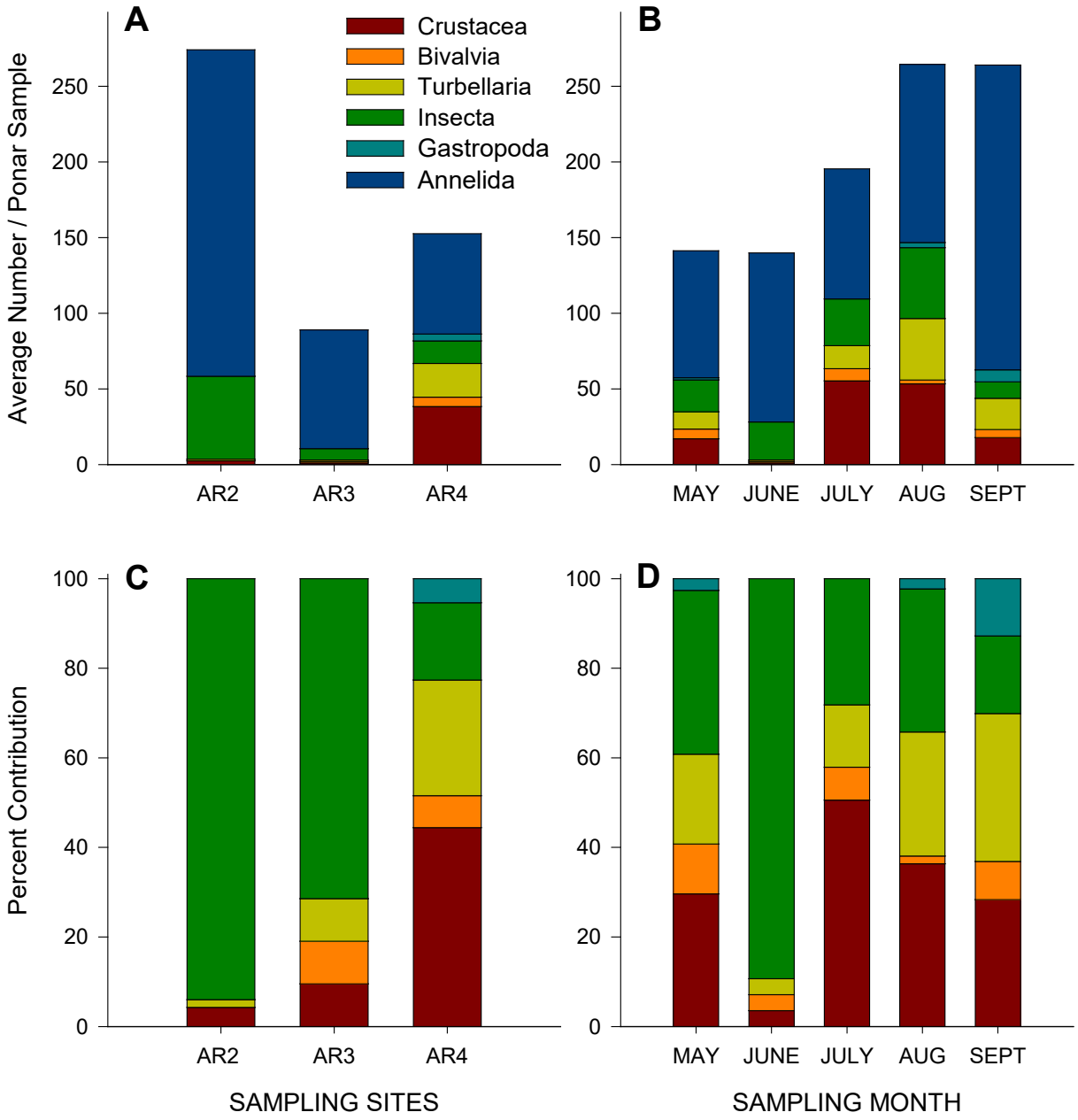

Figure 129. Average number per ponar sample of all benthic macroinvertebrate taxa (A, B) and percent contribution of all non-Annelida benthic macroinvertebrate (C, D) in petite ponar samples separated by site and month.

Multivariate analyses: Due to the multispecies aspect of benthic communities, it is often useful to use multivariate analyses or ordination to examine relationships among samples. This allows multiple taxa to be considered simultaneously when assessing these relationships. In order to get the most meaningful relationships, the full macroinvertebrate sample/taxa matrix was condensed. Taxa that were present in less than three of the original replicate sample matrix were excluded. Then, the remaining, more consistently found taxa were used in the analysis (indicated by asterisks in Table 13, were averaged over the replicates for each date and station combination).

This resulted in one set of taxa values for each station on each date. This reduced matrix (15 samples x 8 taxa) was then subjected to an ordination using a technique called Non-metric Multidimensional Scaling (nMDS). This allows relationships among samples based on their full complement of taxa to be visualized. If successful, relationships among samples can be shown on a two dimensional plot. The taxa differences responsible for the observed relationships can also be examined. The program PRIMER v.6 was used to conduct the ordinations.
The results of an nMDS ordination using the fourth-root transformed data (to decrease the importance of very abundant organisms, like Oligochaetes) is shown in Figure 130. In general, all of the samples separate by site (i.e., the AR4 samples cluster to the left, the AR2 samples cluster to the top right and the AR3 samples cluster in the bottom right). This clustering pattern indicates that the three sampling locations have distinct communities in the types and number of organisms present. Overall AR4 had higher taxa richness across all months (average = 6, range = 6-7) as compared to both AR2 and AR3 (both averages = 3). The higher richness at AR4 is probably due to better habitat conditions, especially large and more heterogeneous sediment particle size.

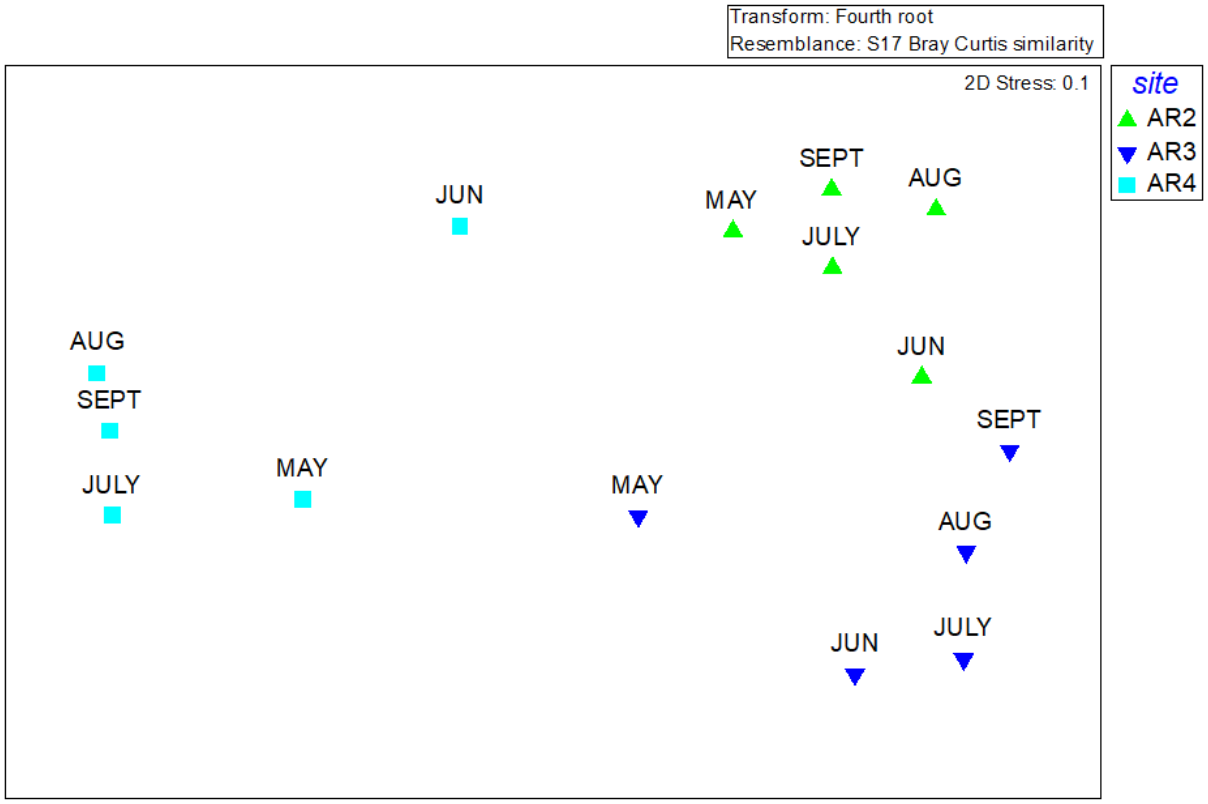

Figure 130. nMDS ordination of benthic samples from tidal stations. The sampling months are placed above each symbol. Colors represent sites. Triplicates were averaged to get a single value for each month-station combination, and then fourth-root transformed. The distance measure was Hellinger.

Influence of Habitat on Community Composition: For this analysis, we assigned all materials greater than 5 mm in the petite ponar sample to one of three categories: leaves/woody debris, mollusc shells, or rocks/sand and calculated the percent contribution of each category to the overall habitat (Table 14). Submerged aquatic vegetation (SAV) was not recovered at any of the

sites. AR2 was dominated by leaves and woody debris throughout the sampling period (average 81%), with little shell or rock/sand collected. In comparison, both AR3 and AR4 are a shelly sites (average 90% and 80%, respectively), with the shell matrix composed of mostly dead Asian clam shells. At AR2, the macroinvertebrate abundance was correlated with the type of large particles available; as the percent organic matter increased and the percent shell decreased, the abundance, but not taxa richness, increased (r = 0.44) (Table 14). Macroinvertebrate richness was not correlated with percent organic matter (r = 0.001). At AR3, there was no relationship between large particle type and total abundance (r = 0.06) or richness (r = 0.19), but this station had variable amounts of large particles present (range of 39 – 99% shell and 1 – 61% leaves or woody debris). AR4 showed an interesting pattern, with a positive relationship between macroinvertebrate richness and percent shell (r = 0.55), but this pattern was reversed for abundance (i.e., a negative relationship between macroinvertebrate abundance and percent shell; r = -0.33).

Table 14. Large substrate composition vs. total abundance of benthic macroinvertebrates in individual replicate samples.

Site	Month	Replicate	% Leaves/Wood	% Shell	% Rock/Sand	Total Abundance	Total Richness
AR2	May	A	32.4	67.2	0.0	85	2
		B	74.5	23.5	0.0	157	3
		C	56.3	43.7	0.0	166	2
	June	A	52.0	42.5	2.5	178	3
		B	84.6	14.1	1.3	243	2
		C	100.0	0.0	0.0	22	1
	July	A	94.1	0.0	0.0	352	2
		B	95.4	0.1	4.5	374	4
		C	95.7	0.0	4.3	72	2
	Aug	A	96.7	3.3	0.0	336	2
		B	85.3	1.3	13.0	314	2
		C	91.1	1.2	6.8	434	2
	Sept	A	74.9	22.3	2.9	527	3
		B	94.2	0.2	5.6	371	3
		C	91.3	0.6	7.1	385	4
AR3	May	A	1.8	98.2	0.0	116	2
		B	2.2	97.8	0.0	60	4
		C	11.1	88.9	0.0	86	4
	June	A	7.5	92.5	0.0	62	2
		B	6.0	94.0	0.0	74	2
		C	2.8	97.2	0.0	60	3
	July	A	7.2	92.8	0.0	47	2
		B	12.6	87.4	0.0	32	2
		C	14.4	85.6	0.0	36	2
	Aug	A	6.5	93.2	0.0	80	3
		B	61.2	38.8	0.0	79	2
		C	3.2	96.8	0.0	75	2
	Sept	A	4.8	95.2	0.0	178	3
		B	12.3	87.7	0.0	199	3

		C	1.4	98.6	0.0	111	2
AR4	**May**	**A**	0.1	99.9	0.0	166	8
		B	0.1	99.9	0.0	146	7
		C	0.1	99.9	0.0	111	7
	June	**A**	82.1	17.0	0.0	298	4
		B	99.6	0.3	0.0	111	2
		C	13.7	86.3	0.0	175	4
	July	**A**	0.3	99.7	0.0	60	5
		B	0.1	99.9	0.0	174	5
		C	0.0	100.0	0.0	53	4
	Aug	**A**	0.0	100.0	0.0	118	6
		B	0.0	98.0	1.9	145	8
		C	0.0	100.0	0.0	156	9
	Sept	**A**	0.2	99.8	0.0	91	7
		B	0.1	49.9	50.0	142	8
		C	0.1	49.9	50.0	79	5

Summary: Similar to previous years, the macroinvertebrate community was dominated by Annelids (including Oligochaetes and Leeches) across sites, with Oligochaetes contributing most to this group. Outside of the Annelids, Crustaceans (dominated by gammarid amphipods) were the most abundant group at AR4, while both AR2 and AR3 were dominated by Insect larvae from the Chironomidae family (midges). Each site had their own unique taxa. Native fingernail clams (family Sphaeriidae) were only found at AR3, while Nematodes and insect larvae from the Leptophlebiidae family were only found at AR2. AR4 had the highest number of unique taxa, with six (three species of gastropods, including the invasive Japanese mystery snails - *Cipangopaludina japonica* and insect larvae from the families Heptageniidae, Aeshnidae, and Leptoceridae). Comparing percent contributions of all non-Annelida taxa across all of the sites, months were dominated by the Crustaceans (July and August), Turbellarians (September) or Insecta (May and June) (Figure 129). Ordination analyses of the communities indicated a clear separation between communities by sampling station. This could be due to the type of habitat found at each site; while the habitat at AR2 is mostly leaves and organic debris, the habitat at both AR3 and AR4 is composed of the shells of dead Asian clams. There was also a change of the community composition throughout the months, as it common for aquatic communities experiencing changes in abiotic conditions and recruitment during the summer months.

Tributary Samples

Duplicate kick net samples were taken in eight tributaries of Hunting Creek on November 3, 2021. The exact locations of the sampling sites are given in Table 15. Individuals from each sample were identified to lowest taxonomic unit, usually genus, except for Oligochaetes (aquatic worms) and Chironomidae (midges).

Table 15. Location of Tributary Benthos Sampling Stations

Station ID	Stream	Location on Stream
CR	Cameron Run	Just below Metrorail bridge
BR	Backlick Run	At trail bridge just upstream of the confluence with Holmes Run
TR	Turkeycock Run	In Bren Mar Park just above Edsall Road
IR	Indian Run	Just below Bren Mar Drive crossing
HR1	Holmes Run	First riffle upstream of confluence with Backlick Run
HR2	Holmes Run	Holmes Run Park just below pedestrian bridge at Pickett Street
TA	Taylor Run	In Angel Park, underneath the trail bridge
TB	Timber Branch	Just east of Ivy Hill Cemetry at W Timber Branch Parkway

Water quality variables were measured on the date of benthic sampling (Table 16) and were generally supportive of aquatic life. It is important to note that all streams were at base flow conditions during the sampling period; water quality is expected to be more degraded during high flow.

Table 16. Water Quality Results from Tributary Benthos Sampling

Station	Temp (°C)	SpCond (uS/cm)	DO (mg/L)	DO (%)	pH	Turbidity YSI units
Cameron Run	11.7	288.3	9.83	90.7	8.0	0.72
Backlick Run	10.5	380.9	11.15	100	7.64	1.63
Turkeycock Run	10.7	266.7	10.56	95.1	7.58	1.12
Indian Run	10.5	334.0	10.79	96.4	7.47	1.58
Holmes Run 1	12.1	204.5	11.12	100	7.88	1.31
Holmes Run 2	13.0	193.3	10.87	100	8.07	1.72
Taylor Run	11.3	323.8	10.74	98.0	7.96	3.36
Timber Branch	11.6	1240	10.07	93.0	7.29	1.15

Taxonomic Groups: Across all sites, 17 different taxa were found. The four most abundant taxa observed included two groups of Tricoptera insect larvae (caddisflies of the families Hydropsychidae and Philopotamidae), a group of Dipteran insect larvae (midges of the Chironomidae family) and Oligochaeta (Table 17, Figure 131). Of these, the Oligochaeta and Chironomidae were found at all of the sites. The Philopotamidae were found at all sites except Timber Branch, and the Hydropsychidae were found at all sites except Backlick Run. All other taxa were significantly less abundant and included Nematodes, Platyhelminthes (flatworms), Hirundea (leeches), Ephemeroptera (mayflies of the family Baetidae), Crustaceans (Gammarid amphipods and Asellidae isopods), Diptera (families Tipulidae, Simuliidae, and Empididae), Coleoptera (family Elmidae), Gastropods (family Physidae), Collembola (springtails), and Trichoptera (familiy Hydroptilidae). (Figure 131). Of the less abundant taxa, none were present at all sites.

Spatial trends: Turkeycock had the highest average abundance of the four dominant taxa (N = 92) (Figure 131). Interestingly, dominant taxa differed by site. Philopotamidae was the dominant group for Holmes Run 2, Indian Run, and Turkeycock Run, while Chironomidae was the dominant group for Cameron Run, Timber Branch and Taylor Run (Figure 131). Hydropsychidae larvae (caddisflies) were dominant only at Holmes Run 1. There were five taxa at were only found at a single location. For example, Hirundea (leeches), the native gastropod

Physa acuta, and the Asellidae isopod were only found at Timber Branch, Gammarid amphipods only at Cameron Run, and the Elmidae riffle beetles were only found at Turkeycock Run.

Table 17. Taxa Identified in Hunting Creek Stream Benthic Samples.

Taxon	Common Name	Average # / kicknet							
		Backlick Run	Cameron Run	Homes Run 1	Holmes Run 2	Indian Run	Taylor Run	Timber Branch	Turkeycock Run
Platyhelminthes	Flatworms	0	5	9.5	0.5	4.5	0.5	1	1
Nematoda	Round worms	0	1	0.5	0.5	1	0	1.5	1.5
Annelida-Oligochaeta	Oligochaete worms	1.5	5.5	4	11	2.5	5.5	26	14
Annelida-Hirundea	Leeches	0	0	0	0	0	0	3.5	0
Gastropoda-Physidae-*Physa acuta*	Physid snail	0	0	0	0	0	0	0.5	0
Crustacea-Amphipoda-Gammarus	Amphipods	0	2	0	0	0	0	0	0
Crusteacea-Isopoda-Asellidae	Isopods	0	0	0	0	0	0	0.5	0
Collembola	Springtails	0.5	0	0	0	0	0	0.5	0
Ephemeroptera-Baetidae	Small minnow mayflies	0	2	4	0.5	0	0	1	0.5
Diptera-Tipulidae	Crane fly	0	0	0	0	0.5	0	2	0
Diptera-Chironomidae	Midges	4	20.5	17.5	6.5	13.5	15.5	34	9
Diptera-Empididae	Dagger fly	0	1	1	0.5	0	1	1	0
Diptera-Simuliidae	Black fly	0.5	1.5	12	0.5	2	2.5	3	0
Coleoptera-Elmidae	Riffle beetle	0	0	0	0	0	0	0	5
Trichoptera-Hydroptilidae	Microcaddisfly	0	7.5	0	1	0	0	0	0
Trichoptera-Hydropsychidae	Hydropsychid caddisfly	0	13	30	6.5	16.5	14	25.5	20
Trichoptera-Philopotamidae	Finger-net caddisfly	2	12.5	21.5	37	32	12.5	0	49
	TOTAL	8.5	71.5	100	64.5	72.5	51.5	100	100
	TAXA RICHNESS	5	11	9	10	8	7	13	8

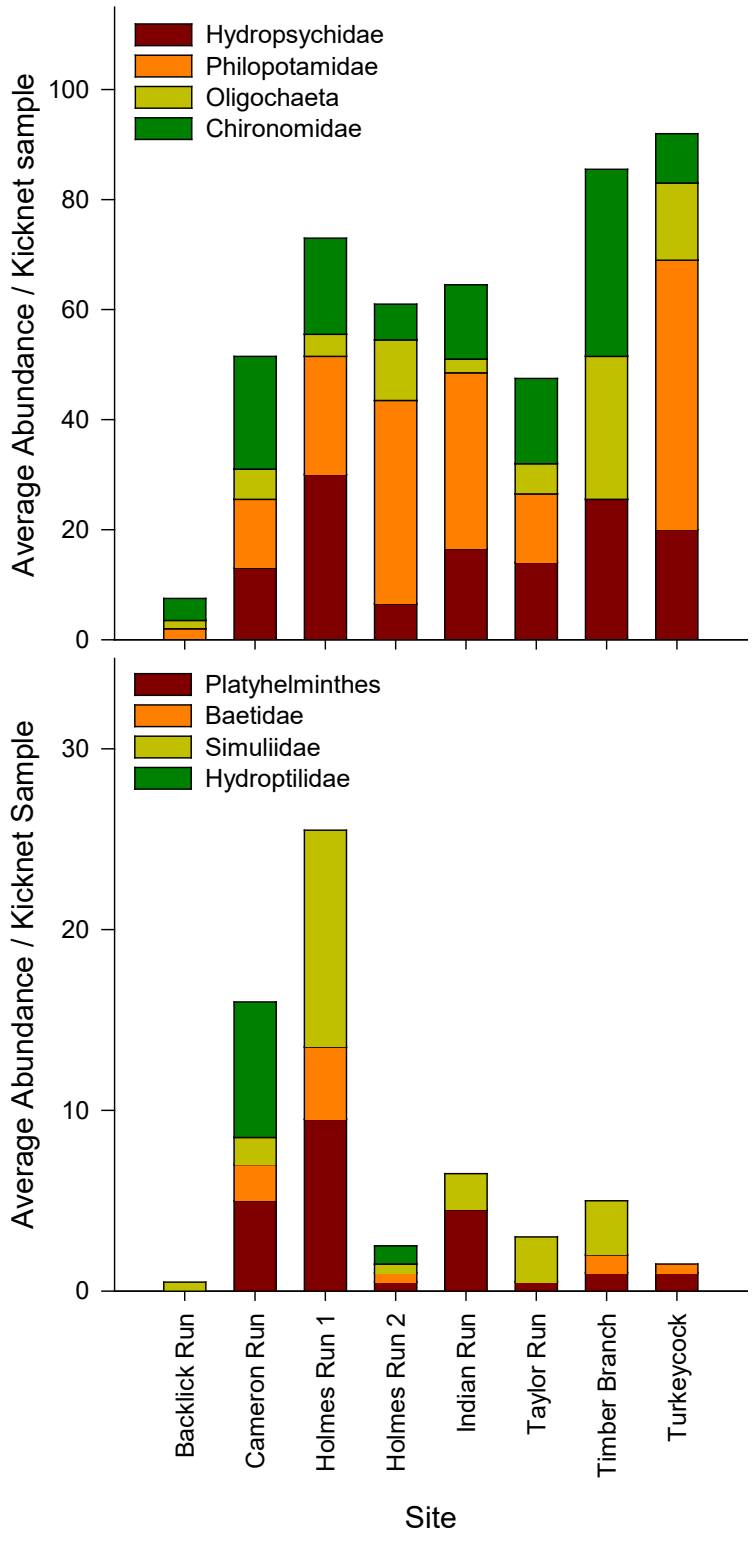

Figure 131. TOP: Average abundance per kicknet sample of the four dominant benthic invertebrate taxa in tributary kick samples. BOTTOM: Average abundance per kicknet sample of four less dominant benthic invertebrate taxa in tributary kick samples. Note the different scales of the y-axes between the two graphs.

Benthic Invertebrate Community Metrics: In general, increasing taxa richness reflects increasing water quality, habitat diversity, or habitat suitability. Taxa richness across all eight sites ranged from 5 to 13 taxa, with lowest richness at Backlick Run and highest richness at Timber Branch (Table 18). "Good" sites were classified as having more than 14 taxa, while "moderate" sites had between 7 and 13; "poor" sites had less than 6 taxa present.

A subset of abundance, EPT richness is the number of species from the generally more environmentally sensitive Insecta groups Ephemeroptera, Plecoptera, and Trichoptera. In general, if the EPT richness is ≤ 2, then conditions are poor. If between 3 and 5, then conditions are moderate. If ≥ 5, then conditions are good. EPT richness in only three of the sampled locations ≤ 2, indicating poor conditions. All sites had at least three species, except for Backlick Run, Indian Run, Timber Branch and Taylor Run. Cameron Run, and Holmes Run 2 had four species, while Holmes Run 1 and Turkerycock had three species.

Calculating the percentage of total organisms that are from the Ephemeroptera, Plecoptera, and Trichoptera groups, without including the family Hydropsychidae, provides another metric for stream condition. In this case, if the value is >9.3%, then conditions are good. If the value is between 4.7 and 9.3%, then conditions are moderate. If the value is < 4.7%, then conditions are poor. Only Timber Branch and Taylor Run had values below the threshold of 4.7%. All of the sites, except Timber Branch, had a high percent of EPT taxa (>20%). Timber Branch had the lowest value at 1%.

Examining the Trichopteran families (without Hydropsychidae) closer can provide more detail about the site conditions, as this insect group has a range of tolerance values for abiotic conditions. Here, good conditions are when the percentage of total organisms >50%, moderate are 25 – 50%, and poor are <25%. Only Holmes Run 2 had percent Trichopteran values higher than 50%; the rest of the sites were either considered moderate (Cameron Run, Indian Run, and Turkeycock Run) or poor (Backlick Run, Holmes Run 1, Taylor Run, and Timber Branch).

Looking at the Coleopteran (beetle) family can also tell us about the stream conditions. In this case, good conditions are values above 1.5, moderate values are 0.75-1.5, and poor conditions are values less than 0.75. Beetles were not found at the majority of sites; only Turkeycock Run had a good percentage of beetles (Elmidae larvae).

The Family Biotic Index (FBI) estimates the overall tolerance of the community in a sampled area toward organic (nutrient) enrichment, weighted by the relative abundance of each taxonomic group (family, genus, etc.). Organisms are assigned a tolerance number from 0 to 10 pertaining to that group's known sensitivity to organic pollutants; 0 is most sensitive, 10 is most tolerant. Low HBI values reflect a higher abundance of sensitive groups, thus a lower level of pollution. Family-level tolerance values from USEPA (Barbour et al. 1999) were used for organisms that could not be identified to the genus level because of size or condition. Taxa with tolerance values ≤3 were considered *intolerant,* whereas those with values ≥7 were considered *tolerant.* Low FBI (≤4.7) values reflect a higher abundance of sensitive groups, indicative of a lower level of pollution. Two locations (Holmes Run 2 and Turkeycock) had "good" FBIs. Two other locations (Holmes Run 1 and Indian Run) fell into the "moderate" category (values 4.7 –

5.4), indicating some organic pollution is probable. The majority of locations were categorized as "poor" (values >5.4) (Backlick Run, Cameron Run, Taylor Run, and Timber Branch), indicating that very substantial pollution was likely (Table 19).

In most cases, as the diversity of a community declines, a select few taxa will dominate the assemblage. Tolerant taxa can replace specialized species, and these communities are indicative of poor stream quality. Percent dominance is calculated as the total number of individuals in the top four most abundant taxa divided by the total number of individuals. A percent dominance above 79% is considered "poor" quality, a value between 57 and 79 is "moderate", and anything below 57% is "good." This year, the top four taxa were the Trichopteran families Hydropsychidae and Philopotamidae, the Chironomidae and the Oligochaeta. The majority of sites were dominated by these top taxa, including Backlick Run, Taylor Run, Timber Branch. Holmes Run 2, Indian Run, and Turkeycock Run. Only Cameron Run and Holmes Run 1 were classified as moderate.

The percent of organisms that are clingers, which are those that have fixed retreats or adaptations for attachment to surfaces in flowing water, is another indicator of environmental quality. While this metric would normally also include the percent of organisms are from the Plecoptera group (which are one of the first groups to disappear as human disturbance increases); none of the organisms sampled this year were from that group. Increasing metric values indicate increasing substrate stability. In this case, if the value is >14%, then conditions are good. If the value is between 7 and 14%, then conditions are moderate. If the value is <7%, then conditions are poor. All of the locations had values >14%, indicating good substrate stability.

Shredder taxa are those that tear apart organic material, usually leaves, and dominate low-velocity, high-retention pools. Sites were categorized as "poor" if the percent of shredders was <2, as "moderate" if the percent was between 2 and 4, and as "good" is the percent was higher than 4. As Chironomidae are considered shredder taxa, and that was a dominant group this year, all locations had high percentages of shredders indicating good conditions.

Predator taxa are at the top of the food web and depend on a reliable source of other invertebrate prey items. The percentage of taxa that are obligate predators can provide a measure of how trophically complex a site is. Less distributed sites support a greater abundance and diversity of prey items, thus supporting a greater number and diversity of predators. Sites were categorized as "poor" if the percent of predators was <3.2, as "moderate" if the percent was between 3.2 and 6.5, and as "good" is the percent was higher than 6.5. All sites were classified as "poor" except for Timber Branch. This may be due to the fact that only three identified organisms were recognized as predators (Hirundea, Tipulidae, and Empididae), and these organisms were not very common across sampled locations.

Using these 10 measures of biological health, we can calculate a summary statistic of relative overall health of these streams (Table 19). In this case, we assign values of high (6), moderate (3), or low (0) health for each metric at each site, sum these values for each site and divide by 60 (i.e., the maximum score achievable). Streams characterized as "excellent" would achieve summary statistics of 80-100% of the maximum summary statistic. "Good" streams would be between 60 and 79%, "fair" streams would come in at between 40 and 59% of the summary

statistic, while "poor" streams would be between 20 to 39%. Using the criteria for each metric laid out above, two streams were categorized as "good" (i.e., Holmes Run 2 and Turkeycock Run), three were categorized as "fair" (i.e., Cameron Run, Holmes Run 1, and Indian Run), and three were categorized as "poor" (i.e., Backlick Run, Taylor Run, and Turkeycock Run) (Table 19). Those that are "good" are slightly degraded sites with decreasing numbers of intolerant species. "Fair" sites have a marked decrease in intolerant species, and the community has shifted to be dominated by a few species. Lastly, "poor" sites lack intolerant species and have an overall decrease in taxa diversity.

Table 18. Benthic invertebrate community metrics on the sum total of organisms found from both replicate kicknets. EPT include the Insecta from Ephemeroptera, Plecoptera, and Trichoptera. Color shading indicates relatively good (green), moderate (yellow), or poor (red) conditions for each of the metrics and the summary statistic.

	Abundance	Taxa Richness	EPT Richness	% EPT w/o Hydropsychidae	% Trichoptera w/o Hydropsychidae	% Coleoptera	Family Biotic Index	% Dominance	% Clingers + % Plecoptera	% Shredders	% Predators
Backlick Run	17	5	1	23.5	23.5	0	7.2	88.2	29.4	47.1	0
Cameron Run	143	11	4	30.8	28.0	0	5.8	72	51	39.2	1.4
Holmes Run 1	200	9	3	25.5	21.5	0	5.2	73	67.5	17.5	1
Holmes Run 2	129	10	4	59.7	58.9	0	4.3	94.6	70.5	11.6	0.8
Indian Run	145	8	2	44.1	44.1	0	4.8	89	70.4	19.3	0.7
Taylor Run	103	7	2	24.3	24.3	0	5.8	92.2	56.3	30.1	1.9
Timber Branch	200	13	2	1.0	0	0	6.6	85.5	31.5	36	6.5
Turkeycock Run	200	8	3	49.5	49.0	5	4.3	92	74.5	9	0

Table 19. Index scores of the benthic invertebrate community metrics on the sum total of organisms found from both replicate kicknets. Color shading indicates relatively good (green), moderate (yellow), or poor (red) conditions for each of the metrics and the summary statistic.

	Taxa Richness	EPT Richness	% EPT w/o Hydropsychidae	% Trichoptera w/o Hydropsychidae	% Coleoptera	Family Biotic Index	% Dominance	% Clingers + % Plecoptera	% Shredders	% Predators	**Index Score**
Backlick Run	0	0	6	0	0	0	0	6	6	0	**30%**
Cameron Run	3	3	6	3	0	0	3	6	6	0	**50%**
Holmes Run 1	3	3	6	0	0	3	3	6	6	0	**50%**
Holmes Run 2	3	3	6	6	0	6	0	6	6	0	**60%**
Indian Run	3	0	6	3	0	3	0	6	6	0	**45%**
Taylor Run	3	0	0	0	0	0	0	6	6	0	**35%**
Timber Branch	3	0	0	0	0	0	0	6	6	3	**30%**
Turkeycock Run	3	3	6	0	6	6	0	6	6	0	**65%**

Summary: Seventeen taxa were identified across all sites in 2021. In general, the top four most abundant taxa observed across all sites stayed the same as in previous years. In 2021, Turkeycock had the highest abundance of all macroinvertebrates and the four dominant taxa, mostly composed of the Insecta family Philopotamidae. In contrast to previous years in which Hydropsychidae larvae (caddisflies) were the dominant group at the majority of the sites, Philopotamidae were dominant across sites in 2021. Taxa richness across all sites ranged from 5 to 13 taxa, with lowest richness at Backlick Run and highest richness at Timber Branch. Using 10 measures of biological health, we calculated a summary statistic of relative overall health of these streams. Using the criteria for each metric laid out above, two streams were categorized as "good", three were categorized as "fair", and three were categorized as "poor".

DISCUSSION

A. 2021 Synopsis

Air temperature was above normal for all months. There were 38 days with maximum temperature above 32.2°C (90°F) in 2021 as in 2020 which is well above the median number over the past decade. Precipitation closer to normal in 2021 than in the extremely wet year 2018. However, it was again well above normal in 2021, especially in June and August. This was reflected by Cameron Run inflows which were also well above normal in June and August. This runoff could have direct impacts on late June and late August water quality-plankton sampling dates. As Figure 132 shows periods of rain and associated runoff peaks were concentrated in late May, June, and August.

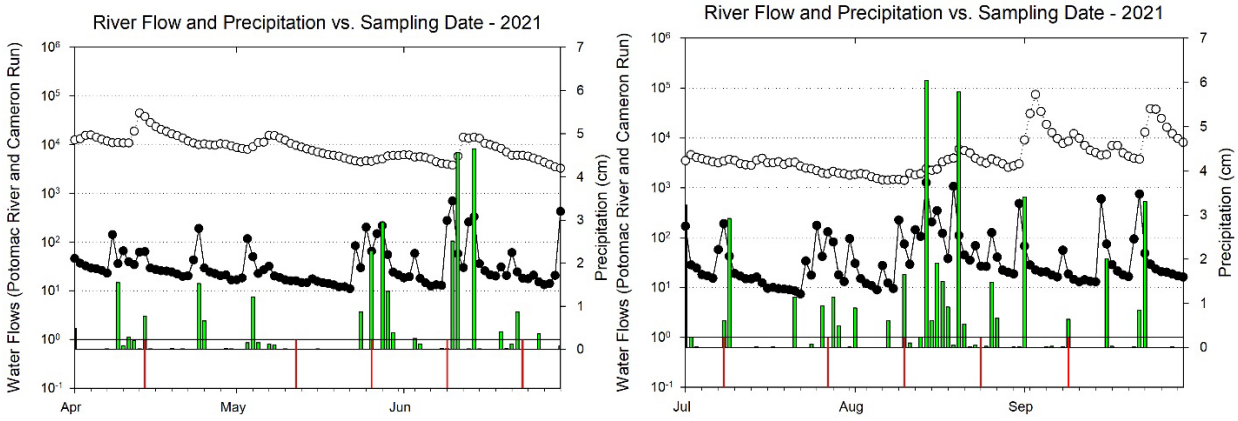

Figures 132. Precipitation (green bars), Cameron Run flows (solid circles), Potomac River flows (open circles) and water quality/plankton sampling events (red lines at bottom).

Water temperature followed a typical seasonal pattern at all tidal stations with highest values approaching 30°C in early June, July, and August. A marked drop in water temperature occurred in late June corresponding with a cool snap and associated precipitation. Specific conductance did not show much variation at most stations. Chloride showed a marked drop in late June at some stations. Dissolved oxygen peaked in early June indicating strong phytoplankton photosynthesis at that time. Field pH also peaked at that time at the embayment stations AR2 and AR3, further evidence of phytoplankton photosynthesis. Total alkalinity was in the 60-100 range at all tidal river sites, similar to past years.

Light penetration was generally higher in the river than in the embayment. In the Hunting Creek embayment there was a consistent decline in Secchi disk depth and light attenuation coefficient over the study period. There were also substantial declines in late June and last July corresponding with elevated Cameron Run inflows. Field turbidity readings also reflected these trends.

Almost all ammonia nitrogen values were below the 0.2 mg/L detection limits at the tidal stations so little could be said about trends. Nitrate showed a general pattern of decline from April into August which is probably attributable to less input and uptake by phytoplankton and other biota. A marked peak was observed in late June attributable to substantial excess runoff from the watershed during June. Nitrate recovered strongly in late August and September. Nitrite was low at all stations and did not show consistent seasonal patterns. Organic N was generally low and fairly constant at the Tidal Main Stations, but higher and more variable at some of the Tidal CSO Impact Stations. Total P exhibited a similar pattern. All ortho-P values were below the 0.05 detection limit so no patterns could be discerned. N/P ratio consistently pointed to P limitation, with values generally in the 10-30 range being greater than 7.2 threshold in all samples. BOD was consistently below 4 mg/L at most stations. TSS values did not vary much over most stations at dates although there were a few spikes at AR1 and AR25.

The grouping of tidal stations into Tidal Main Stations and Tidal Impact Stations did not reveal any major differences in any variables other than perhaps more variability at the Tidal CSO Impact stations.

In the tributaries, seasonal temperature patterns were similar to the tidal stations with the marked drop in late June, but somewhat reduced maximum values near 25°C. In contrast to the tidal stations, specific conductance exhibited a marked seasonal decline especially at the Cameron Run Axis stations probably due to the slow flushing of road salt residuals from surface groundwater. The patterns in chloride, a main component of road salt, backed up these trends in specific conductance. Dissolved oxygen was at or near saturation at the tributary stations except for AR34 which is at the lower end of the Hooffs Run Axis and influenced by the AR effluent and perhaps by near shore tidal Hunting Creek stations. AR34 showed values at low as 3 mg/L or 30% saturation. Field pH followed a very similar seasonal pattern at all stations with most values centered around 7.5. Lab pH values were even more consistent over time and stations, centered slightly below 7.5. YSI turbidity was very low at all tributary stations on all dates except for AR23, AR13, and AR34. These stations are at the lower end of their axes and near the influence of the AR effluent. Total alkalinity was quite consistent at most stations and throughout the year. Again, the exception was AR23 which often showed elevated values.

Total phosphorus values were frequently below the detection limit of 0.05 mg/L except at AR23, AR13, and AR34, similar to turbidity. Virtually all ortho-P values were below the detection limit of 0.05 mg/L. Organic N at most stations was below 0.5 mg/L. Exceptions again were AR23 and AR34 which had substantially higher and more variable values. Ammonia N was generally near or below detection limits with only one higher value at AR23. Nitrate N was generally low and followed a declining trend at most stations in the Cameron Run Axis. AR23 was often higher. Nitrate on the Hooffs Run Axis was generally somewhat higher, especially at AR33 in the middle of a residential area which was consistently higher reaching 2.5 mg/L. Nitrite N was consistently very low. TSS and VSS were consistently low at most tributary stations. Exceptions again were AR23, AR13, and AR34 which had variable and elevated values.

Phytoplankton biomass as indicated by chlorophyll *a* exhibited two distinct maxima and early June and in early August 2021 at the two Hunting Creek embayment stations (AR2 and AR3).

The early June peak occurred during a period of low rainfall and corresponded with high dissolved oxygen and high pH indicating strong photosynthesis by phytoplankton.This peak in late July and early August of 40 µg/L is similar to that attained in 2020 and is among the highest values observed in the nine years of study. At the river station AR4 chlorophyll values were fairly constant at about 10 µg/L. Phytoplankton cell density at AR2 peaked at the same date as chlorophyll *a* at AR2. Cyanobacteria were the dominant group on that date with a roughly even mixture of *Merismopedia*, *Chroococcus*, and *Oscillatoria*. At AR4 phytoplankton cell density peaked in late July led by green algae and cyanobacteria. Phytoplankton biovolume was generally dominated by diatoms notably *Melosira* and some unidentified pennate diatoms at both AR2 and AR4. Other algae such as Euglena and Peridinium were also dominant on some occasions.

Rotifers were very abundant in early June reaching nearly 8000/L at AR2 and over 4000/L at AR4. As is typical, *Brachionus* was the dominant rotifer. The small cladoceran *Bosmina* had a high short-lived peak in late May of over 500/L. *Diaphanosoma* was the dominant large cladoceran and was very abundant at both AR2 and AR4 and reached maxima in late May and early June, again a period of low precipitation and thus low flushing. *Leptodora* reached a very strong peak of over 6000/m^3 in late May. Among the copepods the immature copepod nauplii reached a strong peak in late May at both AR2 and AR4 and then showed a slow decline thereafter. *Eurytemora* as the most abundant larger copepod with a maxima of over 4000/m^3 in early June at AR4 and almost 2000/m^3 at AR2. *Mesocyclops* was also abundant at AR4.

B. Correlation Analysis of Hunting Creek Data: 2013-2021

To better understand the ecological relationships in Hunting Creek and the nearby Potomac River, relationships among parameters were assessed using correlation analysis. Since all samples were collected by PEREC personnel at the same time, it was possible to pool the data on all field and lab water quality parameters at the level of depth-averages and/or surface samples. Three tables were constructed: PEREC field and lab parameters correlated against each other, ARE lab parameters correlated against each other, and all water quality parameters correlated against Cameron Run flow. This final set of correlations was added this year to determine the effect of freshwater flow pulses into Hunting Creek on the water quality variables.

Table 20 shows the correlations among PEREC-collected water quality parameters from the regular sampling. These reflect relationships over all nine years of the study. Indicators of photosynthesis (DOPPM, DOSAT, Field pH) were highly intercorrelated. Also, measures of particles in the water column and resultant water clarity (turbidity, TSS, Secchi disk depth, and extinction coefficient) were also highly intercorrelated. Indicators of phytoplankton abundance (CHLDI, CHLSF, and VSSSF) were highly intercorrelated.

Pearson Correlation Matrix													
	TEMP	SPC	DOPPM	DOSAT	FLDPH	SD	EXTCO	CHLDI	CHLSF	TSSSF	VSSSF	YSITUR	YSICHL
TEMPC	1.0000												
SPC	0.384	1.000											
DOPPM	-0.323	-0.155	1.000										
DOSAT	0.056	-0.017	0.920	1.000									
FIELDPH	0.220	0.060	**0.616**	**0.727**	1.000								
SECCHI	0.002	0.332	0.010	0.006	0.136	1.000							
EXTCOEF	0.012	0.362	-0.009	-0.013	0.203	**0.833**	1.000						
CHLDI	**0.465**	0.250	-0.043	0.121	0.096	-0.269	-0.318	1.000					
CHLSF	**0.455**	0.226	-0.068	0.095	0.075	-0.291	-0.341	**0.986**	1.000				
DRYWTSF	-0.048	-0.297	-0.019	-0.044	-0.368	**-0.747**	**-0.844**	**0.413**	**0.431**	1.000			
AFDWSF	0.163	-0.077	-0.026	0.035	-0.194	**-0.537**	**-0.682**	**0.615**	**0.630**	**0.848**	1.000		
YSITURB	-0.060	-0.359	-0.018	-0.036	-0.232	**-0.639**	**-0.803**	0.173	0.187	**0.730**	**0.547**	1.000	
YSICHL	0.311	0.228	0.016	0.151	0.236	-0.071	-0.070	**0.440**	**0.458**	-0.058	0.052	0.073	1.000

Table 20. Correlations among PEREC collected water quality parameters from regular sampling. Depth-integrated samples unless otherwise indicated. AR2 and AR3 pooled. 2013-2021. April-September. Strongest correlations (r>0.400) are have **bolded** text. N=126-179.
TEMP – water temperature (°C), SPC – specific conductance (µS), DOPPM – dissolved oxygen (mg/L), DOSAT – dissolved oxygen (% saturation), FLDPH – field pH,SD - secchi disk depth (m), EXTCO (light attenuation coefficient (m^{-1}), CHLDI – depth-integrated chlorophyll a (µg/L), CHLSF – surface chlorophyll a (µg/L), , TSSSF - TSS on surface samples (mg/L), VSSSF – VSS on surface samples (mg/L) YSITUR – Turbidity as measured by YSI sonde *in situ*.

The correlation coefficients among AR lab parameters are shown in Table 21. Among the most highly correlated variables in this dataset were TSS and VSS (0.794). Total P was positively correlated with organic N, TSS and VSS. Most phosphorus is bound to particles so these correlations make sense. TP was negatively correlated with N to P ratio and this makes sense since it is in the denominator of this ratio. Organic N was highly correlated with TSS, VSS, and BOD. VSS and TSS were highly correlated with BOD. Lab pH was negatively correlated with ammonia nitrogen, but this may just reflect that lab pH is highest in summer when ammonia nitrogen is lowest. Other correlations were not strong.

Pearson Correlation Matrix													
	PHLAB	**ALK**	**TP**	**OP**	**ON**	**NO3**	**NH4**	**NO2**	**CLD**	**TSS**	**VSS**	**BOD**	**NTOP**
PHLAB	1.000												
ALK	0.279	1.000											
TP	-0.225	-0.134	1.000										
OP	-0.162	-0.280	-0.058	1.000									
ON	-0.142	0.018	**0.499**	-0.238	1.000								
NO3	-0.162	-0.006	0.313	0.101	-0.195	1.000							
NH4	**-0.426**	-0.327	0.322	0.326	0.033	**0.438**	1.000						
NO2	-0.165	0.031	0.180	-0.116	0.303	-0.002	0.095	1.000					
CLD	-0.015	0.131	-0.017	-0.129	0.257	-0.274	0.051	0.013	1.000				
TSS	-0.328	-0.020	**0.699**	-0.057	**0.514**	0.393	0.358	0.195	-0.050	1.000			
VSS	-0.182	0.065	**0.606**	-0.054	**0.571**	0.194	0.240	0.154	0.101	**0.794**	1.000		
BOD	-0.130	-0.085	0.334	-0.121	**0.508**	-0.140	0.121	0.056	0.252	**0.496**	**0.530**	1.000	
NTOP	-0.013	0.200	**-0.604**	0.044	-0.372	0.187	-0.023	-0.141	0.056	-0.287	-0.296	-0.215	1.000

Table 21. Correlation coefficients between AR lab parameters. AR2 and AR3 pooled. 2013-2021. April-September. Strongest correlations (r>0.400) are **bolded**. N=172-177..

PHLAB – lab pH, ALK – total alkalinity (mg/L as $CaCO_3$), TP – total phosphorus (mg/L), OP – orthophosphorus (mg/L), NO3N – nitrate nitrogen (mg/L), NH4N – ammonia nitrogen (mg/L), NO2N – nitrite nitrogen (mg/L), CLD – chloride (mg/L), TSS – total suspended solids (mg/L), VSS – volatile suspended solids (mg/L), NTOP – nitrogen to phosphorus ratio by mass.

Since the study began in 2013 it has been noted that certain water quality variables appear to be impacted by major rainfall and runoff events. In this year's report we have tested the correlations between recent runoff coming down Cameron Run and a wide array of water quality variables (Table 22). This analysis reveals that many variables are strongly correlated with recent stream flow. Specific conductance, chloride, pH, and alkalinity are all significantly reduced by increased streamflow, probably due to the dilution effects of the runoff on the water already in the river. Turbidity, Secchi depth, light attenuation, and TSS are all increased by runoff because solids are either brought in or resuspended by the higher runoff resulting in poorer light penetration. Ammonia nitrogen is increased at all except AR4; the reason for this is unclear.

Table 22. Pearson Correlation Coefficients between Water Quality Parameters and Log_{10}(5 day flow) where 5-day flow is the average stream flow on Cameron Run as measured at USGS Gaging Station 01653000 for the day of sampling and the 4 previous days. N=64-80.

Water Quality Parameter	AR 1 GW Pkwy Br	AR 2 N. Hunting Cr	AR 3 S. Hunting Cr.	AR 4 River Mainstem
Temperature (°C)	-0.438**	-0.428**	-0.407**	-0.431**
Sp. Conductance (µS/cm)	-0.520**	-0.635**	-0.773**	-0.743**
Dissolved Oxygen (mg/L)	0.081	0.062	-0.036	0.390*
Dissolved Oxygen (%sat)	-0.152	-0.087	-0.178	0.234
Field pH	-0.090	-0.291	-0.296	0.050
Secchi Disk Depth (m)	-----	-0.301*	-0.338*	-0.224
Light Atten. Coef. (m^{-1})	-----	-0.339*	-0.439**	-0.230
YSI Turbidity (NTU)	0.430**	0.451**	0.392*	0.084
YSI Chlorophyll (µg/L)	0.097	-0.084	-0.096	-0.099
Chlorophyll a, DI (µg/L)	-----	-0.162	-0.197	-0.273
Chlorophyll a, Surf (µg/L)	-----	-0.117	-0.179	-0.330
TSS, Surf, GMU (mg/L)	0.146	0.389*	0.279	0.083
VSS, Surf, GMU (mg/L)	-0.082	0.132	0.091	-0.019
pH Lab	-0.445**	-0.400**	-0.449**	-0.346*
Total Alk. (mg/L as $CaCO_3$)	-0.572**	-0.572**	-0.542**	-0.523**
Total Phosphorus (mg/L)	0.084	0.296	0.254	0.040
Ortho Phosphorus (mg/L)	0.206	0.254	0.267	0.386*
Organic Nitrogen (mg/L)	-0.163	-0.080	0.005	-0.182
Nitrate Nitrogen (mg/L)	0.122	0.333	0.284	0.281
Ammonia Nitrogen (mg/L)	0.384*	0.392*	0.475**	0.150
Nitrite Nitrogen (mg/L)	-0.113	-0.032	-0.009	-0.312
Chloride (mg/L)	-0.142	-0.206	-0.352*	-0.472**
TSS, DI, ARE (mg/L)	0.242	0.398*	0.208	0.021
VSS, DI, ARE (mg/L)	0.131	0.233	0.097	-0.016
BOD (mg/L)	0.079	0.179	0.130	0.149
N to P ratio	-0.152	-0.091	-0.123	0.073

C. Water Quality: Comparison among Years

Since nine years of data are now available for the Hunting Creek area, comparisons were made for each parameter among years. In order to assess overall patterns in the data among years and stations, box plots were constructed for each station and year. In a box plot, the spread of the middle 50% of the data is shown by a box with a line in the middle which is the median. Whiskers extend out to the limits of the data.

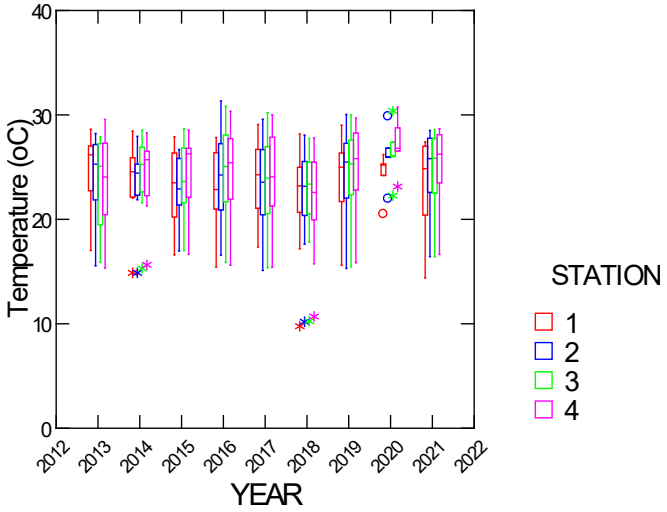

Figure 133. Box plots comparing values of Temperature between years. April through September.

Temperature did not show much difference between the years with the medians in the 24-27ºC range at all sites and years (Figure 133). The 2021 medians were at the higher end of that range and varied very little between stations. Specific conductance showed clear differences among stations in most years with AR 1 consistently higher due to input from AR effluent (Figure 134). In 2021 values at all stations were similar to most years and higher than the wet year 2018.

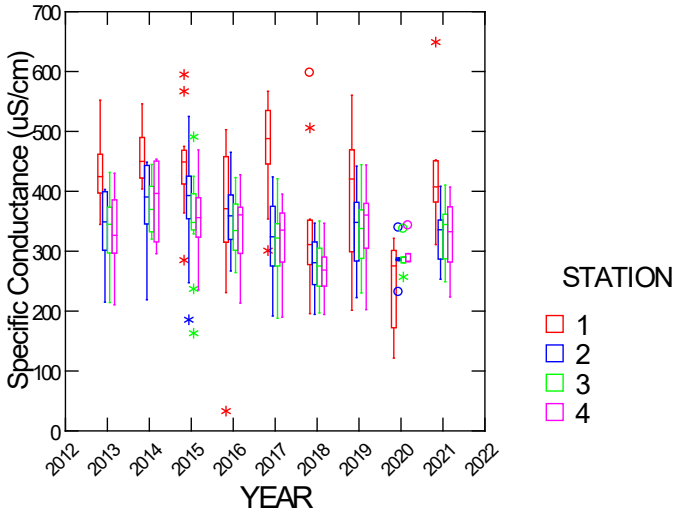

Figure 134. Box plots comparing values of Specific Conductance between years. April through September.

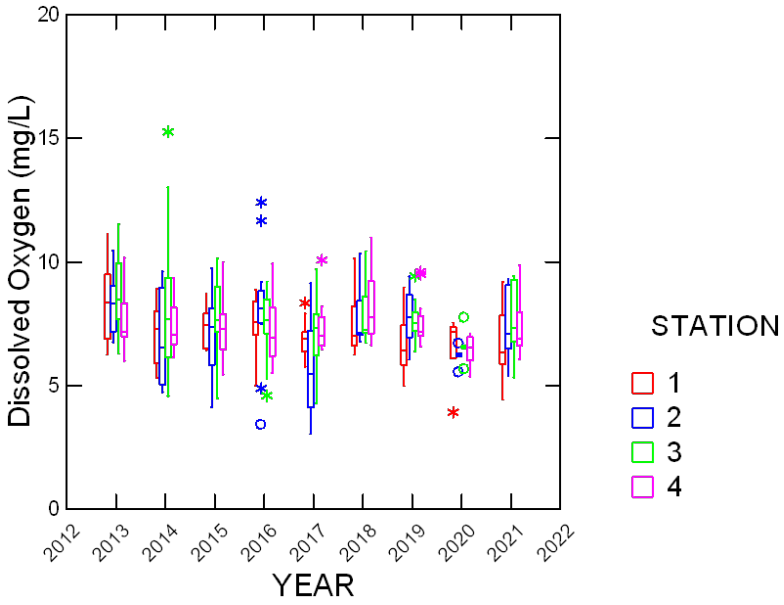

Figure 135. Box plots comparing values of dissolved oxygen as mg/L between years. April through September.

Dissolved oxygen showed little difference among stations in 2021 compared with some more marked differences in previous years (Figure 135). The interquartile range was similar to most previous years. A similar pattern was observed in dissolved oxygen (as % saturation) (Figure 136).

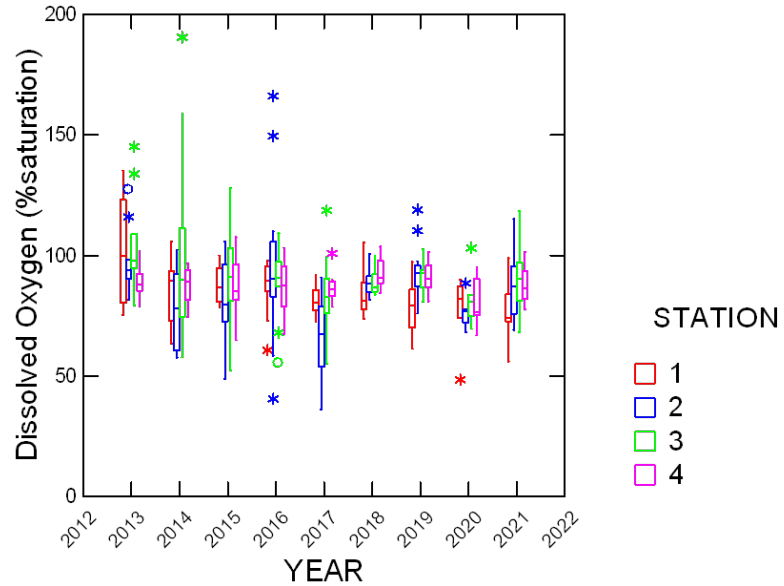

Figure 136. Box plots comparing values of dissolved oxygen as percent saturation between years. April through September.

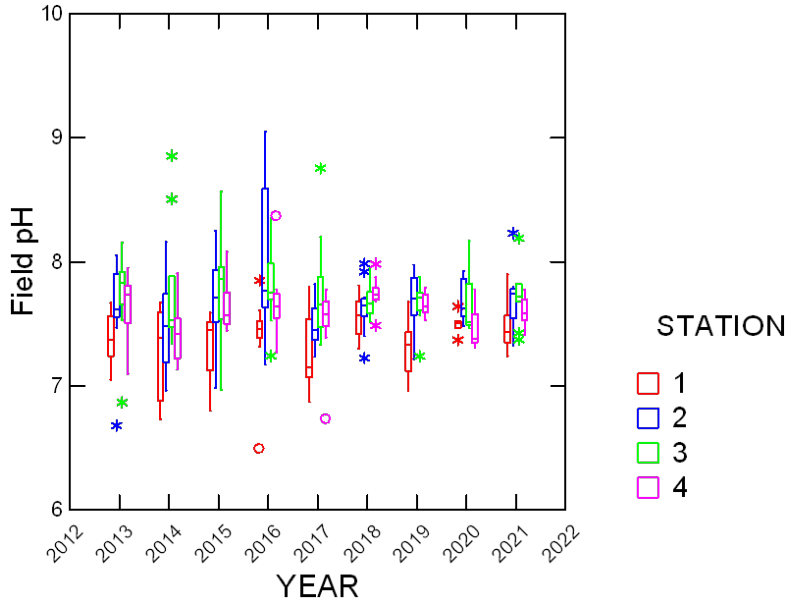

Figure 137. Box plots comparing values of field pH between years. April through September.

Field pH values fell into a relatively narrow range in 2021 as in 2018-2020 (Figure 137). In some years median values at AR2 and AR3 were much higher than at the other two stations. This was attributed to photosynthesis by SAV which tends to increase pH since the high values were observed in July and August when SAV was most abundant. In the period 2018 to 2021 SAV was minimal in Hunting Creek.

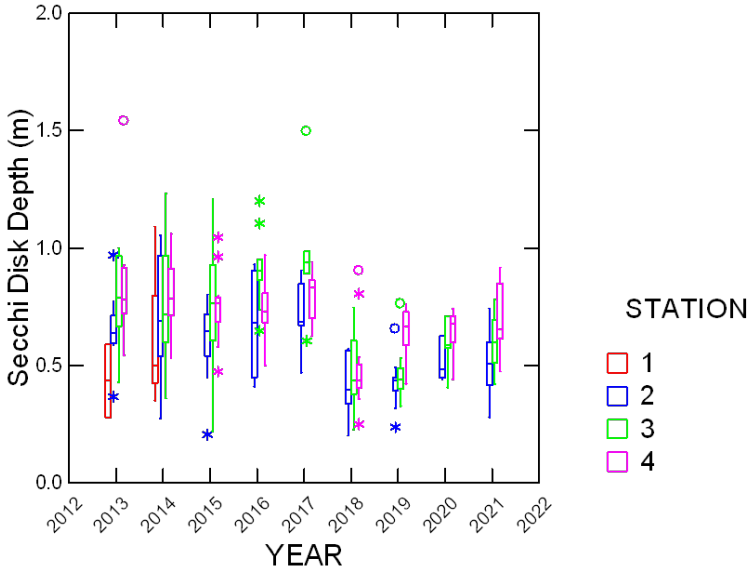

Figure 138. Box plots comparing values of Secchi disk depth between years. April through September.

Secchi disk depth (Figure 138) has generally shown major and consistent differences between stations, attributable to major differences in SAV abundance between the stations. In particular AR3 was often much higher than the other stations. However, starting in 2018 and continuing through 2021, Secchi depths were lower overall and were generally lower at AR2 and AR3 (in the embayment) than at AR4 in the river channel. Light attenuation coefficient is another way of measuring water clarity: less negative values of light attenution coefficient indicate clearer water. Median values in light attenuation coefficient were similar from year to year until 2018 (Figure 139). As with Secchi disk depth, values for light attenuation in 2018 to 2021 showed much reduced water clarity than previous years.

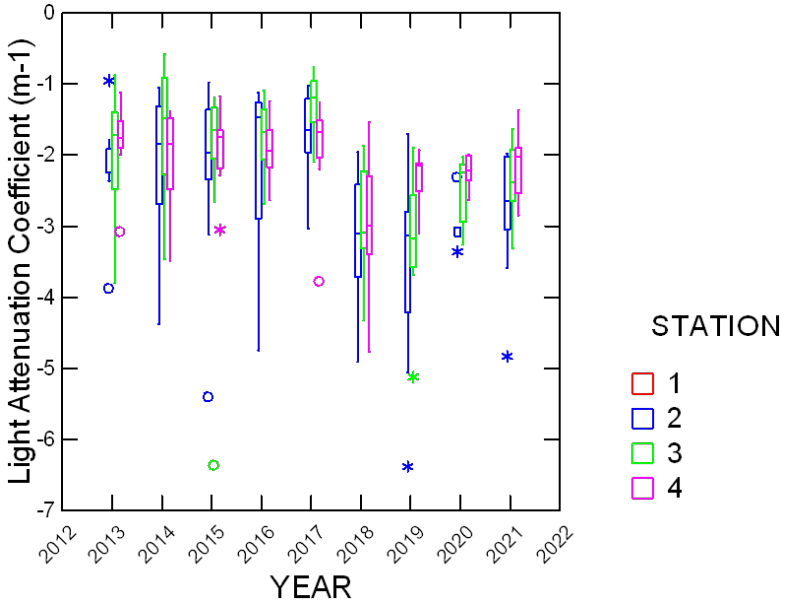

Figure 139. Box plots comparing values of Light Attenuation Coefficient between years. April through September.

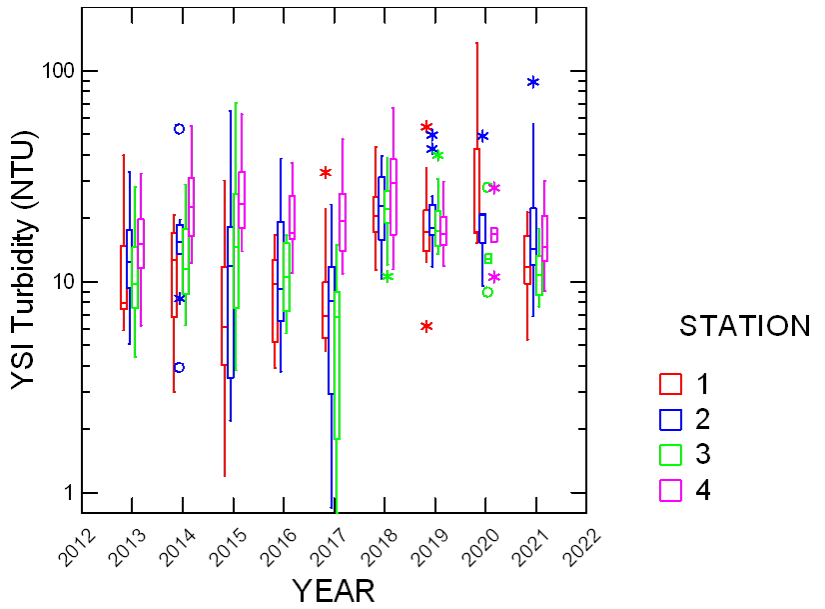

Figure 140. Box plots comparing values of Turbidity between years. April through September.

Turbidity, another measure of water clarity, continued to exhibit much higher values at AR2 and AR3 in 2021 as compared to 2013-2017 (Figure 140). Values at AR4 were not as different as in previous years. Total phosphorus values were again higher in many samples at AR1 than in previous years. Values at AR2, AR3, and AR4 were similar to previous years (Figure 141).

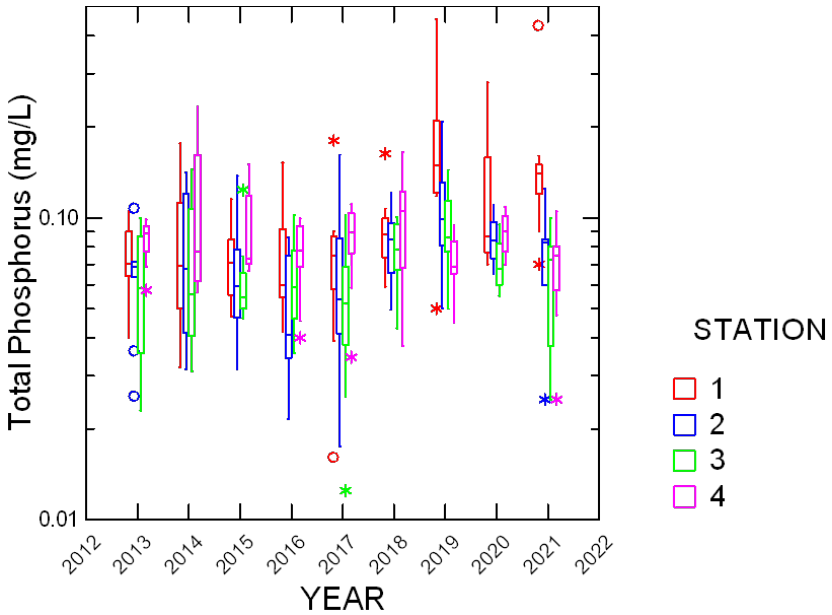

Figure 141. Box plots comparing values of Total Phosphorus between years. April through September.

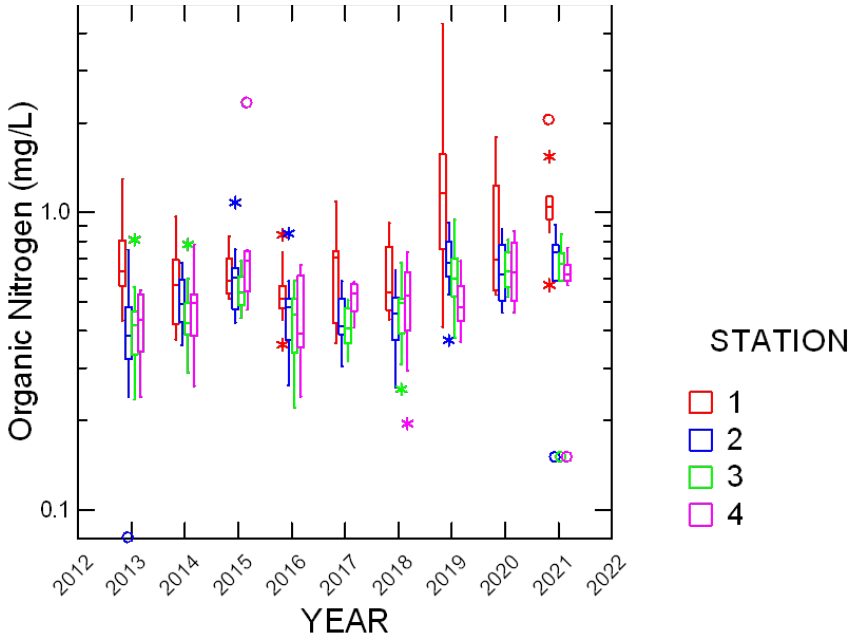

Figure 142. Box plots comparing values of Organic Nitrogen between years. June through September.

Organic nitrogen values in 2021 overlapped extensively with the ranges from previous years (Figure 142). Since 2018 there was the suggestion of an increase. A clear spatial pattern was observed with AR1 highest and greater than normal, while AR4 was little changed compared with previous years. Nitrate nitrogen values in 2021 were consistently lower at all stations than in 2018 and 2019, returning to the ranges found in previous years (Figure 143).

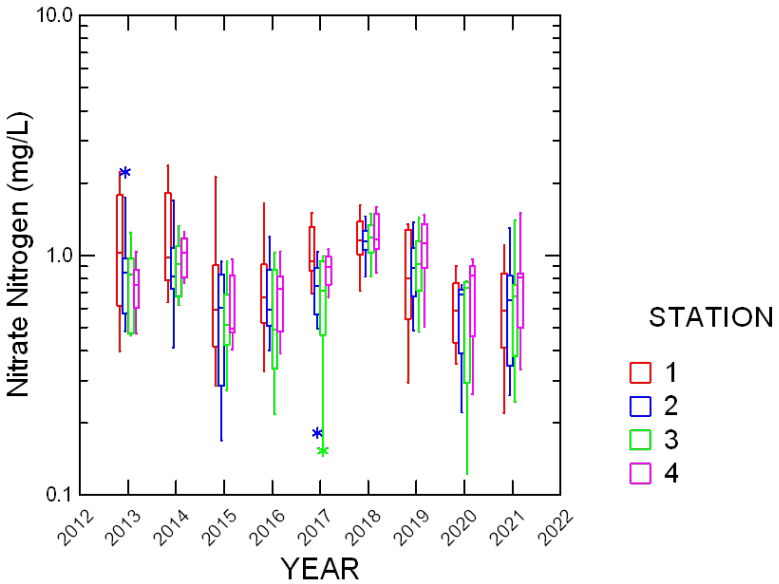

Figure 143. Box plots comparing values of Nitrate Nitrogen between years. June through September.

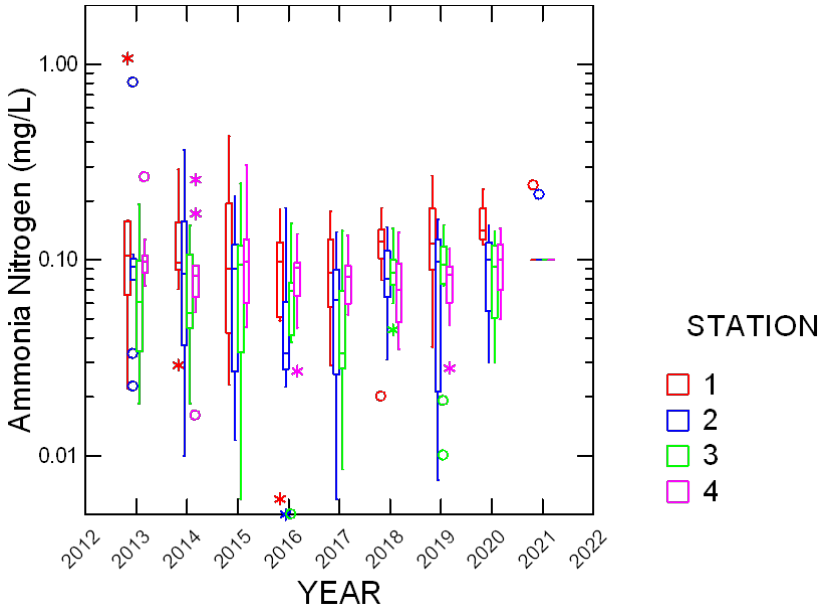

Figure 144. Box plots comparing values of Ammonia Nitrogen between years. April through September.

Ammonia nitrogen values in 2021 were almost all at the limits of detection so little could be discerned in terms of trends (Figure 144). Nitrite nitrogen values in 2020 were in the middle of the range for previous years and did not vary much among stations (Figure 145).

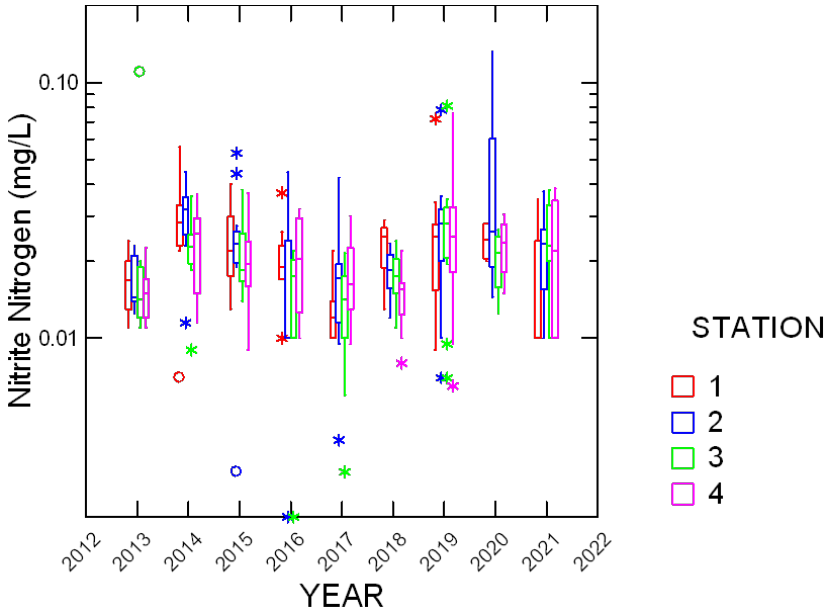

Figure 145. Box plots comparing values of Nitrite Nitrogen between years. April through September.

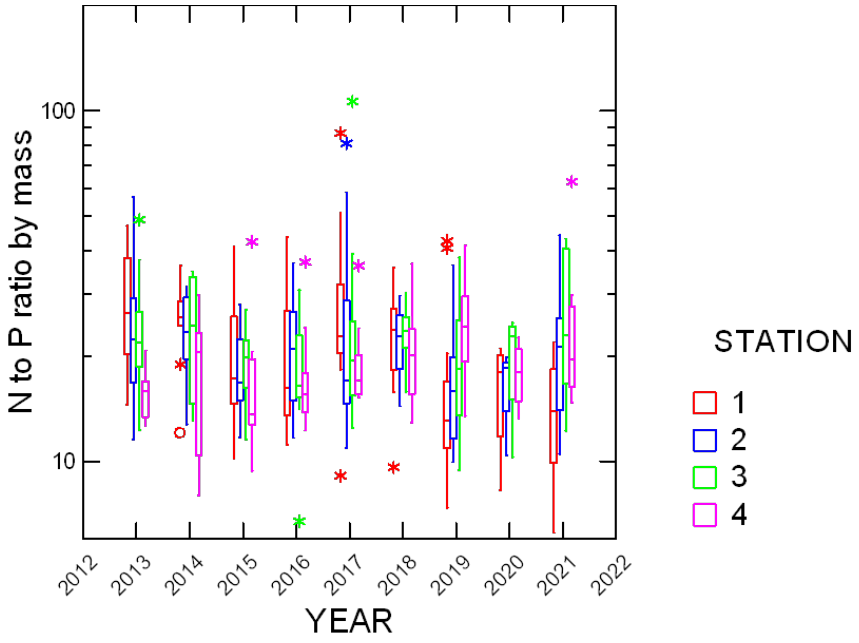

Figure 146. Box plots comparing values of N to P ratio between years. April through September.

N to P ratio for 2020 was in the lower range of values from previous years, but still within the range indicating phosphorus limitation (Figure 146). Since 2019 values have generally been lower at AR1, AR2, and AR3 while AR4 does not exhibit an obvious change over the years.

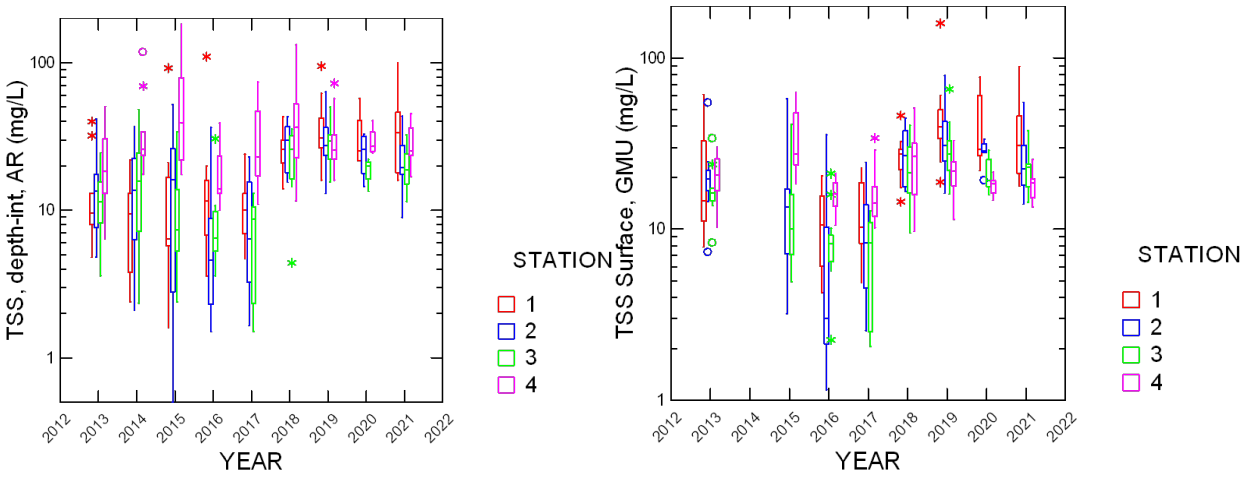

Figure 147. Box plots comparing values of Total Suspended Solids between years. Alex Renew data (a. left) and GMU data (b. right). June through September.

As in 2018 through 2020 total suspended solids (TSS) for AR1, AR2, and AR3 was higher in 2021 than in previous years (Figure 147a,b). The patterns were similar in samples analyzed by both Alex Renew and GMU. Volatile suspended solids (VSS) was in 2021 was similar to 2019 and 2020 and higher than in many previous years (Figure 148a,b).

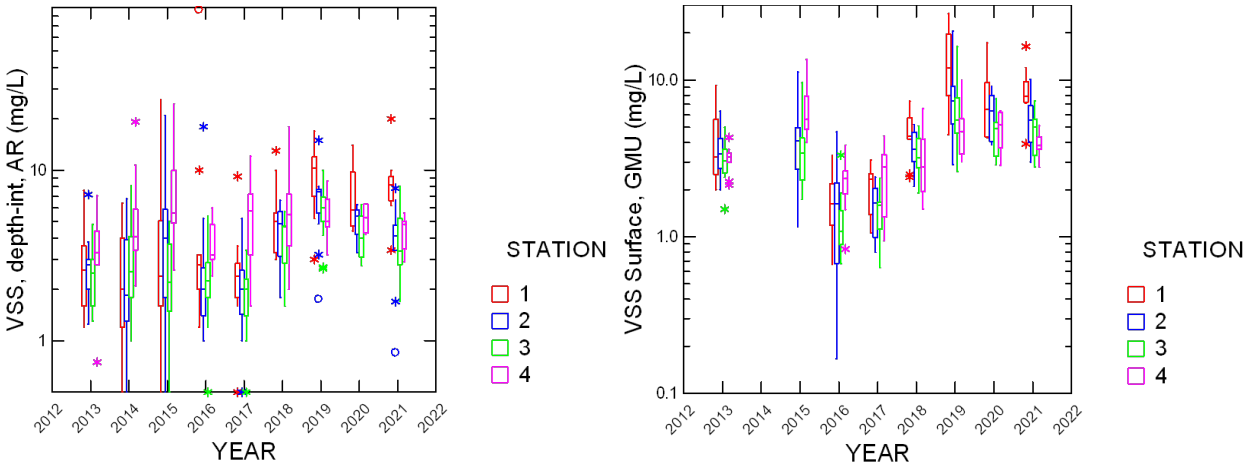

Figure 148. Box plots comparing values of Volatile Suspended Solids between years. Alex Renew Lab data (left) and GMU Lab data (right). June through September.

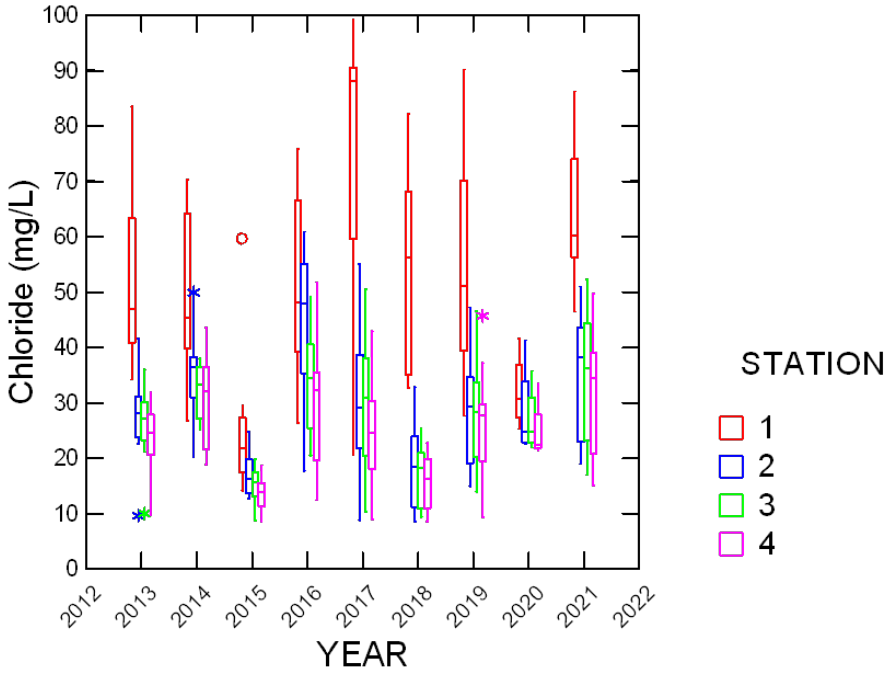

Figure 149. Box plots comparing values of Chloride between years. April through September.

As in most previous years, chloride was higher at AR1 than at the other stations (Figure 149). Total alkalinity was about equal to the early years of the study (Figure 150). In contrast to chloride, total alkalinity was generally lower at AR1 than at the other stations.

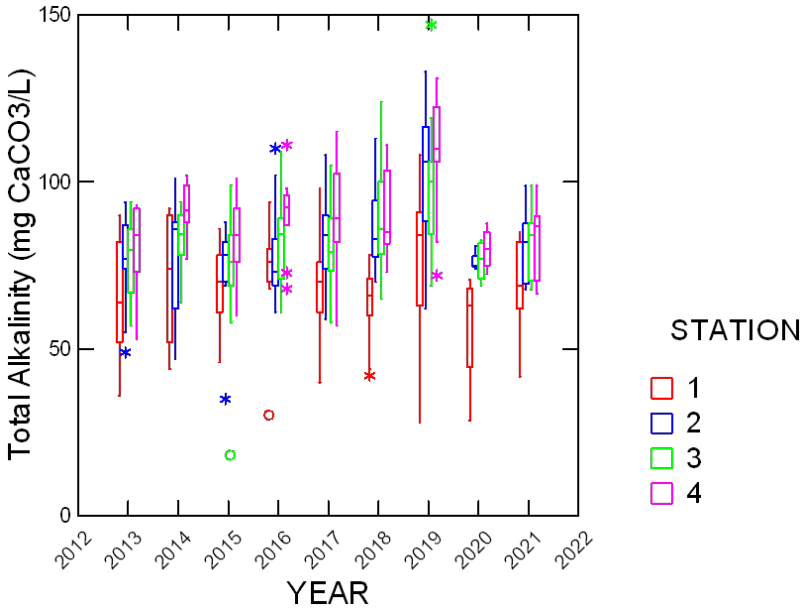

Figure 150. Box plots comparing values of Total Alkalinity between years. April through September.

In 2018 frequent very high flows scoured and washed all of the SAV out of the Hunting Creek embayment. They have not become re-established. To understand the impact of this fundamental change in ecosystem structure the data set was divided into two periods: 2013-2017 and 2018-2021. Statistical and graphical techniques were used to examine the differences between the two periods. Means and standard errors were compiled for 28 parameters for the two periods at each sample site (Appendix A). Most of the significant differences between the two periods were found for Stations AR2 and AR3 and involved changes in the ambient light environment due to increased suspended solids and phytoplankton. Box plots of some of the most significant parameters are shown below (Figures 151 to 153). Note that indicators of light transparency (Secchi Disk and Light Attenuation Coefficient) have decreased substantially and consistently at both AR2 and AR3 since 2018. Also, TSS has increased indicating more suspended sediments in the water column which contributes to poor light penetration. With no competition from SAV, phytoplankton chlorophyll has increased.

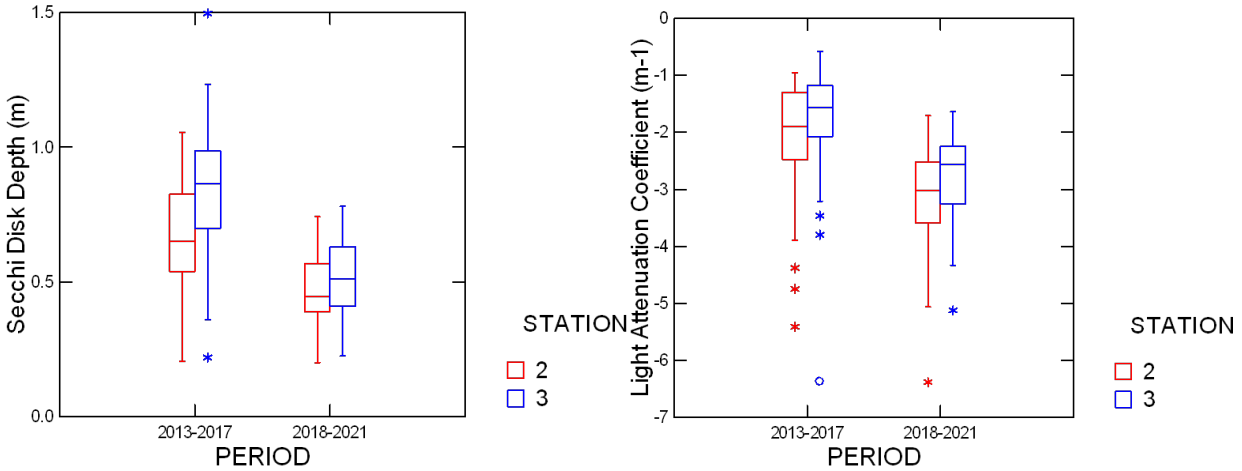

Figure 151. Measures of Light Transparency at Hunting Creek Embayment Stations Comparing 2013-2017 to 2018-2021.

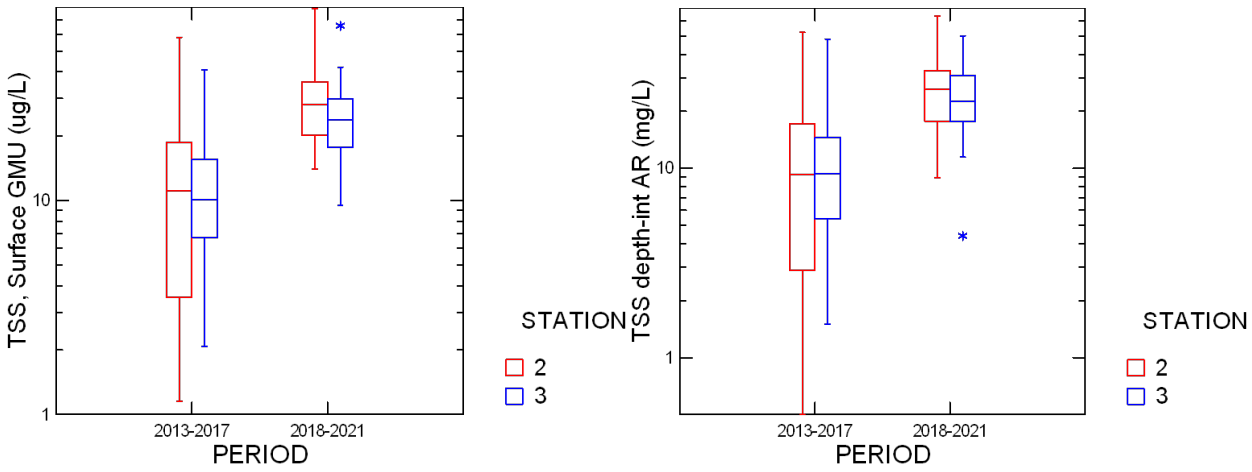

Figure 152. Measures of Suspended Solids at Hunting Creek Embayment Stations Comparing 2013-2107 to 2018-2021.

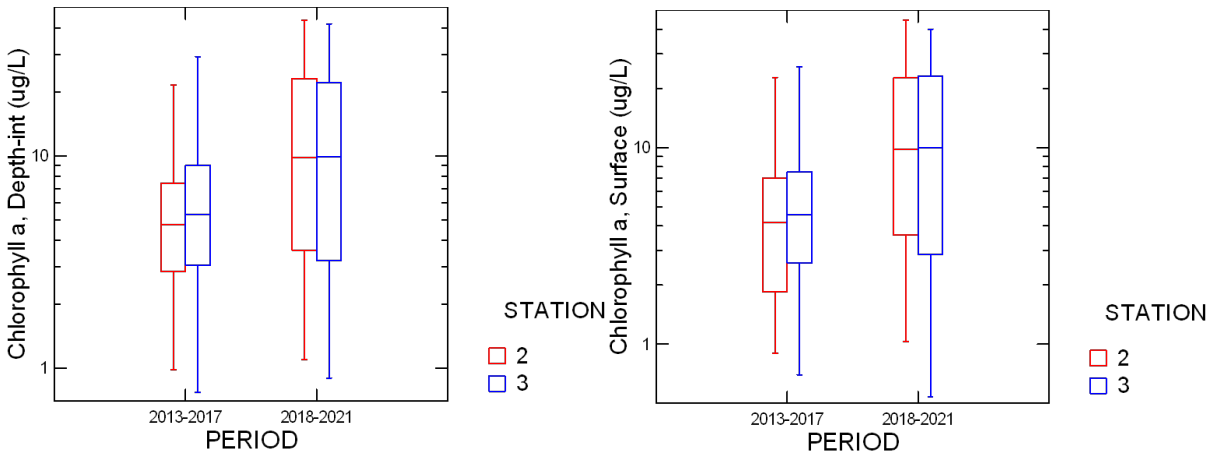

Figure 153. Measures of Phytoplankton Chlorophyll a at Hunting Creek Embayment Stations Comparing 2013-2107 to 2018-2021.

D. Phytoplankton: Comparison among Years

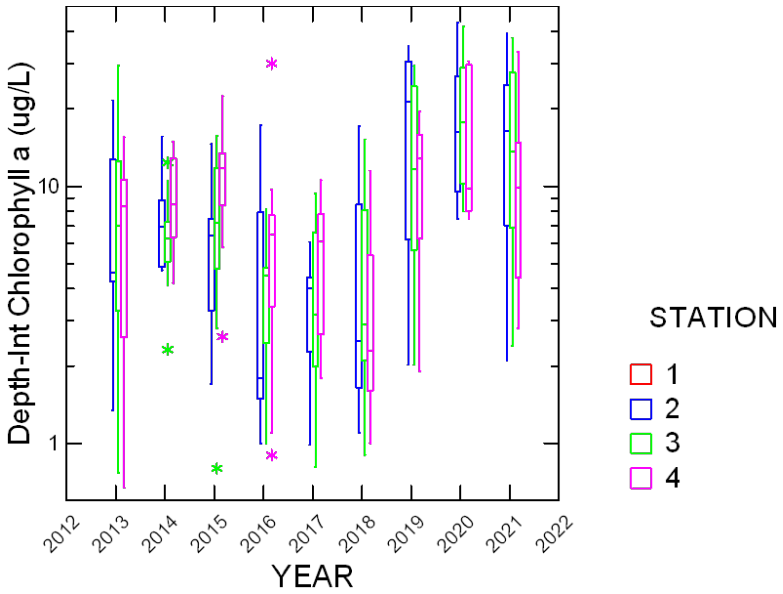

Figure 154. Box plots comparing values of depth-integrated Chlorophyll *a* among years. April through September.

In 2021 chlorophyll *a* levels were similar to 2019 through 2020, reflecting a strong rebound from the generally low levels found in 2018 and were actually among the highest of all previous years (Figure 154, 155). Similar results were observed with surface chlorophyll. Chlorophyll values in the water are a measure of phytoplankton populations which compete with SAV for light and nutrients. Since SAV is now absent in the embayment, phytoplankton have increased.

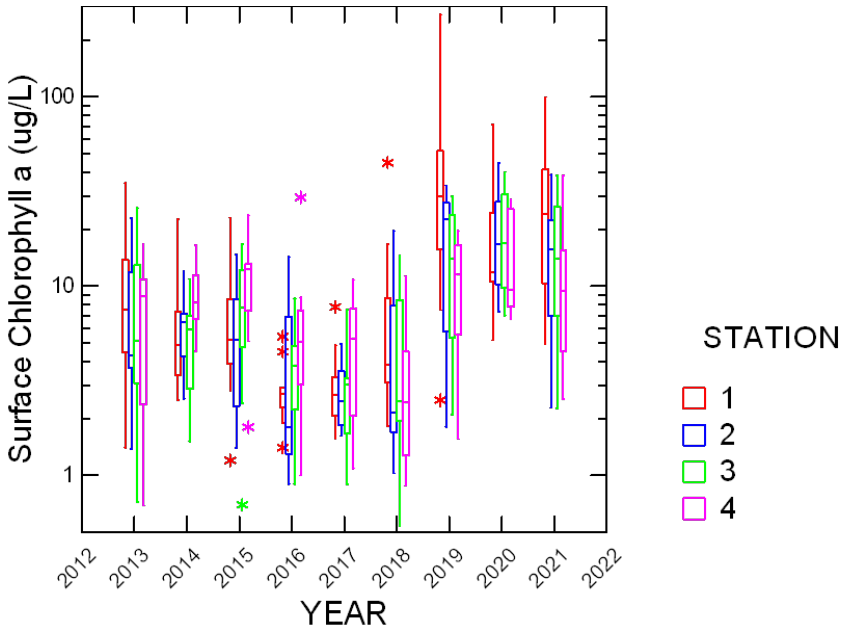

Figure 155. Box plots comparing values of surface Chlorophyll *a* among years. April through September.

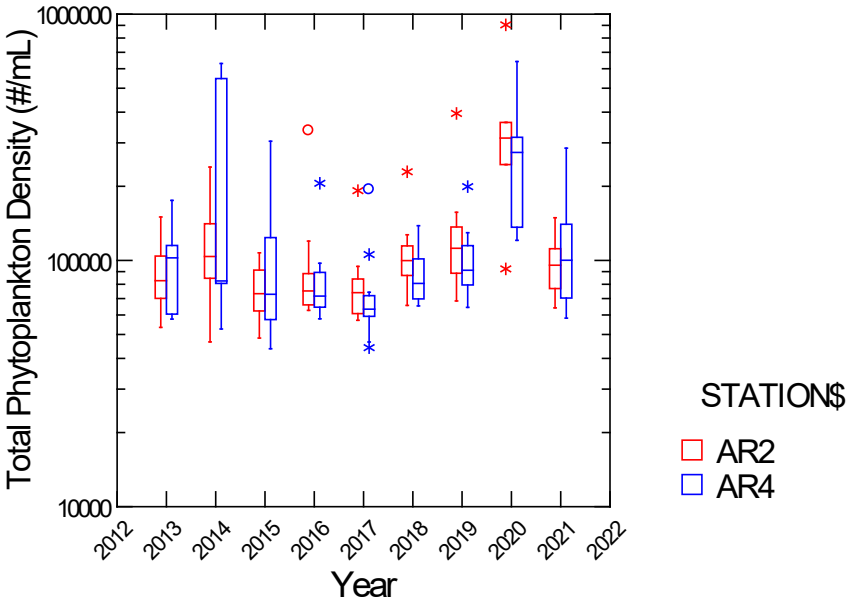

Figure 156. Box plots comparing values of Total Phytoplankton Density.

The median values for total phytoplankton cell density in 2021 were similar to previous years and substantially lower than in 2020 (Figure 156). The high 2020 values may be partially due to the fact that data were only available for the July to September period which often has the highest densities. Total cyanobacterial cell density in 2021 also dropped back from 2020 values to values similar to previous years (Figure 157).

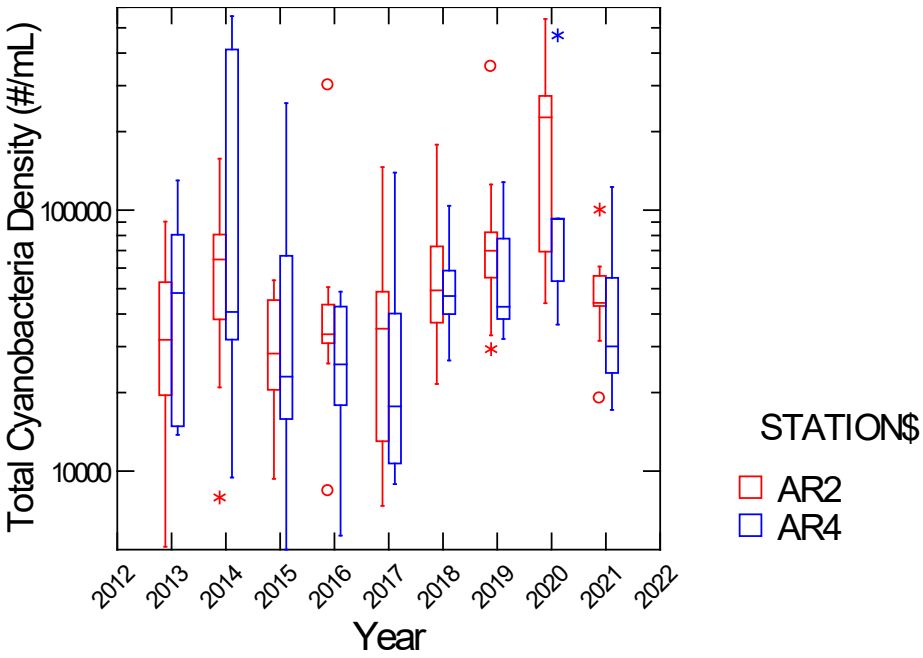

Figure 157. Box plots comparing values of Cyanobacterial Density.

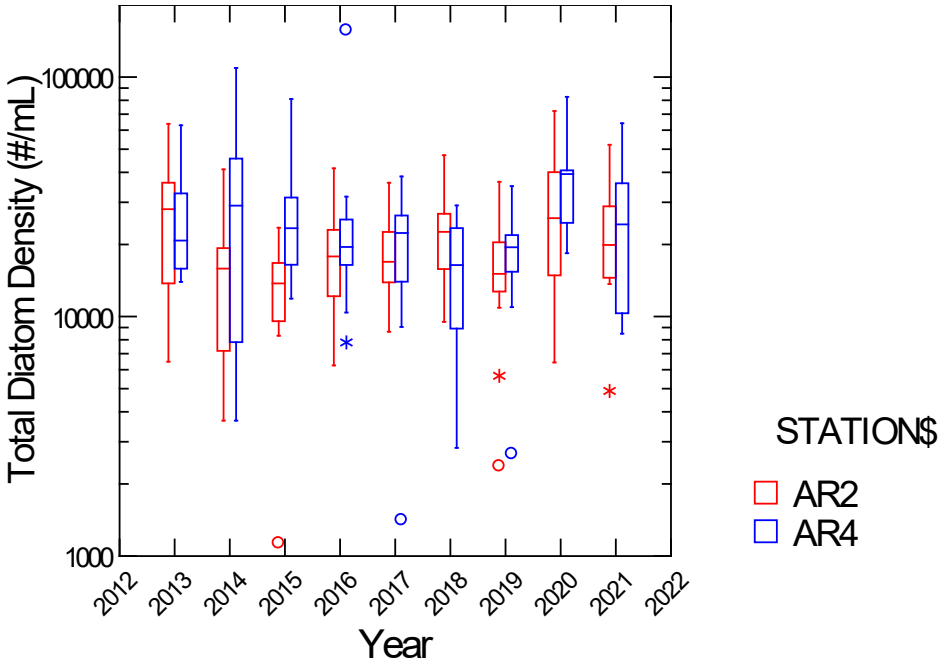

Figure 158. Box plots comparing values of Diatom Density among years.

Median diatom densities in 2021 at both stations were within the range observed in previous years (Figure 158). Green algal cell densities also were lower in 2021 than in 2020 with a few higher values at AR4 (Figure 159).

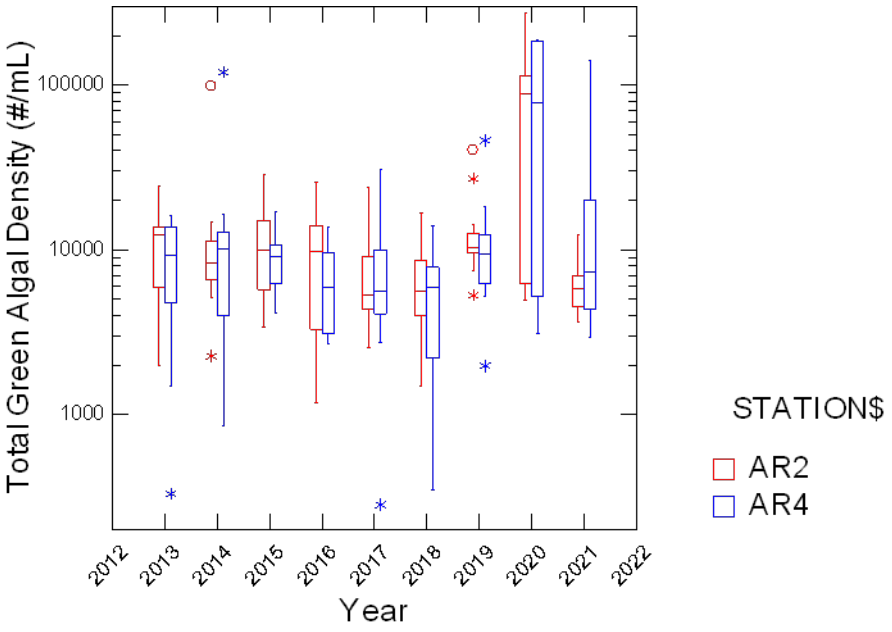

Figure 159. Box plots comparing values of Green Algal Density among years.

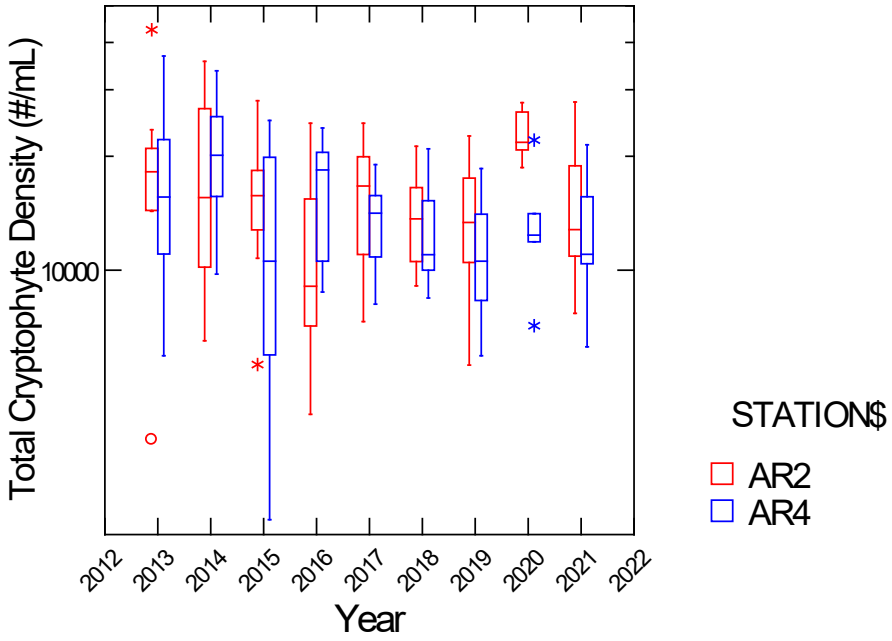

Figure 160. Box plots comparing values of Cryptophyte Density among years.

Median cryptophyte cell densities at AR2 returned to typical values in 2021 after very high values in 2020 (Figure 160). At AR4 cryptophyte densities were in the middle to lower end of the range of previous years. Other taxa includes those species of phytoplankton in groups not tallied above. These are mainly dinoflagellates, crysophytes and euglenoids whose abundances are somewhat sporadic in the study area. Nonetheless, values in this group were much higher than in 2020 and similar to past years (Figure 161).

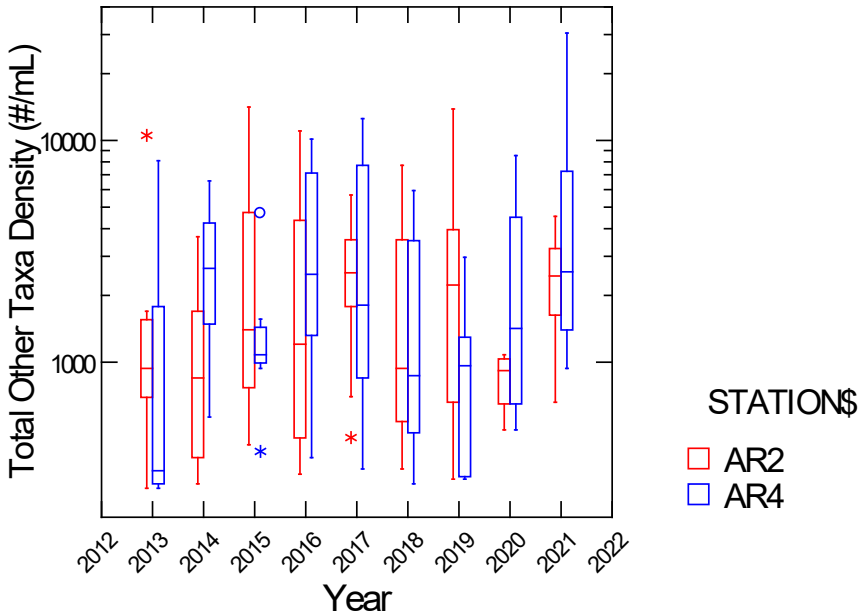

Figure 161. Box plots comparing values of Miscellaneous Taxa Density among years.

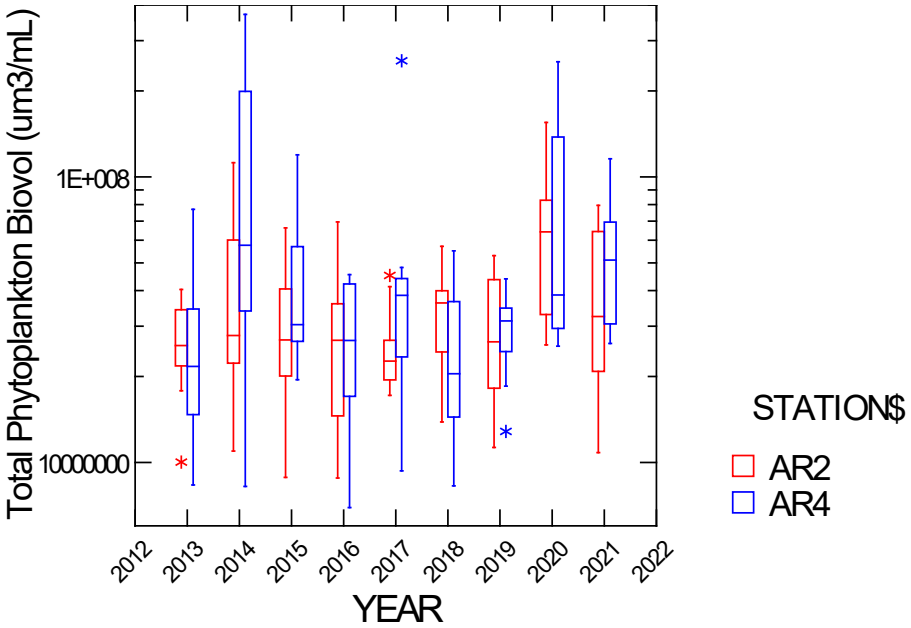

Figure 162. Box plots comparing values of Total Phytoplankton Biovolume among years.

Biovolume takes into account both the number of cells and their relative size. In 2021 total biovolumes were at the higher end of the range of previous years similar to 2014 and 2020 (Figure 162). Total cyanobacterial biovolume median in 2021 declined strongly from 2020 values which were among the highest observed to date (Figure 163).

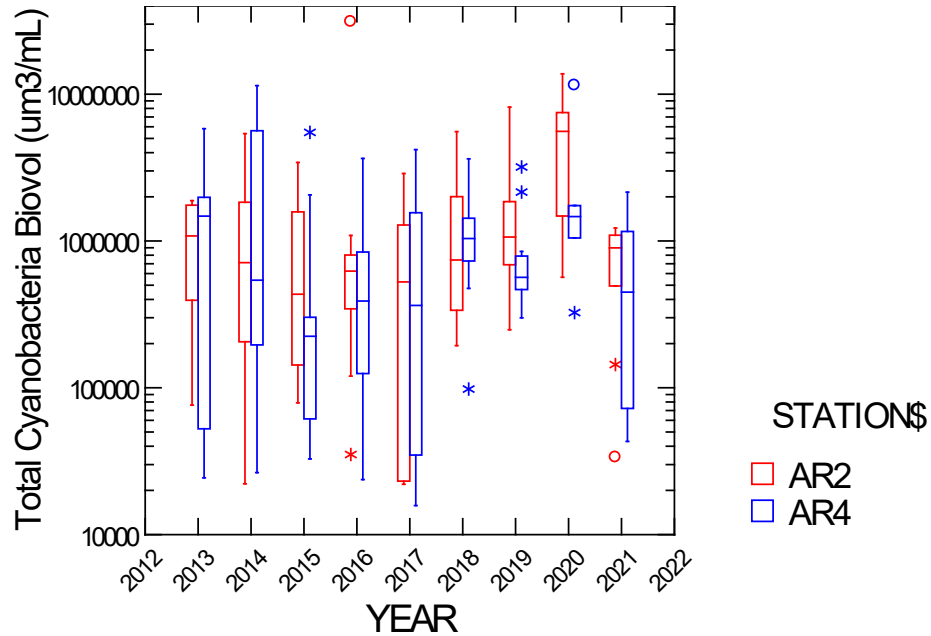

Figure 163. Box plots comparing values of Cyanobacterial Biovolume among years.

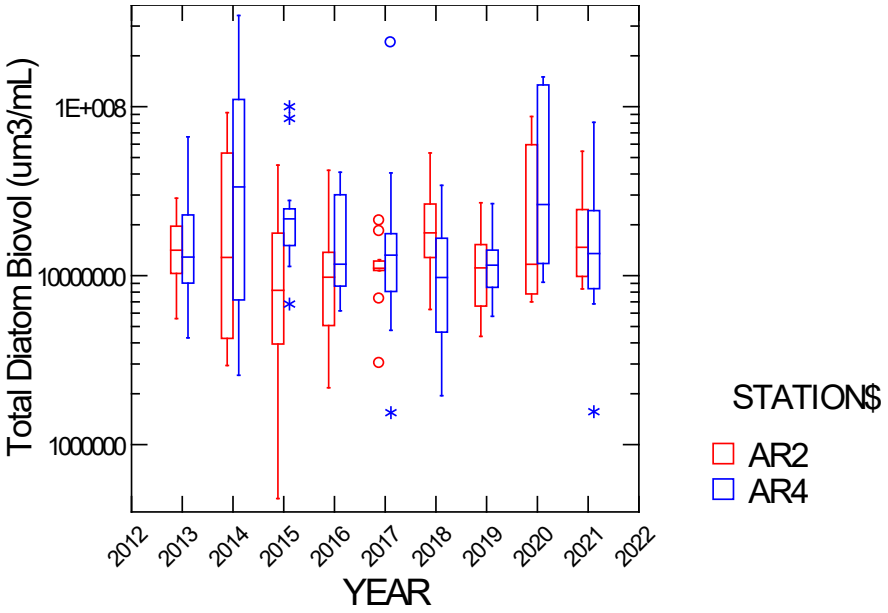

Figure 164. Box plots comparing values of Diatom Biovolume among years.

Median diatom biovolume in 2021 was similar at both stations, falling within the range of previous years (Figure 164). Median values in green algal biovolume were also very similar between the two stations and much reduced at AR2 from 2020 (Figure 165).

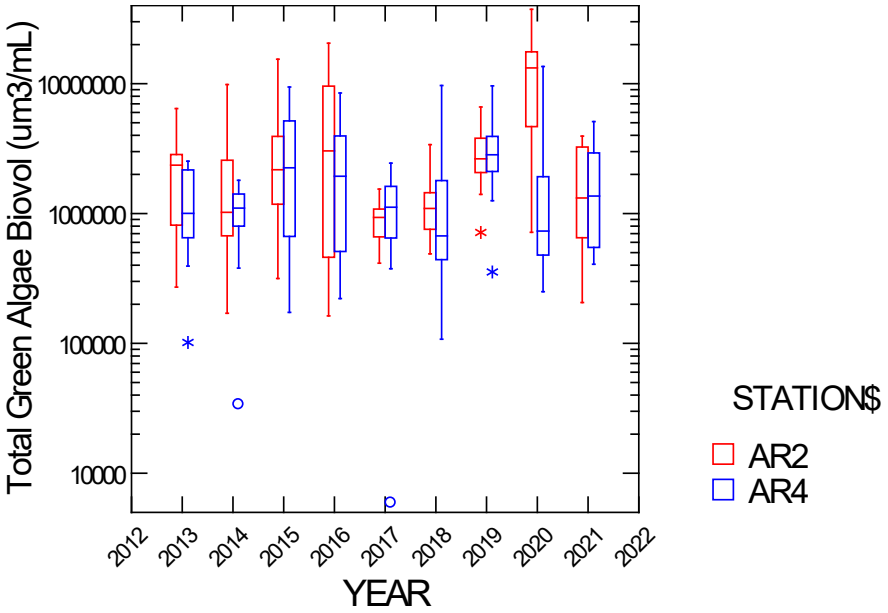

Figure 165. Box plots comparing values of Green Algal Biovolume among years.

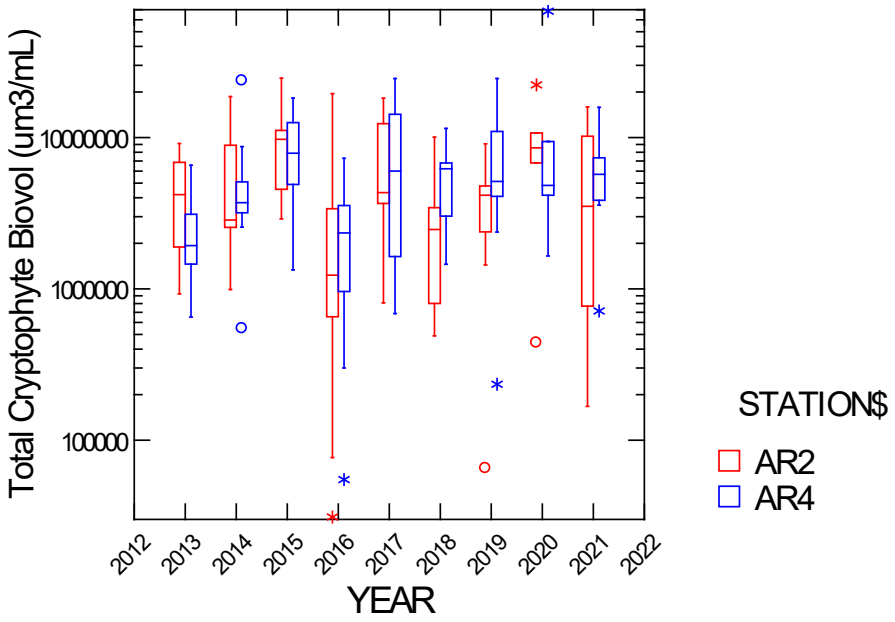

Figure 166. Box plots comparing values of Cryptophyte Biovolume among years.

Cryptophyte biovolume declined at AR2 in 2021 after increasing for the three straight years (Figure 166). Levels at AR4 were somewhat higher and more in line with previous years. The patterns in Miscellaneous Taxa Biovolume continued to increase for the fourth straight year at both stations (Figure 167).

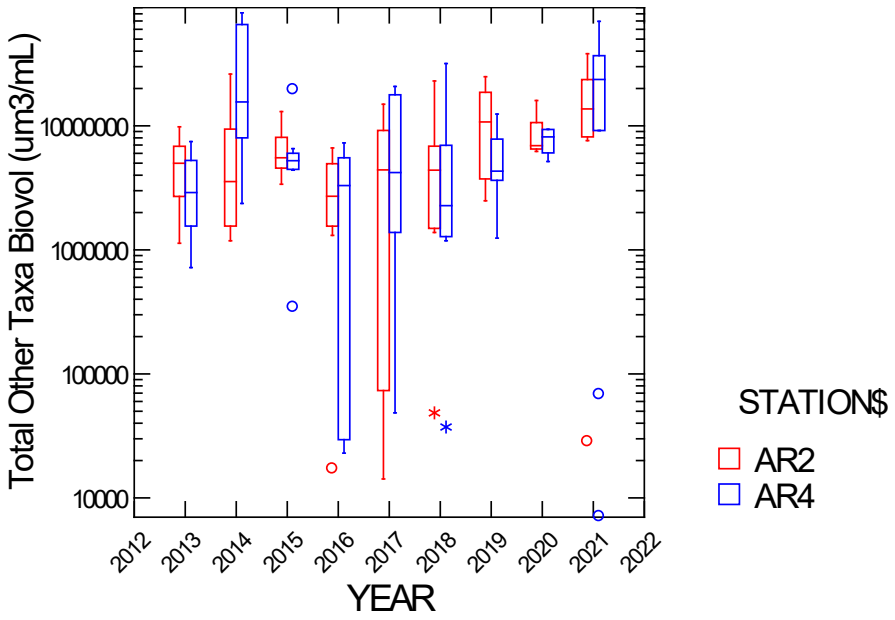

Figure 167. Box plots comparing values of Miscellaneous Biovolume among years.

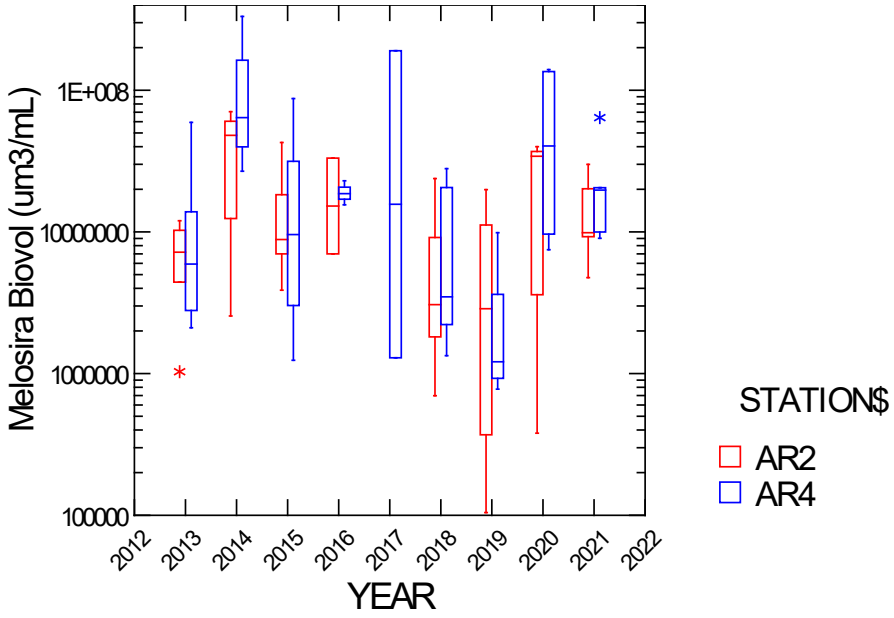

Figure 168. Box plots comparing values of *Melosira* Biovolume among years.

An analysis of interannual and seasonal effects also done for selected individual taxa. Median biovolume values of the filamentous diatom *Melosira* showed a clear peak in 2014 at both stations, then declined steadily through 2019, but cameb back strongly in 2020 and 2021 (Figure 168). Discoid centric biovolume in 2021 was higher at AR4, but similar to previous years after a low value in 2019 (Figure 169).

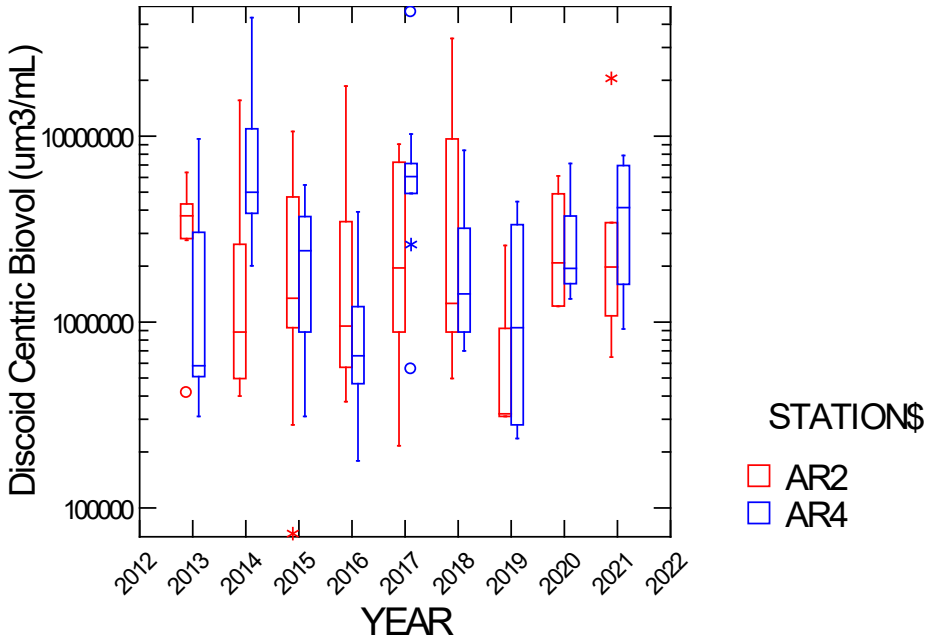

Figure 169. Box plots comparing values of Discoid Centric Diatom Biovolume among years.

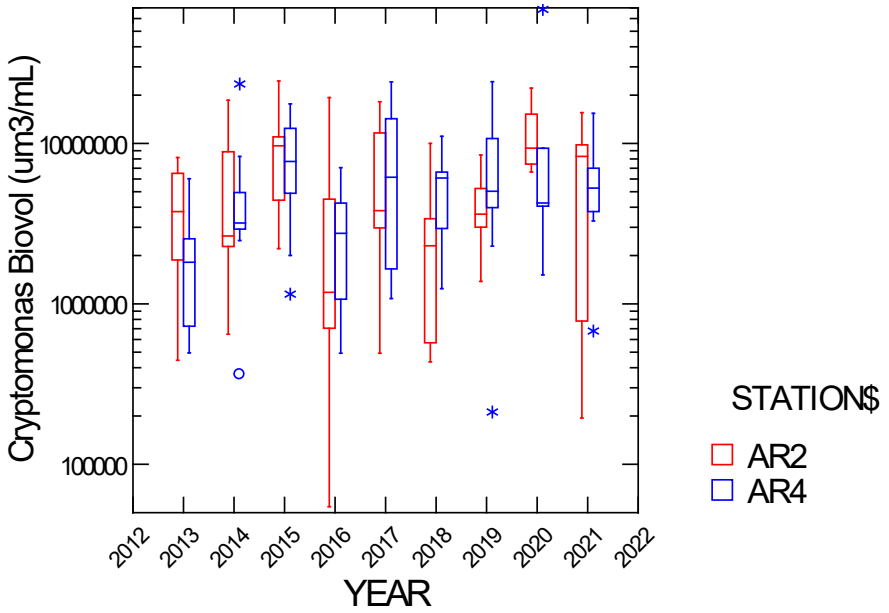

Figure 170. Box plots comparing values of *Cryptomonas* Biovolume among years.

Cryptomonas biovolume at both stations was similar and in the same range as previous years (Figure 170). *Oscillatoria* is the most consistently abundant cyanobacterium in the study area. In 2020 levels recovered strongly at AR2, but in 2021 they dropped back to among the lowest levels observed. *Oscillatoria* remained somewhat depressed at AR4 (Figure 171).

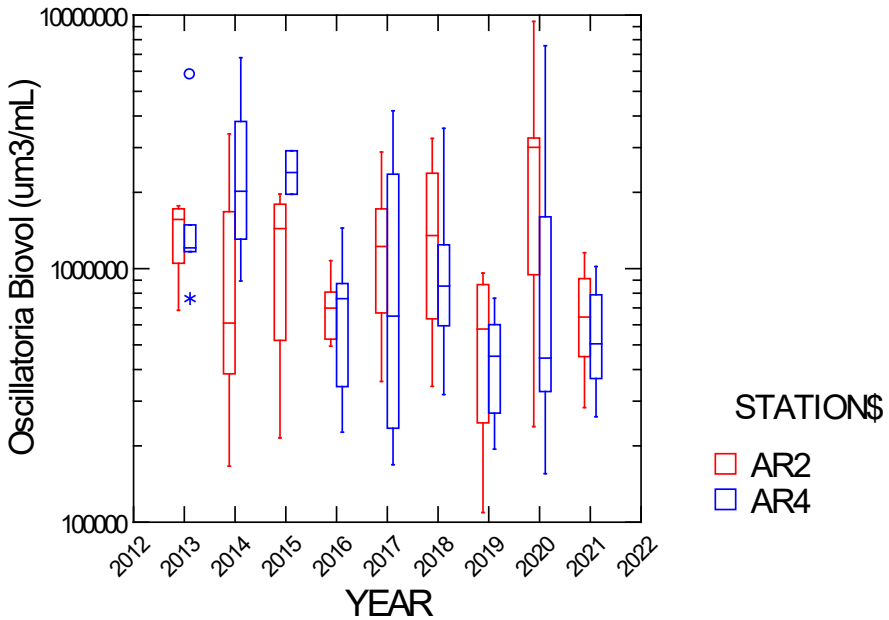

Figure 171. Box plots comparing values of *Oscillatoria* Biovolume among years.

E. Zooplankton: Comparison among Years

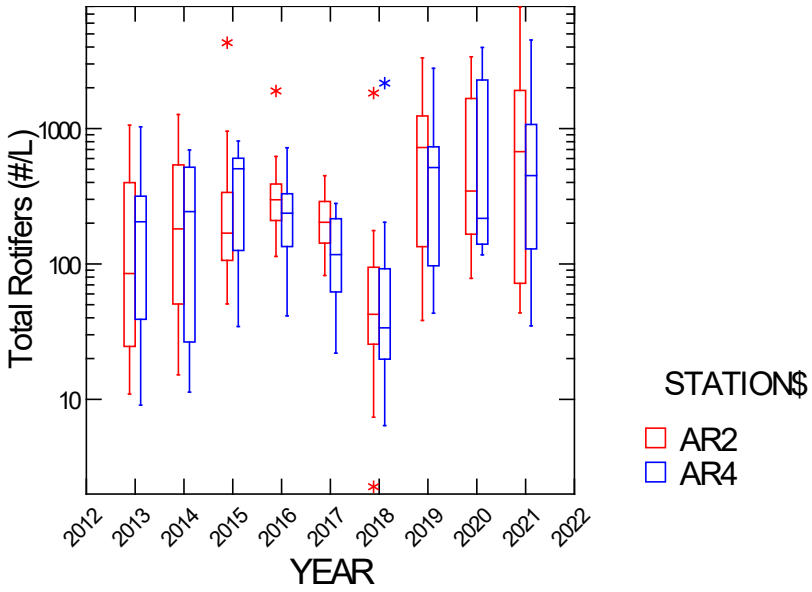

Figure 172. Box plots comparing values of Total Rotifers among years.

Total rotifer densities were very robust in 2021 similar to 2019 and 2020 and consistently higher than during the pre-2018 period (Figure 172). Of particular interest was the strong recovery from the record low values of 2018 which were probably a result of the high rainfall and subsequent flushing of organisms observed that year. Episodic flushing occurred in 2019-2021 and may have actually stimulated the rotifers. The common rotifer *Brachionus* (Figure 173) was the dominant taxon and displayed a similar trend as total rotifers with 2019-2021 levels very high and 2018 the lowest year to date. *Brachionus* exhibited similar values at both station in most years.

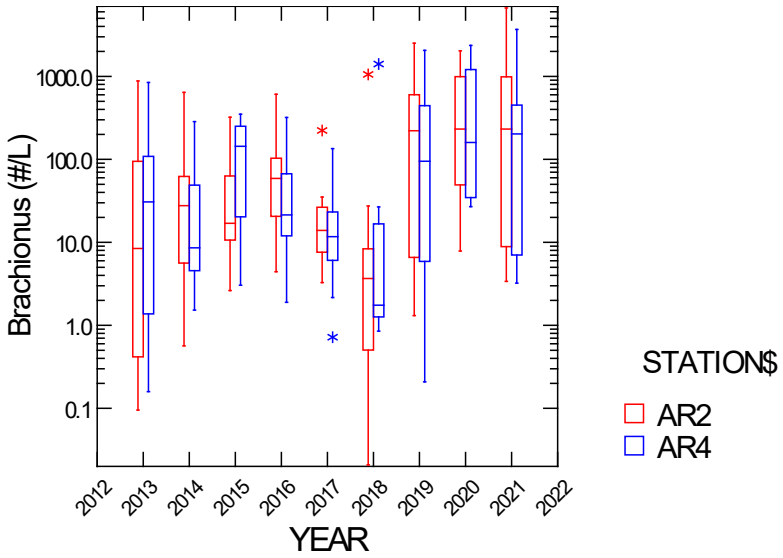

Figure 173. Box plots comparing values of *Brachionus* among years.

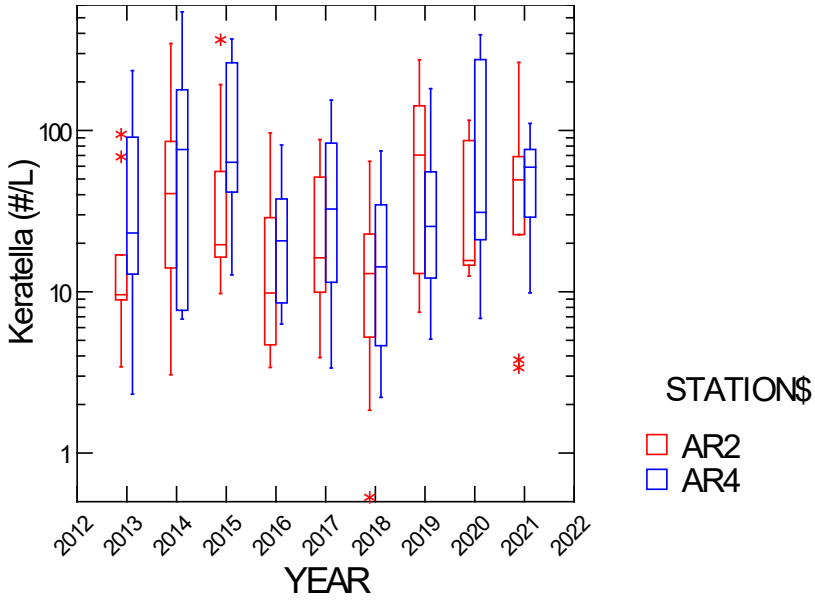

Figure 174. Box plots comparing values of *Keratella* among years.

Another common rotifer *Keratella* exhibited a similar, but less dramatic trend. Values in 2019-2021 were higher in 2018, but 2018 was not as low relative to other years (Figure 174). *Polyarthra*, consistently observed, but less common than *Brachionus* or *Keratella*, also showed a continued rebound from low 2018 levels (Figure 175).

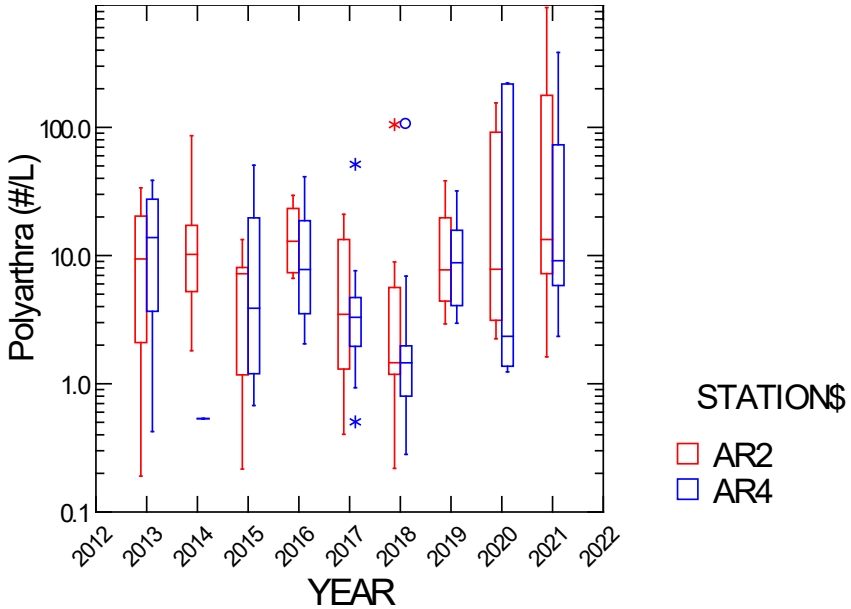

Figure 175. Box plots comparing values of *Polyarthra* among years.

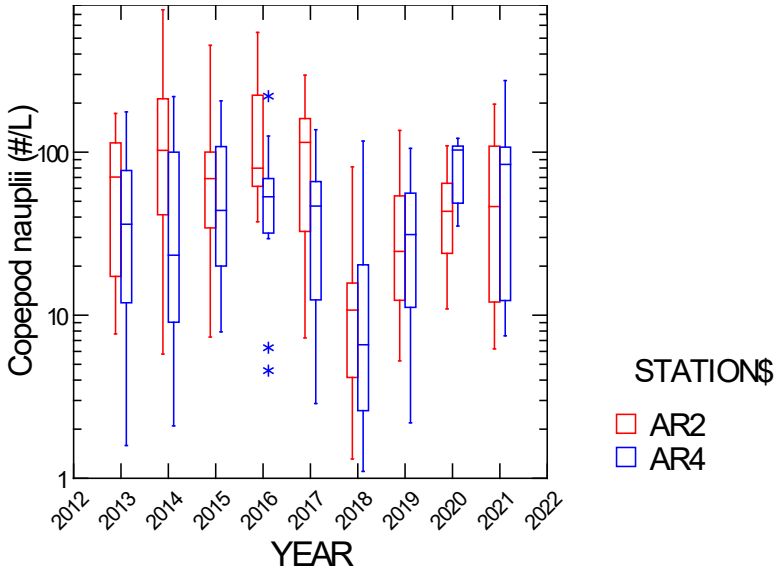

Figure 176. Box plots comparing values of Copepod Nauplii among years.

Nauplii are the juvenile stages of copepods. As such it is hard to identify them to species since they do not have mature characteristics so they have been lumped for all copepod taxa. Nauplii showed a continued recovery in 2021 after the low values of 2018 (Figure 176). Values were similar at the two stations and similar to pre-2018 values. *Bosmina* is a small cladoceran enumerated in the 44 µm samples, but related to *Daphnia* and *Diaphanosoma* collected in the 202 µm nets. As with copepod nauplii, *Bosmina* continued to recover in 2021 after the sharp decline in 2018 to values similar to those observed in the pre-2018 period (Figure 177). There was not a consistent difference in *Bosmina* levels between the two stations.

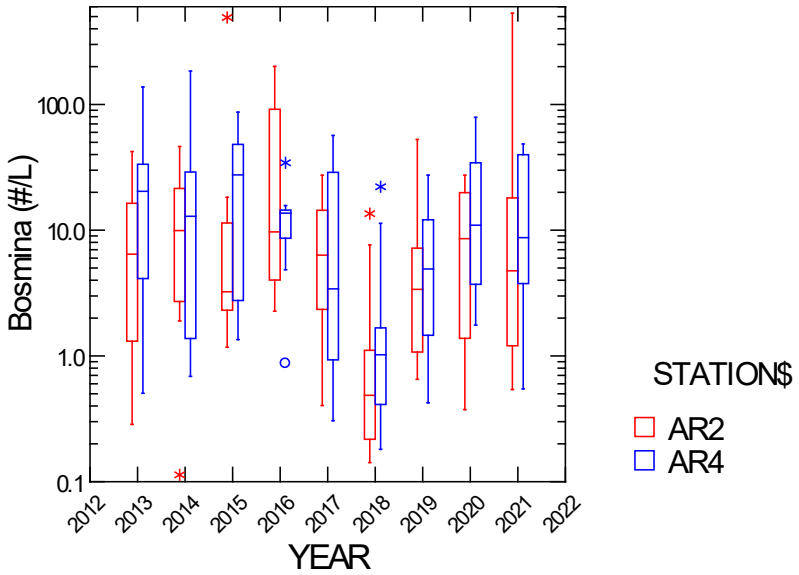

Figure 177. Box plots comparing values of *Bosmina* among years.

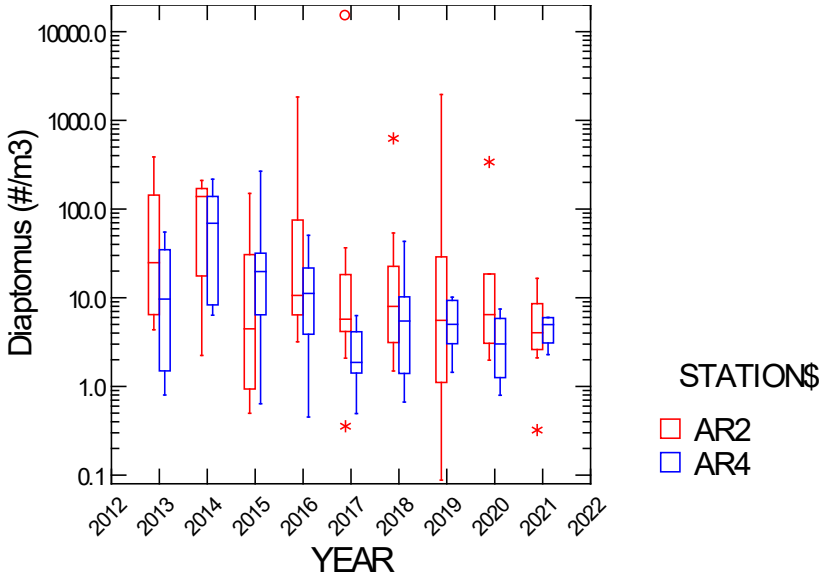

Figure 178. Box plots comparing values of *Diaptomus* among years.

Median *Diaptomus* densities remained at the low end of values observed during the study at both stations in 2021 (Figure 178). *Eurytemora* is the most common calanoid copepod (Figure 179). It consistently was more abundant at the river station AR4 than at AR2 in Hunting Creek. *Eurytemora* did not exhibit much response to the very different flow regimes of 2018 and to the changes in SAV since 2018.

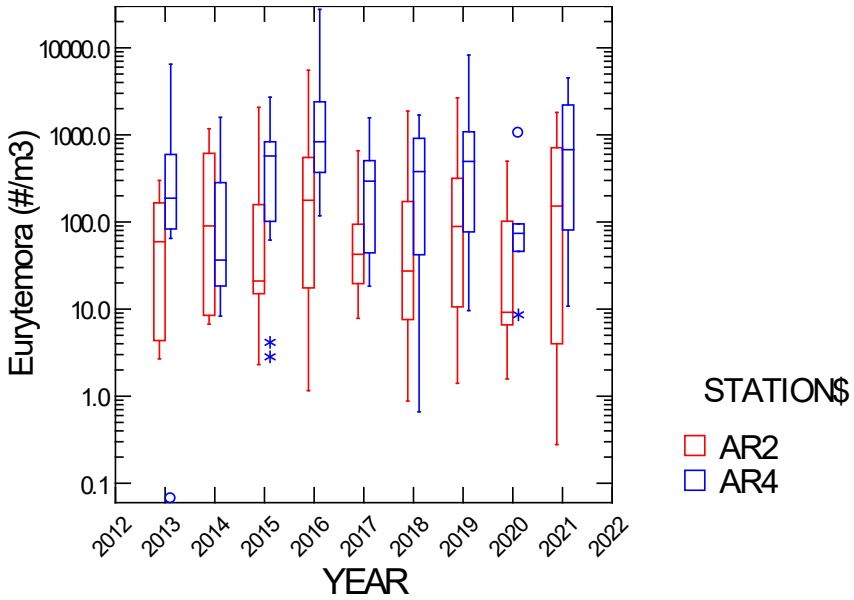

Figure 179. Box plots comparing values of *Eurytemora* among years.

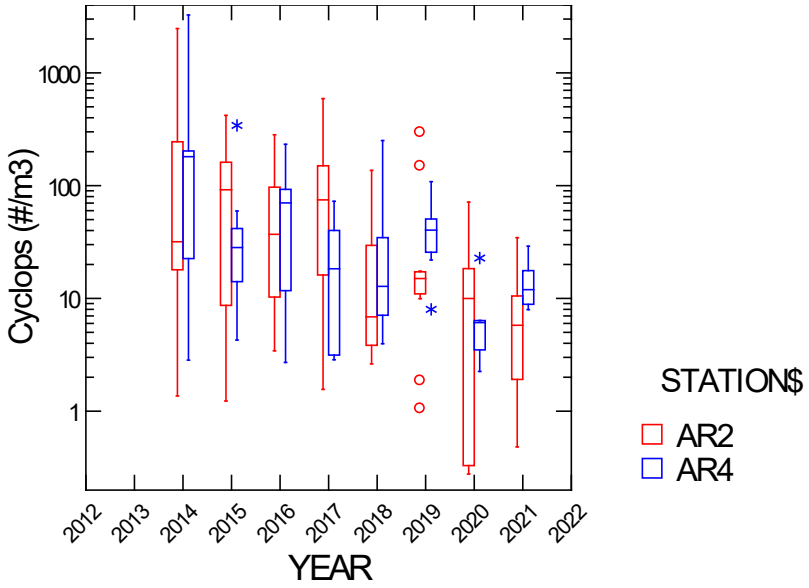

Figure 180. Box plots comparing values of *Cyclops* among years.

The copepod *Cyclops* was present at lower levels in 2021 at AR2 continuing a downward trend over the study period (Figure 180). At AR4 values in 2021 were higher than 2020 and similar to the long term levels. *Mesocyclops* is one of the more common cyclopoid copepods. Median values of *Mesocyclops* at AR2 continued to be at the low end of the range of previous years (Figure 181). However, values at AR4 were the highest yet observed.

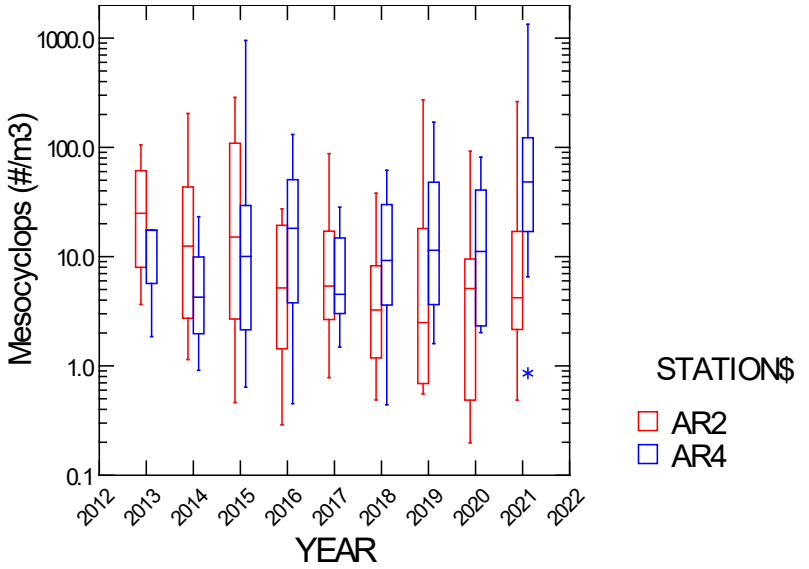

Figure 181. Box plots comparing values of *Mesocyclops* among years.

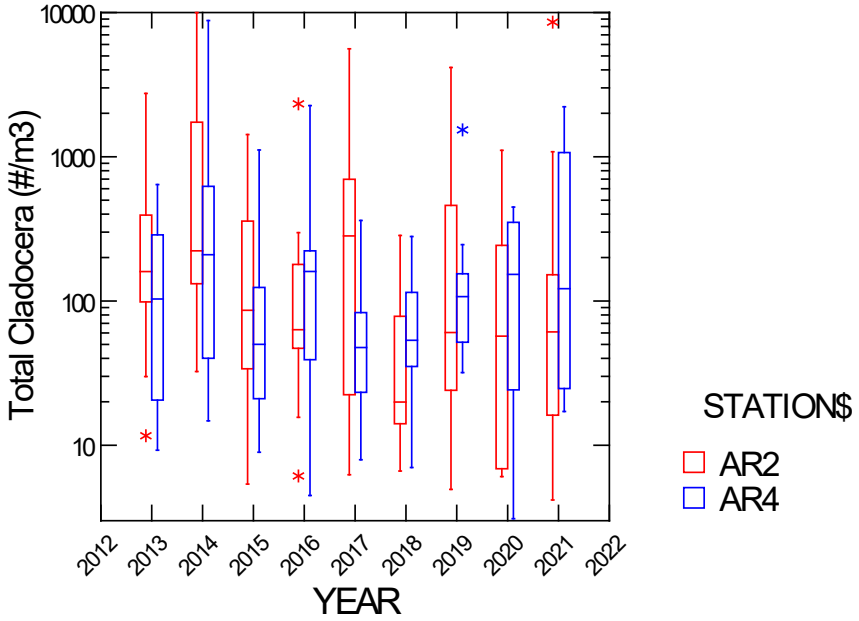

Figure 182. Box plots comparing values of Total Cladocerans among years.

Total cladoceran values (excluding *Bosmina*) at AR2 continued to recover in 2021 after the low levels in 2018, but were slightly below pre-2018 values (Figure 182). Values at AR4 remained within the range of previous years. *Daphnia* was found at clearly higher levels in 2014 than in the other years of the study (Figure 183). Values observed in 2021 were in the middle range of those observed to date.

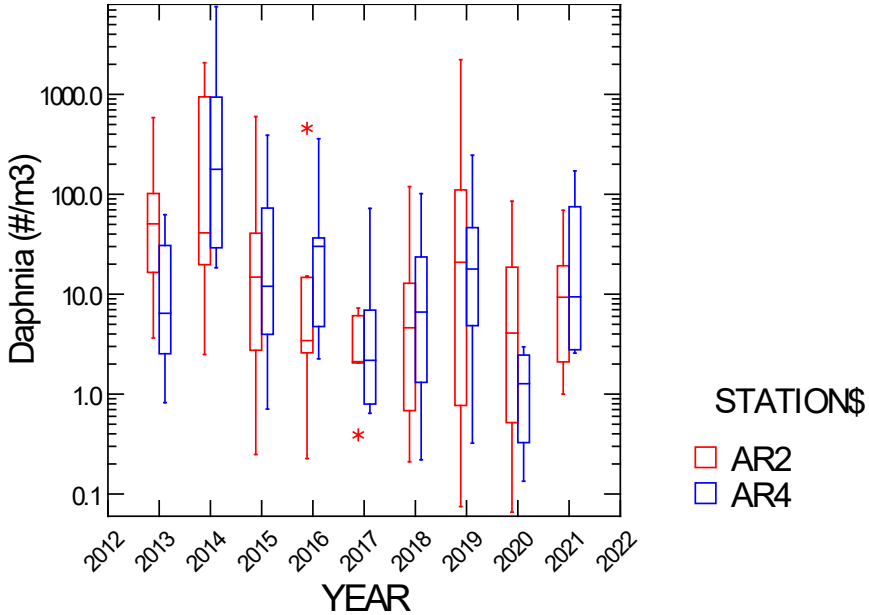

Figure 183. Box plots comparing values of *Daphnia* among years.

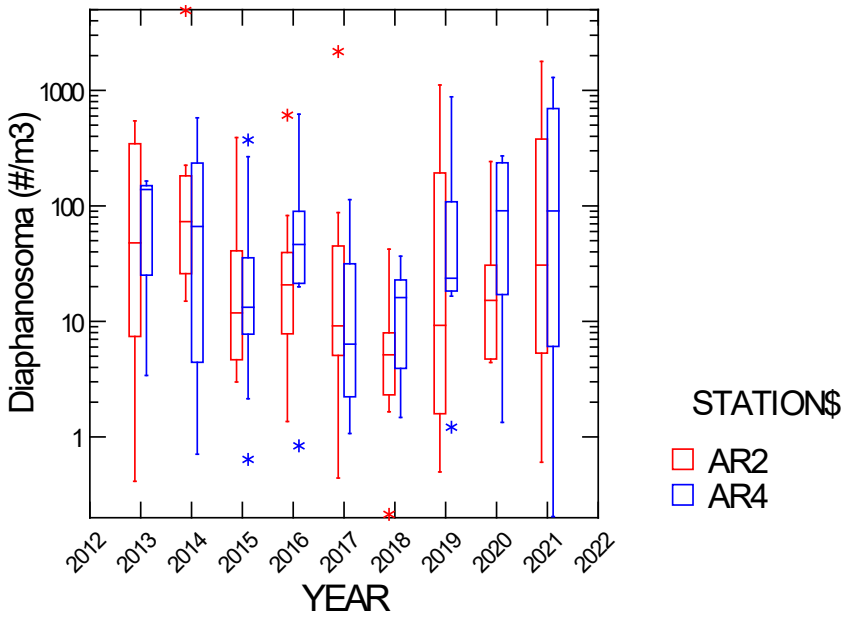

Figure 184. Box plots comparing values of *Diaphanosoma* among years.

Diaphanosoma is a very abundant cladoceran in Gunston Cove, but has proven to be less abundant in the Hunting Creek area, although still important. *Diaphanosoma* levels at AR2 were at record lows in 2018, and showed continued recovery in 2021 to near pre-2018 levels (Figure 184). Levels at AR4 were also higher in 2020 and 2021 than in 2018 and among the highest of the entire study period. *Sida* was generally less abundant than *Diaphanosoma*, It suffered a marked decline in 2018 and has not recovered since then (Figure 185).

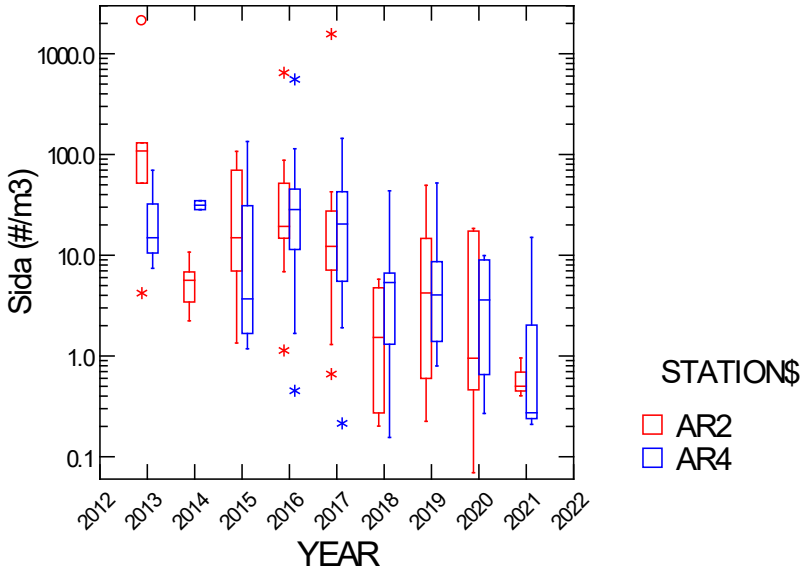

Figure 185. Box plots comparing values of *Sida* among years.

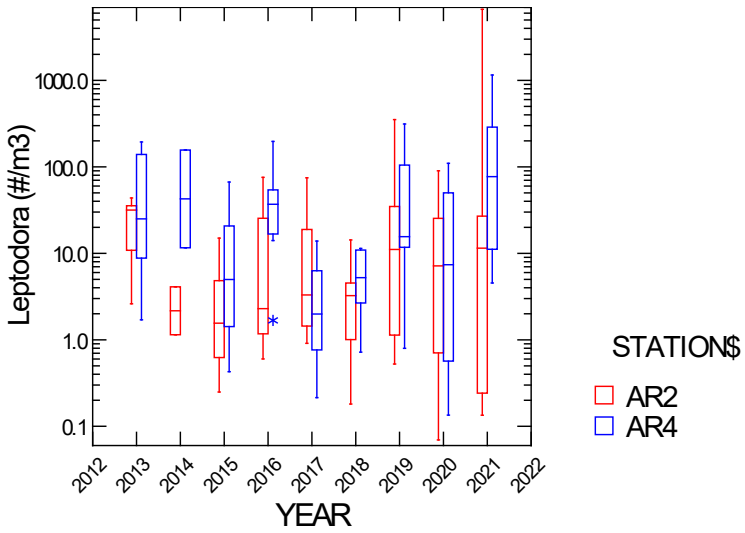

Figure 186. Box plots comparing values of *Leptodora* among years.

Leptodora is a large predacious cladoceran which occurs consistently in the study area (Figure 186). Values in 2021 were among the highest observed to date, particularly at AR4 and were distinctly higher than in 2017 and 2018. Total macrozooplankton, those collected in the 202 µm net, showed a clear interannual pattern with greatest numbers at both stations in 2014 (Figure 187). 2021 values were among the highest at AR4, but were on the low end of previous years at AR2.

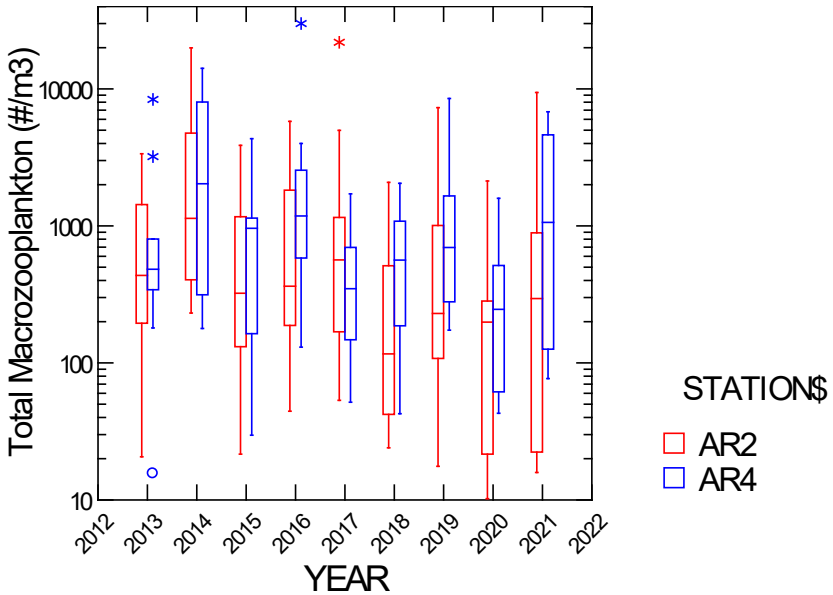

Figure 187. Box plots comparing values of Total Macrozooplankton among years.

F. Ichthyoplankton: Comparison among Years

2021 marks the ninth year of our fish collections in Hunting Creek. Both trends and inter-annual variability become apparent when comparing the years of data. Total larval density is lower than previous years except for 2018 and 2020, which was poorly represented (Table 14). Although total abundance was lower, River Herring and other Clupeids remained the most abundant species similar to previous years. Interestingly, White Perch larvae was the second most abundant we have seen this year, only being surpassed by collections in 2019. Although abundances were somewhat diminished, all four anadromous *Alosa* species were still collected in Hunting Creek, demonstrating that this waterbody remains an important nursery and rearing habitat for these imperiled species of concern.

Table 14. Density of larvae collected all years.

Scientific Name	Common Name	2013	2014	2015	2016	2017	2018	2019	2020	2021	
Alosa aestivalis	Blueback Herring	61.69	200.35	382.05	91.54	205.29	56.54	271.72	4.89	112.1	
Alosa mediocris	Hickory Shad	4.80	4.13	12.11	9.63	4.28	1.58	11.36	0.00	5.93	
Alosa pseudoharengus	Alewife	139.8	57.71	265.97	78.52	81.75	38.85	214.34	3.65	103.2	
Alosa sapidissima	American Shad	0.12	1.32	0.61	1.97	2.80	0.15	0.00	0.00	0.35	
Alosa sp.	unk. Alosa species	0.00	18.49	0.00	0.00	0.00	0.00	0.00	0.00	0.17	
Carassius auratus	Goldfish	56.78	0.89	0.00	0.30	7.02	0.00	0.00	0.00	0.00	
Carpiodes cyprinus	Quillback	0.00	0.00	0.00	0.78	0.00	0.92	8.14	0.00	0.19	
Catostomidae	unk. catostomid	0.00	0.00	0.00	0.00	0.00	0.00	0.17	0.00	0.00	
Centrarchidae	unk. centrarchid	0.00	0.00	0.00	0.13	0.00	0.00	0.00	0.00	0.00	
Clupeidae	unk. clupeid	423.0	781.67	444.54	175.5	193.3	129.3	169.13	5.55	152.8	
Cyprinidae	unk. cyprinidae	1.14	0.00	0.59	0.00	0.00	0.00	0.00	0.00	0.00	
Cyprinus carpio	Carp	0.00	0.00	0.00	0.00	2.98	0.00	0.00	0.00	0.00	
Dorosoma cepedianum	Gizzard Shad	438.4	381.85	592.25	221.5	293.5	83.18	1999.5	0.98	172.5	
Eggs	eggs	0.16	3.09	2.69	17.80	25.66	11.17	62.25	0.00	0.00	
Enneacanthus gloriosus	Bluespotted Sunfish	0.00	0.24	0.00	0.00	0.00	0.00	0.00	0.00	0.00	
Etheostoma olmstedi	Tessellated Darter	0.00	0.00	0.00	0.13	0.00	0.00	0.00	0.00	0.00	
Etheostoma sp.	unk. darter species	0.00	0.00	0.00	0.00	0.00	0.00	0.19	0.00	0.00	
Fundulus diaphanus	Banded Killifish	0.00	0.00	0.00	0.00	0.50	0.00	0.00	0.00	0.00	
Hybognathus regius	East Silvery Minnow	0.00	0.00	0.00	0.00	0.50	0.00	0.19	0.00	0.00	
Lepisosteus osseus	Longnose Gar	0.00	0.00	0.00	0.00	0.25	0.00	0.00	0.00	0.00	
Lepomis cyanellus	Green Sunfish	0.00	0.00	0.00	0.41	0.50	0.00	0.00	0.37	0.00	
Lepomis gibbosus	Pumpkinseed	0.00	0.00	0.00	1.62	0.99	0.39	0.35	0.00	0.00	
Lepomis macrochirus	Bluegill	0.00	0.00	0.00	0.00	0.50	0.00	0.00	2.38	0.00	
Lepomis sp.	unk. sunfish	0.60	2.83	0.49	0.00	8.23	0.00	0.19	0.31	0.19	
Menidia beryllina	Inland Silverside	2.48	3.32	1.98	20.36	60.78	0.66	1.21	1.78	4.89	
Micropterus dolomieu	Smallmouth Bass	0.00	0.00	0.00	0.00	0.25	0.00	0.00	0.00	0.00	
Morone americana	White Perch	0.00	5.90	15.93	8.60	17.54	15.48	66.30	0.14	33.67	
Morone saxatilis	Striped Bass	0.00	4.02	0.00	1.10	7.71	0.00	0.00	0.00	0.00	
Morone sp.	unk. moronid	39.06	43.46	4.32	14.11	3.71	0.00	0.00	0.00	0.00	
Notemigonus crysoleucas	Golden Shiner	0.00	0.84	0.00	0.00	0.00	0.00	0.00	0.00	0.00	
Notropis hudsonius	Spottail Shiner	0.00	0.00	0.00	0.39	2.48	4.94	0.23	0.00	0.00	
Perca flavescens	Yellow Perch	38.22	1.41	0.00	0.65	0.50	0.74	0.73	0.00	0.58	
Strongylura marina	Atlantic Needlefish	0.00	0.12	0.00	0.00	0.13	0.00	0.00	0.00	0.00	
Unidentified	unidentified	11.45	84.35	27.42	34.65	84.23	6.43	126.74	1.03	10.77	
Total		**1218**	**11596**	**1751**	**680**	**1006**	**351**	**2933**	**22**	**598**	

G. Adult and Juvenile Fish: Comparison among Years

The total number of adult and juvenile fishes collected in 2021 was similar to other years falling within the mid-range of our annual abundances. Once again, White Perch was the dominant species collected, continuing a trend that started in 2019 (Table 15). Banded Killifish abundances were similar to 2019, but lower than the years prior to 2018. In 2021, we collected our highest numbers of Blueback Herring to date, which was driven by high abundances in our September collections. The relative abundances of other species are pretty similar to previous years. Unlike 2020, Alewife numbers were back down to normal levels, but the high Alewife abundances in 2020 coupled with the strong Blueback Herring in 2021 indicate that Hunting Creek is a valuable nursery and rearing habitat for these imperiled species. Continued monitoring of these trends will indicate if the moratorium on fishing has resulted in population level responses.

The continued low Banded Killifish numbers, coupled with the elevated White Perch abundance is likely a result of the SAV loss in 2018 that has not reestablished in the system. Looking at our long-term trends in species percentages, it is clear that the community was dominated by Banded Killifish prior to this loss, but now remains dominated by White Perch (Figure 188). The opposite trend was seen in the longer survey record of Gunston Cove (Jones and De Mutsert 2018), which seems mostly due to SAV resurgence since 2005. The decline in SAV cover in Hunting Creek in recent years could be a reason for the decreasing Banded Killifish abundances and increasing White Perch abundances. This loss of SAV may also be favoring other open water species like the Blue Catfish, which was once again present in high numbers this year, when compared to earlier collection seasons (Table 15). Investigating the impacts of this invasive species on the fish community assemblage would be a valuable avenue for future work. Furthermore, predation studies to determine if Blue Catfish are predating upon the imperiled River Herring should also be conducted to protect these imperiled species.

Table 15. Abundances of species collected all years. Columns with an asterisk (*) include Fyke net collections.

Scientific Name	Common Name	2013	2014	2015	2016	2016*	2017	2017*	2018	2018 *	2019	2019 *	2020	2020 *	2021	2021 *
Alosa aestivalis	Blueback Herring	16	8	12	29	29	0	0	0	0	32	33	0	0	290	291
Alosa mediocris	Hickory Shad	0	0	0	0	0	0	0	0	0	8	8	4	4	0	0
Alosa pseudoharengus	Alewife	6	23	28	12	12	0	0	14	14	67	69	113	113	26	26
Alosa sapidissima	American Shad	208	32	163	19	19	2	2	2	2	12	12	0	0	2	2
Alosa sp.	unk. Alosa	299	8	55	11	12	3	3	433	433	822	822	18	18	88	89
Ameiurus catus	White Bullhead	0	0	0	1	2	0	0	8	8	1	1	4	4	2	2
Ameiurus natalis	Yellow Bullhead	0	0	0	0	0	0	0	0	0	4	4	0	0	0	0
Ameiurus nebulosus	Brown Bullhead	3	2	3	3	3	2	5	13	13	2	2	1	1	0	0
Anchoa mitchilli	Bay anchovy	69	70	7	0	0	0	0	0	0	86	86	8	8	22	22
Anguilla rostrata	American Eel	1	3	2	0	0	0	0	0	1	2	2	0	0	0	0
Brevoortia tyrannus	Atlantic Menhaden	0	0	0	0	0	0	0	0	0	30	30	0	0	12	12
Carassius auratus	Goldfish	20	39	2	0	9	18	107	1	1	0	0	0	0	2	2
Carpiodes cyprinus	Quillback	9	19	2	0	0	0	0	0	0	72	72	13	13	6	6
Cyprinella spiloptera	Spotfin shiner	0	0	1	0	0	0	0	0	0	0	0	0	0	0	0
Cyprinus carpio	Carp	0	3	1	7	14	3	3	2	2	4	4	0	0	5	5
Dorosoma cepedianum	Gizzard Shad	5	1	3	0	0	0	0	50	50	52	52	71	71	20	22
Dorosoma petenense	Threadfin Shad	0	0	0	0	0	0	0	0	0	0	0	24	24	29	29
Enneacanthus gloriosus	Bluespotted Sunfish	0	0	0	0	0	27	47	0	0	0	0	0	0	0	0
Erimyzon oblongus	Creek Chubsucker	0	0	0	0	0	0	0	1	1	0	0	0	0	0	0
Etheostoma olmstedi	Tessellated Darter	292	49	39	3	8	33	35	212	221	29	30	11	11	29	29
Fundulus diaphanus	Banded Killifish	1798	2382	2723	1387	1547	692	769	777	777	423	424	147	147	342	343
Fundulus heteroclitus	Mummichog	53	152	174	16	16	62	62	20	20	14	14	4	4	50	50
Gambusia holbrooki	Mosquitofish	11	69	19	0	0	1	1	0	0	7	7	6	6	1	1

Scientific Name	Common Name	2013	2014	2015	2016	2016*	2017	2017*	2018	2018 *	2019	2019 *	2020	2020 *	2021	2021 *
Hybognathus regius	EastSilvery Minnow	0	6	31	2	4	40	40	13	14	6	6	0	0	0	0
Ictalurus furcatus	Blue Catfish	12	4	4	1	1	6	6	57	57	93	93	61	61	56	56
Ictalurus punctatus	Channel Catfish	0	0	2	0	0	0	0	2	2	2	2	3	3	0	0
Lepisosteus osseus	Longnose Gar	0	0	3	1	1	1	1	0	0	0	0	0	0	1	1
Lepomis auritus	Redbreast Sunfish	0	0	1	2	2	0	0	0	0	0	0	0	0	0	0
Lepomis cyanellus	Green Sunfish	0	0	2	0	0	4	7	0	0	0	0	0	0	0	0
Lepomis gibbosus	Pumpkinseed	6	17	11	11	22	39	180	91	100	16	22	6	6	4	4
Lepomis macrochirus	Bluegill	12	52	21	8	20	28	188	75	81	3	5	1	1	5	6
Lepomis megalotis	Longear Sunfish	0	0	0	0	0	1	1	0	0	0	0	0	0	0	0
Lepomis microlophus	Redear Sunfish	6	11	5	2	8	0	0	0	0	0	0	0	0	0	0
Lepomis sp.	unk. sunfish	5	12	5	27	85	50	169	0	2	1	4	1	1	0	0
Menidia beryllina	Inland Silverside	15	6	73	209	210	114	124	107	120	84	86	4	4	42	44
Micropogonias undulatus	Atlantic Croaker	1	0	0	0	0	0	0	0	0	0	0	0	0	1	1
Micropterus dolomieu	Smallmouth Bass	5	5	9	6	6	62	70	20	20	10	10	6	6	1	1
Micropterus punctulatus	Spotted Bass	1	0	0	0	0	0	0	0	0	0	0	0	0	0	0
Micropterus salmoides	Largemouth Bass	3	7	0	5	5	2	2	4	4	2	3	0	0	5	5
Micropterus sp.	unk. bass species	1	0	0	0	0	0	0	0	0	0	0	0	0	0	0
Morone americana	White Perch	574	107	693	19	57	393	439	667	675	1353	1364	2920	2920	1346	1378
Morone saxatilis	Striped Bass	2	0	2	1	5	5	8	2	2	6	6	0	0	2	2
Morone sp.	unk. perch/bass species	0	1	0	0	0	0	0	0	0	0	0	0	0	13	13
Moxostoma erythrurum	Golden Redhorse	0	0	0	0	0	0	0	0	0	3	3	0	0	0	0
Moxostoma macrolepidotum	Shorthead Redhorse	0	0	0	0	0	0	0	1	1	0	0	0	0	0	0
Notemigonus crysoleucas	Golden Shiner	2	3	13	2	2	2	2	5	5	1	1	0	0	0	0
Notropis hudsonius	Spottail Shiner	338	666	87	13	17	11	13	124	125	109	113	96	96	66	69
Perca flavescens	Yellow Perch	22	16	7	7	7	1	2	36	37	6	6	0	0	0	0

Scientific Name	Common Name	2013	2014	2015	2016	2016*	2017	2017*	2018	2018 *	2019	2019 *	2020	2020 *	2021	2021 *
Pomoxis nigromaculatus	Black Crappie	0	0	4	0	1	0	0	3	3	3	4	0	0	0	0
Pylodictis olivaris	Flathead Catfish	0	0	0	0	0	0	0	0	0	0	0	1	1	0	0
Sander vitreus	Walleye	0	0	0	0	0	0	0	1	1	0	0	0	0	0	0
Strongylura marina	Atlantic Needlefish	2	4	3	0	0	9	9	1	1	2	2	0	0	1	1
Trinectes maculatus	Hogchoker	0	0	0	0	0	0	0	0	0	0	0	0	0	1	1
Unidentified	unidentified	2	0	0	0	0	0	0	0	0	0	0	0	0	0	0
Total		**3798**	**3777**	**4210**	**1804**	**2125**	**1611**	**2294**	**2742**	**2794**	**3367**	**3402**	**3524**	**3524**	**2470**	**2512**

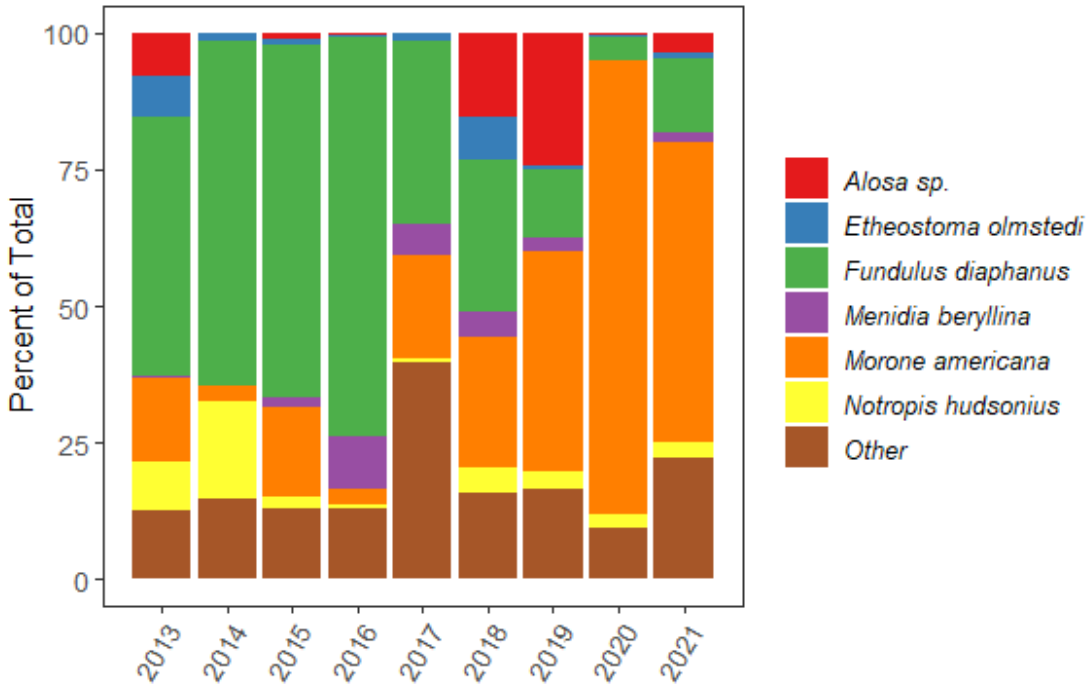

Figure 188. Percentage of total of dominant species collected in all years.

In 2021, we collected at least 27 different species, an improvement over our 2020 collections, likely because we were able to complete our normal sampling effort. The Simpson's Index of Diversity (calculated as 1-(Σ (ni/N)2)) was calculated for all years based on adult and juvenile abundances. Note that in the 2016 report the Simpson's index (D) was reported, in which communities with higher diversity or evenness approach zero. In the reports since 2016 we calculated the Simpson's Index of Diversity, which is 1-D. In this index the communities with higher diversity have higher values (approaching 1) which is more intuitive to interpret. While evenness was reduced each year of sampling before 2017, 2017 and 2018 showed high Simpson's Index of Diversity values, with 2019 slightly lower but still very close to that. 2020 was the lowest on record with a value of 0.309, which should not be interpreted as a reflection of true diversity. In 2021, our Simpson's diversity index was almost double that of 2020 and close to previous years collections indicating that while abundance trends have switched in recent years, species diversity remains similarly high.

H. Submersed Aquatic Vegetation: Comparison among Years

According to annual reports of the Virginia Institute of Marine Science (VIMS) SAV Monitoring Program (http://web.vims.edu/bio/sav/maps.html), virtually the entire surface area of the Hunting Creek embayment was covered with submersed aquatic vegetation during the first five years of this study (2013-2017). In 2018 there was a severe decline in SAV coverage. Furthermore, due to the frequent rainfall events and resulting poor water clarity, VIMS was unable to conduct the aircraft remote sensing so we were not able to make direct comparisons of 2018 coverage with 2016 and 2017. In 2019 VIMS was able to obtain aerial imagery which appears to show no SAV growing in Hunting Creek. In 2016 and 2017 mapping of species was done via boat in association with the water quality mapping surveys and the results have been reported in the results section of these reports. In 2017 the native SAV species *Ceratophyllum demersum* was substantially more abundant than the exotic species *Hydrilla verticillata* in contrast to 2016 when they had a similar abundance. The boat transects studies in 2018, 2019, 2020, and 2021 confirmed the severe dieback has persisted.

I. Benthic Macroinvertebrates: Comparison among Years

River and Embayment Samples

Comparison among Years: As we expected, the macroinvertebrate community from the embayment of Hunting Creek has been dominated by Oligochaete worms across all sites and years (Figure 189). However, if Annelids are removed and we examine the other dominant taxon groups, we see a few different trends in dominant taxa between the three Hunting Creek sites across years (Figure 190). In general, AR2 is dominated by the insect larvae of Chironomids (midges), AR3 is dominated by Gastropods (mostly composed of the invasive Japanese mystery snails), Chironomids, and Gammarid amphipods, and AR4 is dominated by Gammarid amphipods. AR2 is the site closest to the outflow from Hunting Creek, and across years, this site is mostly dominated by Chironomids (2013, 2014, 2018, 2019, 2020, and 2021), but some years Gammarid amphipods (2016 and 2017) and Gastropods (2015) dominate (Figure 190). The AR4 site is the closest to the Potomac River and has been consistently dominated by Gammarid amphipods between 2014 and 2019 and again last summer in 2021; however, in 2020 this site was dominated by the Turbellarians (flatworms). Only in 2013 were the samples dominated by Chironomid insect larvae (Figure 190). The AR4 site also has the highest relative abundances of Bivalvia (mostly driven by the invasive Asian clam *Corbicula fluminea*) and Isopoda (Crustacean) compared to the other two sites. AR4 receives higher water flow and movement, which many species of Bivalvia require, and may help explain why there are higher abundances of Bivalvia located closer to the Potomac River. The site with the most fluctuations in percent contributions of macroinvertebrate taxa was AR3, which is located in the middle of the embayment. In any given year, dominant macroinvertebrate groups change from Gastropods (2013, 2015, and 2016) to Gammarid amphipods (2014, 2017, 2018, and 2020) or Chironomid insect larvae (2019 and 2021). AR3 is also the only site where Gastropods dominate the community composition frequently. This site is probably influenced by both the Potomac River, through the daily movement of the tidal freshwater water body, and by the outfall of Hunting Creek, which moves nutrients and sediments from terrestrial sources. Only in a few years do AR2 and AR3 share the same dominant taxa; in 2015, they were both dominated by Gastropods

(mostly composed of the invasive Japanese mystery snails), in 2017 by Gammarid amphipods, and in 2019 and 2021 by Chironomid insect larvae. In comparison, AR4 seems to show different patterns of dominance than either of the other two sites further in the embayment. The relative importance of both of these waterbodies on determining benthic macroinvertebrate community structure probably varies annually due to climatic events.

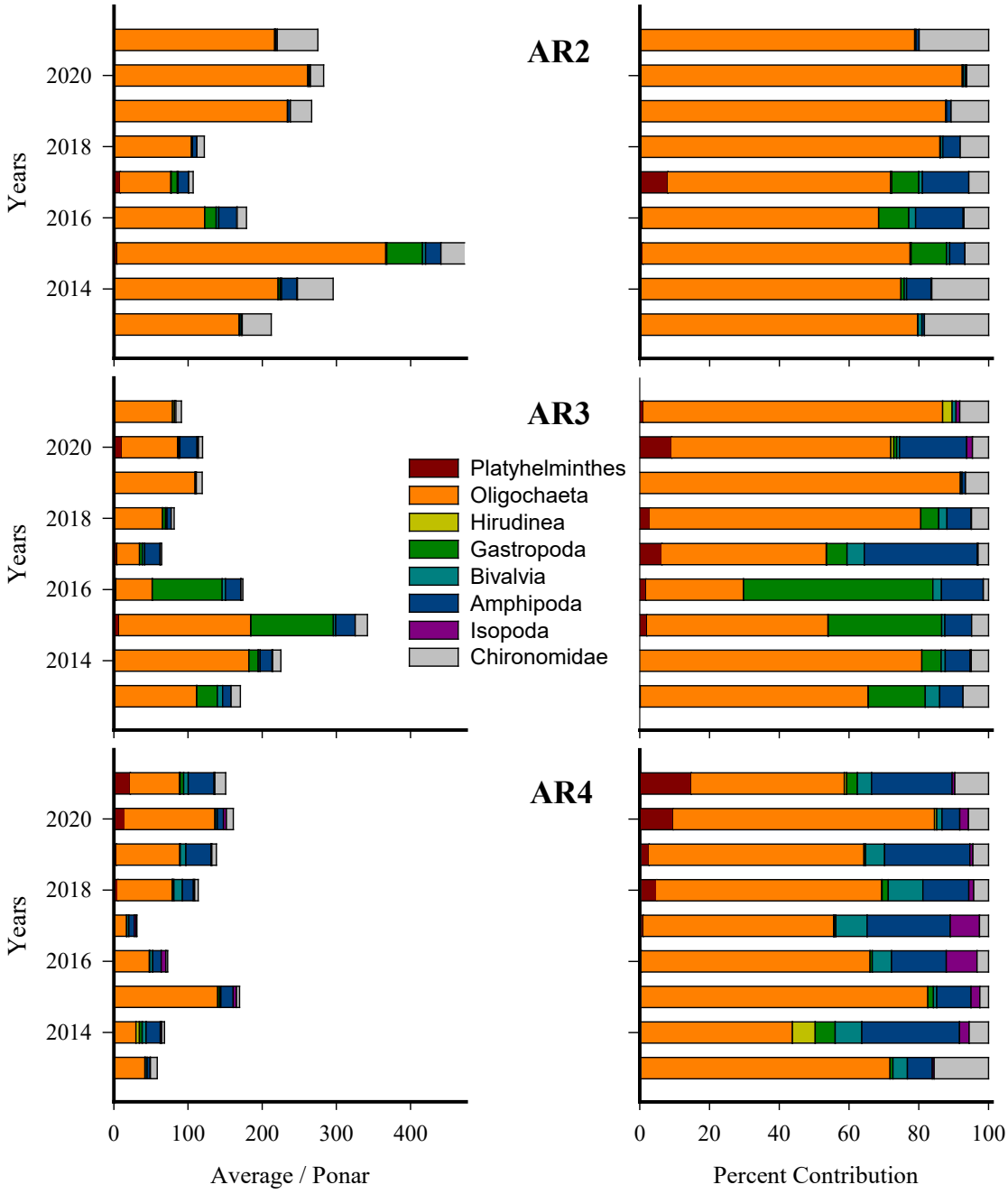

Figure 189. Average number per ponar sample (Left) and percent contribution (Right) of the eight dominant benthic invertebrate taxa in Hunting Creek embayment samples collected between 2013 and 2021 separated by site and year. Note the dominance of the Oligochaeta (worms).

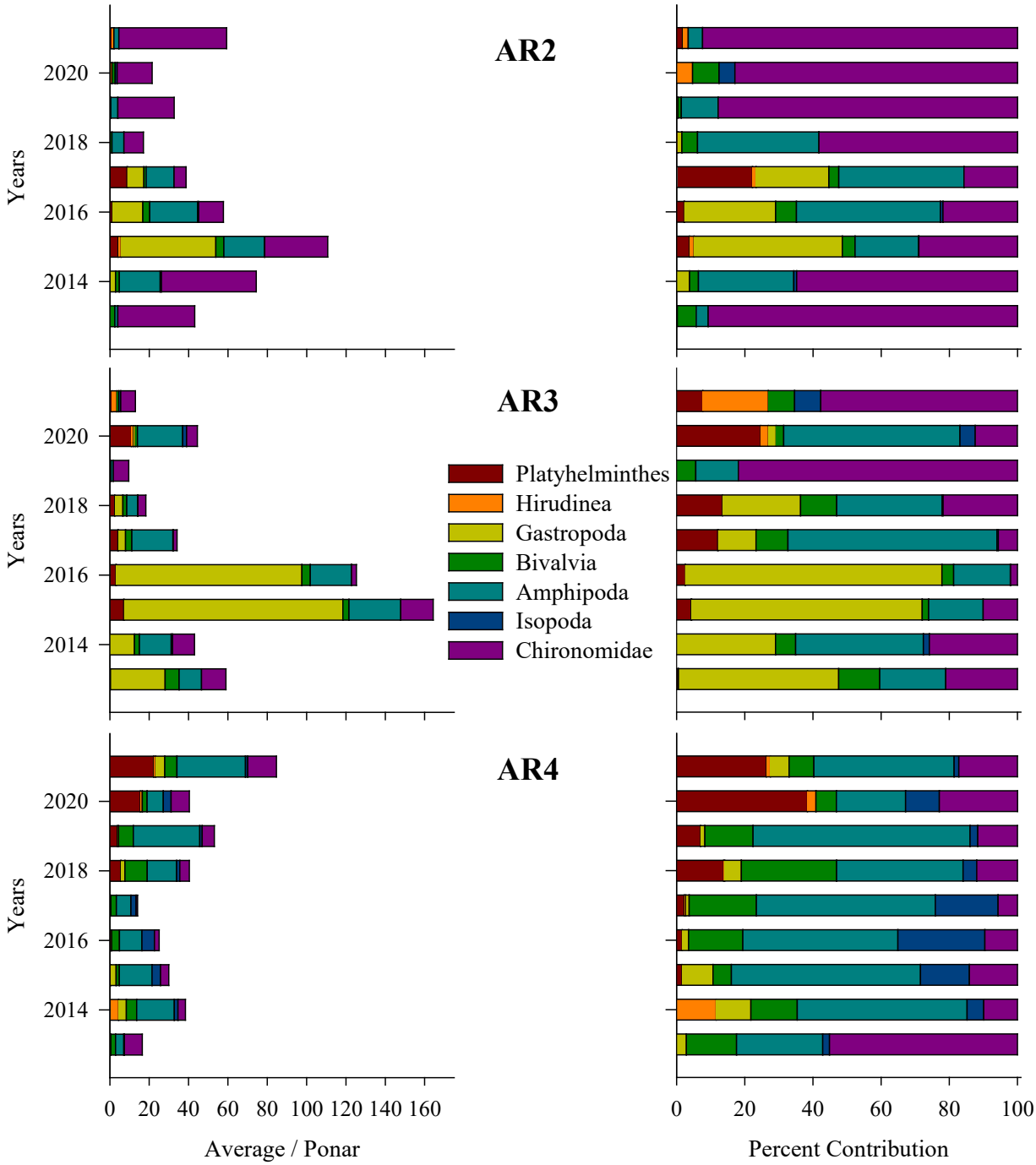

Figure 190. Without Oligochaeta, average number per ponar sample (Left) and percent contribution (Right) of the dominant benthic invertebrate taxa in Hunting Creek embayment samples collected between 2013 and 2021 separated by site and year.

Tributary Samples

Comparison among Years: We have been collecting benthic macroinvertebrate samples from the original six streams emptying into Hunting Creek since 2016. Taylor Run and Timber Branch are excluded from the analyses here, as they were first sampled in 2018. Looking across all sites and years, the taxa that dominates are members of the Insecta family Hydropsychidae (Figure 191). They are the most dominant group 39% of the time across all years and sites. Members within this family are netspinning caddisflies, which live in debris and under stones and spin concave silken nets that face upstream to capture floating or swimming prey. However, only one site from 2021, Holmes Run 1, was dominated by Hydropsychidae. The next most dominant group across all sites and years are members of the Insecta family Chironomidae (28% across all years and sites), known as midges. Chironomid larvae are filter-feeders and often live in tubes in the mud. Backlick Run and Cameron Run were dominated by Chironomidae in 2021. Other macroinvertebrate groups can dominate a site during particular years. For example, Oligochaetes (worms) have been the most frequently encountered group at Cameron Run during 2017 and at Holmes Run-1 and Turkeycock Run in 2018. Turbellarians (flatworms) have only been the most dominant group at Holmes Run-1 during 2016 and at Turkeycock Run in 2019. Members of the Insecta family Philopotamidae and Baetidae are rarely the most dominant group at a site; although Philopotamidae were the most frequently encountered group at Indian Run in 2019 (accounting for 43% of organisms counted) and Cameron Run in 2020 (41% of organisms counted). Surprisingly, Philopotamidae was the dominant group for two sites in 2021 (Holmes Run 2 and Indian Run). In general, across all years, Backlick Run and Cameron Run are dominated by Chironomidae, and both Holmes Run sites are dominated by Hydropsychidae. Depending on the year, Indian Run fluctuates in being dominated by either of the two Trichopteran families – either Hydropsychidae or Philopotamidae. Turkeycock Run is an interesting site, as it has been dominated by all of the groups, except the two Trichopteran families, at some point over the last six years of sampling. All of these sites are probably influenced by differences in the types and amounts of nutrients and sediments moving from terrestrial sources, the flow of water, and anthropogenic impacts to the system. The relative importance of a variety of abiotic factors on determining benthic macroinvertebrate community structure probably varies annually, and even monthly, due to climatic events. Therefore, site-level trends may be apparent with continued annual sampling.

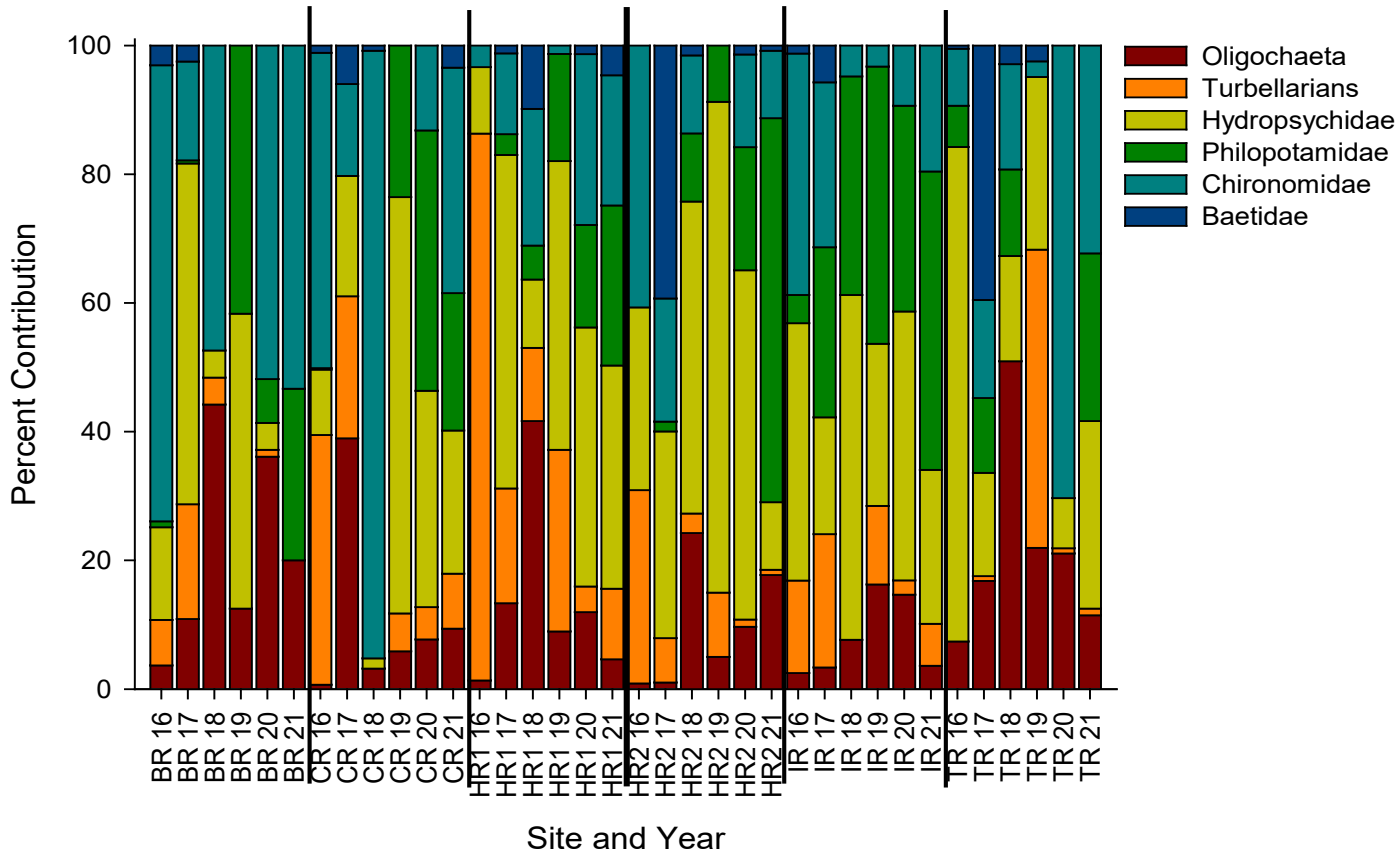

Figure 191. Percent contribution of of the six dominant benthic invertebrate taxa in tributary kick samples collected between 2016 and 2021 separated by site and year. Sites have been separated with black lines for ease of interpretation. Abbreviations for sites are noted in Table XXX.

LITERATURE CITED

Bigelow, H.B. and W.C.Schroeder. 1953. Fishes of the Gulf of Maine. Fishery bulletin No. 74, Vol. 53. U.S. Government Printing Office. Washinton, D.C. 577 pp.

Carter, V., P.T. Gammon, and N.C. Bartow. 1983. Submersed Aquatic Plants of the Tidal Potomac River. Geological Survey Bulletin 1543. U.S. Geological Survey. 63 pp.

Chesapeake Bay Program. 2006 Ambient water quality criteria for dissolved oxygen, water clarity, and chlorophyll *a* for the Chesapeake Bay and its tidal tributaries. 2006 Addendum. Downloaded from Bay Program website 10/13/2006.

Cummings, H.S., W.C. Purdy, and H.P. Ritter. 1916. Investigations of the pollution and sanitary conditions of the Potomac watershed. Treasury Department, U.S. Public Health Service Hygienic Laboratory Bulletin 104. 231 pp.

Dahlberg, M.D. 1975. Guide to coastal fishes of Georgia and nearby states. University of Georgia Press. Athens, GA 187 pp.

Douglass, R.R. 1999. A Field Guide to Atlantic Coast Fishes: North America (Peterson Field

Guides). Houghton Mifflin Harcourt, Boston. 368 pp.
Eddy, S. and J.C. Underhill. 1978. How to know the freshwater fishes. 3rd Ed. W.C. Brown Co. Dubuque, IA. 215 pp.
Froese, R. and D. Pauly (Eds.). 2012. Fish Base. World Wide Web electronic publication. www.fishbase.org, version (04/2012).
Hildebrand and Schroeder. 1928. Fishes of the Chesapeake Bay. U.S. Bureau of Fisheries Bulletin 53, Part 1. Reprinted 1972. T.F.H. Publishing, Inc. Neptune, NJ. 388 pp.
Hogue, J.J, Jr., R.Wallus, and L.K. Kay. 1976. Preliminary guide to the identification of larval fishes in the Tennessee River. Technical Note B19. Tennessee Valley Authority. Knoxville, TN.
Huntley, M., K. Tande, and H.C. Eilertsen. 1987. On the trophic fate of *Phaeocystis pouchetii* (Hariot). Grazing rates of *Calanus hyperboreus* (Kroyer) on diatoms and different size categories of *Phaeocystis pouchetii*. J. Exp. Mar. Biol. Ecol. 110: 197-212.
Islam, S. 2001. Seasonal dynamics of micro-, nanno-, and picoplankton in the tidal freshwater Potomac River in and around Gunston Cove. Ph.Dissertation. George Mason University. 127 pp.
Jenkins, R.E. and N.M. Burkhead. 1994. The freshwater fishes of Virginia. American Fisheries Society. Washington, DC. 1080 pp.
Jones, P.W., F.D. Martin, and J.D. Hardy, Jr. 1978. Development of fishes of the Mid-Atlantic bight. Volumes I-VI. Fish and Wildlife Service, U.S. Department of the Interior. FWS/OBS-78/12.
Kraus, R.T. and R.C. Jones. 2011. Fish abundances in shoreline habitats and submerged aquatic vegetation in a tidal freshwater embayment of the Potomac River. Environmental Monitoring and Assessment. Online: DOI 10.1007/s10661-011-2192-6.
Kelso, D.W., R.C. Jones, and P.L. deFur. 1985. An ecological study of Gunston Cove - 1984-85. 206 pp.
Lippson, A.J. and R.L. Moran. 1974. Manual for identification of early development stages of fishes of the Potomac River estuary. Power Plant Siting Program, Maryland Department of Natural Resources. PPSP-MP-13.
Loos, J.J., W.S. Woolcott, and N.R. Foster. 1972. An ecologist's guide to the minnows of the freshwater drainage systems of the Chesapeake Bay area. Association of Southeastern Biologists Bulletin 19: 126-138.
Lund, J.W.G., C. Kipling, and E.C. LeCren. 1958. The inverted microscope method of estimation algal numbers and the statistical basis of estimations by counting. Hydrobiologia 11: 143-170.
Mansueti, A.J. and J.D. Hardy, Jr. 1967. Development of fishes of the Chesapeake Bay region: an atlas of egg, larvae and juvenile stages: Part 1. Natural Resources Institute. University of Maryland. 202 pp.
Merritt, R.W. and K.W. Cummins. 1984. An introduction to the aquatic insects of North America. 2nd edition. Kendall/Hunt Publishing Co., Dubuque, IA. 722 pp.
Pennack, R.W. 1978. Fresh-water invertebrates of the United States. 2nd ed. Wiley-Interscience. New York, NY.
Schloesser, R.W., M.C. Fabrizio, R.J. Latour, G.C. Garman, G.C., B. Greenlee, M. Groves and J. Gartland. 2011. Ecological role of blue catfish in Chesapeake Bay communities and implications for management. American Fisheries Society Symposium 77:369-382.
Scott, W.B. and E.J. Crossman. 1973. Freshwater fishes of Canada. Bulletin 184. Fisheries

Research Board of Canada. Ottawa, Canada. 966 pp.
Standard Methods for the Examination of Water and Wastewater. 1980. American Public Health Association, American Waterworks Association, Water Pollution Control Federation. 15th ed. 1134 pp.
Thorp, J.H. and A.P. Covich, eds. 1991. Ecology and classification of North American Freshwater Invertebrates. Academic Press. San Diego, CA. 911 pp.
Wetzel, R.G. 1983. Limnology. 2nd ed. Saunders. 767 pp.
Wetzel, R.G. and G.E. Likens. 1991. Limnological analyses. 2nd ed. Springer-Verlag. 391 pp.

Anadromous Fish Survey Cameron Run: 2021

T. Reid Nelson
Assistant Professor, Department of Environmental Science and Policy
Potomac Environmental Research and Education Center

Introduction

Anadromous river herring and shad live as adults in the coastal ocean and return to freshwater creeks and rivers to spawn. In the mid-Atlantic region, four species are present: American Shad (*Alosa sapidissima*), Blueback Herring (*Alosa aestivalis*), Alewife (*Alosa pseudoharengus*), and Hickory Shad (*Alosa mediocris*). Two other Clupeids are semi-anadromous and spawn in Potomac River tributaries. These are Gizzard Shad (*Dorosoma cepedianum*) and Threadfin Shad (*Dorosoma petenense*). Previous reports describe the history of herring populations in the Potomac River watershed (Jones et al. 2019).

The focus of the Cameron Run fish survey is river herring, the collective name of Blueback Herring and Alewife. River herring populations have declined drastically over their range, spurring conservation efforts since 1970, which have been intensified since 2005 with implementation of moratoria. Identifying all areas used as spawning habitat by Alewife and/or Blueback Herring is an important component of their conservation. Since 1988, George Mason University researchers have focused a monitoring program on the spawning of these species in other tributaries such as Pohick Creek, Accotink Creek, and, less regularly, Dogue Creek. With this study Cameron Run was added in 2013, which has not been monitored for presence of river herring or other anadromous species by either George Mason or other fisheries biologists before the start of this study (Jim Cummins, pers. comm.). Historically, local anglers reported anadromous fishes spawning in Cameron Run (Neves et al. 1988); however, our 2013 survey provided the first confirmation of Cameron Run as River Herring spawning habitat (Alan Weaver, VDGIF, pers. comm.). Use of Cameron Run by river herring upstream from where the effluent of Alexandria Renew Enterprises enters Cameron Run signifies that the effluent does not deter river herring from using Cameron Run as spawning habitat. In 2014 we moved the collection site approximately 500 m downstream (still above the Alexandria Renew Enterprises effluent), which increased our catches, and allows us to estimate the size of the spawning population. The new location proved successful and will remain the collection site for any subsequent surveys.

Methods

We conducted weekly sampling trips from March 11 to May 12 in 2021. During each trip (when conditions allowed it) a hoop net was set with wings blocking the complete creek (referred to as block net) to collect adults swimming upstream, and ichthyoplankton nets were set to collect larvae floating downstream. Cross-section and flow were measured to calculate discharge, and physical parameters were measured using a handheld YSI. In some occasions, the conditions were not right to complete one or more procedures, Table 1 provides the information on which procedures were completed each sampling day in 2021. The sampling location was chosen to be

upstream from the Alex Renew effluent, and downstream of the first dam in Cameron Run (Figure 1).

Table 1. Procedures completed each sampling date

Date	Block Net	Plankton	Flow
3/11/2021	24 hours	20 mins	Yes
3/17/2021	No Net Set	20 mins	Yes
3/25/2021	No Net Set	10 mins	Yes
3/31/2021	No Net Set	20 mins	Yes
4/8/2021	24 hours	20 mins	Yes
4/15/2021	No Net Set	10 mins	Yes
4/22/2021	24 hours	20 mins	Yes
4/29/2021	24 hours	20 mins	Yes
5/6/2021	24 hours	20 mins	Yes
5/12/2021	24 hours	20 mins	Yes

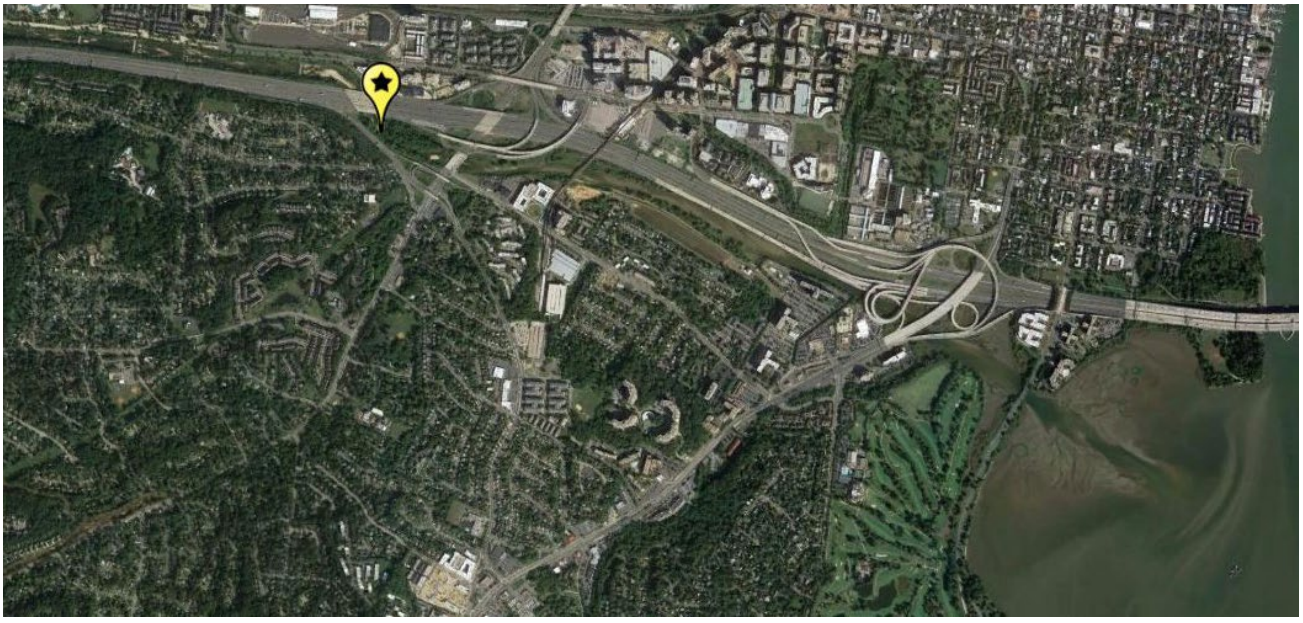

Figure 1. Sampling location Cameron Run.

We collected ichthyoplankton by setting two conical plankton nets with a mouth diameter of 0.25 m and a square mesh size of 0.333 mm in the stream current for 20 minutes. To estimate water volume filtered by the net, we suspended a mechanical flow meter designed for low velocity measurements in the net opening. The number of rotations of the flow meter attached to the net opening was multiplied by 5760 and then divided by 999999 to gain volume filtered (m^3) based on the correction equations provided by the General Oceanics flow meter user manual (https://www.forestry-suppliers.com/Documents/588_msds.pdf). Larval density (#/m^3) per species was calculated using the following formula: Larval density (#/m^3) = number of larvae in one sample (#) /volume filtered (m^3).

We collected 2 ichthyoplankton samples per trip, and these were spaced out evenly along the stream cross-section. Coincident with plankton samples, we calculated stream discharge rate from measurements of stream cross-section area and current velocity using the following equation:

Depth (m) x Width (m) x Velocity (m/s) = Discharge (m^3/s)

We measured velocity using a handheld digital flow meter that measures flow in cm/s, which had to be converted to m/s to calculate discharge. We measured depth and current velocity at 12 to 20 locations along the cross-section. During each sampling trip, we recorded other physical parameters (water temperature, dissolved oxygen, pH, and specific conductivity) as well.

We preserved ichthyoplankton samples in 70% ethanol and transported them to the GMU laboratory for identification and enumeration. To identify larvae, we used multiple taxonomic resources: primarily Lippson & Moran (1974), Jones et al. (1978), and Walsh et al. (2005). River herring (both species) have semi-demersal eggs (tend to sink to the bottom) that are frequently adhesive. As this situation presents a significant bias, we are not treating egg abundance in the samples as a reliable estimate of egg abundance, and this is not used in population productivity estimates. We estimate total larval production (P) during the period of sampling by multiplying the larval density (m^{-3}) with total discharge (m^3) during the spawning period, which we assume is represented our sampling period.

The block net was deployed once each week in the morning and retrieved the following morning (Figure 2). Fish in the block net were identified, enumerated, and measured.

Since the net was set 24 hours per week during the spawning season, and the spawning season is estimated to last 10 weeks, we approximated total abundance of spawning river herring during the time of collection by extrapolating the mean catch per hour per species during the time the creeks were blocked over the total collection period as follows:

Average catch/24 hours * 1680 hours = total abundance of spawners

We assumed our total collection period to be a good approximation of the total time of the river herring spawning run.

In response to problems with animals tearing holes in our nets in previous sampling experiences, we used a fence device in front of the mouth of the net that significantly reduces this problem. The device effectively excluded wildlife such as otters and turtles, while it has slots that allowed up-running fish to be captured.

Figure 2. Hoop net deployed in new location in Cameron Run. The hedging is angled downstream in order to funnel up-migrating herring into the opening of the net.

Results and Discussion

During the sampling period, we caught only 36 Alewife on a single sampling date, April 8th 2021 (Table 2). However, this abundance of Alewife was similar to our overall Alewife abundance in previous sampling years. However, we cannot compare to 2020, given that our field sample was canceled as a result of COVID-19. We set the net so that fishes must swim upstream into Cameron Run to be caught in the net, which is a behavior associated with spawning. The high water during this sampling season precluded nets being set for the majority of March, which likely caused us to miss many spawning River Herring. Although we did not intercept any adult Blueback Herring this year, we did collect larval Blueback Herring and Alewife indicating that this creek was used for spawning by both species. Since the spawning populations is small and sampling variability high (for larval density, a small portion of the water column is sampled for 20 minutes per week), sampling over multiple years provides us with increasingly better estimates of the spawning population of Alewife and Blueback Herring in Cameron Run. Given that we only collected adult Alewife, we were only able to estimate the Alewife spawning population.

Table 2. Species collected in Cameron Run with hoop net during weekly sampling. River herring are indicated by bold font.

Date	ScientificName	CommonName	Count
2021-04-08	***Alosa pseudoharengus***	**Alewife**	**36**
2021-04-08	*Catostomus commersonii*	White Sucker	1
2021-04-08	*Erimyzon oblongus*	Creek Chubsucker	1
2021-04-08	*Lepomis macrochirus*	Bluegill	1
2021-04-29	*Lepomis auritus*	Redbreast Sunfish	4
2021-04-29	*Lepomis gibbosus*	Pumpkinseed	1
2021-04-29	*Lepomis macrochirus*	Bluegill	11
2021-04-29	*Micropterus salmoides*	Largemouth Bass	7
2021-04-29	*Morone americana*	White Perch	3
2021-05-06	*Lepomis auritus*	Redbreast Sunfish	1
2021-05-06	*Lepomis macrochirus*	Bluegill	3
2021-05-06	*Morone americana*	White Perch	2
	Total		71

We collected more larvae this year than we did in 2019, unfortunately the 2020 field season was cancelled as a result of COVID-19 so we have a gap in our data for that year. In our samples, we positively identified 219 Alewife, and 11 Blueback Herring larvae (Table 3), which is almost identical to our 2019 numbers of each species respectively (211, 10). The unidentified larvae could have also been river herring potentially increasing our numbers. Once again, the collection of Blueback Herring larvae confirms that they were spawning in Cameron Run, even though we did not intercept any adults. In addition to river herring, we also collected Gizzard Shad, Goldfish, Spottail Shiners, White Perch, Common Carp, Inland Silversides, and Quillback (Table 3).

Table 3. Larvae collected in Cameron Run. Herring larvae (river herring and other clupeids) are in bold. Fish larvae too damaged for identification to species level were identified at the highest level possible.

Date	Scientific Name	Common Name	Count	Volume	AveDensity
2021-03-25	*Eggs*	Eggs	20	29.580	1.122
2021-03-31	***Alosa pseudoharengus***	**Alewife**	**5**	**0.175**	**0.000**
2021-04-08	***Alosa aestivalis***	**Blueback Herring**	**5**	**38.782**	**0.137**
2021-04-08	***Alosa pseudoharengus***	**Alewife**	**78**	**38.782**	**2.082**
2021-04-08	*Clupeidae*	Unk. Clupeidae	2	38.782	0.052
2021-04-08	*Dorosoma cepedianum*	Gizzard Shad	1	38.782	0.024
2021-04-08	*Eggs*	Eggs	134	38.782	3.505
2021-04-08	*Notropis hudsonius*	Spottail Shiner	4	38.782	0.109
2021-04-08	*Unidentified*	Unknown	2	38.782	0.057
2021-04-15	***Alosa pseudoharengus***	**Alewife**	**7**	**2.797**	**0.954**
2021-04-15	*Eggs*	Eggs	162	2.797	26.711
2021-04-15	*Notropis hudsonius*	Spottail Shiner	1	2.797	0.000
2021-04-22	***Alosa aestivalis***	**Blueback Herring**	**1**	**31.818**	**0.037**
2021-04-22	***Alosa pseudoharengus***	**Alewife**	**40**	**31.818**	**1.248**
2021-04-22	*Carassius auratus*	Goldfish	1	31.818	0.027
2021-04-22	*Eggs*	Eggs	59	31.818	1.884
2021-04-22	*Notropis hudsonius*	Spottail Shiner	1	31.818	0.037
2021-04-29	***Alosa aestivalis***	**Blueback Herring**	**5**	**5.431**	**0.565**
2021-04-29	***Alosa pseudoharengus***	**Alewife**	**89**	**5.431**	**25.087**
2021-04-29	*Carassius auratus*	Goldfish	1	5.431	0.498
2021-04-29	*Clupeidae*	Unk. Clupeidae	2	5.431	0.226
2021-04-29	*Dorosoma cepedianum*	Gizzard Shad	2	5.431	0.997
2021-04-29	*Eggs*	Eggs	17	5.431	3.076
2021-04-29	*Morone americana*	White Perch	25	5.431	3.594
2021-04-29	*Notropis hudsonius*	Spottail Shiner	5	5.431	0.950
2021-04-29	*Unidentified*	Unknown	3	5.431	0.724
2021-05-06	*Carassius auratus*	Goldfish	4	36.437	0.100
2021-05-06	*Cyprinus carpio*	Common Carp	1	36.437	0.030
2021-05-06	*Eggs*	Eggs	118	36.437	3.340
2021-05-06	*Menidia beryllina*	Inland Silverside	3	36.437	0.091
2021-05-06	*Notropis hudsonius*	Spottail Shiner	1	36.437	0.030
2021-05-06	*Unidentified*	Unknown	1	36.437	0.025
2021-05-12	*Carassius auratus*	Goldfish	5	25.407	0.206

Date	Scientific Name	Common Name	Count	Volume	AveDensity
2021-05-12	*Carpiodes cyprinus*	Quillback	2	25.407	0.080
2021-05-12	*Cyprinus carpio*	Common Carp	1	25.407	0.045
2021-05-12	*Eggs*	Eggs	9	25.407	0.409
2021-05-12	*Menidia beryllina*	Inland Silverside	3	25.407	0.115
2021-05-12	*Notropis hudsonius*	Spottail Shiner	7	25.407	0.286
	Total		827		

We measured creek discharge and other physical parameters at the same location and times where ichthyoplankton samples were taken, which was about 100 m downstream from the block net (Table 4). Mean creek discharge was less than 2019 but in the same range as previous years. Mean discharge in 2021 was 0.552 m^3 s^{-1}, ranging from 0.03 m^3 s^{-1} to 1.46 m^3 s^{-1}. Water temperature was above 10 °C on all sampling days, except for March 17th, which is the presumed minimum temperature for river herring spawning. The first sampling date where we found Alewife (larvae) was March 31, following this low temperature period. However, larvae were present through late April. Dissolved oxygen (DO), and pH were in the benign range for occurrence of river herring throughout the sampling period (Table 4).

Table 4. Physical parameters measured at Cameron Run during each sampling week.

Date	Discharge m^3 s^{-1}	Temperature °C	Spcond µS s^{-1}	DO mg L^{-1}	pH
2021-03-11	0.99	15.7	NA	11.29	7.97
2021-03-17	0.14	8.9	0.75	13.09	7.67
2021-03-25	1.46	13.2	647.00	10.80	7.56
2021-03-31	0.03	14.7	695.00	11.50	7.92
2021-04-08	0.48	20.4	719.00	11.65	9.48
2021-04-15	0.72	17.1	662.00	10.81	8.43
2021-04-22	0.55	11.2	662.00	12.08	8.34
2021-04-29	0.41	23.5	620.00	9.71	8.16
2021-05-06	0.46	18.6	554.00	9.79	7.51
2021-05-12	0.28	17.6	624.00	10.92	8.00

During the sampling period of 10 weeks, the total discharge was estimated to be on the order of 3.33 million cubic meters (Table 5), similar to 2019 and previous years. Given the observed mean densities of larvae (3.01 m^{-3}), the total production of river herring larvae was estimated at approximately 10.05 million for Cameron Run (Table 5). Note that the estimate is based on a small sample of the total discharge. With 36 adult Alewife collected, and extrapolating over period of the spawning run as explained in the methods, this could mean that the river herring spawning population in 2019 was 420 individuals, which is higher than recorded in 2019, but still in the range that is similar to previous years.

Table 5. Estimation of river herring (alewife and blueback herring) larval production and spawner abundance from Cameron Run during spring 2021.

Parameter	**Cameron Run**
Mean discharge (m3s-1)	0.552
Total discharge, (m3)	3337098.921
Total plankton nets volume sampled (m^3)	213.015
Mean Alosa larvae density (m^{-3})	3.011
Total river herring production (# larvae)	10048188.473
Total adult Alewife(#)	420.000

Conclusions

After we found that Cameron Run is used as river herring spawning habitat with just one adult river herring and seven larvae in 2013, we were able to confirm this finding by collecting more river herring adults and larvae from 2014-2021 (Figure 3), albiet with the exception of 2020 when sampling did not occur because of COVID-19. By moving our sampling site approximately 500 m downstream in 2014 we have found a better sampling location. Even further downstream Cameron Run becomes too deep and wide for our sampling strategy.

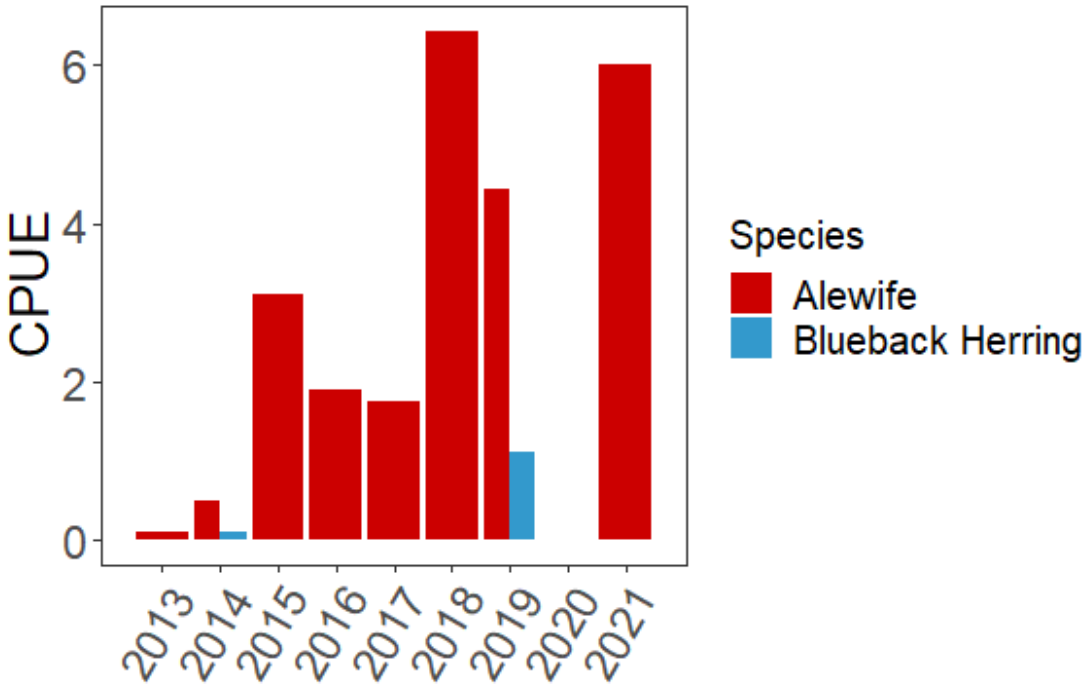

Figure 3. Catch per Unit Effort of Alewife and Blueback Herring (number of individuals per block net) collected with the block net in each year.

The finding of river herring adults and larvae in an area above the outflow of the Alexandria Renew Enterprises wastewater reclamation facility signifies that the water of Cameron Run is clean enough to use as spawning habitat for these species of concern. These finding will not

affect AlexRenew, but will affect the terms of construction permits in and around Cameron Run (i.e. some construction activities may be restricted by the Virginia Department of Wildlife Resources (VADWR) during the annual spawning period (mid-March to mid-May) of river herring (Alan Weaver, VADWR, pers. comm.).

Although the current evidence suggests that the importance of Cameron Run may be marginal to Alewife and Blueback Herring populations, it is important to recognize that marginal habitats may sustain fish populations during periods of declining abundance and low recruitment (Kraus and Secor 2005). Due to the moratorium on river herring set in place bay-wide in 2012, annual estimation of spawner abundance should be a continued priority for annual monitoring of this and other Potomac River tributaries. In 2015, 3 years after the 2012 moratorium, Alewife CPUE greatly increased, which is about the time it takes for Alewife to grow to adulthood and return to their spawning grounds. This peak has been seen in other tributaries to the Potomac River as well (Jones and De Mutsert 2016) and could signify the effect of the release from the fishery. This effect was not seen throughout Virginia however (Alan Weaver, VDGIF, pers. comm.), and was not maintained to the same level in the subsequent years (2016 and 2017). Anadromous fishes typically exhibit strong year-class fluctuations, and we expected a high return of river herring in 2018 if the offspring of the successful 2015 year-class was able to return. We indeed saw even higher numbers return in 2018, which is a sign that the high abundance in 2015 may have given a lasting boost to the population. It is a good sign that the same level of return spawners was registered in 2019, and that adult Blueback Herring were among the river herring collected this year. Unfortunately, we were not able to collect fishes during 2020, but our trends from 2021 also indicate many Alewife spawners. Furthermore, these spawners came from a limited sample size given environmental constraints on our sampling methods and the overall spawning population may have been even higher than we detected. While our total adult Alewife population numbers are similar to 2019, the larval production is much higher potentially indicating better spawning and larval survival conditions. Additional years of data collection (at least through 2 generation lengths ~ a decade) will allows us to see if this cycle continues into the future and helps with the slow built-up of river herring populations.

Literature Cited

General Oceanics. ND. General Oceanics digital flowmeter mechanical and electronic operators manual. https://www.forestry-suppliers.com/Documents/588_msds.pdf.

Jones, P. W., F. D. Martin, and J. D. Hardy, Jr. 1978. Development of fishes of the Mid-Atlantic Bight: an atlas of egg, larval, and juvenile stages, volume 1. Acipenseridae through Ictaluridae. U.S. Fish and Wildlife Service, FWS/OBS-78/12.

Jones, R. C., De Mutsert, K., and G. D. Foster. 2014. An Ecological Study of Hunting Creek-2013. Final report to Alexandria Renew Enterprises, Alexandria, VA. 123 p.

Jones, R. C. and De Mutsert, K. 2016. An Ecological Study of Gunston Cove-2015. Final report. Potomac Environmental research and education Center, Fairfax, VA.

Kraus, R. T. and D. H. Secor. 2005. Application of the nursery-role hypothesis to an estuarine fish. Marine Ecology Progress Series 290:301-305.

Neves, R. J., M. Cooper. Odom, J. J. Ney, and Virginia. Dept. of Transportation. 1988. Use of Virginia's tributaries of the Potomac River by anadromous fishes : final report for phase four of an analysis of the impediments to spawning migrations of anadromous fish in Virginia rivers.

ESCHERICHIA COLI ABUNDANCES IN HUNTING CREEK/CAMERON RUN AND ADJACENT POTOMAC RIVER - 2021

Final Report
By

Benoit Van Aken
Associate Professor, Department of Chemistry & Biochemistry
George Mason University

1. Introduction

During 2021, in connection with examination of ecological and chemical parameters, a study of *Escherichia coli* in the areas of the Hunting Creek/Cameron Run watershed and adjacent waters of the Potomac River was continued with samples being collected at 17 sites. These sites included 10 sites sampled in the period 2016 – 2018 (AR-1, AR-2, AR-3, AR-4, AR-10, AR-12, AR-13, AR-21, AR-23, and AR-30). AR-11 (outlet of Lake Cook) was not sampled beyond 2019 because it was considered redundant with a nearby downstream site in Camron Run: AR-21. Note that AR-22, sampled in 2016 and 2017, has not been accessible since 2018 due to existence of large-scale construction projects and earthwork along the stream bank of Huntington Park. Three new sites sampled in 2019 included one off-shore site: AR-32 (Potomac Mainstem downstream of Outfall 001) and two shore sites: AR-33 (Hooffs Run at Linden St) and AR-34 (Hooff Run at Alex Renew). Note that site AR-31 (Potomac Mainstem upstream of Outfall 001), which was sampled in 2019, was not sampled in 2020 and 2021. In 2020, four new sites were added, including three shore sites: AR-24 and AR-25 by the Hunting Creek Embayment near shore just west and east of Royal St. combined sewage outfall (CSO), respectively, and AR-35 by the Timber Branch of Hoofs Run at downstream end of Ivy Hill Cemetery, and one off-shore site in the Potomac River at Daingerfield Island (marker '6'): AR-38.

This work provides current microbiological water quality information in these aquatic ecosystems adjacent to and receiving water from the wastewater reclamation facility operated by Alexandria Renew Enterprises (hereafter Alex Renew). The research continues to determine the ambient levels of *E. coli* and if these waters are impaired under the Clean Water Act in terms of their uses as designated by the Commonwealth of Virginia.

The text of the Virginia Water Quality Standards (9 VAC 25-260-10) is as follows:

"All state waters, including wetlands, are designated for the following uses: recreational uses, e.g., swimming and boating; the propagation and growth of a balanced, indigenous population of aquatic life, including game fish, which might reasonably be expected to inhabit them; wildlife; and the production of edible and marketable natural resources, e.g., fish and shellfish" (VSWCB 2011).

Section 9VAC25-260-170 of the Virginia Water Quality Standards (amended as of January 2011) specifies the bacteriological criteria for *E. coli* that apply to primary contact recreational use surface waters:

1. "*E. coli* bacteria shall not exceed a monthly geometric mean of **126 CFU/100 mL** in freshwater […]."

2. "Geometric means shall be calculated using all data collected during any calendar month with a minimum of four weekly samples."

3. "If there are insufficient data to calculate monthly geometric means in freshwater, no more than 10% of the total samples in the assessment period shall exceed **235 *E. coli* CFU/100 mL** […]."

5. "For beach advisories or closures, a single sample maximum of **235 *E. coli* CFU/100 mL** in freshwater […] shall apply." (VSWCB 2011b)

Of all of the conditions in rivers and streams which can lead to a listing of 'impaired water', the one criterion that, more than any other, results in such a listing is coliform bacteria or *E. coli* abundances (USEPA 2014). Both Hunting Creek and Cameron Run were listed as impaired under the Clean Water Act for exceedances of Virginia's water quality criterion for *E. coli* bacteria (VADEQ, 2012), although the earlier impairment listing of Hunting Creek was based on the then applicable fecal coliform criterion (VADEQ 2010). The fecal coliform criterion was subsequently changed to *E. coli* based on the understanding that this subset of fecal coliforms is more specifically associated with fecal material from humans and other warm-blooded animals. The U.S. EPA (USEPA 2012) recommended and the Commonwealth of Virginia accepted *E. coli* as the better indicator of health risk related to recreational water contact. That is the current microbiological water quality criterion.

Due to this impairment, total maximum daily load (TMDL) allocations for *E. coli* were developed for both of these watersheds in late 2010 (VADEQ 2010). The City of Alexandria is working toward achieving the bacteriological criteria for these waters through a variety of programs including a storm water program, minimizing combined storm water sewer system overflows and eventually eliminating those discharges, reductions in pet waste sources, and discovery of illegal discharges. Because the sources of *E. coli* to water systems are many and varied, including wildlife sources which are generally not controlled unless at a nuisance level, continued monitoring of *E. coli* in these waterways is an important aspect of maintaining and improving water quality. The results reported here add to the understanding of the microbiological quality of these systems.

2. Methods

Sampling Regime & Methods

In the prior years, the approach was to sample on a biweekly basis in May through September with one sampling in April. In 2021, samples were collected on 10 dates, from April 14, 2021 to September 8, 2021. The last scheduled sampling on September 22, 2021 was cancelled due to inclement weather (**Table EC1**). Water samples were collected at 17 stations on each sampling day. Station identifiers and locations are shown in **Table EC2** (the map of EC sampling stations is provided in Appendix A, **Figure A1**). Samples were collected in clean, steam sterilized (autoclaved), 1-liter, wide-mouth polypropylene bottles. Eleven stations were approached from the shore: AR-1, AR-12, AR-13, AR-21, AR-23, AR-24, AR-25, AR-30, AR-33, AR-34, and AR-35, and 6 stations were sampled from an outboard-powered research vessel: AR-2, AR-3, AR-4, AR-10, AR-32, and AR-38. Among the shore stations, stations AR-21, AR-24, AR-25, AR-30, and AR-35 were sampled from the shore without wading into the stream. At these stations, samples were collected as grab samples using the 1-liter bottle. Sampling was operated in the most active flow zone that could be reached from the shore. At station AR-1, AR-23, and AR-34, samples were collected remotely using a sterilized, 1- or 4-liter round, polypropylene wide-mouth bottle fitted with a harness and nylon line. At station AR-1, the sample bottle was deployed from atop the George Washington Parkway Bridge over Hunting Creek on the downstream side approximately at mid-span. At stations AR-23 and AR-34, the sample bottle was deployed from the shore and thrown to about 5-10 yards into the water. When accumulation of surface debris prevented the collection of grab samples, AR-25 was also sampled using a bottle fitted with a harness and nylon line. Collection of three shore-approached samples was achieved wading in the streams: AR-12, AR-13, and AR-33. At station AR-12, we waded into the water downstream of the collection site to approximately midstream, waited for the current to carry away any disturbed sediment and then collected the sample by submerging the 1-liter bottle upstream of the sample collector. At station AR-13, the bottom of the stream at the approach site is paved with concrete. At this site, we waded to approximately midstream and to the edge of the concrete paved segment. After waiting for any disturbed sediment to be washed away, the sampled was collected by submerging the sterile 1-liter bottle in the stream. At station AR-33, the bottom of the stream is entirely paved with concrete. At this site, we waded to approximately midstream. After waiting for any disturbed sediment to be washed away, the sample was collected again by submerging the sterile 1-liter bottle in the stream. Boat-approached sites, AR- 2, AR-3, AR-4, AR-10, AR- 32, and AR-38, were sampled by submerging the collection bottles over the side of the research vessel as the vessel coasted on final approach to the station.

In all cases, the bottles were rinsed twice with sample water and then the final sample was collected. Immediately after collection, samples were placed in dark, insulated containers packed with ice. Samples were returned to the George Mason University at the Potomac Science Center, where they were processed within about 4 hour of collection.

Table EC1. Sampling Dates

Date	Date Codes
14-apr-2021	20210414
5-may-2021	20210505
26-may-2021	20210526
9-jun-2021	20210609
24-jun-2021	20210624
8-jul-2021	20210708
27-jul-2021	20210727
10-aug-2021	20210810
24-aug-2021	20210824
8-sep-2021	20210908

Table EC2. Station identifiers, locations and access type

Station ID	Access Type	Location Description	Latitude	Longitude
AR-1	Shore	Hunting Cr just above GW Parkway Bridge	38.78992	-77.05126
AR-2	Boat	Northern portion of Hunting Cr.	38.78509	-77.04951
AR-3	Boat	Southern portion of Hunting Cr.	38.78181	-77.04890
AR-4	Boat	Potomac River Channel off Hunting Cr.	38.78124	-77.03529
AR-10	Boat	Potomac River North of Wilson Bridge	38.79816	-77.03907
AR-12	Shore	Last Riffle of Cameron Run near Beltway crossing	38.80218	-77.08467
AR-13	Shore	Hooffs Run upstream of Alex renew outfall	38.80278	-77.05848
AR-21	Shore	South side of Cameron Run downstream from Lake Cook drain	38.80318	-77.09565
AR-23	Shore	South side of Cameron Run across from AlexRenew outfall	38.79372	-77.05966
AR-24	Shore	Hunting Creek Embayment near shore just west of Royal St CSO outfall	38.79156	-77.04680
AR-25	Shore	Hunting Creek Embayment near shore just east of Royal St CSO outfall	38.79205	-77.04538
AR-30	Shore	Cameron Run upstream near metro rail bridge	38.80545	-77.10745
AR-32	Boat	Potomac Mainstem downstream of Outfall 001	38.80940	-77.03727
AR-33	Shore	Hooffs Run at Linden St	38.81103	-77.05993
AR-34	Shore	Hooffs Run at Alex Renew	38.79918	-77.05997
AR-35	Shore	Timber Branch of Hoof's Run at downstream end of Ivy Hill Cemetery	38.8175	-77.070654
AR-38	Boat	Potomac River at Daingerfield Island; at marker '6'	38.82348	-77.03802

Analytical Methods

Determination of the abundance of *E. coli* was performed following the EPA Method 1603 (*Escherichia coli* in Water by Membrane Filtration Using Modified Membrane-Thermotolerant *Escherichia coli* Agar–Modified mTEC, USEPA 2009). This is an EPA-approved method for determining abundance of *E. coli* in fresh water. It is a one-step modification of the EPA Method 1103.1. It is based on *E. coli* production of β-D-glucuronidase and the consequent metabolism of 5-bromo-6-chloro-3-indolyl-β-D-glucuronide in the medium to glucuronic acid and a red- or magenta-colored product (USEPA 2009).

For this work, mTEC medium (Fisher) was prepared in our laboratory at George Mason University (Potomac Science Center) shortly before each sampling trip. The medium

was prepared as per package directions, and ~5 mL of the molten medium was placed aseptically into sterile, 50-mm Petri dishes with tight fitting lids. Prepared medium was stored at 4°C in the dark until use. Phosphate buffered saline (PBS) was prepared as per Method 1603 and autoclave sterilized. PBS was added to smaller samples (1.0 mL and 10 mL) to make volumes up to at least 20 mL before filtration. This aids in distributing bacteria uniformly across the membrane surface. The PBS was also used for blank controls.

Upon return to the laboratory, samples were processed immediately. Sterile, gridded, 0.45 µm membrane filters were aseptically positioned, grid side up, on the base of a sterile, polycarbonate filter holder, and the filter tower was placed in position on a vacuum flask over the filter and base. Samples were shaken vigorously to assure complete mixing and appropriate volumes (1.0 mL, 10.0 mL, and 100.0 mL) of sample were added to each of three replicate filter systems. Before adding the two smaller volume aliquots to the filter funnels, sufficient PBS was added to make the final volume approximately 20 mL. Samples were then filtered with vacuum (approximately 10 in. Hg). Each filter was then removed from the filter holder base aseptically with sterile, blunt-tipped forceps and placed onto the surface of the mTEC agar without trapping any air bubbles beneath the filter. After replacing the Petri dish tops, the plates were incubated in a 35°C incubator for 2 ± 0.5 hours. They were then removed, placed in heat-sealed plastic bags and submerged in a water bath at 44.5°C ± 0.2°C for 22 ± 2 hours. Three blank controls, consisting of 3 x 100 mL of PBS, were checked each time samples were processed. Generally, no *E. coli* were detected in these blank controls, although occasionally controls had one or two presumptive *E. coli* colonies. The data were not corrected for this low background as it was generally far less than 1 percent of the abundances on countable plates.

After the water bath incubation, samples were retrieved and observed immediately for typical red or magenta *E. coli* colonies. All Petri dishes (3 volumes x 3 replicates = 9 Petri dishes per sample) were observed. Although only dilutions yielding colony counts between 20 and 80 needed to be enumerated, we generally recorded colonies for each countable dilution. Often, however, when *E. coli* were too abundant, the higher volume samples were not countable due to overgrowth. Calculation of final *E. coli* abundances followed the procedures described in Appendix B of the EPA Method 1603 (USEPA 2009). In brief, *E. coli* abundance were reported as 'colony forming units (CFUs) per 100 mL'. Since there were triplicate analyses of each dilution, the colony count per Petri dish was separately converted to CFUs per 100 mL and then the triplicates were averaged. If no dilution gave individual counts between 20 and 80, the nearest count was selected and used for the final calculation as described in appendix B of the EPA Method 1603. If all counts were too numerous to count (TNTC), the colony count was reported as greater than the highest acceptable count for the lowest dilution: in our case, 'greater than 8,000 CFUs per 100 mL', according to appendix B of the EPA Method 1603. If no samples showed positive counts, which was the cases for most of negative controls, results were reported as 'less than 1 CFU per 100 mL', according to appendix B of the EPA Method 1603.

3. Results & Discussion

In 2021, typical *E. coli* colonies were observed in some dilution(s) of every sample tested. There was then a point estimate of *E. coli* CFUs per 100 mL for each sample. In some instances, even the lowest volume plates (1 mL) were TNTC and reported as 'greater than 8,000 CFUs per 100 mL'. *E. coli* abundances grouped by station are shown in **Figure EC1** and *E. coli* abundances grouped by sampling date are shown in **Figure EC3** (tabular data is in Appendix A, **Table A1**). One of the three controls analyzed in Aug 10 showed a positive count (i.e., 1 count per 100 mL). Other controls did not show any counts and were reported as 'less than 1 CFU per 100 mL' (data not presented).

Since there was no situation in which four weekly samples were collected in a single calendar month, the '235 CFUs per 100 mL' (in more than 10% of the samples) criterion is applicable in determining impairment.

Data Grouped by Station

The different stations sampled have been selected with the purpose of capturing the potential contribution of Alex Renew's CSOs to receiving waters. These CSOs include the Cameron Run CSO across station AR-23 on Cameron Run, the Hooffs Run CSO between station AR-13 and AR-34 on Hooffs Run, the Royal St. CSO between stations AR-24 and AR-25 on the Potomac River, and the Pendleton St. CSO by station AR-32 on the Potomac River.

In 2021, thermotolerant *E. coli* abundances grouped by station exceed the 235 CFUs per 100 mL 'impaired water' criterion at all shore stations and five out of the six off-shore stations (AR-2, AR-3, AR-10, AR-32, and AR-38) at some time during the sampling period. Only the off-shore site AR-4 did not show any exceedance during the sampling period (**Figure EC1**). This is well in accordance to observations made in 2015, 2016, 2017, and 2019, where all stations showed exceedance for at least one sampling date. Only in 2020, three off-shores stations did not show any exceedance, likely because only five sampling campaigns were conducted versus 10-11 in other years. One shore station showed exceedance of 235 CFUs per 100 mL on all sampling dates: AR-13. All other stations on shore showed exceedance of 235 CFUs per 100 mL on at least 5 sampling dates out of 10. Six shore stations showed exceedance in at least 8 sampling dates: AR-13, AR-24, AR-25, AR-30, AR-33, AR-34, and AR-35. As usual, off-shore stations showed less exceedances: 4 or less over all sampling dates.

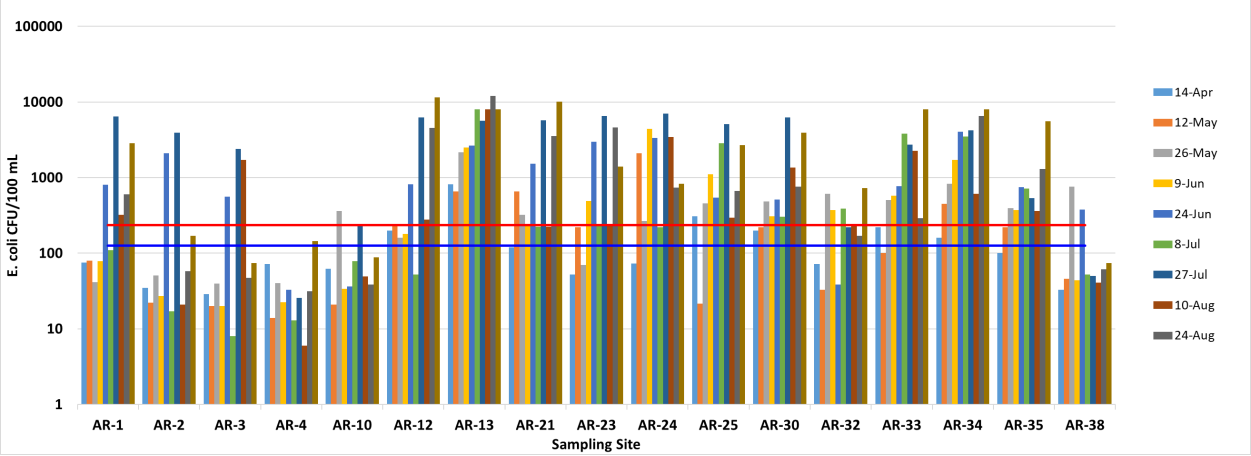

Figure EC1. *E. coli* abundance per 100 mL in Cameron Run, Hunting Creek, and the adjacent Potomac River grouped by stations from April to September 2021. The blue horizontal line represents the *E. coli* criterion for the geometric monthly mean allowable abundance (126 CFUs per 100 mL), and the red line represents the criterion for allowable abundance in the absence of four monthly samples (235 CFUs per 100 mL).

Figure EC2 shows the 'box plots' of *E. coli* numbers per 100 mL as arrayed by site. In this figure, the stations were grouped by streams, including the shore stations on Cameron Run (orange), the shore stations on Hooff Run (green), the shore stations on the Potomac River near the Royal St. CSO outfall (purple), and the off-shore stations (blue). Five sampling stations are located along Cameron Run and include, from upstream to downstream: AR-30, AR-21, AR-12, AR-23, and AR-1. AR-30 and AR-21 are in flowing Cameron Run, AR-12, AR-23, and AR-1 are in tidal Cameron Run. Four stations are located along Hooff Run (a tributary of Cameron Run) and include, from upstream to downstream: AR-35, AR-33, AR-13, and AR-34. Hooff Run is a tributary of Cameron Run, which is suspected to contribute to the *E. coli* contamination observed in Cameron Run. Two shore stations are located on Potomac River near the Royal St. CSO and include AR-24 and AR-25. Off-shore stations include two stations in the Hunting Creek embayment, near the Hunting Creek discharge point, AR-2 and AR-3, and four stations in the mainstem Potomac River, from upstream to downstream: AR-38, AR-32, AR-10, and AR-4.

On average, we observed first an increase of the detected *E. coli* numbers on Cameron Run when moving downstream from AR-30 (1,430 CFUs/100 mL) to AR-12 (2,422 CFUs/100 mL). Then the numbers decreased from AR-12 to AR-1 (1,142 CFUs/100 mL). We observed a significant decrease of the numbers between AR-12 and AR-23, indicating that the contribution of the Cameron Run CSO (located at almost the same level as AR-23) to the contamination of Cameron Run may not be significant.

On average, we also observed an increase of the *E. coli* numbers when going downstream along Hooff Run from AR-35 (1,028 CFUs/100 mL) to AR-34 (3,001 CFUs/100 mL), with a maximum of 5,042 CFUs/100 mL at AR-13. We observed a significant decrease of the counts between AR-13 and AR-34, which again indicates that the contribution of Hoof Run CSO (located between AR-13 and AR-34) to Hooff Run contamination may not be significant.

The shore Potomac stations nearby the Royal St. CSO outfall showed average numbers of 2,247 and 1,399 CFUs/100 mL for AR-24 and AR-25, respectively. These numbers are much higher than the nearby off-shore numbers at stations AR-10 (101 CFUs/100 mL) or AR-2 (643 CFUs/100 mL), indicating a possible contribution of the Royal St. CSO outfall to water contamination at these sites.

All off-shore numbers were on average much lower than the shore numbers (40 – 643 versus 1,028 – 5,042 CFUs/100 mL). Off-shore stations by the Hunting Creek Embayment, AR-2, AR-3, and AR-4, showed a steady decrease of the counts when increasing the distance from Cameron Run discharge: from AR-1 (1,142 CFUs/100 mL) to AR-4 (40 CFUs/100 mL), which suggests that Cameron Run may be a significant source of *E. coli* to the Potomac River. All off-shore stations in the mainstream Potomac River, AR-38, AR-32, AR-10, and AR-4, showed similarly low numbers (40 – 286 CFUs/100 mL). Station AR-32, which is nearby the Pendelton St. CSO in Orinoco Bay shows slightly higher average counts (286 CFUs/100mL) than the downstream stations in mainstem Potomac river, AR-38, AR-10, and AR-4, It is noteworthy that these numbers are low and the difference may not be significant.

In summary, the average *E. coli* counts by stations increased from upstream to downstream, along both Cameron Run and Hooff Run. These streams also showed the highest counts that we recorded among all stations. Examination of the *E. coli* counts along Cameron Run and Hooff Run does not indicate a significant contribution of the Cameron Run CSO and Hoof Run CSO to the contamination of these streams. The Potomac River stations near the Royal St. CSO outfall showed numbers much higher than nearby off-shore numbers at stations, suggesting a contribution of the Royal St. CSO outfall to water contamination at these sites. The off-shore counts were about one or more orders of magnitude lower that the shore counts, which is easily explained by dilution of the stream water.

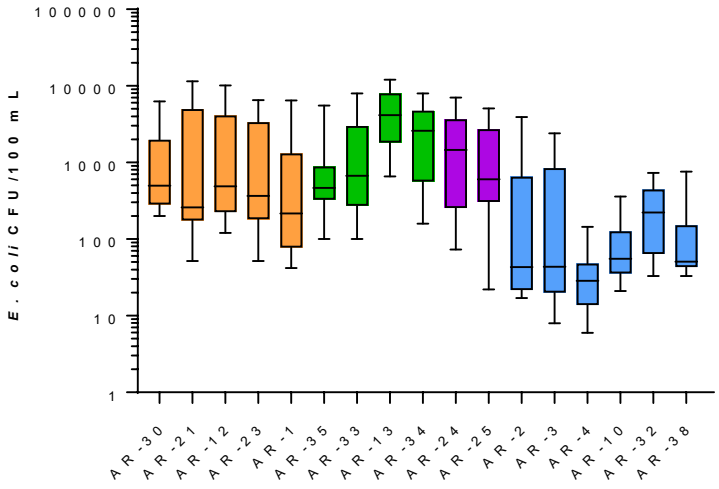

Figure EC2. Box plots of *E. coli* abundance per 100 mL for each site in Cameron Run, Hunting Creek, and the adjacent Potomac River from April to September 2021. The bars show the minimum and maximum counts, the boxes show the 25 and 75-percentile, and the median. Shore stations on Cameron

Run are in orange, shore stations on Hooff Run are in green, shore station on the Potomac River are purple, and off-shore stations are blue.

Data Grouped by Date

E. coli abundances grouped by dates are presented in **Figure EC3** and **EC4**. The highest average *E. coli* numbers were observed on July 27 and September 8 (~3,700 average CFUS/100 mL). The frequency of exceedances of 235 CFUs/100 mL was the highest on June 24, July 27, and September 8, with 14, 12, and 14 exceedances over the 17 sites sampled. Unlike what was observed in several prior years, in 2021, we did not detect significant correlation between the *E. coli* numbers and the Cameron Run flow (recorded at Wheeler Ave), evaluated as daily flow or 3- and 5-day average (Pearson correlation coefficient < 0.5).

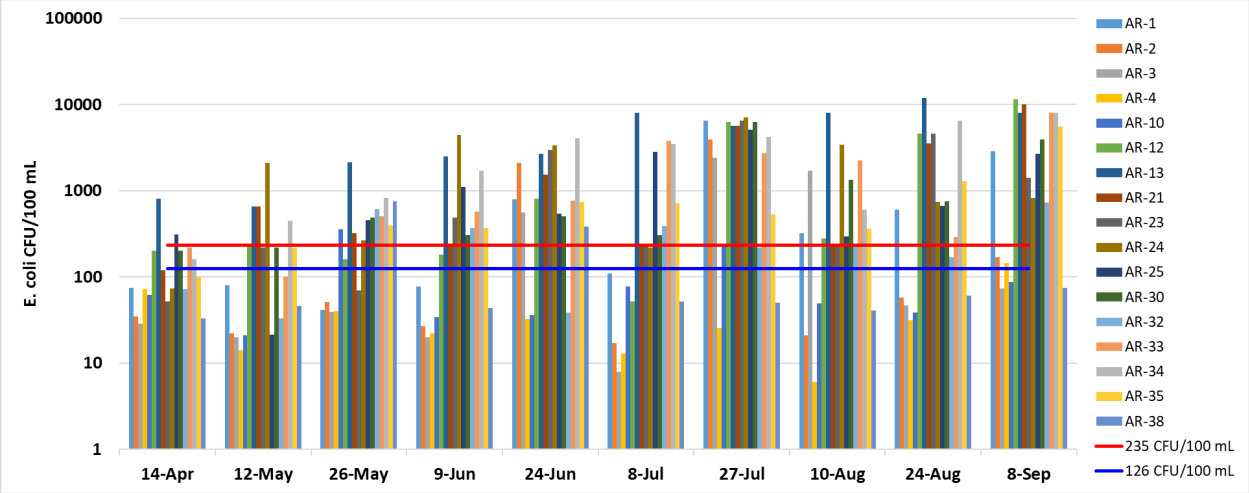

Figure EC3. *E. coli* abundance per 100 mL in Cameron Run, Hunting Creek, and the adjacent Potomac River grouped by sampling dates for all stations. The blue horizontal line represents the *E. coli* criterion for the geometric monthly mean allowable abundance (126 CFUs per 100 mL), and the red line represents the criterion for allowable abundance in the absence of four monthly samples (235 CFUs per 100 mL).

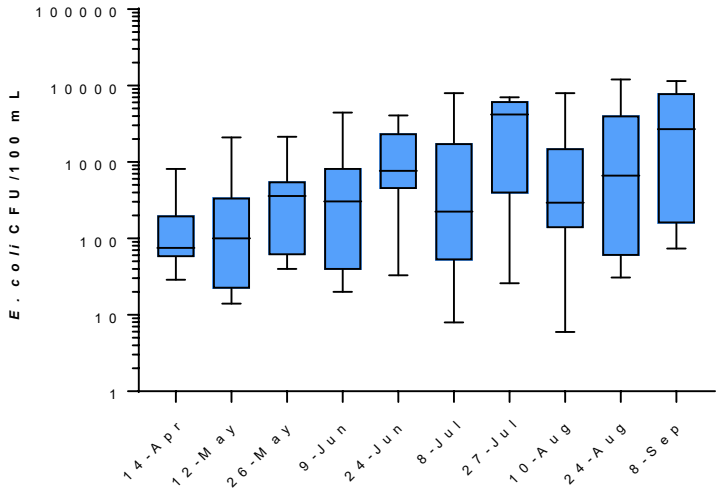

Figure EC4. Box plots of *E. coli* abundance per 100 mL for each sampling dates in Cameron Run, Hunting Creek, and the adjacent Potomac River over all sites. The bars show the minimum and maximum

values, the boxes show the 25 and 75-percentile, and the median.

Temporal Trends

The number of stations and sampling events have increased between 2014 and 2021 (i.e., 8 sites and 6 sampling times in 2014 to 17 sites and 10 sampling times in 2021), with the exception of 2020, which was marked by a reduction of the sampling campaigns due to COVID-19. We present here a timeline of changes in the percentage of samples that exceeded the 235 CFUs per 100 mL standard (**Figure EC5**). We also present the average *E. coli* abundances per 100 mL over the period 2017 – 2021 (**Figure EC6**). Even though over the period 2014 – 2017, both the percent exceedances and average counts globally suggested worsening of the water conditions, these trends are not observed for the period 2018 - 2021. We observe globally comparable numbers in the years 2019, 2020, and 2021.

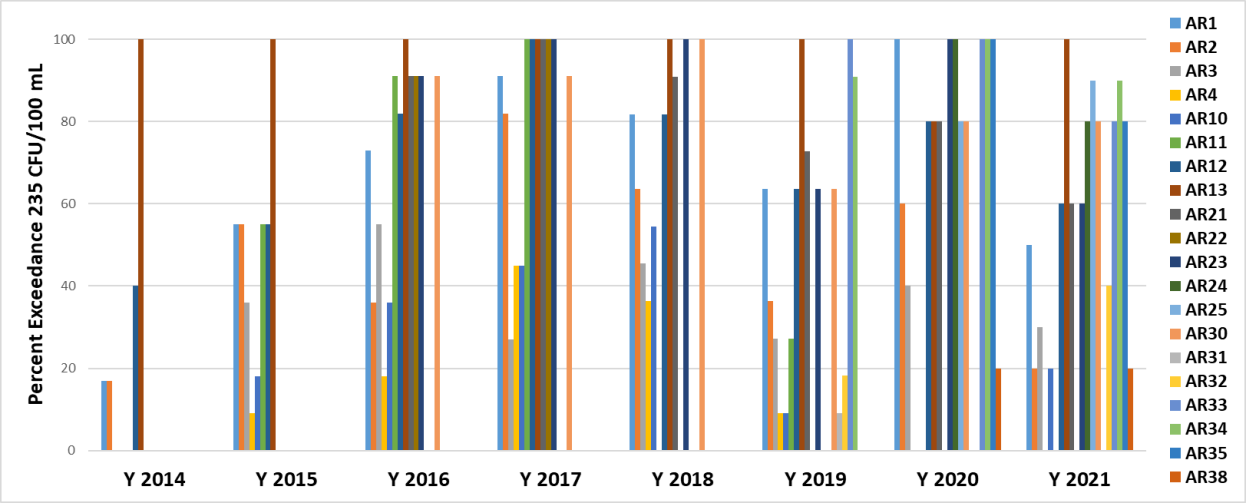

Figure EC5: Percentage of sample events when *E. coli* abundances exceeded 235 per 100 mL in the years 2014 -- 2021. Samples were collected 6 times during 2014, whereas in each of the subsequent years, samples were collected 10 or 11 times.

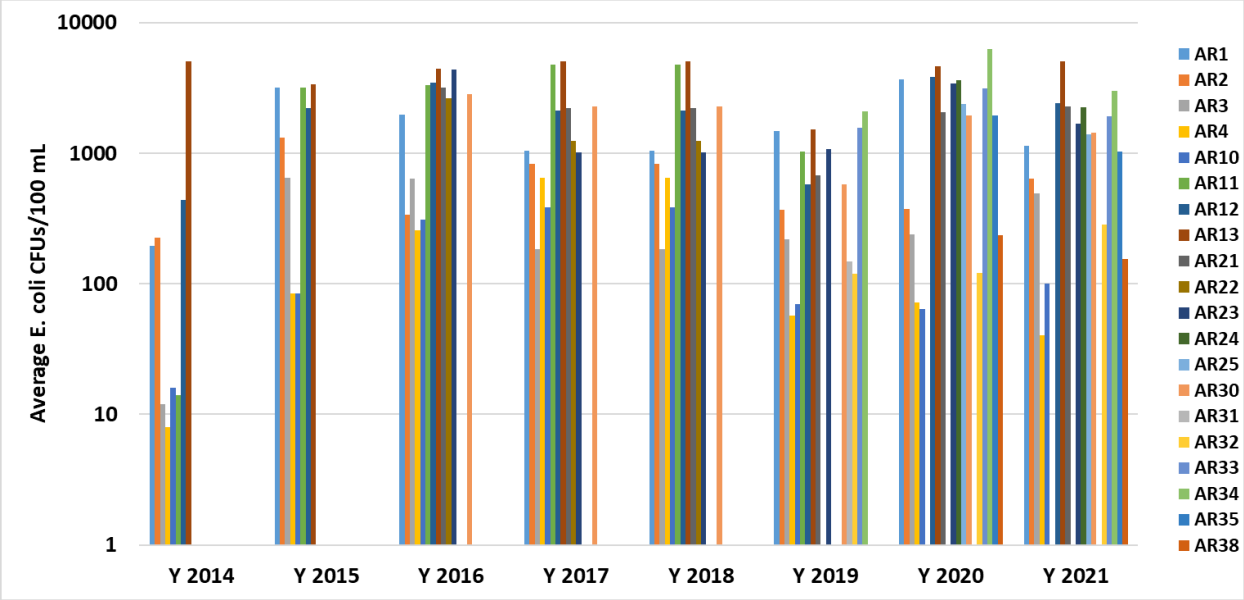

Figure EC6: *E. coli* abundances per 100 mL in the years 2014 – 2021. Samples were collected 6 times during 2014, whereas in each of the subsequent years, samples were collected 10 or 11 times.

4. Conclusions

The data continue to support a conclusion that the entire area sampled, including the mainstem of the Potomac River, is impaired for the bacteriological water quality criterion (*E. coli*) under Section 9VAC25-260-170 of the Virginia Water Quality Standards that applies to primary contact recreational use surface waters. Although our data showed globally an increase of the *E. coli* abundances and percent exceedances of the 235 CFUs per mL criterion from 2014 to 2017, these numbers seemed to have peaked in 2017 and even showed a slight decrease in the subsequent years.

Sampling additional sites in Hooff Run/Cameron Run and the Potomac River helped to determine the potential contribution of Alex Renew CSOs to receiving waters. The 2021 data does not indicate a significant contribution of the Cameron Run CSO and Hoof Run CSO to the contamination of these streams by *E. coli*. However, the 2021 data may indicate a contribution of the Royal St. CSO outfall to contamination of the Potomac River. The 2021 data does not show a significant contribution of the Pendelton St. CSO to the mainstem Potomac river.

Literature Cited

U.S. Environmental Protection Agency (USEPA). 2009. Method 1603: *Escherichia coli* (*E. coli*) in Water by Membrane Filtration Using Modified membrane-Thermotolerant *Escherichia coli* Agar (Modified mTEC). Available at: < http://water.epa.gov/scitech/methods/cwa/bioindicators/> search Method 1603, December 2009.

U.S. Environmental Protection Agency (USEPA). 2012. Water: Monitoring &

Assessment: 5.11 Fecal Bacteria. Available at: http://water.epa.gov/type/rsl/monitoring/vms511.cfm

U.S. Environmental Protection Agency (USEPA). 2014. National Water Quality Assessment Report, water Quality Assessment and Total Maximum Daily Loads Information. Available at: <http://ofmpub.epa.gov/waters10/attains_index.control>

Virginia Department of Environmental Quality (VADEQ). 2010. Bacteria TMDLs for the Hunting Creek, Cameron Run, and Holmes Run Watersheds. Available at: <deq.state.va.us>

Virginia Department of Environmental Quality (VADEQ). 2012. 2012 Impaired Waters: Category 4 & 5 by Basin and Stream Name, Potomac and Shenandoah River Basins, Cause Group Code: A13R-03-BAC - Cameron Run/Hunting Creek. Available at: <http://www.deq.virginia.gov/Programs/Water/WaterQualityInformationTMDLs/WaterQualityAssessments.aspx>

Virginia. *State Water Control Board* (VSWCB). 2011. 9 VAC 25-260-10 Designation of uses. Virginia Water Quality Standards. Available at: <http://lis.virginia.gov/cgi-bin/legp604.exe?000+reg+9VAC25-260-10>

Virginia. *State Water Control Board* (VSWCB). 2011b. 9 VAC 25-260-170 Bacteria; other recreational waters. Virginia Water Quality Standards. Available at: <http://lis.virginia.gov/cgi-bin/legp604.exe?000+reg+9VAC25-260-170>

Appendix A

Figure A1. Maps of sampling sites

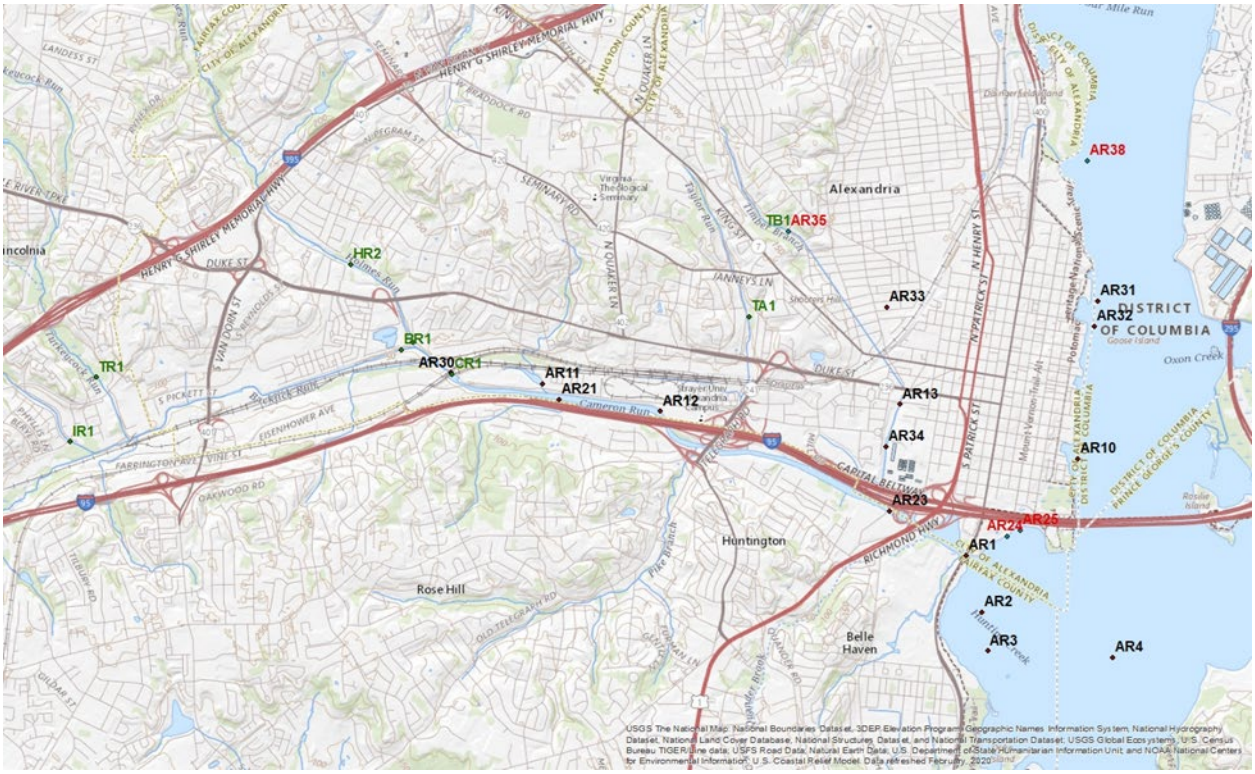

Table A1. 2021 *E. coli* abundances per 100 mL for all station, all sampling dates

Stations	Sampling Dates									
# CFU Per 100 mL	04/14/21	05/12/21	05/26/21	06/09/21	06/24/21	07/08/21	07/27/21	08/10/21	08/24/21	09/08/21
AR-1	75	80	42	78	800	110	6467	323	600	2850
AR-2	35	22	51	27	2100	17	3933	21	58	170
AR-3	29	20	40	20	557	8	2400	1700	47	74
AR-4	72	14	40	22	33	13	26	6	31	145
AR-10	62	21	360	34	36	78	240	49	38	88
AR-12	200	240	160	180	810	52	6233	280	4567	11500
AR-13	810	660	2150	2500	2667	8000	5633	8000	12000	8000
AR-21	120	660	323	230	1528	225	5700	225	3567	10100
AR-23	52	220	70	490	2967	227	6500	245	4600	1400
AR-24	73	2100	267	4433	3333	220	7050	3433	735	830
AR-25	310	22	457	1100	540	2833	5067	293	667	2700
AR-30	200	220	487	307	510	303	6267	1347	760	3900
AR-32	72	33	610	370	39	387	220	227	170	730
AR-33	220	100	507	573	770	3800	2733	2250	290	8000
AR-34	160	447	830	1700	4067	3500	4200	607	6500	8000
AR-35	100	220	395	370	745	715	537	363	1300	5533
AR-38	33	46	760	44	380	52	50	41	61	75

Table A2. Mean of *E. coli* abundances per 100 mL, seasonal means and standard deviations and percent exceedances of the 126 and 235 CFUs/100 mL criteria

Station	Seasonal Mean (*E. coli* /100 mL)	Seasonal St. Dev. (*E. coli* /100 mL)	Percent Exceedance 126 CFUs/100 mL	Percent Exceedance 235 CFUs/100 mL
AR1	1142	2055	50	50
AR2	643	1324	30	20
AR3	489	855	30	30
AR4	40	41	10	0
AR10	101	111	20	20
AR12	2422	3861	90	60
AR13	5042	3838	100	100
AR21	2268	3314	90	60
AR23	1677	2272	80	60
AR24	2247	2297	90	80
AR25	1399	1625	90	90
AR30	1430	2033	100	80
AR32	286	238	70	40
AR33	1924	2478	90	80
AR34	3001	2724	100	90
AR35	1028	1619	90	80
AR38	154	237	20	20

Station	Seasonal Mean (*E. coli* /100 mL)	Seasonal St. Dev. (*E. coli* /100 mL)	Percent Exceedance 126 CFUs/100 mL	Percent Exceedance 235 CFUs/100 mL
AR1	3655	4157	100	100
AR2	374	214	100	60
AR3	238	180	60	40
AR4	72	84	20	0
AR10	64	11	0	0
AR12	3865	4769	100	80
AR13	4619	3480	80	80
AR21	2069	2086	100	80
AR23	3433	2280	100	100
AR24	3601	2835	100	100
AR25	2375	2352	100	80
AR30	1946	1579	100	80
AR32	121	72	60	0
AR33	2681	3328	100	100
AR34	4498	5040	100	100
AR35	1951	1695	100	100
AR38	235	306	60	20